Post-fire carbon, fuels, and vegetation dynamics in wet temperate forests: implications for future fire and management in the Pacific Northwest

Jenna Morris

A dissertation

submitted in partial fulfillment of the

requirements for the degree of

Doctor of Philosophy

University of Washington

2025

Reading Committee:

Brian J. Harvey, Chair

Joshua S. Halofsky

Crystal L. Raymond

Program Authorized to Offer Degree:

School of Environmental and Forest Sciences

University of Washington

Abstract

Post-fire carbon, fuels, and vegetation dynamics in wet temperate forests: implications for future fire and management in the Pacific Northwest

Jenna Morris

Chair of the Supervisory Committee:

Brian J. Harvey

School of Environmental and Forest Sciences

Forecasting ecosystem dynamics under warming climate and increasing fire activity is a critical priority for contemporary ecology and ecosystem management. However, fundamental understanding of fire effects is missing in ecosystems where fire is infrequent, including wet temperate forests west of the Cascade Range crest in Washington and northern Oregon, USA ("northwestern Cascadia"). In this dissertation, I combined empirical and simulation insights from recent fires in northwestern Cascadia to address research priorities for anticipating the effects of large infrequent fires on future forest dynamics. First, I characterized initial (2–5 years) post-fire aboveground biomass in long-term monitoring plots within five fires to explore the relative influence of pre-fire stand age and burn severity on two important post-fire disturbance legacies: carbon and fuel profiles. I found that pre-fire stand age drove total legacy amounts

while burn severity modified legacy condition. Regardless of burn severity, most biomass present pre-fire persisted following fire. These findings suggest that, when burned, older stands may have greater potential than younger stands to support several ecosystem functions, due to more abundant and complex disturbance legacies. Next, I characterized the relative importance of bottom-up and top-down drivers on short-interval reburn potential. I used the Fire and Fuels Extension to the Forest Vegetation Simulator to model potential fire behavior and effects in each field plot under two fire weather scenarios. I found that initial fuel variability influenced some aspects of potential fire behavior and effects in reburns under moderate fire weather conditions. However, extreme fire weather is likely to override these effects and result in stand-replacing fire effects regardless of differences in initial fuel variability among stands. Microclimate responding to differences in stand structure buffered potential fire behavior and effects, particularly in unburned stands, but did not change overall patterns. These findings suggest the dominance of top-down drivers on influencing short-interval reburn potential in wet temperate forests. Finally, I examined potential tradeoffs for managing post-fire forest trajectories, specifically focusing on early-seral conditions, tree regeneration, and fuel profiles. I initialized each high severity field plot in the individual-based landscape model, iLand, and simulated 80 years of stand development under two future climate scenarios. I found that pre-fire stand age had lasting effects on forest recovery following stand-replacing fire, with older stands having longer persistence of early-seral conditions, more abundant and diverse live tree regeneration, and greater canopy and surface fuel loads. Post-fire trajectories were similar under both warming and current future climate scenarios. These findings suggest that post-fire recovery may be more robust in older stands, and negative effects of warming are unlikely through the end of the century in the absence of additional disturbance. Further, common post-fire management

interventions present likely tradeoffs for post-fire forest structure and function. Collectively, this work builds understanding of the drivers and consequences of fire in forests shaped by long intervals between severe disturbances. Exploring the immediate and future effects of fire on ecosystem functions, disturbance interactions, and management outcomes supports our ability to manage post-fire recovery trajectories in some of the world's highest biomass forests.

TABLE OF CONTENTS

LIST OF FIGURES

LIST OF TABLES

ACKNOWLEDGEMENTS

I am overwhelmed with gratitude for everyone who has made this accomplishment possible (though clearly not lost for words with which to express this gratitude).

This dissertation took place on traditional lands stewarded since time immemorial by Indigenous peoples including the Cowlitz Indian Tribe, Duwamish Tribe, Confederated Tribes of Grand Ronde, Muckleshoot Indian Tribe, Puyallup Tribe of Indians, Confederate Tribes of Siletz Indians, Suquamish Tribe, Tulalip Tribes, Confederated Tribes of Warm Springs, and Confederated Tribes and Bands of the Yakama Nation. I honor with gratitude the land itself and these peoples, past and present, who thrive in these places.

Immense thank you to Brian Harvey – I couldn't have asked for a better graduate advisor. You have cultivated a lab culture rooted in respect, compassion, and community. You encourage us to be ambitious, support us in our pursuits, and celebrate our efforts regardless of the outcome. Your mentorship prioritizes both professional development and our overall wellbeing. You demystify the academic world and provide space for difficult conversations. You are approachable, understanding, patient, and kind. For all of this, I am so grateful. Thank you for the time and energy you've invested in my graduate experience, and for building my confidence while stoking the stoke along the way.

Thank you to my committee members for your wisdom and guidance. I am grateful for the experience of learning from such fantastic scientists and really value the unique perspectives and expertise you each bring to this field. Crystal Raymond, thank you for helping me place my work within context of climate adaptation, and for providing me with valuable opportunities to build my training in actionable science. It's been so rewarding to learn from your experiences working at the boundary between science and management. Josh Halofsky, thank you for your encouragement, practicality, and constant consideration of my goals and perspectives. I really value your mentorship style and am lucky to collaborate with you on westside fire research. Abby Swann, thank you for your climate insights and helping me to engage more thoughtfully with modeling tools. You have been a fantastic GSR, both ensuring the PhD process was fair and strengthening my knowledge base. Jerry Franklin, it has been an honor to have you on my committee. I am grateful for your insightful comments and practical approaches, informed by

decades of experience and deep knowledge of these ecosystems, and remain inspired by your generous support for early career ecologists, storytelling prowess, and passion for preserving the legacies of permanent plot networks and long-term research studies.

I am grateful to the many collaborators and partners with whom I have had the pleasure of working and learning. Dan Donato, it's been so rewarding to study westside fires under the mentorship of someone so knowledgeable, well-rounded, and kind. Thank you for investing so much time into my graduate experience, and for your willingness to always offer helpful and practical advice. Thank you to our agency partners from the Tulalip Tribes, Forest Service, Washington Department of Natural Resources, and National Park Service for facilitating invaluable access and logistical support for our post-fire research, and for providing insightful perspectives on the unique challenges and opportunities for managing forest and fire dynamics across northwestern Cascadia. I recognize the (often overlooked and undervalued) impact of your public service and sincerely appreciate your hard work in support of sustainable land management!

I also want to acknowledge my undergraduate mentor, Grant Casady, for his investment in my education of mind and heart. Thank you for encouraging my interest in ecological research and providing me with training opportunities, field experience, and guidance with which to pursue a career in this field. I remain inspired by your approach to science rooted in stewardship of our natural world and am grateful for the continual kindness of you and your family.

This work was supported by funding from the following agencies: the USDA Forest Service – PNW Research Station under award 20-JV-11261927-060 as part of the Westside Fire and Climate Adaptation Research Initiative; the intramural research program of the U.S. Department of Agriculture, National Institute of Food and Agriculture, McIntire Stennis accession no. 1027380; a Graduate Research Innovation award (No. 23-1-01-15) from the Joint Fire Science Program; Grant / Cooperative Agreement G20AC00115 from the United States Geological Survey Northwest Climate Adaptation Science Center; and a U.S. Geological Survey Northwest Climate Adaptation Science Center award G17AC00218. An additional thank you to the College of the Environment, School of Environmental and Forest Sciences, Graduate School, and Graduate and Professional Student Senate at the University of Washington for providing funding to support my attendance and presentation of research at professional conferences.

The foundation of this research rests on the collective efforts of everyone who has supported our field data collection across the western Cascades. Enormous gratitude for the hard work of all our incredible field technicians from 2019–2022, including Ellie Aosved, Ali Brown, Eric Burres, Sarah Burrington, Francesca Dezza Parada, Mark Elbrecht, Davien Graham, Ben Hagedorn, Ashley Hillis, Hiruni Jayasekera, Nic Katz, Sofia Kruszka, Nicole Lau, Madison Laughlin, Alex MacKinnon, Marwa Mahmoud, Michael McNorvell, Sienna Patton, Allison Phillips, Christian Rolfson, Margalit Shetreat-Klein, Maddy Stone, Libby Taylor-Manning, Sam Tharpgeorge, Marcela Todd Zaragoza, Spencer Vieira, Hannah Wilson, Roni Woodard, and Cameron Zinke. Thank you for your relentless enthusiasm, trust, and perseverance. As challenging as these field seasons were—enduring long and smoky days, arduous terrain, UCAR troubles, a global pandemic, the Heat Dome, and difficult human encounters—they were even more rewarding, and the source of many cherished memories, thanks to each of you. I want to extend additional gratitude to Don Radcliffe, Madison Laughlin, Liliana Rangel-Parra, and Sofia Kruszka for helping to organize and lead these field seasons. I so appreciate your expertise, patience, thoughtfulness, and emotional support that were critical to pulling off these ambitious 3+ month excursions each summer. I'd also like to acknowledge critical support and assistance provided by Gene Brandow and his kind crew during a rough patch on the Mount Hood National Forest; Colin and the other helpful folks who enabled our lawn lodgings at Wind River; the many camp hosts who accommodated our oversized groups; and Les Schwab, GreenTree Towing, and Topline Towing (for obvious reasons).

Massive gratitude to my Harvey Lab friends and colleagues. I could not have asked for a more supportive, impressive, and fun lab group to work with and learn from! I am a better ecologist and person thanks to your perspectives. To the original lab ladies—Michelle Agne, Saba Saberi, and Michele Buonanduci—thank you for being such incredible personal and academic role models, and for all your efforts establishing the foundational values of the lab. You're amazing women and I'm so grateful for your friendship! Michelle, you are an exceptional person in so many ways. Thank you for your openness, advocacy, and infinite wisdom. Saba, your authenticity and candidness are so refreshing. Thank you for your generosity, solidarity, and honesty. Michele, I am lucky to have had someone so thoughtful and brilliant with whom to navigate all stages of grad school. Thank you for your reliability and solid advice on every topic (especially statistics). Don Radcliffe, I so appreciate the sincerity, ambition, and levity you

cultivate around you. Thank you for fostering so much community within and outside of SEFS, and for the much-needed reminders to take breaks and prioritize life outside grad school when possible. Madison Laughlin, I am constantly in awe of your ambition, empathy, intuition, and creativity. Thank you for your willingness to always lend a hand or an ear, and for the steadiness you cultivate. Liliana Rangel-Parra, I have so much respect for your perseverance, humility, courage, and karaoke skills. Thank you for your constant kindness and infectious curiosity. Sofia Kruszka, you are one of the most selfless, dependable, and determined people I know. Thank you for being my iLand partner, and for your help on so many dimensions both in and out of the office. Angie Liotta, I deeply admire your work ethic, levelheadedness, and willingness to offer help in a heartbeat. Thank you for all your advice, your leadership in SEFS, and your partnership in TA'ing 200 undergrads together. Kristin Braziunas, thank you for offering me so much of your time and invaluable guidance to be able to complete my iLand analyses, and for encouraging us to eat lunch together. I'm grateful for your mentorship and excited to continue to work with and learn from you. I also want to thank Sienna Patton for all her contributions to this research during her capstone – it was so rewarding to be your mentor. I am additionally grateful for the unique perspectives, insights, and opportunities for collaboration from all the honorary lab members and visitors over the years, including Kavya Pradhan, Kyra Clark-Wolf, Royale Williams, Sarah McColl-Gausden, and Ella Plumanns-Pouton.

Thank you to the SEFS community for all your support. I am grateful to have had such welcoming graduate peers and role models to help me navigate grad school and provide some fun along the way. I've learned so much from all of you, especially the importance of collective action. I remain inspired by your passion for research and teaching, perseverance in pursuit of a graduate education, and commitment to building a more equitable and just department, field, and world. It is encouraging to know our future is filled with so many incredible people working to address all dimensions of environmental stewardship!

Thank you to all my friends for the care and excitement you bring to my life. To the friends I've met in Seattle—including Elena, Tyler, Lila, Olivia, Saba, Michele, Sarah, Vivian, Gina, et al.—I feel so lucky to have been surrounded by such cool, talented, genuine, and welcoming people. I truly value all the conversations, meals, laughter, new experiences, and celebrations we've shared, and am appreciative for your solid advice. To my friends in Spokane—Beth, Steven, et

al.—thank you for all the fun opportunities to take a break, get back to the eastside, and build on our college memories. To my longtime friends—Piper and Allie—thank you for your unconditional support. I'm unbelievably grateful to have a friendship so comfortable, effortless, and secure across a variety of life stages and long distances. You two have kept me grounded and brought me immeasurable joy – love you both!

Huge thank you to my family for your love and support. I am grateful to my parents, Keeli and Andy, for your unwavering encouragement to pursue my interests, invaluable assistance in accessing my education, and trust in my decisions. Thank you for fostering my curiosity, creativity, and appreciation for nature. Thank you as well to my brother, Drew, for your steady presence and assurance. I also want to acknowledge the generosity of the entire Jaeger family – thank you all for helping support our lives in Seattle and providing opportunities for much needed fun and celebration together.

Finally, I want to acknowledge my partner, Evan, for your steadfastness through it all. I am especially grateful for your humor, and for persuading us to adopt a cat, Fey – who knew a little void could provide so much joy and comfort? I know it hasn't been easy accommodating my late nights, months of field work, and financial limitations while also navigating your own challenges. Thank you for your constant support and encouragement despite these difficulties, helping to build my confidence and reminding me I am capable when I felt otherwise. Looking forward to continuing to brave the future together!

INTRODUCTION

Forest dynamics are shifting in response to global change (McDowell et al. 2020). In addition to direct effects on demographic processes, warming climate has indirect effects on forest ecosystems through natural disturbances (Seidl et al. 2017). These disturbances (i.e., discrete disruptive events that alter the state and trajectory of ecosystems; Pickett and White 1985) are important drivers of forest patterns and processes (Bowd et al. 2021). However, disturbance frequency, severity, and extent are changing in response to warming climate (Sommerfeld et al. 2018), threatening ecosystem services and creating uncertainty about future forest trajectories (Seidl et al. 2016). As climate continues to warm in the future (Lee et al. 2021), understanding the drivers and anticipating the effects of disturbances on forest ecosystems will be critical for adapting to climate change (Turner 2010).

Characterizing future disturbance dynamics is particularly important in forest ecosystems shaped by large infrequent disturbances (Turner and Dale 1998). These disturbances, such as the 1980 eruption of Mount St. Helens and the 1988 Yellowstone fires in western North America, can produce qualitatively different outcomes for ecosystems compared to smaller and more frequent disturbance events (Romme et al. 1998). Variability in the magnitude of large infrequent disturbances interacts with the pre-disturbance ecosystem state to produce complex spatial patterns of disturbance legacies (i.e., individuals, materials, and adaptations from the pre-disturbance system that persist following disturbance; Franklin et al. 2000). These legacies can influence post-disturbance structure and function and interactions with other disturbances for decades to centuries (Foster et al. 1998, Turner et al. 1998). However, despite their profound role in shaping landscape patterns and processes, the ecological effects of large infrequent disturbances are not well understood due to the rarity of these events and limited data on long-

term effects (Turner and Dale 1998). Therefore, when these disturbances do occur, it is crucial to characterize the immediate effects and post-disturbance recovery over time to inform future forest management (Dale et al. 1998).

Fire is a major disturbance agent and fundamental ecological process in forest ecosystems (Bowman et al. 2009, McLauchlan et al. 2020). However, changing climate has increased fire activity in forests across the world (Bowman et al. 2020). In western North America, warmer and drier conditions have promoted increases in area burned (Westerling 2016, Abatzoglou and Williams 2016), high severity burn area (Parks and Abatzoglou 2020, Parks et al. 2023), fire season length (Jolly et al. 2015), and number of large fires (Dennison et al. 2014). Fire activity is expected to continue to increase with future warming (Jones et al. 2022), highlighting uncertainties and challenges for understanding the implications of future fires on forest ecosystems.

One research priority for addressing these challenges is characterizing the drivers and effects of fires on forest structure and function (McLauchlan et al. 2020). Biological legacies, shaped by the pre-fire ecosystem state and fire severity, are major determinants of post-fire outcomes (Peters et al. 2011, Johnstone et al. 2016). Given the role of forests as the largest terrestrial carbon sink (Pan et al. 2011), live and dead post-fire biomass components are key legacies that support carbon cycling (Kashian et al. 2006) and feedbacks to future disturbances (Burton et al. 2020). Thus, characterizing these legacies immediately following fire can provide a baseline condition for monitoring change over time and supporting forest resilience to future fire (Seidl and Turner 2022).

A second priority for addressing key challenges in ecology is examining interactions and feedbacks among disturbances (McLauchlan et al. 2020). Disturbance interactions shape

ecosystem dynamics across scales with important consequences for forest structure and function (Buma 2015, Burton et al. 2020). Multiple fires can interact as linked disturbances (Simard et al. 2011) where one fire alters the occurrence or effects of a subsequent fire. Past fires can often act as temporary barriers to the spread and severity of subsequent fires by consuming fuels and altering vegetation structure and composition (Parks et al. 2014, 2015). When occurring at short intervals, disturbance interactions can also produce compound effects on structure and composition (Paine et al. 1998) that may cause abrupt shifts in forest dynamics (Turner et al. 2020), such as conversion of forest to non-forest or homogenization of landscape patterns (Prichard et al. 2017, Hoecker and Turner 2022, Harvey et al. 2023). Since increasing fire activity may promote the likelihood of reburns, characterizing how one fire interacts with subsequent fires is important for managing post-fire landscapes.

A third priority for addressing key challenges in ecology is understanding the long-term consequences of disturbances (McLauchlan et al. 2020). Forests are long-lived ecosystems and stand development after severe disturbances can take decades to centuries (Franklin et al. 2002, Seidl and Turner 2022). While initiating empirical studies shortly after disturbance can help fill knowledge gaps and provide important ecological and management insights (Lindenmayer et al. 2010), process-based ecosystem models allow for examination of responses over time and under novel conditions (Grimm et al. 2017, Turner and Carpenter 2017). Thus, combining empirical and simulation modeling approaches can be especially powerful for exploring the drivers and effects of changing climate and fire activity on forest ecosystems (Seidl 2017).

While fire dynamics are relatively well-studied in forests adapted to frequent fire (e.g., Hessburg et al. 2021), critical insights on large and severe fire effects are missing in forests shaped by infrequent fires. Wet forests at temperate latitudes in coastal margins worldwide (e.g.,

northwestern North America, southwestern South America, southeastern Australia) are characterized by fire regimes that include large stand-replacing fires occurring at intervals of several decades to centuries (McCarthy et al. 1999, Veblen et al. 2008, Reilly et al. 2021). Fire occurrence is limited primarily by fuel flammability, requiring prolonged periods of high heat and low moisture conditions to sufficiently dry fuels for fire ignition and spread (Bradstock 2010, Littell et al. 2018). When fires do occur, abundant fuel loads can facilitate high fire intensity and result in near-total tree mortality and conversion of forests from carbon sinks to carbon sources for several decades (Kashian et al. 2006). After fire, live fuels can recover rapidly in these high productivity systems, suggesting past fires may not reduce the likelihood or severity of subsequent fire (Buma et al. 2020). However, given the long intervals between these large severe fire events, there are inherently few opportunities to study the drivers and effects of fire in wet temperate forests, and examine post-fire recovery trajectories over longer time scales.

Using concepts and approaches from disturbance and fire ecology, forest ecology, and ecosystem modeling, this dissertation explores the immediate and mid- to longer-term consequences of large infrequent fires in wet temperate forests. Specifically, I focus on wet temperate forests west of the Cascade Range crest in Washington and northern Oregon, USA (hereafter 'northwestern Cascadia') as an archetype of systems shaped by stand-replacing fires at multi-century intervals (Agee 1993, Reilly et al. 2021). Conifer-dominated forests in northwestern Cascadia support exceptionally high levels of biomass (Waring and Franklin 1979) and are continually at the forefront of global forest, carbon, and climate change policy (Spies et al. 2018). Historical records suggest these forests have a tendency to reburn at short intervals following an initial fire (Gray and Franklin 1997, Reilly et al. 2022), though mechanisms are uncertain. Recent fires have burned nearly a quarter million hectares in the region (Reilly et al.

2022), creating an opportunity to build understanding of forest recovery after large infrequent fires in wet temperate forests.

In collaboration with local, state, tribal, and federal agencies, this dissertation uses empirical and simulation insights from these recent fires in northwestern Cascadia to address priorities for anticipating the effects of large infrequent fires on future forest dynamics. In Chapter 1, I characterize aboveground biomass in recently burned stands across the region to explore drivers of variability in initial post-fire carbon and fuel profiles. In Chapter 2, I use detailed fuels data from these field-measured stands and a mechanistic fire behavior model to address uncertainties about drivers of early post-fire reburn potential. In Chapter 3, I use landscape simulation modeling to extend empirical insights from Chapters 1 and 2 into the future, examining potential tradeoffs for managing post-fire forest trajectories under changing climate. Together, these chapters build fundamental understanding of the mechanisms behind disturbance-mediated change and feedbacks in systems shaped by long intervals between large, severe disturbances.

REFERENCES

Abatzoglou, J. T., and A. P. Williams. 2016. Impact of anthropogenic climate change on wildfire across western US forests. Proceedings of the National Academy of Sciences 113:11770–11775.

Agee, J. 1993. Fire ecology of Pacific Northwest forests. Island Press, Washington D.C.

Bowd, E. J., S. C. Banks, A. Bissett, T. W. May, and D. B. Lindenmayer. 2021. Direct and indirect disturbance impacts in forests. Ecology Letters 24:1225–1236.

Bowman, D. M. J. S., J. K. Balch, P. Artaxo, W. J. Bond, J. M. Carlson, M. A. Cochrane, C. M. D'Antonio, R. S. DeFries, J. C. Doyle, S. P. Harrison, F. H. Johnston, J. E. Keeley, M. A. Krawchuk, C. A. Kull, J. B. Marston, M. A. Moritz, I. C. Prentice, C. I. Roos, A. C. Scott, T. W. Swetnam, G. R. van der Werf, and S. J. Pyne. 2009. Fire in the Earth System. Science 324:481–484.

Bowman, D. M. J. S., C. A. Kolden, J. T. Abatzoglou, F. H. Johnston, G. R. van der Werf, and M. Flannigan. 2020. Vegetation fires in the Anthropocene. Nature Reviews Earth &

Environment 1:500–515.

Bradstock, R. A. 2010. A biogeographic model of fire regimes in Australia: current and future implications. Global Ecology and Biogeography 19:145–158.

Buma, B. 2015. Disturbance interactions: characterization, prediction, and the potential for cascading effects. Ecosphere 6:1–15.

Buma, B., S. Weiss, K. Hayes, and M. Lucash. 2020. Wildland fire reburning trends across the US West suggest only short-term negative feedback and differing climatic effects. Environmental Research Letters 15:034026.

Burton, P. J., A. Jentsch, and L. R. Walker. 2020. The Ecology of Disturbance Interactions. BioScience 70:854–870.

Dale, V. H., A. E. Lugo, J. A. MacMahon, and S. T. A. Pickett. 1998. Ecosystem Management in the Context of Large, Infrequent Disturbances. Ecosystems 1:546–557.

Dennison, P. E., S. C. Brewer, J. D. Arnold, and M. A. Moritz. 2014. Large wildfire trends in the western United States, 1984–2011. Geophysical Research Letters 41:2928–2933.

Foster, D. R., D. H. Knight, and J. F. Franklin. 1998. Landscape Patterns and Legacies Resulting from Large, Infrequent Forest Disturbances. Ecosystems 1:497–510.

Franklin, J. F., D. Lindenmayer, J. A. MacMahon, A. McKee, J. Magnuson, D. A. Perry, R. Waide, and D. Foster. 2000. Threads of continuity. Conservation in Practice 1:8–17.

Franklin, J. F., T. A. Spies, R. V. Pelt, A. B. Carey, D. A. Thornburgh, D. R. Berg, D. B. Lindenmayer, M. E. Harmon, W. S. Keeton, D. C. Shaw, K. Bible, and J. Chen. 2002. Disturbances and structural development of natural forest ecosystems with silvicultural implications, using Douglas-fir forests as an example. Forest Ecology and Management 155:399–423.

Gray, A. N., and J. F. Franklin. 1997. Effects of multiple fires on the structure of southwestern Washington forests. Northwest Science 71:174–185.

Grimm, V., D. Ayllón, and S. F. Railsback. 2017. Next-Generation Individual-Based Models Integrate Biodiversity and Ecosystems: Yes We Can, and Yes We Must. Ecosystems 20:229–236.

Harvey, B. J., M. S. Buonanduci, and M. G. Turner. 2023. Spatial interactions among short-interval fires reshape forest landscapes. Global Ecology and Biogeography:geb.13634.

Hessburg, P. F., S. J. Prichard, R. K. Hagmann, N. A. Povak, and F. K. Lake. 2021. Wildfire and climate change adaptation of western North American forests: a case for intentional management. Ecological Applications 31:e02432.

Hoecker, T. J., and M. G. Turner. 2022. A short-interval reburn catalyzes departures from historical structure and composition in a mesic mixed-conifer forest. Forest Ecology and Management 504:119814.

Johnstone, J. F., C. D. Allen, J. F. Franklin, L. E. Frelich, B. J. Harvey, P. E. Higuera, M. C. Mack, R. K. Meentemeyer, M. R. Metz, G. L. Perry, T. Schoennagel, and M. G. Turner. 2016. Changing disturbance regimes, ecological memory, and forest resilience. Frontiers in Ecology and the Environment 14:369–378.

Jolly, W. M., M. A. Cochrane, P. H. Freeborn, Z. A. Holden, T. J. Brown, G. J. Williamson, and

D. M. J. S. Bowman. 2015. Climate-induced variations in global wildfire danger from 1979 to 2013. Nature Communications 6:1–11.

Jones, M. W., J. T. Abatzoglou, S. Veraverbeke, N. Andela, G. Lasslop, M. Forkel, A. J. P. Smith, C. Burton, R. A. Betts, G. R. van der Werf, S. Sitch, J. G. Canadell, C. Santín, C. Kolden, S. H. Doerr, and C. Le Quéré. 2022. Global and Regional Trends and Drivers of Fire Under Climate Change. Reviews of Geophysics 60:e2020RG000726.

Kashian, D. M., W. H. Romme, D. B. Tinker, M. G. Turner, and M. G. Ryan. 2006. Carbon Storage on Landscapes with Stand-replacing Fires. BioScience 56:598–606.

Lee, J.-Y., J. Marotzke, G. Bala, L. Cao, S. Corti, J. P. Dunne, F. Engelbrecht, E. Fischer, J. C. Fyfe, C. Jones, A. Maycock, J. Mutemi, O. Ndiaye, S. Panickal, and T. Zhou. 2021. Future Global Climate: Scenario-Based Projections and Near-Term Information. Cambridge University Press, Cambridge, United Kingdom and New York, NY, USA.

Lindenmayer, D. B., G. E. Likens, and J. F. Franklin. 2010. Rapid responses to facilitate ecological discoveries from major disturbances. Frontiers in Ecology and the Environment 8:527–532.

Littell, J. S., D. McKenzie, H. Y. Wan, and S. A. Cushman. 2018. Climate Change and Future Wildfire in the Western United States: An Ecological Approach to Nonstationarity. Earth's Future 6:1097–1111.

McCarthy, M. A., A. Malcolm Gill, and D. B. Lindenmayer. 1999. Fire regimes in mountain ash forest: evidence from forest age structure, extinction models and wildlife habitat. Forest Ecology and Management 124:193–203.

McDowell, N. G., C. D. Allen, K. Anderson-Teixeira, B. H. Aukema, B. Bond-Lamberty, L. Chini, J. S. Clark, M. Dietze, C. Grossiord, A. Hanbury-Brown, G. C. Hurtt, R. B. Jackson, D. J. Johnson, L. Kueppers, J. W. Lichstein, K. Ogle, B. Poulter, T. A. M. Pugh, R. Seidl, M. G. Turner, M. Uriarte, A. P. Walker, and C. Xu. 2020. Pervasive shifts in forest dynamics in a changing world. Science 368:eaaz9463.

McLauchlan, K. K., P. E. Higuera, J. Miesel, B. M. Rogers, J. Schweitzer, J. K. Shuman, A. J. Tepley, J. M. Varner, T. T. Veblen, S. A. Adalsteinsson, J. K. Balch, P. Baker, E. Batllori, E. Bigio, P. Brando, M. Cattau, M. L. Chipman, J. Coen, R. Crandall, L. Daniels, N. Enright, W. S. Gross, B. J. Harvey, J. A. Hatten, S. Hermann, R. E. Hewitt, L. N. Kobziar, J. B. Landesmann, M. M. Loranty, S. Y. Maezumi, L. Mearns, M. Moritz, J. A. Myers, J. G. Pausas, A. F. A. Pellegrini, W. J. Platt, J. Roozeboom, H. Safford, F. Santos, R. M. Scheller, R. L. Sherriff, K. G. Smith, M. D. Smith, and A. C. Watts. 2020. Fire as a fundamental ecological process: Research advances and frontiers. Journal of Ecology 108:2047–2069.

Paine, R. T., M. J. Tegner, and E. A. Johnson. 1998. Compounded perturbations yield ecological surprises. Ecosystems 1:535–545.

Pan, Y., R. A. Birdsey, J. Fang, R. Houghton, P. E. Kauppi, W. A. Kurz, O. L. Phillips, A. Shvidenko, S. L. Lewis, J. G. Canadell, P. Ciais, R. B. Jackson, S. W. Pacala, A. D. McGuire, S. Piao, A. Rautiainen, S. Sitch, and D. Hayes. 2011. A Large and Persistent Carbon Sink in the World's Forests. Science 333:988–993.

Parks, S. A., and J. T. Abatzoglou. 2020. Warmer and drier fire seasons contribute to increases in area burned at high severity in western US forests from 1985-2017. Geophysical

Research Letters 47:e2020GL089858.

Parks, S. A., L. M. Holsinger, K. Blankenship, G. K. Dillon, S. A. Goeking, and R. Swaty. 2023. Contemporary wildfires are more severe compared to the historical reference period in western US dry conifer forests. Forest Ecology and Management 544:121232.

Parks, S. A., L. M. Holsinger, C. Miller, and C. R. Nelson. 2015. Wildland fire as a self-regulating mechanism: the role of previous burns and weather in limiting fire progression. Ecological Applications 25:1478–1492.

Parks, S. A., C. Miller, C. R. Nelson, and Z. A. Holden. 2014. Previous fires moderate burn severity of subsequent wildland fires in two large western US wilderness areas. Ecosystems 17:29–42.

Peters, D. P. C., A. E. Lugo, F. S. Chapin III, S. T. A. Pickett, M. Duniway, A. V. Rocha, F. J. Swanson, C. Laney, and J. Jones. 2011. Cross-system comparisons elucidate disturbance complexities and generalities. Ecosphere 2:art81.

Pickett, S. T. A., and P. S. White, editors. 1985. The Ecology of Natural Disturbance and Patch Dynamics. Academic Press, Inc, San Diego, California.

Prichard, S. J., C. S. Stevens-Rumann, and P. F. Hessburg. 2017. Tamm Review: Shifting global fire regimes: Lessons from reburns and research needs. Forest Ecology and Management 396:217–233.

Reilly, M. J., J. E. Halofsky, M. A. Krawchuk, D. C. Donato, P. F. Hessburg, J. D. Johnston, A. G. Merschel, M. E. Swanson, J. S. Halofsky, and T. A. Spies. 2021. Fire Ecology and Management in Pacific Northwest Forests. Pages 393–435 in C. H. Greenberg and B. Collins, editors. Fire Ecology and Management: Past, Present, and Future of US Forested Ecosystems. Springer International Publishing, Cham.

Reilly, M. J., A. Zuspan, J. S. Halofsky, C. Raymond, A. McEvoy, A. W. Dye, D. C. Donato, J. B. Kim, B. E. Potter, N. Walker, R. Davis, C. J. Dunn, D. M. Bell, M. J. Gregory, J. D. Johnston, B. J. Harvey, J. E. Halofsky, and B. K. Kerns. 2022. Cascadia Burning: the historic, but not historically unprecedented, 2020 wildfires in the Pacific Northwest, USA. Ecosphere 13:e4070.

Romme, W. H., E. H. Everham, L. E. Frelich, M. A. Moritz, and R. E. Sparks. 1998. Are Large, Infrequent Disturbances Qualitatively Different from Small, Frequent Disturbances? Ecosystems 1:524–534.

Seidl, R. 2017. To Model or not to Model, That is no Longer the Question for Ecologists. Ecosystems 20:222–228.

Seidl, R., T. A. Spies, D. L. Peterson, S. L. Stephens, and J. A. Hicke. 2016. Searching for resilience: addressing the impacts of changing disturbance regimes on forest ecosystem services. Journal of Applied Ecology 53:120–129.

Seidl, R., D. Thom, M. Kautz, D. Martin-Benito, M. Peltoniemi, G. Vacchiano, J. Wild, D. Ascoli, M. Petr, J. Honkaniemi, M. J. Lexer, V. Trotsiuk, P. Mairota, M. Svoboda, M. Fabrika, T. A. Nagel, and C. P. O. Reyer. 2017. Forest disturbances under climate change. Nature Climate Change 7:395–402.

Seidl, R., and M. G. Turner. 2022. Post-disturbance reorganization of forest ecosystems in a changing world. Proceedings of the National Academy of Sciences 119:e2202190119.

Simard, M., W. H. Romme, J. M. Griffin, and M. G. Turner. 2011. Do mountain pine beetle outbreaks change the probability of active crown fire in lodgepole pine forests? Ecological Monographs 81:3–24.

Sommerfeld, A., C. Senf, B. Buma, A. W. D'Amato, T. Després, I. Díaz-Hormazábal, S. Fraver, L. E. Frelich, Á. G. Gutiérrez, S. J. Hart, B. J. Harvey, H. S. He, T. Hlásny, A. Holz, T. Kitzberger, D. Kulakowski, D. Lindenmayer, A. S. Mori, J. Müller, J. Paritsis, G. L. W. Perry, S. L. Stephens, M. Svoboda, M. G. Turner, T. T. Veblen, and R. Seidl. 2018. Patterns and drivers of recent disturbances across the temperate forest biome. Nature Communications 9:4355.

Spies, T. A., P. A. Stine, R. Gravenmier, J. W. Long, and M. J. Reilly. 2018. Synthesis of science to inform land management within the Northwest Forest Plan area. Gen. Tech. Rep. PNW-GTR-966, U.S. Department of Agriculture, Forest Service, Pacific Northwest Research Station, Portland, OR.

Turner, M. G. 2010. Disturbance and landscape dynamics in a changing world. Ecology 91:2833–2849.

Turner, M. G., W. L. Baker, C. J. Peterson, and R. K. Peet. 1998. Factors Influencing Succession: Lessons from Large, Infrequent Natural Disturbances. Ecosystems 1:511–523.

Turner, M. G., W. J. Calder, G. S. Cumming, T. P. Hughes, A. Jentsch, S. L. LaDeau, T. M. Lenton, B. N. Shuman, M. R. Turetsky, Z. Ratajczak, J. W. Williams, A. P. Williams, and S. R. Carpenter. 2020. Climate change, ecosystems and abrupt change: science priorities. Philosophical Transactions of the Royal Society B: Biological Sciences 375:20190105.

Turner, M. G., and S. R. Carpenter. 2017. Ecosystem Modeling for the 21st Century. Ecosystems 20:211–214.

Turner, M. G., and V. H. Dale. 1998. Comparing Large, Infrequent Disturbances: What Have We Learned? Ecosystems 1:493–496.

Veblen, T. T., T. Kitzberger, E. Raffaele, M. Mermoz, M. E. González, J. S. Sibold, and A. Holz. 2008. The historical range of variability of fires in the Andean - Patagonian Nothofagus forest region. International Journal of Wildland Fire 17:724.

Waring, R. H., and J. F. Franklin. 1979. Evergreen coniferous forests of the Pacific Northwest. Science 204:1380–1386.

Westerling, A. L. 2016. Increasing western US forest wildfire activity: sensitivity to changes in the timing of spring. Philosophical Transactions of the Royal Society B: Biological Sciences 371:1–10.

Chapter 1. STRUCTURAL LEGACIES DRIVE VARIABILITY IN POST-FIRE ABOVEGROUND CARBON AND FUEL PROFILES IN WET TEMPERATE FORESTS

1.1 ABSTRACT

Disturbance legacies shape ecosystem functioning and feedbacks to future disturbances, yet how legacies are driven by pre-disturbance state and disturbance magnitude is poorly understood – especially in ecosystems influenced by infrequent and severe disturbances. Focusing on wet temperate forests as an archetype of these ecosystems, we characterized live and dead aboveground biomass 2–5 years post-fire in western Washington and northwestern Oregon, USA to ask: How do pre-fire stand age (i.e., pre-disturbance ecosystem state) and burn severity (i.e., disturbance magnitude) drive variability in initial post-fire (1) aboveground biomass carbon and (2) fuel profiles? Dominant drivers of post-fire legacies and potential disturbance feedbacks varied widely by response variable, with pre-disturbance ecosystem state driving total legacy amounts and disturbance magnitude moderating legacy condition. Total post-fire carbon was ~3–4 times greater in mid- and late-seral stands compared to young stands. In unburned and low-severity fire stands, >70% of post-fire total carbon was live, and canopy fuel profiles were largely indistinguishable between the two fire severity classes, suggesting greater continuity of structure and function pre- and post-fire. Conversely, in high-severity stands, >95% of post-fire total carbon was dead and very little canopy fuel remained. Regardless of burn severity, most biomass present pre-fire persisted following fire, suggesting high-carbon pre-fire stands lead to high-carbon post-fire stands (and vice versa). Persistence of legacy biomass in high-severity stands, even as it decays, will therefore buffer total ecosystem carbon storage as live tree carbon

recovers over time. Further, all burned stands had considerable production of black carbon in charred wood biomass which can support ecosystem functioning and promote long-term carbon storage. Initial post-fire fuel loads are sufficient to support fire in all stands but reburn potential may be greater in high-severity stands due to rapid regeneration of flammable live surface vegetation and more exposed microclimatic conditions. Fuel reduction benefits from fire on subsequent fire occurrence in high-productivity systems therefore appear short-lived. Our findings demonstrate the importance of pre-disturbance ecosystem state in dictating many aspects of initial post-disturbance structure and function, with important implications for managing post-fire recovery trajectories in some of Earth's most productive and highest biomass forests.

1.2 INTRODUCTION

As climate warms and disturbance activity increases (Seidl et al. 2017), understanding drivers of post-disturbance outcomes is essential for forecasting ecosystem futures. Disturbance legacies (i.e., individuals, materials, and adaptations from the pre-disturbance system that persist following disturbance; Franklin et al. 2000) are major determinants of post-disturbance outcomes that can shape ecosystem trajectories for decades to centuries (Seidl and Turner 2022). Two key drivers of disturbance legacies include the pre-disturbance ecosystem state and disturbance magnitude (i.e., degree of effect on ecosystem properties; Pickett and White 1985) (Johnstone et al. 2016, Peters et al. 2011). The pre-disturbance ecosystem state sets the template of structural and compositional material available to persist as legacies. Intervals between disturbances typically dictate the range in biotic structure, composition, and complexity of the pre-disturbance state. Disturbance magnitude then interacts with the ecosystem state to influence the amount, composition, and arrangement of available material that either is removed or persists as legacies.

For example, greater burn severity (i.e., amount of vegetation killed by fire; Keeley 2009) results in greater total loss and conversion from live to dead biomass (Meigs et al. 2011). While individual drivers of post-disturbance legacies have received attention, the relative and combined importance of multiple drivers are less well understood.

Disturbance legacies can strongly shape post-disturbance ecosystem functioning and feedbacks to future disturbances, and are of particular importance in ecosystems influenced by infrequent severe disturbances. For example, stand-replacing fire can shift ecosystems from carbon sinks to sources via mortality and subsequent decomposition of biomass (Kashian et al. 2006). However, live biomass can recover carbon quickly in high-productivity systems and legacy carbon can persist for centuries in large dead and charred material (Hudiburg et al. 2023). Disturbance legacies can also alter the likelihood, extent, or magnitude of a future disturbance via feedbacks (i.e., linked interactions; Simard et al. 2011). For example, fires can temporarily reduce the probability, spread, and severity of subsequent fires due to fuel consumption and changes in vegetation composition, though the strength of these effects diminishes over time as fuels recover (Buma et al. 2020). In highly productive ecosystems, rapid accumulation of fuels after fire may promote the likelihood of short-interval reburns (Gray and Franklin 1997, Reilly et al. 2022) with implications for structure (e.g., Hoecker and Turner 2022a) and rates of recovery (e.g., Braziunas et al. 2023). Given the critical post-disturbance reorganization window (Seidl and Turner 2022), characterizing the structure and function of legacies soon after disturbances is important for ecological forecasting and understanding management options (Lindenmayer et al. 2010). Yet, there are inherently few opportunities to study post-disturbance outcomes in ecosystems with long disturbance-free intervals.

We tested the relative influence of pre-disturbance state and disturbance magnitude on key

disturbance legacies in forests influenced by long-interval stand-replacing fires. We focused on wet temperate forests of the Pacific Northwest, USA – an archetype of infrequent stand-replacing fire regimes shared by other forests at temperate latitudes in coastal margins worldwide (e.g., southwestern South America, southeastern Australia). Forests west of the Cascade Range crest in Washington and northern Oregon (hereafter 'northwestern Cascadia') are shaped by a fire regime that includes stand-replacing fires with multi-century return intervals and extensive area burned (>50%) at high severity (Agee 1993). Among the range of intermediate fires that can occur between these long-interval events, historical records suggest a strong tendency of these forests to reburn in the initial decades following a stand-replacing fire (i.e., fire begets fire; Gray and Franklin 1997, Reilly et al. 2022), though mechanisms are not well understood. These forests are among the most productive and carbon dense in the world, representing a vital carbon sink and economic resource (Case et al. 2021). Accordingly, the region is continually at the forefront of global forest and climate change policy and displays a wide variety of past disturbance and management legacies (Spies et al. 2018). Recent fires have burned more than 200,000 ha across the region (Reilly et al. 2022), creating an opportunity to examine post-fire structure, function, and implications for future disturbances and management. Using field data from five recent fires in northwestern Cascadia, we asked: how do pre-fire stand age and burn severity drive variability in initial post-fire (1) aboveground biomass carbon and (2) fuel profiles?

1.3 METHODS

1.3.1 *Study area*

Northwestern Cascadia comprises 6.1 Mha of wet temperate forests. Current structural conditions, which bear the legacy of more than a century of timber harvest activity, are

dominated by dense young plantations and mid-seral forests among unharvested old growth stands (Donato et al. 2020, Spies et al. 2018). Forests are dominated by obligate-seeding gymnosperm species, with composition varying by elevation. At lower elevations (<1,000 m), Douglas-fir (*Pseudotsuga menziesii*), western hemlock (*Tsuga heterophylla*), and western redcedar (*Thuja plicata*) are dominant, with noble fir (*Abies procera*) and Pacific silver fir (*Abies amabilis*) prevalent at relatively cooler and wetter middle elevations (1,000–1,600 m). Angiosperm tree species are less common, but can resprout and exist at high densities in mesic and recently-disturbed areas (Franklin and Dyrness 1973). Understory composition is dominated by abundant cover of shrub, fern, and forb species (Spies 1991). Climate is Mediterranean with mild seasonal temperatures, wet winters, and dry summers (Franklin and Dyrness 1973). Across our sampled area, 30-year normals (1991–2020) of annual mean temperature and total precipitation range from 4.0–10.7°C and 1,435–3,273 mm, with 76% of precipitation occurring November through April (PRISM Climate Group 2024). Soils are primarily loamy, well-drained Inceptisols derived from pyroclastic and igneous parent materials (Franklin and Dyrness 1973).

The long interval (200–600 years) stand-replacing fire regime of northwestern Cascadia is limited primarily by climatic controls on region-scale weather events and fuel moisture (Agee 1993). More frequent fires may occur in the interim periods, commonly associated with the use of fire as a management tool by Indigenous peoples (Boyd 1999, Johnston et al. 2023). Most large and severe fires occur toward the end of summer following prolonged periods of high temperature and low humidity that allow for sufficient drying of fine fuels to ignite and carry fire (Reilly et al. 2021). Such fires typically produce large patches (>10,000 ha) of area burned at high severity (Agee 1998, Reilly et al. 2022) due to intense burning conditions and lack of fire resistant traits for most tree species (Minore 1979, Stevens et al. 2020), but also tend to include

substantial portions burned at lower severity arising from periods of mild fire weather (Reilly et al. 2022). The largest fires (>50,000 ha) are driven by extreme weather events such as synoptic dry east winds that drive rapid fire spread (Reilly et al. 2021).

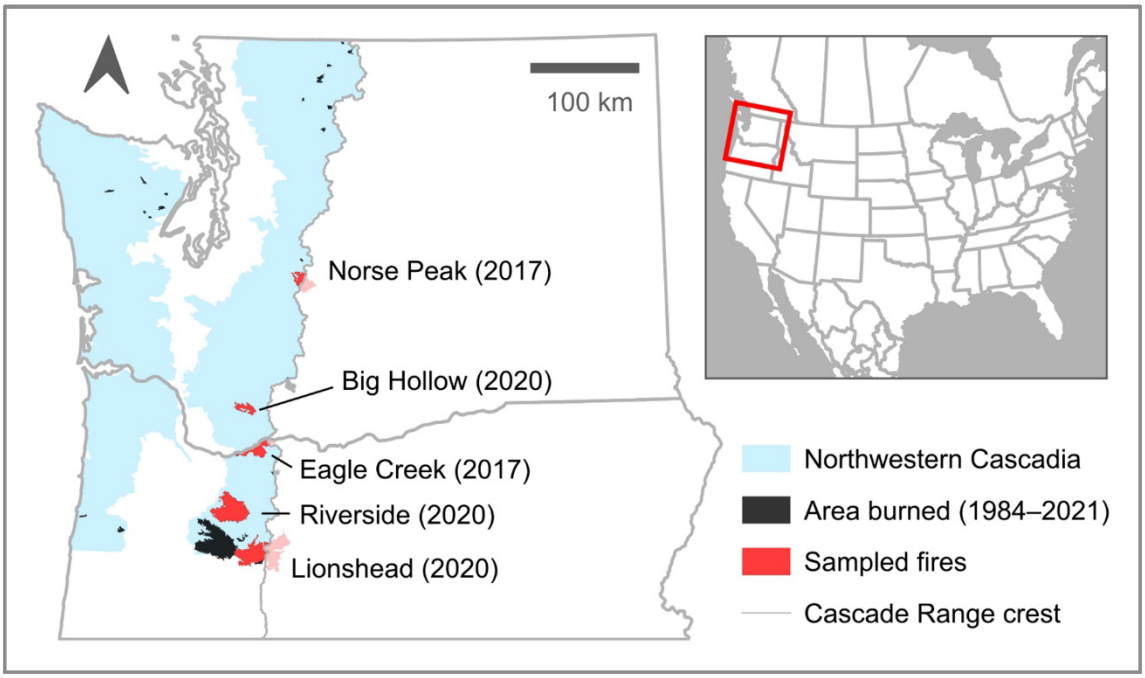

Fire	Fire year	Fire size (ha)	Location	Sampling time since fire (yr)	Plots (*n*)
Big Hollow	2020	9,811	Gifford Pinchot National Forest	2	26
Eagle Creek	2017	17,666	Columbia River Gorge National Scenic Area & Mount Hood National Forest	4–5	3
Lionshead	2020	42,220	Willamette National Forest	3	4
Norse Peak	2017	8,922	Mount Baker-Snoqualmie National Forest	2–4	55
Riverside	2020	55,920	Mount Hood National Forest	2–3	7

Figure 1.1. Study area. *Top*: Sampled fire perimeters (red) and recent area burned (1984–2021; black) within northwestern Cascadia, USA (blue). *Bottom*: Location, timing, and number of plots ($N = 95$) across sampled fires. Fire size only includes area burned on the west side of the Cascade Range crest (source: Monitoring Trends in Burn Severity, https://www.mtbs.gov/).

1.3.2 *Sampling design*

We established 1-ha long-term monitoring plots ($N = 95$) in forest stands within five recent (2017–2020) fires across northwestern Cascadia (Figure 1.1). Plots were established 2–5 years post-fire and systematically stratified by field-determined pre-fire stand age and burn severity (Figure 1.2; Appendix A). We defined pre-fire stand age (i.e., age prior to the recent focal fires in our study) by developmental stage as a function of structural and compositional attributes (Van Pelt 2007), and classified as young, mid-seral, or late-seral (Appendix A: Table 1.1). In general, young stands (~30–50 years) established after clearcut harvest in the late 1900s and had high densities of small-diameter shade-intolerant conifer trees starting to develop overlapping canopies. Mid-seral stands (~70–150 years) originated from fire or clearcut harvest after Euro-American settlement and were dominated by scant understory and near-total canopy cover of rapidly growing trees. Late-seral stands (~160–500+ years) originated from fire generally prior to Euro-American settlement and were characterized by spatial heterogeneity in live and dead vegetation structures including multilayered tree canopies, abundant tree regeneration and down wood, and large diameter trees (Franklin et al. 2002). We classified burn severity by percent of fire-killed basal area as unburned (0%), low (<30%), or high (≥90%). We could not locate any young stands that burned at low severity, thus this condition is not represented in this analysis.

Figure 1.2. Representative photos taken two years post-fire within sampled stands illustrating the range in initial fire effects across pre-fire stand age × burn severity classes. Note differences in the abundance, size, and arrangement of live and dead biomass between strata. Young stands burned at low severity were not represented due to rare occurrence across the study area.

1.3.3 *Field data collection*

We characterized post-fire aboveground biomass in each 1-ha plot using standard methods (Appendix A). Live and dead trees were measured in four variable-radius subplots according to size class based on diameter at breast height (dbh, 1.37 m): trees (dbh ≥ 10 cm); saplings (height ≥ 0.3 m, dbh < 10 cm). Large trees (dbh ≥ 100 cm) were measured across the entire plot. Live tree seedlings (height < 0.3 m), woody shrubs, and herbaceous vegetation were measured in 12 fixed-radius subplots. Down woody debris (height < 2 m) and forest floor fuel (litter, duff) were measured along planar intercept transects (Brown 1974, Lutes et al. 2006). In young stands, subplot radii and transect lengths for measures of trees and down woody debris were reduced by approximately half to reflect the generally smaller-stature, higher-frequency vegetation. Post-fire stand structure is summarized in Appendix A: Table 1.4.

1.3.4 *Biomass and fuels calculations*

We derived aboveground biomass carbon, surface, and canopy fuel loads for each plot using component-, species-, and region-specific allometric equations (Appendix A). Aboveground biomass carbon (i.e., carbon stored in plant matter) included wood, bark, branch, and foliage biomass for all measured vegetation. We also quantified carbon in charred stem wood (i.e., black carbon; Bird et al. 2015) on standing trees and coarse woody debris. Surface fuels included down woody debris, live seedlings and small saplings (height < 1.37 m), and live understory vegetation (woody shrubs, herbaceous vegetation). Canopy fuels included foliage and branch biomass, available canopy fuel load, canopy bulk density, and canopy base height for live and dead standing trees and large saplings (height ≥ 1.37 m). All measures were scaled to per-ha values.

1.3.5 *Statistical analysis*

We compared mean aboveground biomass carbon and fuel loads across strata using generalized linear models. Model structure was consistent for all response variables, predicting each non-negative continuous response as a function of categorical pre-fire stand age and burn severity. Responses were modeled by a gamma distribution with log link function and included an intercept-only zero-inflation parameter to account for sampling zeros. To compare the relative strength of pre-fire stand age and burn severity in driving post-fire outcomes, we computed pairwise differences in predicted means (i.e., marginal comparisons) for each response across all levels of pre-fire stand age and burn severity. Mean effect size for each predictor was obtained by taking the average of the absolute differences across levels. Analyses and visualizations were performed in R 4.4.0 (see Appendix A for packages; R Core Team 2024).

1.4 RESULTS

1.4.1 *Post-fire aboveground biomass carbon*

Most aboveground biomass carbon (hereafter 'carbon') persisted through fire. On average, burned stands had at least 67% of the total carbon in unburned stands, the majority of which (>95%) was in woody biomass (Appendix B: Table 1.9). Pre-fire stand age was the dominant driver of total carbon, with 2–3x the effect of burn severity on the major carbon components, including all standing trees and down woody debris (Figure 1.3). In general, post-fire carbon increased with pre-fire stand age (Figure 1.4). Compared to young stands, mid- and late-seral stands had 223% and 299% more post-fire total carbon, respectively (Appendix B: Table 1.11, Table 1.16). Burn severity drove conversion from live to dead carbon but did not override the effect of pre-fire stand age on post-fire total carbon (Figure 1.3). Compared to unburned stands,

post-fire live carbon was similar in low-severity stands but 99% less in high-severity stands. Both low- and high-severity stands had 49% and 321% more post-fire dead carbon, including 0.3 Mg C ha^{-1} more charred wood, respectively (Figure 1.4; Appendix B: Table 1.11, Table 1.16).

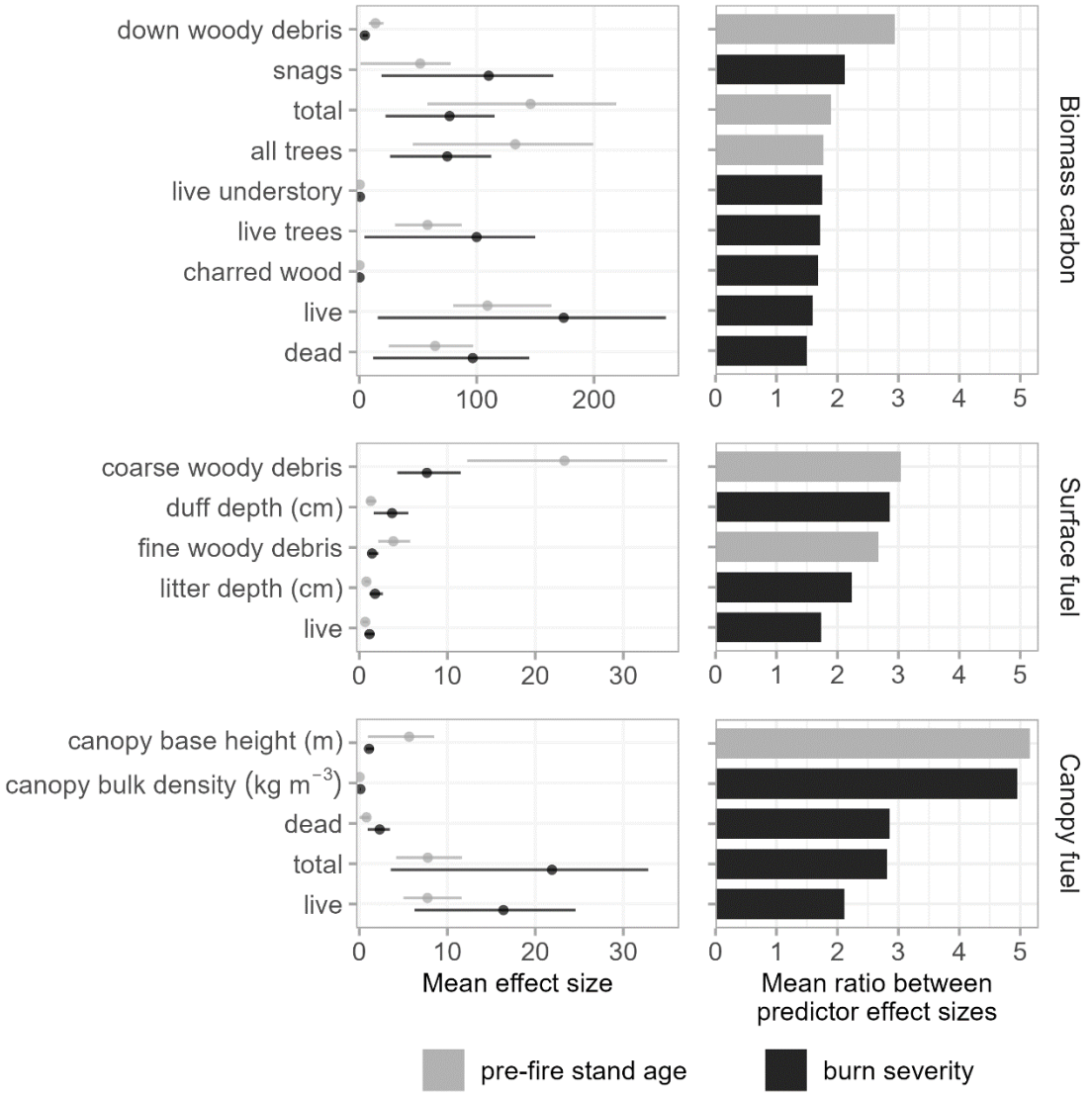

Figure 1.3. Relative effects of pre-fire stand age (gray) and burn severity (black) on initial post-fire aboveground biomass carbon and fuel profiles. *Left*: Marginal comparisons in mean effect sizes. Points and lines are the mean and range (min–max) of absolute differences in predicted means for pairwise comparisons across all predictor levels, on the response scale (Mg ha^{-1}, unless otherwise indicated). Wider ranges indicate larger differences in a single predictor level compared to the other levels. *Right*: Ratio in mean effect sizes relative to the dominant predictor. See Appendix B for marginal comparison summaries and additional response variables.

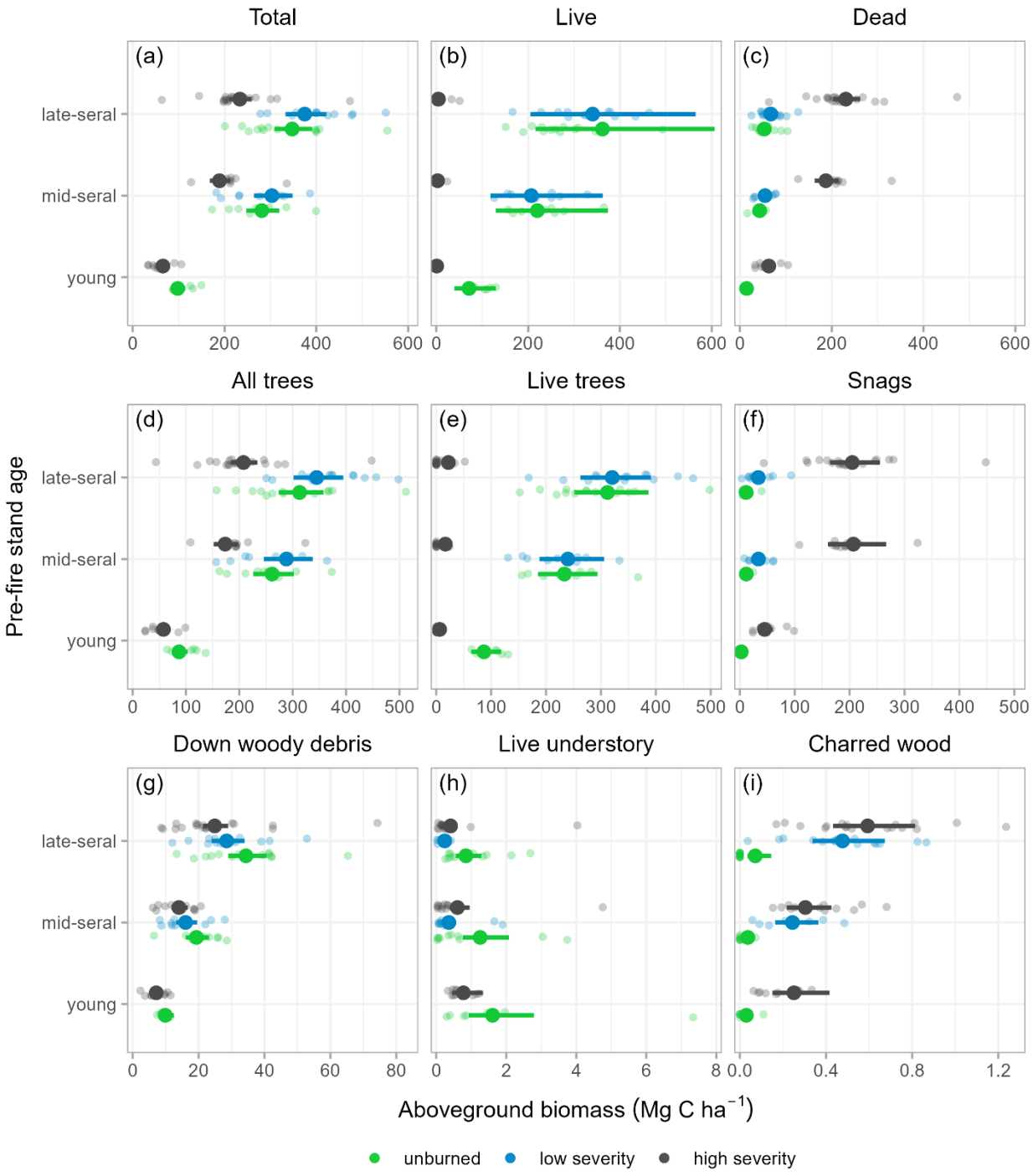

Figure 1.4. Initial post-fire aboveground biomass carbon. Bold points and lines are model-predicted means and 95% confidence intervals for each stand age class, colored by burn severity. Translucent points show plot-level values. See Appendix B for model summaries.

1.4.2 *Post-fire fuel profiles*

Pre-fire stand age was the dominant driver of post-fire surface fuel profiles, with 3x the effect of burn severity on the major surface fuel components, including coarse and fine woody debris (Figure 1.3). In general, post-fire dead surface fuels increased—and live surface fuels decreased—with pre-fire stand age (Figure 1.5). Compared to young stands, mid- and late-seral stands had 197% and 554% more coarse and 37% and 59% more fine woody debris post-fire, respectively (Appendix B: Table 1.12, Table 1.16). However, burn severity was the dominant driver of post-fire fuel depths and live surface fuels, with 2–3x the effect of pre-fire stand age on duff, litter, and live vegetation (Figure 1.3), though these components comprise a minor portion of the post-fire total surface fuel load (Figure 1.5). This effect was unique to each burn severity class; fuel depths and live surface fuels were distinct for unburned, low-, and high-severity stands. In general, post-fire surface fuels decreased with burn severity (Figure 1.5). Compared to unburned stands, low- and high-severity stands had 57% and 89% less duff, 33% and 67% less litter, and 79% and 50% less live surface fuel post-fire, respectively (Appendix B: Table 1.12, Table 1.16).

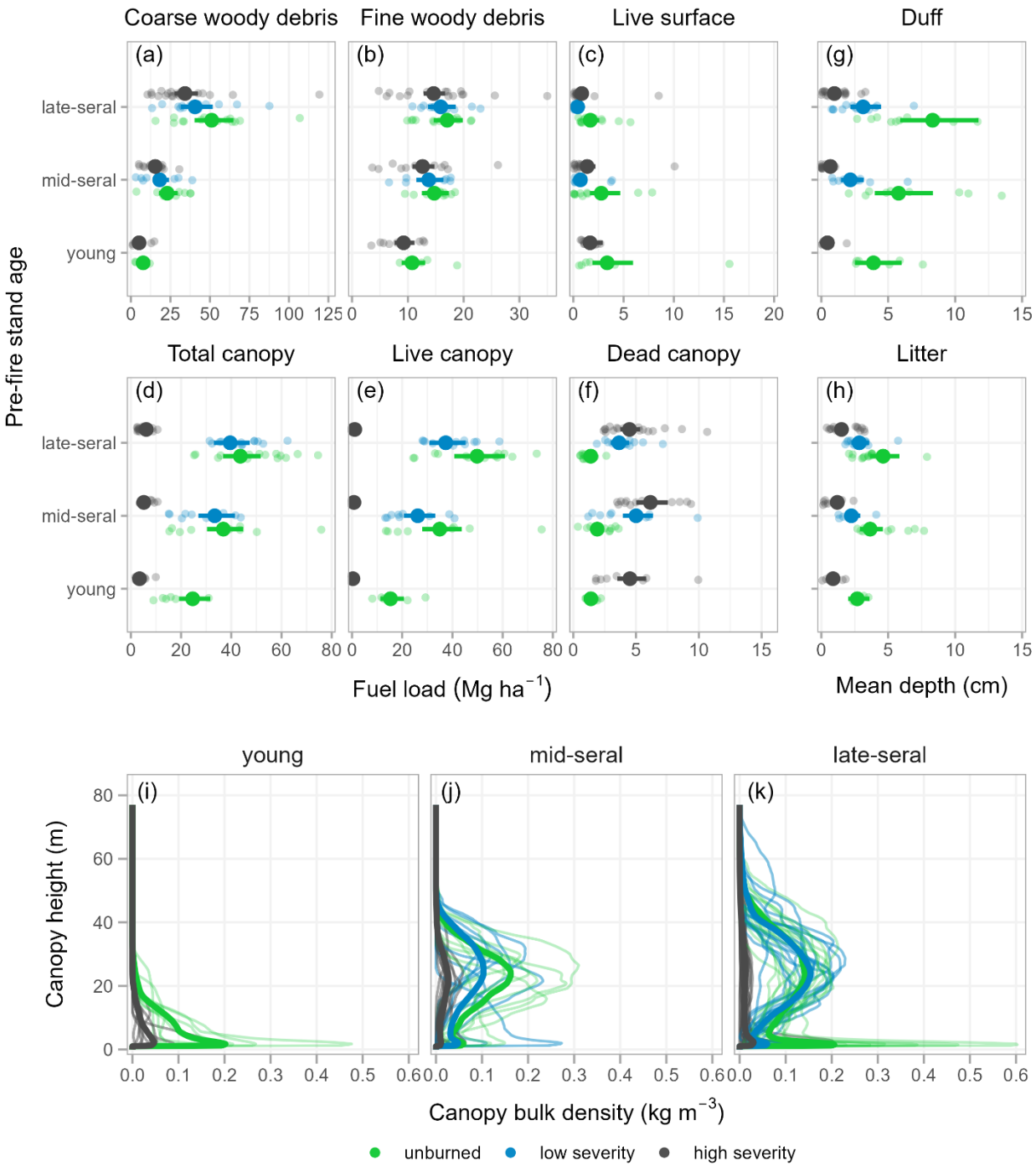

Figure 1.5. Initial post-fire surface (a–c), available canopy (d–f), forest floor (g–h), and vertical (i–k) fuel profiles. Bold points and lines are model-predicted means and 95% confidence intervals (a–h) or simple means (i–k) for each stand age class, colored by burn severity. Translucent points (a–h) and lines (i–k) show plot-level values. See Appendix B for model summaries.

Burn severity was the dominant driver of post-fire canopy fuel profiles, with 2–5x the effect of pre-fire stand age on available canopy fuels and canopy bulk density (Figure 1.3). This burn severity effect was driven primarily by high-severity stands; post-fire canopy fuel profiles were largely indistinguishable between unburned and low-severity stands. In general, post-fire total and live fuels decreased—and dead fuels increased—with burn severity (Figure 1.5). Compared to unburned and low-severity stands, high-severity stands had 86% less post-fire total available canopy fuel, and 82% and 75% less canopy bulk density, respectively. Both low- and high-severity stands had 11% and 98% less live and 163% and 213% more dead post-fire available canopy fuel than unburned stands, respectively (Appendix B: Table 1.13, Table 1.16). However, pre-fire stand age had 5x the effect of burn severity on post-fire canopy base height (Figure 1.3), driven primarily by mid-seral stands. In general, post-fire canopy fuels increased with pre-fire stand age (Figure 1.5). Compared to young stands, mid- and late-seral stands had 86% and 117% more post-fire total available canopy fuel, respectively. Mid-seral stands also had 669% taller post-fire canopy base height than young stands (Appendix B: Table 1.13, Table 1.16).

1.5 DISCUSSION

By testing how multiple drivers affect aboveground post-fire legacies of biomass carbon and fuel profiles, our study demonstrates the importance of pre-disturbance ecosystem state in dictating many aspects of initial post-disturbance structure and function. This work builds understanding of the mechanisms behind disturbance-mediated change and feedbacks in systems shaped by long intervals between severe disturbances, with notable implications for managing post-fire recovery trajectories in some of Earth's most productive and highest biomass forests.

1.5.1 *Pre-fire stand age drives variability in total post-fire legacies*

Pre-fire stand age was the dominant driver of initial patterns in total disturbance legacies after fire. Within each severity class, stands that were older at the time of fire had greater post-fire total aboveground biomass carbon, total tree mass, and down woody debris than younger stands, corresponding to trends in biomass with succession in wet temperate forests in northwestern Cascadia (Agee and Huff 1987, Gray et al. 2016, Spies et al. 1988) and globally (Burrascano et al. 2013, Pregitzer and Euskirchen 2004). Most biomass present pre-fire persisted post-fire, supporting regional trends (Campbell et al. 2007, Donato et al. 2013, Fahnestock and Agee 1983) and suggesting that high-carbon pre-fire stands lead to high-carbon post-fire stands (and vice versa), regardless of burn severity. Woody biomass, particularly within larger trees, accounted for most of the remaining carbon, reflecting expected patterns of combustion (Agee 1993).

These findings suggest that, when burned, late-seral stands may have a greater potential than younger stands to support several ecosystem functions, due to greater abundance and complexity (e.g., greater range of component sizes) of disturbance legacies. Retention of structural legacies, especially woody biomass, is important for supporting critical post-disturbance functions (e.g., nutrient cycling, wildlife habitat, microsite diversity), particularly following stand-replacing disturbances (Franklin et al. 2002). Persistence of legacy biomass on site, even as it decays following high-severity fire, will buffer total ecosystem carbon storage as live carbon recovers over time. Accordingly, alterations to stand age and pre-disturbance structural legacies will have lasting effects on post-fire outcomes and recovery potential (Seidl et al. 2014), underscoring the importance of considering stand ages present on a landscape when managing for desired post-disturbance outcomes.

1.5.2 *Burn severity moderates the condition of post-fire legacies*

Burn severity moderated the condition of disturbance legacies, driving initial patterns in live and dead aboveground biomass carbon and canopy fuel profiles after fire. In stands burned at high severity, >95% of the total post-fire aboveground biomass carbon was in dead material, and very little (<15% of unburned) canopy fuel remained. Given these stands experienced predominantly crown fire which consumes the majority of available fuels (Agee 1993), and are composed of several tree species with few adaptations to resist fire (Minore 1979, Stevens et al. 2020), these outcomes are in line with expectations from similar systems (Kauffman et al. 2019). By contrast, in unburned and low-severity stands, >70% of total post-fire aboveground biomass carbon was stored in live material and canopy fuel loads were similar. This is likely due to low-severity stands experiencing predominantly surface fire behavior which, compared to crown fire, has less influence on vegetation structure and does little to alter available canopy fuels in these systems (Bassett et al. 2017). Regardless of severity, fire produced a considerable amount of black carbon in charred wood – both low- and high-severity stands had a quarter to more than half a metric ton of charred wood biomass carbon per hectare. This mechanism of long-term carbon storage produced values comparable to other systems that have observed similar amounts of black carbon generated from a range of burn severities (Campbell et al. 2007, Volkova et al. 2022).

These findings have different implications following low- and high-severity fire, both of which can play significant roles in forest dynamics of wet temperate systems with long intervals between stand-replacing fires. Retention of mostly live legacies and similarity to unburned stands suggests greater continuity of structure and function pre- and post-fire in low-severity stands compared to high-severity stands. Low-severity stands may also help facilitate recovery of more severely burned areas by providing a live seed source for dispersal into nearby high-

severity patches (Donato et al. 2009, Laughlin et al. 2023). In contrast, retention of mostly dead legacies and rapid growth of non-tree vegetation suggests protracted regeneration timelines and a wider range of potential stand development pathways in high-severity stands compared to low-severity stands (Tepley et al. 2013). Accordingly, high-severity stands can facilitate the development of structurally complex early-seral ecosystems, promoting increased biodiversity and unique ecosystem functions (Swanson et al. 2011), and restoration of the most contemporarily underrepresented landscape condition (Donato et al. 2020).

1.5.3 *Implications for future forest dynamics and management*

Initial patterns of post-fire disturbance legacies have implications for carbon trajectories, reburn potential, and climate-adaptive management. While pre-fire stand age was the dominant driver of initial post-fire total carbon dynamics in these stands, burn severity will define longer-term carbon trajectories. Long-term post-fire carbon trajectories are a function of the balance between carbon lost through biomass consumption and decomposition of fire-killed vegetation, and carbon gained through vegetation regrowth (Pugh et al. 2019), influenced by the distribution of stand structures and ages across the burned landscape (Kashian et al. 2006). Total aboveground biomass carbon remained high in burned stands, though most initial post-fire carbon was stored in live biomass for low-severity stands and dead biomass for high-severity stands. Post-fire carbon trajectories in low-severity stands are likely to be similar to unburned stands and follow expected trends with later successional stages (Janisch and Harmon 2002). High-severity stands are likely to remain carbon sources for several decades post-fire until net primary production exceeds decomposition losses (Law et al. 2004), though dead wood can be an effective long-term carbon store, taking several decades to centuries to fully decompose (Harmon et al. 1986). Black carbon within charred wood biomass is a particularly persistent form of dead carbon that is

resistant to decay (Bird et al. 2015). Our findings suggest that fire, regardless of severity, can promote long-term carbon storage in wet temperate forests via char formation, though many unknowns have yet to be addressed about the role of black carbon (Santín et al. 2016). Further, regional projections of future fire activity generally forecast increased number of fires, area burned by large fires, shorter fire return intervals, and longer fire seasons (Dye et al. 2024). Increased fire frequency may substantially reduce total carbon through conversion of older stands to younger stands (Harmon et al. 1990, Seidl et al. 2014) and less persistent large woody legacies due to more frequent combustion (Donato et al. 2016, Raymond and McKenzie 2012).

Fire occurrence in high-productivity wet temperate forests may increase the risk of reburning in a subsequent fire due to initial fire effects on post-fire disturbance legacies, meaning major fires may effectively occur in episodes of burn-reburn sequences (Agee 1993, Gray and Franklin 1997). Reburn potential appears greater in stands burned at high severity due to rapid regeneration of more flammable live surface vegetation within the first several years post-fire (Landesmann et al. 2021, Thompson et al. 2007) as well as reduced cover and likely microclimatic shifts towards warmer and drier conditions (Chen et al. 1993, though see Cawson et al. 2017). Yet, despite possible differences in reburn potential as a function of burn severity, initial post-fire fuel loads may be sufficient to support fire in all stands. For example, reburn potential may be similar between low-severity and unburned stands because canopy fuels are largely unchanged, and reductions in surface fuels are incremental. In combination with the high ecosystem productivity in the study area, our results suggest fuel reduction benefits from fire are a short-lived limitation on subsequent fire occurrence, though additional research is needed to disentangle the relative importance of structural versus weather drivers of reburn potential in this system.

1.6 APPENDIX A: SUPPLEMENTAL METHODS

A.1 *Field data collection*

A.1.1 Plot establishment and stratification

We established plots on public lands managed by the U.S. Forest Service. Plot centers were located at least 100 m from roads and trails. We excluded confounding features from the plot area (e.g., decommissioned roads, streams, riparian zones, and rock outcroppings). Within a sampled fire, plot centers were located at least 100 m apart for stands of different strata, and at least 400 m apart for stands of the same strata.

We stratified our plots by field-determined pre-fire stand age, burn severity, and forest zone. For pre-fire stand age, we characterized the structural development stage of each stand based on the size, abundance, crown and bark characteristics, and spatial arrangement of the major tree species. We then assigned a categorical age class to each development stage (Table 1.1). For burn severity, we assessed the amount of basal area killed by fire and categorized stands as unburned (no evidence of fire), low (<30% mortality), or high severity (i.e., stand replacing, ≥90% mortality). In low-severity stands, evidence of fire was present across at least 50% of the plot area, though the spatial pattern of burned area was rarely uniform. Due to greater accessibility and similarity with burned stands, we established some unburned stands outside sampled fire perimeters. For forest zone, we used regional keys to classify stands according to Franklin and Dyrness (1973) based on the percent cover of shade-tolerant species (Table 1.2).

Table 1.1. Classification of pre-fire stand age based on development stages via Van Pelt (2007).

Pre-fire stand age class	Stand development stage(s)
Young	Canopy closure
Mid-seral	Biomass accumulation / stem exclusion
	Maturation I
Late-seral	Maturation II
	Vertical diversification
	Horizontal diversification

Note: Stand development stages follow the successional sequence described by Franklin et al. (2002) and are generally based on the size, abundance, bark condition, crown characteristics (e.g., lower branch pruning, presence of epicormic branches), and vertical and horizontal spatial arrangement of the major shade-intolerant (e.g., Douglas-fir, noble fir) and shade-tolerant (e.g., western hemlock, Pacific silver fir) tree species with each 1-ha stand.

Table 1.2. Regional key used for determining forest zones (sensu Franklin and Dyrness 1973) based on cover of shade-tolerant species, modified from Van Pelt (2007) and Topik and others (1986).

1a	Douglas-fir ≥ 10% shade-tolerant cover	. . . . . do not sample
1b	Not as above	 2
2a	Subalpine fir ≥ 10% shade-tolerant cover	. . . . . do not sample
2b	Not as above	 3
3a	Mountain hemlock ≥ 10% shade-tolerant cover	. . . . . *Tsuga mertensiana* Zone
3b	Not as above	 4
4a	Pacific silver fir ≥ 10% shade-tolerant cover	. . . . . *Abies amabilis* Zone
4b	Not as above	 5
5a	Western hemlock ≥ 10% shade-tolerant cover	. . . . . *Tsuga heterophylla* Zone
5b	Not as above	. . . . . re-check above or do not sample

Notes: If sampling at Norse Peak, replace 10% with 20% for couplets 2–5. If sampling in Oregon, replace 10% with 2% for couplets 2–5.

A.1.2 Plot layout and field measurements

See Figure 1.6 for a general diagram of the plot layout, and Table 1.3 for a summary of field measurements. Total area sampled differed by pre-fire stand age, with lengths of cardinal transects, tree subplot radii, and down woody debris transects in young stands reduced by approximately half to account for scaling dynamics and improve sampling efficiency given the much higher tree densities characteristic of earlier successional stages. Lengths of sapling subplot radii, subcardinal plot transects and subplot radii, and fuel depth locations were consistent across all stands. Total plot area was 1 ha in mid- and late-seral stands and 0.25 ha in young stands. Additional details regarding the location, size, and arrangement of the area sampled and corresponding measurements collected for each aboveground biomass component are presented below. See Table 1.4 for a summary of post-fire structure.

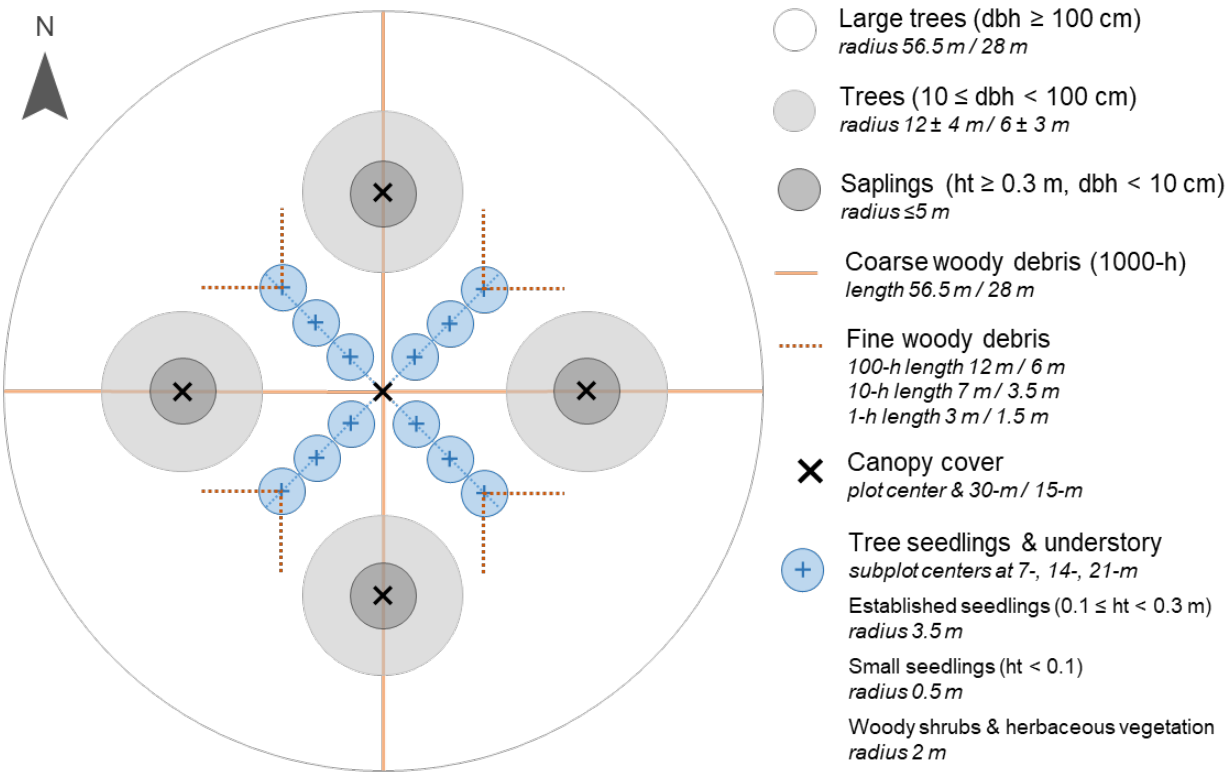

Figure 1.6. Plot layout diagram. Symbols display the size and spatial arrangement of area sampled for each stand component, corresponding to the following colors: grayscale, trees and saplings; orange, coarse and fine woody debris; black, canopy cover; blue, tree seedlings and understory vegetation. For stand components with multiple radii or lengths listed (i.e., separated by a slash), the first value corresponds to sizes in mid- and late-seral stands and the second value corresponds to sizes in young stands. Total plot area was 1 ha for mid- and late-seral stands and 0.25 ha for young stands. dbh, diameter at breast height (1.37 m).

Table 1.3. Summary of field measurements taken for each aboveground biomass component.

Biomass component	Description	Field measurements
Trees		
Trees	overstory trees, dbh ≥ 10 cm	species, status, decay class[1], dbh, total height, percent stem remaining, height to base of live and/or dead crown, percent bark present at dbh, percent of crown volume with needle scorch[2], percent of stem surface area with charred wood[2]
Saplings	understory trees, height ≥ 0.3 m & dbh < 10 cm	species, status, dbh[3], total height, presence of broken top
Seedlings	live tree seedlings, height < 0.3 m	species, height[4], count
Live understory		
Woody shrubs	non-tree woody plants	species, total height, basal diameter of each stem
Herbaceous vegetation	non-woody forbs, graminoids, non-vascular plants	species, percent cover
Down woody debris		
Coarse woody debris	1000-h, diameter ≥ 7.6 cm	species, diameter, decay class, presence of charred wood
Fine woody debris	1-h, diameter < 0.6 cm 10-h, diameter 0.6–2.5 cm 100-h, diameter 2.5–7.6 cm	count by size class
Forest floor		
Litter	dead non-woody plant material	depth
Duff	decomposing litter	depth
Dead fuel	dead woody and non-woody plant material, height ≤ 2 m	depth

Notes: Status refers to live or dead. dbh, diameter at breast height (1.37 m).
[1] Only applicable to dead stems.
[2] Only applicable to trees in burned stands.
[3] Only applicable to individuals with height ≥ 1.37 m.
[4] Only applicable to individuals with height ≥ 0.1 m.

We measured trees (10 ≤ dbh < 100 cm) and saplings (height ≥ 0.3 m, dbh < 10 cm) in four variable radius subplots. We selected subplot radii to ensure at least ~60 trees were measured within each plot. Radii were kept a consistent length for all subplots within a plot. In mid- and late-seral stands, subplots were located 30 m from plot center along each 56.5 m long cardinal plot transect. Tree subplot radii ranged from 8 to 16 m, with a default of 12 m (800–3,217 m^2 total area). In young stands, subplots were located 15 m from plot center along each cardinal plot transect. Tree subplot radii ranged from 3 to 9 m, with a default of 6 m. Sapling subplot radii ranged from 2 to 5 m (50–314 m^2 total area) regardless of pre-fire stand age. We measured large trees (dbh ≥ 100 cm) throughout the entire plot due to their larger stature, rarer occurrence, and outsized ecological role compared to smaller trees. For each stem, we recorded species, status (live or dead), total height, and presence of broken top. For stems taller than 1.37 m, we also recorded dbh, base height of live and dead crown, decay class (1–5; Lutes et al. 2006), percent bark present at dbh, and percent stem remaining. For stumps (i.e., trees with broken top and height < 1.37 m), we recorded diameter at base instead of dbh. Percentages of crown volume with needle scorch and stem wood surface area with char were also recorded for trees in burned stands. See Table 1.5 for the tree species composition across the sampled study area.

We measured live tree seedlings (height < 0.3 m), woody shrubs, and herbaceous vegetation in 12 fixed-radius subplots positioned at the 7-, 14-, and 21-m marks along each 24.5 m long subcardinal plot transect. Subplot radii were 3.5 m for established seedlings (height ≥ 0.1 m; 462 m^2 total area), 0.5 m for small seedlings (height < 0.1 m; 9 m^2 total area), and 2 m for woody shrubs and herbaceous vegetation (150 m^2 total area). For tree seedlings, we tallied individuals by species and recorded height for those taller than 0.1 m. For woody shrubs, we

recorded species, height, and basal diameter of all live stems. For herbaceous vegetation, we measured percent cover by species (non-vascular and graminoid species were grouped by functional type).

We took canopy cover measurements at five fixed locations throughout each plot using the Gap Light Analysis Mobile App (Tichý 2016) run from a Samsung Galaxy tablet. In mid- and late-seral stands, hemispherical digital photographs were taken at plot center and the 30-m mark along each 56.5 m long cardinal plot transect. In young stands, canopy cover photographs were taken at plot center and the 15-m mark along each 28 m long cardinal plot transect. Photographs were taken from the downhill side of a sampling point facing upslope and analyzed immediately within the app to determine canopy cover in the field. We also visually estimated the percent of live canopy in each photograph while in the field.

We measured down woody debris, litter, and duff along planar intercept fuel transects (Brown 1974, Lutes et al. 2006). Fuel transect lengths differed by size class (fine vs. coarse woody debris) and pre-fire stand age. Fine woody debris (1-, 10-, and 100-h fuels; diameter < 7.6 cm) was tallied by size class along eight fuel transects. Fuel transects were arranged in pairs located along each subcardinal plot transect, with the end of each fuel transect crossing the center of the 21-m subplot. Fine woody debris fuel transect pairs were oriented perpendicularly in the cardinal directions bisected by the subcardinal plot transects. Fuel transect lengths were 12 m in mid- and late-seral stands (96 m total sampled length) and reduced to 6 m in young stands (48 m total sampled length). For mid- and late-seral stands, we tallied 1-h fuels (diameter < 0.6 cm) along the first 3 m, 10-h fuels (diameter 0.6–2.5 cm) along the first 7 m, and 100-h fuels (diameter 2.5–7.6 cm) along the entire 12 m. For young stands, we tallied 1-h fuels along the first 1.5 m, 10-h fuels along the first 3.5 m, and 100-h fuels along the entire 6 m.

Coarse woody debris (1000-h fuels; diameter ≥ 7.6 cm) was sampled along four fuel transects originating at plot center and extending in each cardinal direction. Fuel transect lengths were 56.5 m in mid- and late-seral stands (226 m total sampled length) and reduced to 28 m in young stands (112 m total sampled length). We classified 1000-h fuels by level of decay as sound (decay class 1–3) or rotten (decay class 4–5). We measured the overall plot slope and slope of each coarse woody debris fuel transect from plot center using a laser rangefinder.

Litter, duff, and dead fuel depths were measured along each fine woody debris fuel transect at consistent locations across all stands. Litter and duff depths were taken at 0.5 and 1.5 m, and dead fuel depths were taken at three intervals between 0.0–0.5, 0.5–1.0, and 1.0–1.5 m.

A.2 *Post-fire stand structure*

Initial post-fire stand structure varied widely across pre-fire stand age and burn severity strata (Table 1.4). Values of most structural variables increased with pre-fire stand age. In unburned stands, mid- and late-seral stands had on average 93% more total basal area, 149% more tree seedlings, 75% larger total quadratic mean diameter, and 32% less total overstory density compared to young stands. In contrast to pre-fire stand age, values of total and live variables decreased—and dead variables increased—with burn severity. Across all pre-fire stand age classes, burned stands had 3–30% less total basal area (excluding late-seral low severity stands), 6–32% less overstory density, 37–91% less understory density, and 14–87% less canopy cover compared to unburned stands. Differences were greatest in high-severity stands: 98–100% of total basal area, density, and canopy cover in high severity stands were dead, compared to 14–83% in low-severity stands. Quadratic mean diameter of live trees was 30–137% larger in burned stands, while total and dead trees were similar size across all severity classes. Live seedling density was greatest in low-severity and least in high-severity stands (Table 1.4).

Table 1.4. Initial post-fire stand structure summarized across pre-fire stand age × burn severity strata. Values are the mean (standard error) minimum–maximum.

Structural variable	young (n = 16)		mid-seral (n = 31)			late-seral (n = 48)		
	unburned (n = 7)	**high** (n = 9)	**unburned** (n = 10)	**low** (n = 9)	**high** (n = 12)	**unburned** (n = 14)	**low** (n = 15)	**high** (n = 19)
Basal area (m^2 ha^{-1}) height ≥ 1.37 m								
Total	38.8 (4.6) 20.1–58.9	27.2 (3.6) 15.6–41.7	71.8 (5.1) 40.5–88.2	69.3 (4.6) 48.6–85.1	66.1 (2.8) 49.5–83.1	77.6 (5.6) 47.9–120.9	92.2 (3.2) 69.2–110.8	66.3 (4.5) 21.5–126.0
Live	36.0 (3.4) 20.1–47.5	0.0 (0.0) 0.0–0.0	62.9 (4.4) 38.6–82.6	54.1 (3.5) 38.2–68.5	0.5 (0.5) 0.0–5.5	64.9 (4.5) 40.0–102.9	72.8 (3.9) 36.3–99.9	1.1 (0.7) 0.0–11.3
Dead	2.8 (1.6) 0.0–11.4	27.2 (3.6) 15.6–41.7	8.8 (1.6) 1.8–18.8	15.2 (2.4) 4.5–23.3	65.6 (2.8) 49.5–83.1	12.7 (2.1) 4.0–29.3	19.4 (3.1) 4.0–55.2	65.2 (4.5) 21.5–126.0
Overstory density (stems ha^{-1}) dbh ≥ 10 cm								
Total	1,111 (197) 522–1,720	919 (130) 462–1,719	968 (128) 385–1,444	660 (103) 400–1,332	732 (64) 419–1,033	543 (54) 311–1,011	508 (51) 226–800	484 (36) 183–793
Live	1,084 (201) 472–1,688	0 (0) 0–0	720 (93) 329–1,182	375 (60) 211–734	2 (2) 0–25	434 (40) 270–698	277 (35) 142–592	2 (1) 0–17
Dead	26 (12) 0–80	919 (130) 462–1,719	248 (55) 20–648	284 (60) 117–722	730 (64) 419–1,033	109 (31) 24–486	230 (36) 59–450	483 (36) 183–793
Understory density (stems ha^{-1}) dbh < 10 cm, height ≥ 0.3 m								
Total	3,071 (1,305) 765–10,744	1,927 (651) 224–6,544	1,228 (378) 191–4,377	531 (310) 0–2,866	276 (108) 0–1,369	5,944 (1,055) 447–13,706	1,347 (268) 64–3,725	522 (126) 32–2,356
Live	2,693 (1,041) 733–8,754	11 (11) 0–96	931 (395) 191–4,377	89 (60) 0–542	0 (0) 0–0	5,605 (983) 351–13,263	292 (91) 0–1,083	0 (0) 0–0
Dead	378 (270) 32–1,990	1,916 (654) 128–6,544	296 (93) 0–828	442 (255) 0–2,324	276 (108) 0–1,369	339 (114) 0–1,393	1,056 (209) 64–2,642	522 (126) 32–2,356
Seedling density (stems ha^{-1}) height < 0.3 m								
Live	1,304 (292) 499–2,583	291 (88) 22–748	2,559 (1,455) 0–14,666	7,146 (1,711) 2,918–19,477	1,425 (602) 22–7,342	3,934 (704) 310–8,760	5,542 (683) 2,145–11,299	3,071 (614) 22–7,596

Quadratic mean diameter (cm) dbh ≥ 10 cm								
Total	21.6 (1.8) 17.2–29.2	18.5 (1.1) 13.4–24.6	32.2 (2.6) 24.9–53.8	38.2 (2.5) 26.5–49.9	35.0 (2.1) 24.5–50.3	43.3 (2.2) 33.8–60.3	50.5 (2.7) 38.2–67.8	42.7 (2.1) 25.5–63.4
Live	21.4 (1.9) 17.2–29.7	NA	34.9 (2.7) 26.7–56.3	45.5 (3.7) 27.6–64.3	52.9* (–) –	44.3 (2.4) 33.1–62.4	61.1 (3.1) 42.2–84.6	105.2 (7.6) 92.2–124.9
Dead	32.8 (12.1) 11.1–67.2	18.5 (1.1) 13.4–24.6	22.7 (2.0) 14.4–35.8	26.1 (1.7) 19.8–36.2	34.9 (2.1) 24.5–50.3	42.1 (3.9) 26.6–73.9	33.6 (2.8) 20.4–55	42.4 (2.1) 25.5–63.4
Canopy cover (%)								
Total	80.5 (3.5) 68–91.4	10.1 (1.2) 4.1–15.1	89.2 (1.6) 76.7–96.3	77.0 (3.4) 54.1–88.0	28.0 (3.0) 14.9–48.5	83.6 (1.5) 75.9–92.8	66.1 (3.0) 39.4–83.0	26.1 (1.5) 15.6–42.5
Live	79.1 (3.3) 68–89.9	0.1 (0.1) 0.0–0.7	87.8 (1.9) 74.4–95.8	66.6 (4.4) 39.5–81.9	0.0 (0.0) 0.0–0.0	82.0 (1.5) 74.5–90.3	54.8 (4.4) 17.5–81.6	0.2 (0.2) 0.0–3.4
Dead	1.4 (0.6) 0.0–4.4	10.0 (1.2) 4.1–15.1	1.4 (0.3) 0.0–3.5	10.4 (2.2) 3.2–22.1	28.0 (3.0) 14.9–48.5	1.7 (0.3) 0.0–3.3	11.3 (2.5) 1.4–36.5	25.9 (1.5) 15.6–42.5

Note: NA for live quadratic mean diameter in young high severity stands due to no live overstory trees present. Standard error and range are not reported (–) for live quadratic mean diameter in mid-seral high severity stands due to only having a single observation. dbh, diameter at breast height (1.37 m).

Table 1.5. Species, functional group, size range, and relative importance for trees and large saplings (height ≥ 1.37 m) measured across all sampled stands (N = 95).

Scientific name	Common name	Functional group	dbh range (cm)		Importance value
			min	max	
Pseudotsuga menziesii	Douglas-fir	I	0.2	180.3	85.5
Tsuga heterophylla	western hemlock	T	0.1	154.1	76.8
Abies amabilis	Pacific silver fir	T	0.1	140.5	67.3
Abies procera	noble fir	I	0.1	171.9	32.2
Thuja plicata	western redcedar	T	0.1	160.3	13.5
Taxus brevifolia	Pacific yew	T	0.5	25.4	5.5
Chrysolepis chrysophylla	giant chinquapin	B	0.4	16.5	3.6
Abies grandis	grand fir	T	5.2	44.0	3.4
Acer macrophyllum	bigleaf maple	B	9.0	38.2	2.1
Prunus emarginata	bitter cherry	B	0.9	35.1	2.0
Pinus monticola	western white pine	I	13.9	108.7	1.6
Tsuga mertensiana	mountain hemlock	T	1.3	85.0	1.5
Picea engelmannii	Engelmann spruce	T	28.5	44.8	1.1
Callitropsis nootkatensis	Alaska cedar	T	1.0	34.8	0.8
Abies lasiocarpa	subalpine fir	T	18.8	39.5	0.7
Populus balsamifera ssp. *trichocarpa*	black cottonwood	B	25.5	38.0	0.6
Alnus rubra	red alder	B	26.6	34.2	0.6
Larix occidentalis	western larch	I	47.4	59.7	0.4
Acer glabrum	Rocky Mountain maple	B	9.0	11.9	0.3
Cornus nuttallii	Pacific dogwood	B	9.9	9.9	0.3
Pinus contorta var. *latifolia*	lodgepole pine	I	17.1	17.1	0.3

Notes: Functional group describes the reproductive classification and shade tolerance of each species: I, shade-intolerant conifer/gymnosperm; T, shade-tolerant conifer/gymnosperm; B, broadleaf/angiosperm. Importance value is an index of how dominant a species is within an ecosystem, calculated as the sum of relative frequency (i.e., proportion of sampled area in which each species occurs), relative density (i.e., number of individuals per sampled area), and relative dominance (i.e., basal area per sampled area) of each species (Curtis and McIntosh 1951). The importance value index ranges from 0–300, with higher values indicating greater importance of an individual species. dbh, diameter at breast height (1.37 m).

A.3 *Biomass and fuels calculations*

A.3.1 Aboveground biomass carbon

We estimated the aboveground biomass of all measured vegetation using allometric equations specific to each component, described below (Table 1.6). We determined aboveground biomass carbon by multiplying the biomass of each component by its corresponding carbon content, based on species-, component-, position- (i.e., standing vs. down), and decay class-specific values presented in the literature (range 39.4–58.3%; Table 1.7). We also quantified the biomass of black carbon within charred wood using methods from Donato et al. (2009 eq. 4) as described below, assuming a carbon content of 75% (Branca and Di Blasi 2003).

We calculated total aboveground biomass of standing trees and large saplings (height ≥ 1.37 m) by summing individual estimates for crown (foliage, branches) and stem (wood, bark) components. We derived crown biomass using species-, size-, and region-specific allometric equations based on height and/or dbh (Table 1.6). We calculated total crown biomass by summing separate estimates of foliage and branch mass for each individual tree. Equations were sourced primarily from the BIOPAK database (Means et al. 1994). When multiple suitable equations were available for a species (i.e., 2+ equations developed in the western Cascades from trees with size ranges overlapping our field measurements), we took the mean estimate across all sources to account for latitudinal differences in moisture and productivity, as well as derivation methods (e.g., sample size, function shape). When equations specific to the western Cascades were not available, we used equations developed in other regions. When no equations were available for a species, we substituted equations from analogous species based on shared structural and functional attributes.

Table 1.6. References for allometric equations used to convert field measurements into biomass estimates. Equations were species-specific for trees, seedlings and small saplings, woody shrubs, and herbaceous vegetation.

Strata	Biomass component	Source(s)
Down woody debris	total	4
Trees & large saplings (height ≥ 1.37 m)	foliage	8, 14, 20, 21, 24
	branches	6, 8, 14, 20, 22, 24
	stems[1]	8, 14, 20, 21, 24
	crown proportions[2]	6, 22
Seedlings & small saplings (height < 1.37 m)	total	6, 9, 10, 19
Standing trees & coarse woody debris	charred wood	7
Woody shrubs	total[3]	3, 5, 8, 10, 11, 14, 16, 17, 18, 23
Herbaceous vegetation	total	1, 2, 8, 10, 12, 13, 14, 15, 16, 17, 23

Notes: Source codes correspond to the following citations: [1] Acker and Easter 1993; [2] Alaback 1986; [3] Alexander 1978; [4] Brown 1974; [5] Brown and Johnston 1976; [6] Brown 1978; [7] Donato et al. 2009; [8] Gholz et al. 1979; [9] Halpern et al. 1996; [10] Halpern and Miller 1993; [11] Helgerson et al. 1988; [12] Koerper 1983; [13] Losapio et al. 2018; [14] Means et al. 1994; [15] Monzingo et al. 2022; [16] Ohmann et al. 1981; [17] Olson and Martin 1981; [18] Ottmar et al. 2000; [19] Ross and Walstad 1986; [20] Shaw 1979; [21] Sillett et al. 2018; [22] Snell and Little 1983; [23] Spies and Easter 1991; [24] Standish et al. 1985.

[1] We used the sum of stem wood and stem bark equations to estimate total stem biomass.

[2] Crown proportions were applied to the sum of foliage and branch biomass to determine the amount of branch biomass within each fuel size class (1-h, 10-h, 100-h, 1000-h).

[3] When equations for total biomass were unavailable for a shrub species, we used the sum from separate foliage, stem, and branch equations to estimate total biomass.

Table 1.7. References for determining carbon content of each biomass component. The range in carbon content values is shown for all measured species and decay classes within each stratum.

Stratum	Biomass component	Carbon content range (%)	Source(s)
All trees	branches	47.3–52.8	1, 4, 5, 6, 8, 10, 12
Live trees & large saplings	foliage	40.0–52.3	1, 2, 11
	stem wood	47.4–52.8	1, 4, 5, 6, 10
	stem bark	48.9–53.2	1, 4, 8, 12
Dead snags & stumps	stem wood	45.5–55.8	4
	stem bark	44.1–58.3	4
Seedlings & small saplings	total	45.8–51.6	1, 2, 4, 5, 6, 8, 10, 12
Coarse woody debris	stem wood	45.5–57.0	4
	stem bark	44.1–56.4	4
Fine woody debris	total	47.1	5
Herbaceous vegetation	total	39.4–48.2	1, 5, 7, 9
Woody shrubs	total	47.2	5
Standing trees & coarse woody debris	charred wood	75.0	3

Notes: Source codes correspond to the following citations: [1] Ares et al. 2007; [2] Berner and Law 2016; [3] Donato et al. 2009; [4] Harmon et al. 2013; [5] Jain et al. 2010; [6] Lamlom and Savidge 2003; [7] Li and Shipley 2017; [8] Martin et al. 2018; [9] Moore et al. 2007; [10] Namm and Berrill 2012; [11] Smith and Dukes 2017; [12] Thomas and Martin 2012.

Since fewer field measurements were taken on individual large saplings (dbh < 10 cm) compared to trees (dbh ≥ 10 cm), we made several assumptions and approximations necessary for estimating crown biomass for large saplings. We assumed all dead large saplings had a decay class of 1, no bark loss, and no charred wood. We estimated crown length and crown base height for large saplings using species-specific mean ratios of crown length and height from live and dead trees (dbh ≥ 10 cm) with heights overlapping the observed large sapling height range (Table 1.8).

We corrected crown biomass for mass loss due to foliage scorch, broken top, and decay class. For trees with evidence of scorched foliage, we reduced total foliage biomass using the proportion of un-scorched foliage remaining. For trees with a broken top, we adjusted for loss of crown biomass using a correction factor applied to total foliage and branch biomass. Broken top correction factors were based on a regression of crown length and dbh for all live unbroken trees within our dataset (N = 3,440). We calculated crown length as the difference between total height and height to the base of the crown. We derived a separate correction factor for tree species considered shade-intolerant conifers, shade-tolerant conifers, and broadleaf trees (Table 1.5; Figure 1.7). We determined proportional crown remaining for broken top trees by dividing the observed crown length by the regression-predicted crown length. For dead trees, we corrected for loss of volume and density due to decay by reducing total branch biomass using decay class-specific relative volume and density values. We assumed relative volumes of 1.0, 0.8, 0.5, 0.2, and 0.0 for decay classes 1–5, respectively (Donato et al. 2013), and used species-specific relative densities for snags from Harmon et al. (2011).

Table 1.8. Observed height range and mean crown ratio used to estimate crown base height and crown length for large saplings within the canopy fuel profile (height ≥ 1.37 m, dbh < 10 cm).

Species[†]	Status[†]	Sapling height range (m)		Crown ratio
		min	max	
Pacific silver fir	live	1.4	9.0	0.754
	dead	1.4	9.0	0.595
grand fir	dead	2.6	6.5	0.553
noble fir	live	1.5	8.5	1.000
	dead	1.5	11.2	0.929
Rocky Mountain maple	dead	3.8	3.8	0.630
bigleaf maple	dead	1.5	1.5	0.630
Alaska cedar	live	1.6	1.6	0.692
giant chinquapin	dead	1.5	9.7	0.630
Pacific dogwood	live	5.4	5.4	0.630
bitter cherry	live	2.7	3.9	0.630
Douglas-fir	live	1.6	6.7	0.708
	dead	1.4	12.8	0.708
Pacific yew	live	1.4	6.4	0.908
	dead	1.4	4.7	0.760
western redcedar	live	1.4	9.9	0.692
	dead	1.7	9.3	0.562
western hemlock	live	1.4	10.4	0.742
	dead	1.4	9.6	0.623
mountain hemlock	live	1.6	9.4	0.730

Notes: Crown ratios were derived by taking the species-specific mean ratios of crown length and height from unbroken live and dead trees (dbh ≥ 10 cm) with heights overlapping the sapling height range.

[†] Species and status include only individuals represented within our field data. Thus, not all tree species are included here and some species only have a single status reported.

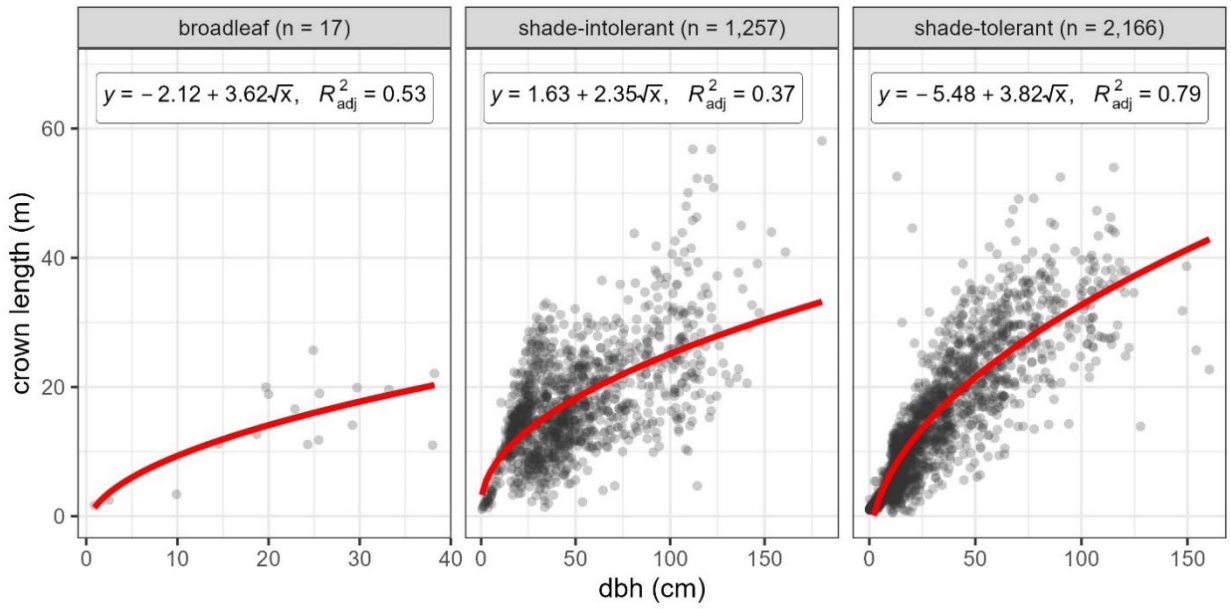

Figure 1.7. Linear regressions (red lines) of crown length (y) ~ diameter at breast height (dbh, x) used to correct crown fuel biomass for trees with broken tops. Regressions were based on observations (gray points) of all live unbroken trees (height ≥ 1.37 m) within our dataset (N = 3,440). Crown length was the difference in total height and height to the base of the crown. Broken top correction factors were derived separately for tree species considered broadleaf trees (left), shade-intolerant conifers (center), and shade-tolerant conifers (right) (Table 1.5). A square root transformation to dbh resulted in the highest goodness-of-fit values for all models.

We derived stem biomass for standing live and dead trees, large saplings (height ≥ 1.37 m), and stumps (broken top and height < 1.37 m) from species- and region-specific allometric equations based on height and/or diameter (Table 1.6) and corrected for mass loss due to broken top, bark loss, decay class, and charred wood. We calculated total stem biomass by summing separate estimates of stem wood and bark mass for each individual tree. Diameter at base (dab) was used in place of dbh within stem mass equations for stumps. For trees with broken tops (including stumps), we reduced total stem biomass using the proportion of stem remaining. For trees and stumps missing bark (i.e., percent bark at dbh/dab < 100), we reduced total bark biomass using the proportion of bark remaining. For dead trees and stumps, we adjusted wood biomass for density loss from decay using species- and decay class-specific relative density reduction factors from Harmon et al. (2011). We also corrected for biomass loss from char on

stem wood following methods from Donato et al. (2009).

We derived total aboveground biomass of live understory vegetation—including tree seedlings and small saplings (height < 1.37 m), woody shrubs, and herbaceous vegetation (i.e., forbs, ferns, and graminoids)—using species- and region-specific allometric equations based on height, percent cover, and/or basal diameter (Table 1.6). Equations were sourced primarily from the BIOPAK and TRY databases (Kattge et al. 2020, Means et al. 1994). When no equations were available for a species, we substituted equations from analogous species based on shared structural and functional attributes.

We derived biomass of down wood debris using standard methods (Brown 1974). We corrected for the slope of each transect using our field-measured slopes and the slope correction factor equation from Brown (1974). For calculating biomass of fine woody debris (1-, 10-, 100-h particles), we used non-slash composite values from Brown (1974) for squared average diameters, specific gravities, and non-horizontal angle correction factor. For calculating biomass of coarse woody debris (1000-h particles), we used species- and decay class-specific wood densities (Harmon et al. 2008). We also corrected for mass loss from wood charring on coarse woody debris following methods from Donato et al. (2009).

We characterized charred wood (i.e., solid organic material that remains after incomplete combustion of woody biomass) in order to (a) correct for loss of mass due to combustion, and (b) explicitly quantify the biomass of black carbon (i.e., carbon fraction of char) due to its role in long-term carbon storage and nutrient cycling (Bird et al. 2015). We quantified biomass of charred wood on coarse woody debris and standing trees (including stumps) using methods from Donato et al. (2009) based on presence and depth of char. During field data collection, we recorded the binary presence or absence of charred wood on coarse woody debris and the

percentage of surface area with charred wood on standing trees. We assumed a char depth of 8.2 mm based on mean values from mesic Douglas-fir forests in western Oregon (Donato et al. 2009). In general, we derived charred wood biomass by subtracting the mass of the uncharred inner portion of each 1000-h particle or stem from the total mass. We determined the total mass of wood using allometric equations, as described above (Table 1.6). We calculated mass of the uncharred inner core by adjusting measured diameter inputs for the allometric equations for both stem wood mass and coarse woody debris load to account for the depth of char and associated mass loss (Donato et al. 2009 eq. 7), assuming 70% loss based on common estimates (e.g., Dietenberger 2002).

For coarse woody debris with presence of char, we first determined the mass of the uncharred inner portion by using the adjusted diameter input within the equation from Brown (1974). We then subtracted the mass of the uncharred inner portion from the total mass and adjusted for proportion of mass remaining (i.e., 0.3) to find the mass of the charred outer portion. We determined total wood mass for coarse woody debris with charred wood by adding the charred and uncharred portions (Donato et al. 2009 eq. 5).

For standing trees with presence of char, we first calculated the amount of total stem wood mass with char by multiplying by the proportion of charred surface area. We then found the mass of the uncharred inner portion of the charred stem wood by using the adjusted diameter input within same allometric equations for total wood mass (Table 1.6). We subtracted the mass of the uncharred inner portion from the total stem wood mass with char and adjusted for proportion of mass remaining (i.e., 0.3) to determine the mass of the charred outer portion. We calculated total wood mass for trees with charred wood by adding the charred and uncharred portions. We acknowledge this approach assumes a cylinder and may slightly overestimate char

mass but was still the best approach given the information we had – i.e., no measures of char height with which to use the conical frustum approach described in Donato et al. (2009).

A.3.2 Fuel profiles

Fuel loads were determined by separating biomass into surface and canopy fuel components.

Surface fuel profiles included fine and coarse woody debris (height < 2 m), live tree seedlings and small saplings (height < 1.37 m), and live understory vegetation (shrubs, forbs, graminoids). We separated down woody debris biomass by standard fuel size and decay (i.e., sound vs. rotten) classes. We separated live surface fuel biomass into woody (tree seedlings and small saplings, shrubs) and herbaceous (forbs, graminoids) components.

Canopy fuel profiles included foliage and branch biomass, available canopy fuel load, canopy bulk density, and canopy base height for all live and dead standing trees and large saplings taller than 1.37 m. We separated live and dead branch biomass into fuel size classes (i.e., 1-, 10-, 100-, 1000-h) using accumulative proportion equations based on species, dbh, and height (Brown 1978, Snell and Little 1983). This approach was developed by Brown and Johnston (1976) and is used in common modeling tools for fuel and fire management including FuelCalc (Reinhardt et al. 2006a) and the Fire and Fuels Extension to the Forest Vegetation Simulator (FFE-FVS; Rebain 2010). For shade-intolerant tree species (Table 1.5), we used separate branch size proportion equations for individual trees in dominant versus intermediate canopy positions. We assigned canopy position based on a tree's height relative to other trees within each stand: if tree height was above the 60^{th} percentile for the stand, a tree was considered dominant (i.e., among the tallest 40% of trees), otherwise it was considered to be intermediate (Rebain 2010).

Available canopy fuel load represents the portion of canopy biomass that would typically

be consumed in a crown fire and included the sum of foliage, dead 1-h branches, and half of live 1-h branches (Reinhardt et al. 2006b). We created vertical canopy fuel profiles for each stand by evenly distributing available canopy fuel in 0.25-m bins along the crown length of each canopy tree and summing by bin (Donato et al. 2013, Simard et al. 2011). Canopy bulk density represents the mean volume of available fuel within the canopy and was defined as the maximum 3-m running mean across the vertical canopy fuel profile (Reinhardt et al. 2006b). Canopy base height represents the height at which there is enough available fuel for fire to travel vertically through the canopy (Scott and Reinhardt 2001) and was defined as the lowest height at which canopy bulk density exceeded 0.04 kg m^{-3} (Cruz et al. 2004, Donato et al. 2013, Sando and Wick 1972).

A.4 *R packages*

We used the following packages for all analyses and visualization in R, version 4.4.0 (R Core Team 2024): *egg*, version 0.4.5 (Auguie 2019); *ggpmisc*, version 0.5.6 (Aphalo 2024); *ggpubr*, version 0.6.0 (Kassambara 2023); *glmmTMB*, version 1.1.9 (Brooks et al. 2017); *janitor*, version 2.2.0 (Firke 2023); *marginaleffects*, version 0.20.1 (Arel-Bundock 2024); *patchwork*, version 1.2.0 (Pedersen 2024); *plotrix*, version 3.8.4 (Lemon 2006); *rtry*, version 1.1.0 (Lam et al. 2023); *tidyverse*, version 2.0.0 (Wickham et al. 2019); and *zoo*, version 1.8.12 (Zeileis and Grothendieck 2005).

1.7 APPENDIX B: SUPPLEMENTAL RESULTS AND STATISTICAL MODEL OUTPUTS

B.1 *Model summaries*

Table 1.9. Model-predicted means and 95% confidence intervals for post-fire aboveground biomass carbon components across pre-fire stand age × burn severity strata.

Biomass component (Mg C ha^{-1})	young		mid-seral			late-seral		
	unburned	high	unburned	low	high	unburned	low	high
All								
Total	98.0 (83.9–114.4)	65.8 (56.8–76.3)	281.2 (247.4–319.6)	303.3 (264.0–348.3)	188.9 (168.0–212.4)	347.4 (308.8–390.8)	374.6 (332.7–421.8)	233.3 (210–259.2)
Live	71.3 (39.2–129.8)	0.9 (0.5–1.7)	220.1 (129.5–374)	207.0 (118.1–362.9)	2.8 (1.7–4.7)	362.0 (216.1–606.5)	340.5 (205.1–565.3)	4.6 (3.1–7.0)
Dead	14.5 (12.0–17.5)	63.0 (52.9–75.1)	43.1 (36.9–50.4)	54.8 (46.6–64.4)	187.3 (162.7–215.6)	53.1 (46.3–61)	67.5 (58.5–78.0)	230.8 (203.5–261.7)
Woody	91.9 (78.7–107.3)	65.7 (56.7–76.1)	264.9 (233.0–301.2)	290.9 (253.2–334.3)	189.2 (168.2–212.8)	325.4 (289.2–366.2)	357.3 (317.3–402.5)	232.4 (209.2–258.2)
Non-woody	14.1 (8.6–23.0)	0.2 (0.1–0.3)	12.6 (8.9–18.0)	11.5 (7.7–17.2)	0.2 (0.1–0.3)	19.6 (14.1–27.2)	17.9 (12.6–25.3)	0.3 (0.2–0.4)
Trees								
Total	86.8 (73.3–102.7)	57.6 (48.8–67.9)	261.2 (225.8–302.2)	287.9 (245.8–337.3)	173.3 (151.7–197.9)	312.9 (273.7–357.8)	344.9 (301.4–394.7)	207.6 (184.2–233.9)
Live	86.7 (63.5–118.4)	6.1 (3.7–10.2)	233.3 (185.2–293.9)	239.7 (187.9–305.8)	16.4 (10.9–24.7)	311.8 (251.5–386.5)	320.3 (262.3–391.2)	21.9 (15.2–31.6)
Snags	2.5 (1.8–3.5)	44.9 (33.6–60.1)	11.6 (9.0–15.0)	33.8 (25.5–44.7)	206.7 (160.4–266.4)	11.5 (9.1–14.6)	33.5 (26.1–42.9)	204.7 (164.3–255.1)
Stumps	1.8 (0.8–3.8)	1.0 (0.4–2.2)	0.8 (0.3–1.7)	0.7 (0.3–1.6)	0.4 (0.2–1.1)	0.3 (0.1–0.5)	0.2 (0.1–0.8)	0.1 (0.1–0.2)
Stem wood								
Total	58.3 (49.2–69)	43.6 (36.9–51.5)	175.7 (151.8–203.4)	202.3 (172.6–237.2)	131.4 (114.9–150.2)	207.2 (180.9–237.2)	238.6 (208.3–273.2)	154.9 (137.4–174.6)
Live	57.2 (39.9–81.9)	4.5 (2.5–8.2)	155.7 (119.4–203)	168.7 (127.2–223.6)	12.3 (7.7–19.7)	201.8 (157.3–258.8)	218.6 (173.7–275.1)	16.0 (10.5–24.3)
Dead	3.0 (2.3–3.9)	41.4 (32.1–53.2)	10.4 (8.3–13.0)	24.8 (19.6–31.4)	143.1 (116.2–176.4)	10.5 (8.6–12.9)	25.2 (20.4–31.1)	145.4 (121.4–174.0)
Stem bark								
Total	12.4 (9.9–15.6)	9.3 (7.4–11.6)	35.5 (29.2–43.2)	42.9 (34.7–53.1)	26.5 (22.1–31.7)	37.1 (30.9–44.6)	44.9 (37.4–53.8)	27.7 (23.6–32.5)
Live	12.7 (8.6–18.8)	1.3 (0.7–2.4)	31.0 (23.3–41.5)	35.8 (26.3–48.7)	3.1 (1.9–5.3)	36.0 (27.4–47.3)	41.5 (32.3–53.3)	3.6 (2.3–5.8)
Dead	0.5 (0.4–0.8)	7.9 (5.5–11.2)	2.1 (1.5–2.8)	5.4 (3.8–7.5)	31.7 (23.5–42.9)	1.7 (1.3–2.3)	4.3 (3.2–5.8)	25.7 (19.9–33.1)

Down woody debris								
Total	9.9 (7.8–12.4)	7.1 (5.8–8.8)	19.3 (16.1–23.2)	16.0 (13.1–19.6)	14.0 (11.7–16.7)	34.4 (29–40.7)	28.5 (23.9–33.9)	24.9 (21.4–29)
Live understory								
Total	1.6 (0.9–2.8)	0.8 (0.4–1.3)	1.3 (0.8–2.1)	0.4 (0.2–0.6)	0.6 (0.4–1.0)	0.8 (0.6–1.3)	0.2 (0.1–0.4)	0.4 (0.3–0.6)
Charred wood								
Total	0.0 (0.0–0.1)	0.3 (0.2–0.4)	0.0 (0.0–0.1)	0.2 (0.2–0.4)	0.3 (0.2–0.4)	0.1 (0.0–0.1)	0.5 (0.3–0.7)	0.6 (0.4–0.8)

Notes: All values are Mg C ha^{-1}. Woody biomass includes branches and stems of standing trees, stumps, down woody debris, and woody shrubs. Non-woody biomass includes tree foliage and total mass of herbaceous vegetation. Tree biomass includes foliage, branches, and stems for all live and dead individuals (i.e., large trees, trees, saplings, seedlings, stumps). Stump biomass includes stem wood and bark of trees with broken top and height < 1.37 m. Stem wood and bark biomass include standing trees (height ≥ 1.37 m) and coarse woody debris. Live understory biomass includes woody shrubs, herbaceous vegetation, and tree seedlings and small saplings (height < 1.37 m). Charred wood biomass includes black carbon in charred stem wood on coarse woody debris and standing live and dead trees.

Table 1.10. Model-predicted means and 95% confidence intervals for post-fire surface and canopy fuel components across pre-fire stand age × burn severity strata.

Fuel component	young		mid-seral			late-seral		
	unburned	high	unburned	low	high	unburned	low	high
Down woody debris (Mg ha^{-1})								
Total	19.4 (15.4–24.5)	13.9 (11.2–17.3)	38.5 (32.1–46.2)	32.0 (26.3–38.9)	27.6 (23.2–32.8)	68.2 (57.7–80.7)	56.7 (47.7–67.3)	48.9 (42.0–56.8)
1-h	3.3 (2.6–4.2)	1.7 (1.3–2.2)	4.6 (3.8–5.7)	4.7 (3.8–5.9)	2.4 (2.0–2.9)	5.8 (4.8–7.0)	5.9 (4.9–7.2)	3.0 (2.6–3.5)
10-h	3.6 (2.9–4.5)	2.9 (2.3–3.6)	4.9 (4.0–5.9)	4.2 (3.4–5.1)	3.9 (3.2–4.7)	5.6 (4.7–6.7)	4.8 (4–5.8)	4.5 (3.8–5.2)
100-h	3.9 (2.9–5.1)	4.8 (3.6–6.3)	5.1 (4.1–6.5)	4.7 (3.6–6.0)	6.3 (5.1–7.9)	5.8 (4.6–7.2)	5.2 (4.2–6.5)	7.1 (5.9–8.6)
Fine woody debris	10.8 (8.9–13.1)	9.2 (7.6–11.2)	14.7 (12.5–17.3)	13.7 (11.5–16.4)	12.6 (10.8–14.7)	17 .0 (14.6–19.9)	15.9 (13.6–18.6)	14.6 (12.8–16.7)
1000-h sound	2.9 (1.8–4.7)	1.9 (1.2–2.9)	11.2 (8.0–15.9)	10.6 (7.4–15.3)	7.2 (5.2–10.2)	31.4 (23–43.1)	29.7 (21.3–41.4)	20.3 (15.2–27)
1000-h rotten	5.3 (3.3–8.8)	3.9 (2.5–6.1)	11.3 (7.9–16.2)	7.3 (4.8–11)	8.3 (5.8–11.8)	19.0 (13.5–26.7)	12.2 (8.7–17.2)	14.0 (10.2–19.1)
Coarse woody debris	7.8 (5.6–10.9)	5.2 (3.9–7.1)	23.0 (17.8–29.7)	18.3 (13.8–24.2)	15.4 (12.0–19.8)	51.1 (40.3–64.8)	40.6 (31.8–51.8)	34.3 (27.6–42.5)
Surface fuel depths (cm)								
Litter	2.7 (2.0–3.6)	0.9 (0.7–1.2)	3.6 (2.9–4.6)	2.2 (1.7–2.9)	1.2 (0.9–1.5)	4.6 (3.7–5.8)	2.8 (2.3–3.6)	1.5 (1.2–1.8)
Duff	3.9 (2.5–6.0)	0.5 (0.3–0.7)	5.8 (4.0–8.3)	2.2 (1.5–3.2)	0.7 (0.4–1.0)	8.3 (5.9–11.7)	3.1 (2.2–4.5)	1.0 (0.7–1.3)
Dead fuel	13.8 (10.1–18.8)	10.9 (8.0–14.9)	16.0 (12.4–20.6)	22.6 (17.2–29.8)	12.7 (9.8–16.4)	18.1 (14.1–23.2)	25.6 (19.9–32.9)	14.3 (11.7–17.6)
Live surface fuels (Mg ha^{-1})								
Total	3.4 (1.9–5.9)	1.7 (0.9–3)	2.8 (1.6–4.7)	0.7 (0.4–1.1)	1.4 (0.9–2.2)	1.7 (1.1–2.6)	0.4 (0.3–0.7)	0.8 (0.6–1.2)
Woody shrubs	2.1 (1–4.2)	0.9 (0.4–2.0)	2.5 (1.2–4.9)	0.3 (0.2–0.6)	1.1 (0.6–2.0)	1.0 (0.6–1.8)	0.1 (0.1–0.3)	0.4 (0.3–0.7)
Herbaceous vegetation	0.5 (0.3–1.0)	0.7 (0.4–1.2)	0.3 (0.2–0.5)	0.3 (0.2–0.6)	0.4 (0.2–0.6)	0.2 (0.1–0.4)	0.3 (0.2–0.5)	0.3 (0.2–0.4)
Conifer tree seedlings	0.1 (0.1–0.2)	0.0 (0.0–0.0)	0.1 (0.1–0.3)	0.0 (0.0–0.0)	0.0 (0.0–0.0)	0.7 (0.4–1.1)	0.0 (0.0–0.1)	0.0 (0.0–0.0)
Broadleaf tree seedlings	0.3 (0.0–3.3)	0.4 (0.1–1.5)	0.0 (0.0–0.1)	0.0 (0.0–0.0)	0.0 (0.0–0.3)	0.1 (0.0–1.1)	0.0 (0.0–0.2)	0.2 (0.0–0.6)
Canopy foliage (Mg ha^{-1})								
Total	11.9 (8.8–16.2)	0.3 (0.2–0.5)	29.0 (23.1–36.4)	22.3 (17.6–28.3)	0.7 (0.5–1.1)	43.8 (35.7–53.7)	33.6 (27.6–40.9)	1.1 (0.8–1.6)

Live	12.1 (8.8–16.5)	0.3 (0.2–0.4)	29.4 (23.3–37.1)	22.1 (17.3–28.3)	0.6 (0.4–0.9)	43.1 (35.0–53.2)	32.5 (26.6–39.7)	0.9 (0.6–1.3)
Dead[1]	0.0 (0.0–0.0)	0.0 (0.0–0.0)	0.0 (0.0–0.0)	0.7 (0.2–1.3)	0.0 (0.0–0.0)	0.0 (0.0–0.0)	0.6 (0.3–0.9)	0.1 (0.0–0.2)
1-h branches (Mg ha^{-1})								
Total	9.5 (7.7–11.8)	3.8 (3.2–4.7)	13.2 (11.1–15.7)	12.4 (10.3–15)	5.3 (4.5–6.2)	13.3 (11.4–15.6)	12.6 (10.7–14.7)	5.4 (4.6–6.2)
Live	6.5 (5.0–8.4)	0.2 (0.1–0.2)	11.1 (9.2–13.5)	8.1 (6.6–9.9)	0.3 (0.2–0.4)	13.3 (11.2–15.8)	9.7 (8.2–11.4)	0.3 (0.2–0.4)
Dead	1.4 (1.1–1.8)	4.5 (3.5–5.8)	1.9 (1.5–2.3)	4.2 (3.3–5.3)	6.1 (5.0–7.5)	1.4 (1.1–1.7)	3.0 (2.5–3.7)	4.4 (3.7–5.3)
10-h branches (Mg ha^{-1})								
Total	11.4 (9.4–13.7)	8.1 (6.7–9.7)	28.4 (24.2–33.3)	26.9 (22.6–31.9)	20.1 (17.5–23.2)	30.0 (26–34.6)	28.4 (24.5–32.8)	21.3 (18.7–24.3)
Live	8.1 (6.2–10.7)	0.2 (0.1–0.3)	19.3 (15.8–23.6)	16.9 (13.6–20.9)	0.5 (0.3–0.6)	23.4 (19.5–28.1)	20.5 (17.2–24.3)	0.6 (0.4–0.8)
Dead	3.2 (2.5–4.1)	8.4 (6.5–10.8)	7.9 (6.3–10.0)	8.7 (6.9–10.9)	20.8 (17.0–25.5)	7.7 (6.4–9.4)	8.5 (6.8–10.4)	20.3 (16.9–24.3)
100-h branches (Mg ha^{-1})								
Total	2.6 (1.9–3.6)	0.8 (0.6–1.2)	26.8 (20.2–35.6)	22.9 (17.1–30.7)	8.6 (6.7–11.0)	58.0 (44.8–75.0)	49.6 (38.4–64.0)	18.6 (14.9–23.2)
Live	3.2 (2.1–4.7)	0.1 (0.1–0.2)	20.0 (15.2–26.3)	19.3 (14.5–25.8)	0.8 (0.5–1.3)	43.8 (34.2–56.1)	42.3 (33.4–53.6)	1.7 (1.1–2.8)
Dead	0.3 (0.2–0.5)	0.7 (0.5–1.1)	3.8 (2.7–5.4)	3.3 (2.3–4.5)	8.3 (6.2–11.1)	9.0 (6.8–12.0)	7.7 (5.6–10.6)	19.6 (15.0–25.6)
1000-h branches (Mg ha^{-1})								
Live	0.0 (0.0–0.1)	0.0 (0.0–0.0)	0.4 (0.2–0.5)	0.5 (0.3–0.8)	0.1 (0.0–0.2)	0.6 (0.4–1.0)	0.9 (0.6–1.3)	0.1 (0.1–0.3)
Available canopy fuel load (Mg ha^{-1})								
Total	24.6 (19.2–31.6)	3.5 (2.8–4.3)	36.9 (30.3–44.7)	33.4 (26.9–41.5)	5.2 (4.3–6.2)	43.6 (36.7–51.8)	39.6 (33.0–47.4)	6.1 (5.2–7.3)
Live	15.3 (11.3–20.7)	0.3 (0.2–0.5)	34.9 (27.9–43.7)	26.2 (20.6–33.2)	0.8 (0.5–1.1)	49.8 (40.7–60.9)	37.3 (30.8–45.2)	1.1 (0.8–1.6)
Dead	1.4 (1.1–1.8)	4.5 (3.5–5.8)	1.9 (1.5–2.3)	5.0 (3.9–6.3)	6.1 (5.0–7.5)	1.4 (1.1–1.7)	3.6 (3.0–4.4)	4.5 (3.8–5.3)
Canopy bulk density (kg m^{-3})								
Total	0.26 (0.18–0.36)	0.04 (0.03–0.06)	0.19 (0.15–0.25)	0.15 (0.11–0.20)	0.03 (0.03–0.04)	0.22 (0.17–0.28)	0.17 (0.13–0.22)	0.04 (0.03–0.05)
Canopy base height (m)								
Total	1.2 (0.7–2.0)	1.4 (0.7–2.8)	8.4 (5.5–12.7)	11.7 (7.7–17.8)	10.2 (5.8–17.8)	2.0 (1.4–2.9)	2.8 (2.0–4.1)	2.5 (1.3–4.6)

Notes: [1] Model for dead foliage did not converge; values are observed mean (± 2 standard error).

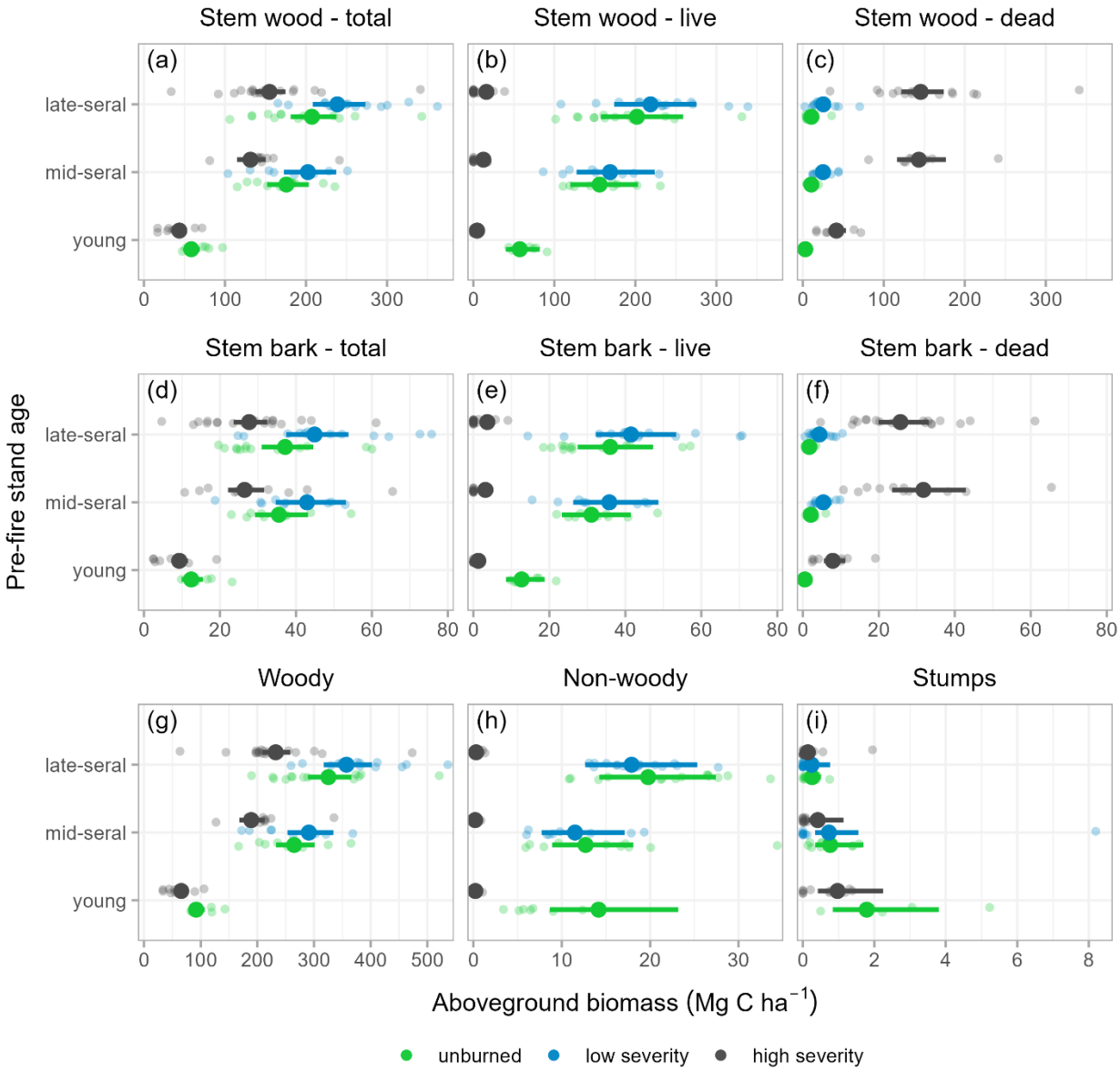

Figure 1.8. Post-fire aboveground biomass carbon across pre-fire stand age × burn severity strata. Stem wood (a–c) and bark (d–f) biomass include standing trees (height ≥ 1.37 m) and coarse woody debris. Woody biomass (g) includes branches and stems of standing trees, stumps, down woody debris, and woody shrubs. Non-woody biomass (h) includes tree foliage and total mass of herbaceous vegetation. Stump biomass (i) includes stem wood and bark of trees with broken top and height < 1.37 m. See Table 1.9 and Table 1.11 for model summaries and outputs.

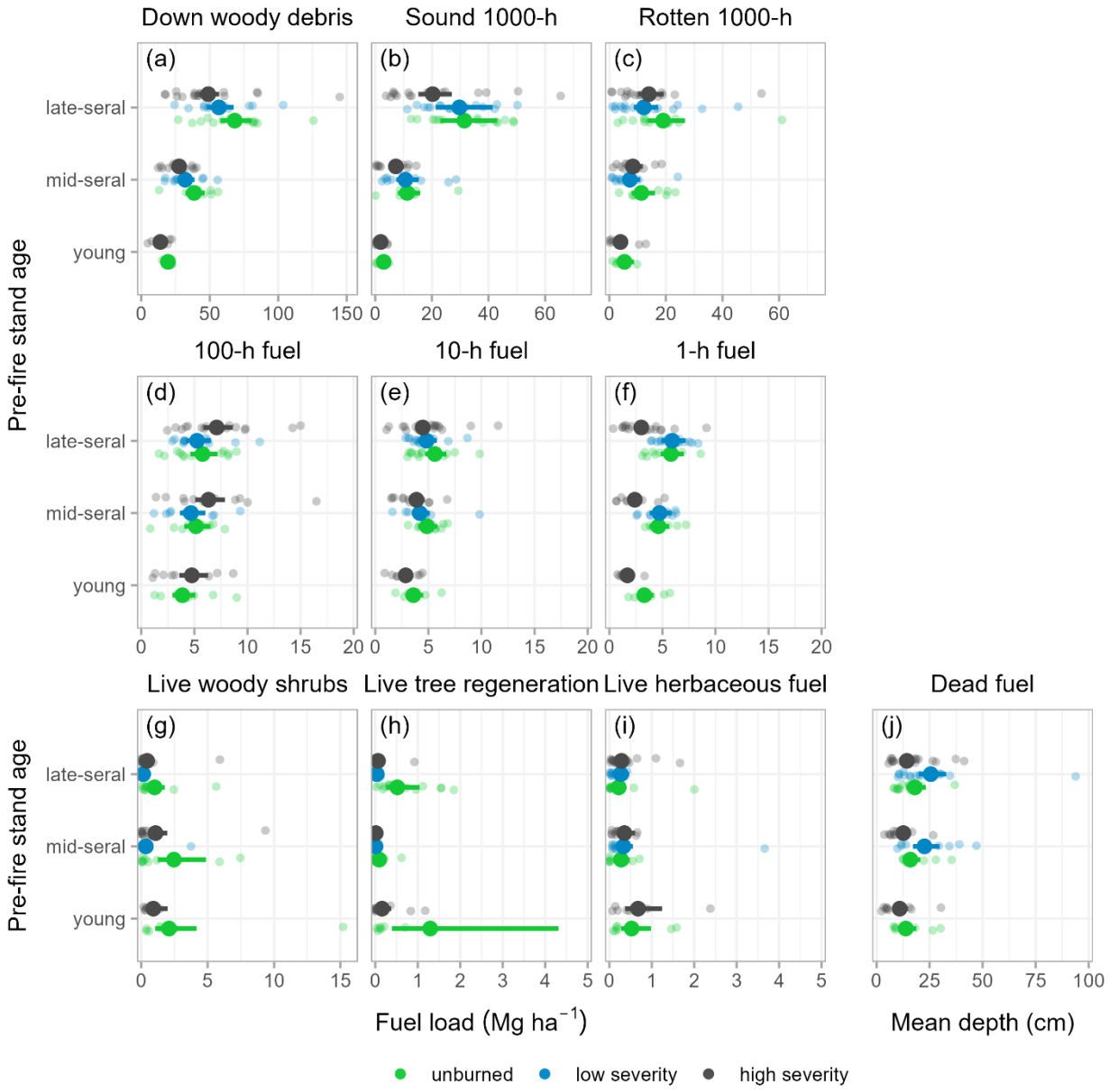

Figure 1.9. Post-fire surface fuel profiles across pre-fire stand age × burn severity strata. Down woody debris (a) includes the sum of all coarse (b–c) and fine (d–f) fuels located on or within two meters above the ground. Dead fuel size class diameters: 1-h, <0.6 cm; 10-h, 0.6–2.5 cm; 100-h, 2.5–7.6 cm; 1000-h, ≥8.0 cm. Live surface fuel (g–i) includes all live woody shrubs (g), tree seedlings and small saplings (h; height < 1.37 m), and herbaceous understory vegetation (i). Dead fuel (j) includes any dead plant material within or above the litter. Bold points and lines are model-predicted means and 95% confidence intervals for each stand age class, colored by burn severity. Translucent points show plot-level values. See Table 1.10 and Table 1.12 for model summaries and outputs.

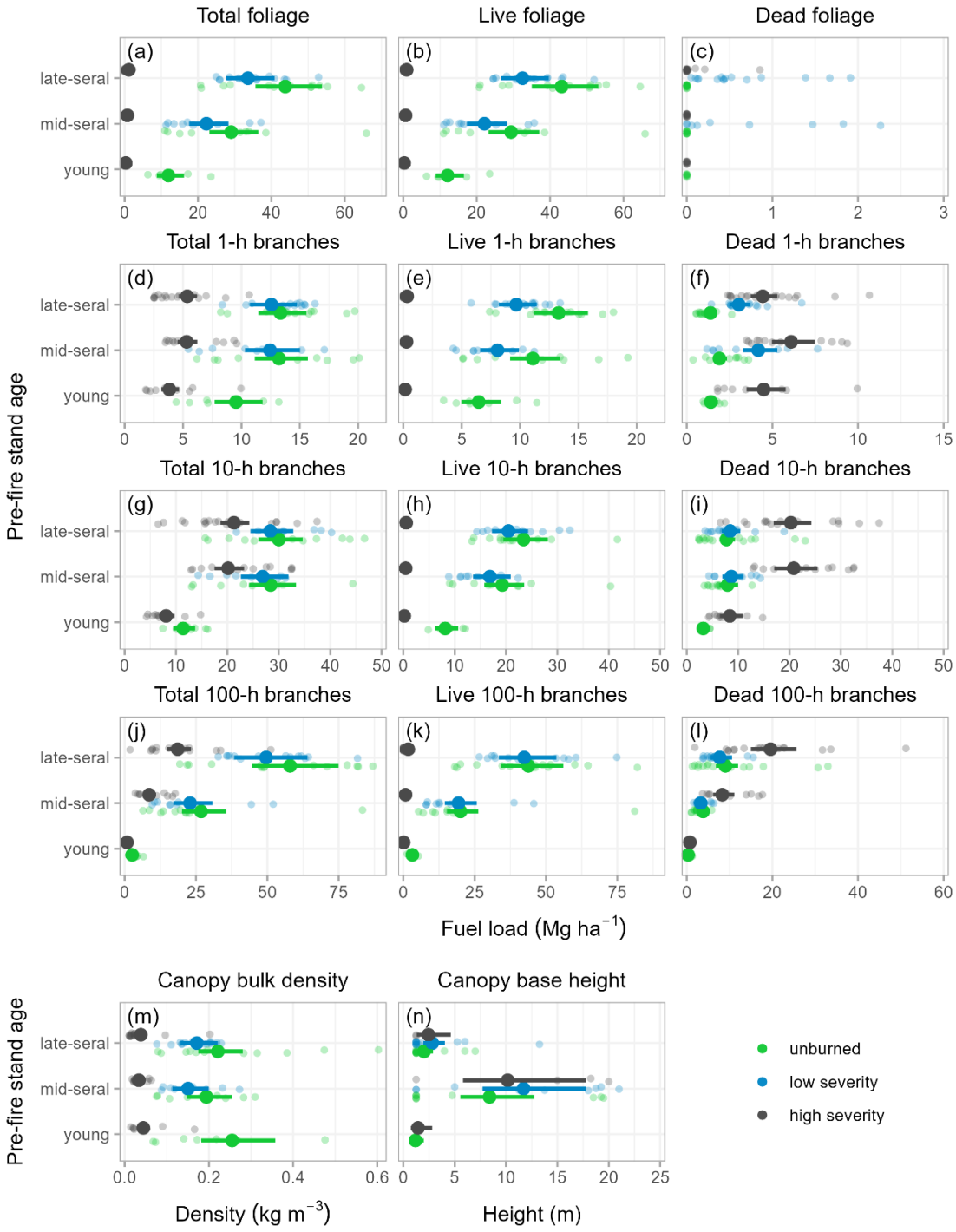

Figure 1.10. Post-fire canopy fuel profiles across pre-fire stand age × burn severity strata. Available canopy fuel includes the sum of live and dead foliage, dead 1-h branches, and half of live 1-h branches. Branch fuel size class diameters: 1-h, <0.6 cm; 10-h, 0.6–2.5 cm; 100-h, 2.5–7.6 cm. Bold points and lines are model-predicted means and 95% confidence intervals for each stand age class, colored by burn severity. Translucent points show plot-level values. Predicted values are not presented for dead foliage (c) due to model convergence failure. See Table 1.10 and Table 1.13 for model summaries and outputs.

B.2 *Model outputs*

Table 1.11. Outputs from generalized linear models testing for effects of pre-fire stand age and burn severity on post-fire aboveground biomass carbon.

Response	**Predictor**	**β**	**SE**	***z***	***p***
Total biomass	young × unburned (intercept)	4.58	0.08	58.08	<0.001
	pre-fire stand age: mid-seral	1.05	0.09	12.10	<0.001
	pre-fire stand age: late-seral	1.27	0.08	15.23	<0.001
	burn severity: low	0.08	0.08	0.97	0.334
	burn severity: high	-0.40	0.07	-5.98	<0.001
Live biomass	young × unburned (intercept)	4.27	0.31	13.96	<0.001
	pre-fire stand age: mid-seral	1.13	0.36	3.13	0.002
	pre-fire stand age: late-seral	1.62	0.34	4.74	<0.001
	burn severity: low	-0.06	0.33	-0.19	0.853
	burn severity: high	-4.36	0.28	-15.55	<0.001
Dead biomass	young × unburned (intercept)	2.68	0.10	28.16	<0.001
	pre-fire stand age: mid-seral	1.09	0.10	10.41	<0.001
	pre-fire stand age: late-seral	1.30	0.10	13.13	<0.001
	burn severity: low	0.24	0.09	2.58	0.010
	burn severity: high	1.47	0.08	18.46	<0.001
Woody biomass	young × unburned (intercept)	4.52	0.08	57.20	<0.001
	pre-fire stand age: mid-seral	1.06	0.09	12.12	<0.001
	pre-fire stand age: late-seral	1.26	0.08	15.18	<0.001
	burn severity: low	0.09	0.08	1.19	0.232
	burn severity: high	-0.34	0.07	-5.05	<0.001
Non-woody biomass	young × unburned (intercept)	2.65	0.25	10.55	<0.001
	pre-fire stand age: mid-seral	-0.11	0.26	-0.43	0.670
	pre-fire stand age: late-seral	0.33	0.24	1.37	0.169
	burn severity: low	-0.10	0.22	-0.45	0.653
	burn severity: high	-4.18	0.20	-21.07	<0.001
Tree biomass – total	young × unburned (intercept)	4.46	0.09	51.86	<0.001
	pre-fire stand age: mid-seral	1.10	0.10	11.31	<0.001
	pre-fire stand age: late-seral	1.28	0.09	13.81	<0.001
	burn severity: low	0.10	0.09	1.09	0.275
	burn severity: high	-0.41	0.08	-5.46	<0.001
Tree biomass – live	young × unburned (intercept)	4.46	0.16	28.09	<0.001
	pre-fire stand age: mid-seral	0.99	0.20	5.01	<0.001
	pre-fire stand age: late-seral	1.28	0.19	6.64	<0.001
	burn severity: low	0.03	0.13	0.21	0.837
	burn severity: high	-2.65	0.21	-12.80	<0.001
Tree biomass – snags	young × unburned (intercept)	0.93	0.17	5.32	<0.001

	pre-fire stand age: mid-seral	1.53	0.18	8.35	<0.001
	pre-fire stand age: late-seral	1.52	0.17	8.80	<0.001
	burn severity: low	1.07	0.16	6.72	<0.001
	burn severity: high	2.88	0.14	20.69	<0.001
Tree biomass – stumps	young × unburned (intercept)	0.58	0.39	1.51	0.132
	pre-fire stand age: mid-seral	-0.85	0.54	-1.56	0.118
	pre-fire stand age: late-seral	-1.94	0.44	-4.45	<0.001
	burn severity: low	-0.05	0.53	-0.09	0.927
	burn severity: high	-0.61	0.39	-1.58	0.114
Stem wood biomass – total	young × unburned (intercept)	4.07	0.09	47.12	<0.001
	pre-fire stand age: mid-seral	1.10	0.10	11.26	<0.001
	pre-fire stand age: late-seral	1.27	0.09	13.57	<0.001
	burn severity: low	0.14	0.09	1.57	0.116
	burn severity: high	-0.29	0.08	-3.84	<0.001
Stem wood biomass – live	young × unburned (intercept)	4.05	0.18	22.09	<0.001
	pre-fire stand age: mid-seral	1.00	0.23	4.40	<0.001
	pre-fire stand age: late-seral	1.26	0.22	5.66	<0.001
	burn severity: low	0.08	0.15	0.53	0.599
	burn severity: high	-2.54	0.24	-10.59	<0.001
Stem wood biomass – dead	young × unburned (intercept)	1.10	0.13	8.25	<0.001
	pre-fire stand age: mid-seral	1.24	0.15	8.27	<0.001
	pre-fire stand age: late-seral	1.26	0.14	8.89	<0.001
	burn severity: low	0.87	0.14	6.42	<0.001
	burn severity: high	2.62	0.12	22.78	<0.001
Stem bark biomass – total	young × unburned (intercept)	2.52	0.12	21.89	<0.001
	pre-fire stand age: mid-seral	1.05	0.13	8.00	<0.001
	pre-fire stand age: late-seral	1.10	0.13	8.74	<0.001
	burn severity: low	0.19	0.12	1.57	0.115
	burn severity: high	-0.29	0.10	-2.90	0.004
Stem bark biomass – live	young × unburned (intercept)	2.54	0.20	12.68	<0.001
	pre-fire stand age: mid-seral	0.90	0.25	3.60	<0.001
	pre-fire stand age: late-seral	1.04	0.24	4.28	<0.001
	burn severity: low	0.14	0.17	0.85	0.394
	burn severity: high	-2.29	0.26	-8.73	<0.001
Stem bark biomass – dead	young × unburned (intercept)	-0.66	0.19	-3.44	0.001
	pre-fire stand age: mid-seral	1.39	0.21	6.60	<0.001
	pre-fire stand age: late-seral	1.18	0.20	5.92	<0.001
	burn severity: low	0.95	0.19	4.95	<0.001
	burn severity: high	2.72	0.16	16.69	<0.001
Down woody debris biomass	young × unburned (intercept)	2.29	0.12	19.26	<0.001
	pre-fire stand age: mid-seral	0.67	0.13	5.27	<0.001
	pre-fire stand age: late-seral	1.25	0.12	10.33	<0.001
	burn severity: low	-0.19	0.11	-1.66	0.097

	burn severity: high	-0.32	0.10	-3.32	0.001
Live understory biomass	young × unburned (intercept)	0.47	0.28	1.69	0.092
	pre-fire stand age: mid-seral	-0.25	0.33	-0.76	0.447
	pre-fire stand age: late-seral	-0.64	0.30	-2.14	0.032
	burn severity: low	-1.26	0.29	-4.26	<0.001
	burn severity: high	-0.73	0.25	-2.96	0.003
Charred wood biomass	young × unburned (intercept)	-3.50	0.33	-10.76	<0.001
	pre-fire stand age: mid-seral	0.19	0.29	0.66	0.510
	pre-fire stand age: late-seral	0.86	0.30	2.86	0.004
	burn severity: low	1.90	0.37	5.10	<0.001
	burn severity: high	2.12	0.34	6.28	<0.001

Notes: Both pre-fire stand age and burn severity were categorical predictors with three levels: young, mid-seral, and late-seral age; unburned, low-, and high-severity. Young unburned stands were incorporated into model intercepts. β, coefficient estimate. SE, standard error. *z*, test statistic. *p*, p-value. Woody biomass includes branches and stems of standing trees, stumps, down woody debris, and woody shrubs. Non-woody biomass includes tree foliage and total mass of herbaceous vegetation. Tree biomass includes foliage, branches, and stems for all live and dead individuals (i.e., large trees, trees, saplings, seedlings, stumps). Stump biomass includes stem wood and bark of trees with broken top and height < 1.37 m. Stem wood and bark biomass include standing trees (height ≥ 1.37 m) and coarse woody debris. Live understory biomass includes woody shrubs, herbaceous vegetation, and tree seedlings and small saplings (height < 1.37 m). Charred wood biomass includes black carbon in charred stem wood on coarse woody debris and standing live and dead trees.

Table 1.12. Outputs from generalized linear models testing for effects of pre-fire stand age and burn severity on post-fire surface fuels.

Response	Predictor	β	SE	*z*	*p*
Down woody debris	young × unburned (intercept)	2.97	0.12	25.06	<0.001
	pre-fire stand age: mid-seral	0.68	0.13	5.33	<0.001
	pre-fire stand age: late-seral	1.26	0.12	10.31	<0.001
	burn severity: low	-0.19	0.11	-1.66	0.096
	burn severity: high	-0.33	0.10	-3.46	0.001
Coarse woody debris – total (1000-h)	young × unburned (intercept)	2.05	0.17	11.93	<0.001
	pre-fire stand age: mid-seral	1.08	0.18	5.91	<0.001
	pre-fire stand age: late-seral	1.88	0.17	10.83	<0.001
	burn severity: low	-0.23	0.16	-1.46	0.144
	burn severity: high	-0.40	0.14	-2.91	0.004
Sound 1000-h	young × unburned (intercept)	1.08	0.24	4.50	<0.001
	pre-fire stand age: mid-seral	1.34	0.26	5.22	<0.001
	pre-fire stand age: late-seral	2.37	0.24	9.77	<0.001
	burn severity: low	-0.06	0.21	-0.27	0.785
	burn severity: high	-0.44	0.19	-2.37	0.018
Rotten 1000-h	young × unburned (intercept)	1.68	0.25	6.65	<0.001
	pre-fire stand age: mid-seral	0.75	0.27	2.82	0.005
	pre-fire stand age: late-seral	1.27	0.26	4.97	<0.001
	burn severity: low	-0.44	0.23	-1.96	0.050
	burn severity: high	-0.31	0.20	-1.56	0.119
Fine woody debris – total (1-, 10-, 100-h)	young × unburned (intercept)	2.38	0.10	23.88	0.000
	pre-fire stand age: mid-seral	0.31	0.11	2.77	0.006
	pre-fire stand age: late-seral	0.46	0.11	4.29	<0.001
	burn severity: low	-0.07	0.10	-0.70	0.487
	burn severity: high	-0.15	0.09	-1.79	0.073
1-h fuel	young × unburned (intercept)	1.19	0.12	9.69	<0.001
	pre-fire stand age: mid-seral	0.34	0.14	2.45	0.014
	pre-fire stand age: late-seral	0.57	0.13	4.30	<0.001
	burn severity: low	0.02	0.12	0.17	0.866
	burn severity: high	-0.66	0.11	-6.20	<0.001
10-h fuel	young × unburned (intercept)	1.28	0.12	10.93	<0.001
	pre-fire stand age: mid-seral	0.30	0.13	2.31	0.021
	pre-fire stand age: late-seral	0.45	0.12	3.60	<0.001
	burn severity: low	-0.15	0.12	-1.29	0.198
	burn severity: high	-0.23	0.10	-2.27	0.023
100-h fuel	young × unburned (intercept)	1.35	0.14	9.53	<0.001
	pre-fire stand age: mid-seral	0.28	0.16	1.76	0.079
	pre-fire stand age: late-seral	0.40	0.15	2.60	0.009
	burn severity: low	-0.09	0.15	-0.65	0.513
	burn severity: high	0.21	0.12	1.68	0.092
Dead fuel depth	young × unburned (intercept)	2.63	0.16	16.61	0.000

	pre-fire stand age: mid-seral	0.15	0.18	0.81	0.417
	pre-fire stand age: late-seral	0.27	0.17	1.59	0.113
	burn severity: low	0.35	0.16	2.16	0.031
	burn severity: high	-0.23	0.14	-1.70	0.090
Duff depth	young × unburned (intercept)	1.36	0.22	6.15	<0.001
	pre-fire stand age: mid-seral	0.39	0.26	1.50	0.135
	pre-fire stand age: late-seral	0.76	0.23	3.24	0.001
	burn severity: low	-0.98	0.22	-4.44	<0.001
	burn severity: high	-2.14	0.20	-10.64	<0.001
Litter depth	young × unburned (intercept)	0.99	0.15	6.60	<0.001
	pre-fire stand age: mid-seral	0.31	0.17	1.83	0.067
	pre-fire stand age: late-seral	0.54	0.16	3.41	0.001
	burn severity: low	-0.49	0.15	-3.26	0.001
	burn severity: high	-1.12	0.13	-8.70	<0.001
Live fuel – total	young × unburned (intercept)	1.21	0.29	4.19	<0.001
	pre-fire stand age: mid-seral	-0.19	0.34	-0.56	0.576
	pre-fire stand age: late-seral	-0.69	0.31	-2.23	0.026
	burn severity: low	-1.37	0.30	-4.53	<0.001
	burn severity: high	-0.70	0.25	-2.79	0.005
Live fuel – woody vegetation	young × unburned (intercept)	0.99	0.35	2.87	0.004
	pre-fire stand age: mid-seral	0.04	0.42	0.08	0.933
	pre-fire stand age: late-seral	-0.62	0.37	-1.66	0.096
	burn severity: low	-2.08	0.37	-5.62	<0.001
	burn severity: high	-1.00	0.31	-3.26	0.001
Live fuel – herbaceous vegetation	young × unburned (intercept)	-0.64	0.32	-2.02	0.044
	pre-fire stand age: mid-seral	-0.64	0.37	-1.73	0.084
	pre-fire stand age: late-seral	-0.86	0.33	-2.58	0.010
	burn severity: low	0.19	0.32	0.59	0.554
	burn severity: high	0.25	0.27	0.93	0.353
Live fuel – woody shrubs	young × unburned (intercept)	0.74	0.35	2.09	0.037
	pre-fire stand age: mid-seral	0.16	0.45	0.37	0.715
	pre-fire stand age: late-seral	-0.73	0.40	-1.82	0.068
	burn severity: low	-1.97	0.39	-4.98	<0.001
	burn severity: high	-0.83	0.33	-2.52	0.012
Live tree seedlings & small saplings – total	young × unburned (intercept)	0.26	0.61	0.42	0.675
	pre-fire stand age: mid-seral	-2.63	0.61	-4.33	<0.001
	pre-fire stand age: late-seral	-0.91	0.56	-1.62	0.106
	burn severity: low	-2.71	0.48	-5.65	<0.001
	burn severity: high	-2.10	0.46	-4.57	<0.001
Live tree seedlings & small saplings – conifer	young × unburned (intercept)	-2.06	0.33	-6.17	<0.001
	pre-fire stand age: mid-seral	0.08	0.41	0.20	0.839
	pre-fire stand age: late-seral	1.65	0.39	4.27	<0.001
	burn severity: low	-3.13	0.37	-8.53	<0.001
	burn severity: high	-6.32	0.31	-20.09	<0.001
Live tree seedlings	young × unburned (intercept)	-2.06	0.33	-6.17	<0.001

& small saplings – broadleaf	pre-fire stand age: mid-seral	0.08	0.41	0.20	0.839
	pre-fire stand age: late-seral	1.65	0.39	4.27	<0.001
	burn severity: low	-3.13	0.37	-8.53	<0.001
	burn severity: high	-6.32	0.31	-20.09	<0.001

Notes: Both pre-fire stand age and burn severity were categorical predictors with three levels: young, mid-seral, and late-seral age; unburned, low-, and high-severity. Young unburned stands were incorporated into model intercepts. β, coefficient estimate. SE, standard error. *z*, test statistic. *p*, p-value.

Table 1.13. Outputs from generalized linear models testing for effects of pre-fire stand age and burn severity on post-fire canopy fuels.

Response	Predictor	β	SE	*z*	*p*
Available canopy fuel – total	young × unburned (intercept)	3.20	0.13	25.19	<0.001
	pre-fire stand age: mid-seral	0.40	0.13	3.01	0.003
	pre-fire stand age: late-seral	0.57	0.13	4.43	<0.001
	burn severity: low	-0.10	0.12	-0.83	0.404
	burn severity: high	-1.96	0.10	-19.10	<0.001
Available canopy fuel – live	young × unburned (intercept)	2.73	0.15	17.66	<0.001
	pre-fire stand age: mid-seral	0.82	0.19	4.34	<0.001
	pre-fire stand age: late-seral	1.18	0.18	6.45	<0.001
	burn severity: low	-0.29	0.13	-2.29	0.022
	burn severity: high	-3.82	0.20	-19.52	<0.001
Available canopy fuel – dead	young × unburned (intercept)	0.34	0.13	2.57	0.010
	pre-fire stand age: mid-seral	0.31	0.15	2.10	0.035
	pre-fire stand age: late-seral	-0.01	0.14	-0.06	0.954
	burn severity: low	0.97	0.13	7.28	<0.001
	burn severity: high	1.17	0.11	10.38	<0.001
Canopy bulk density	young × unburned (intercept)	-1.37	0.17	-7.91	<0.001
	pre-fire stand age: mid-seral	-0.27	0.19	-1.47	0.141
	pre-fire stand age: late-seral	-0.14	0.18	-0.82	0.413
	burn severity: low	-0.26	0.16	-1.58	0.115
	burn severity: high	-1.75	0.14	-12.45	<0.001
Canopy base height	young × unburned (intercept)	0.17	0.26	0.64	0.522
	pre-fire stand age: mid-seral	1.96	0.32	6.22	<0.001
	pre-fire stand age: late-seral	0.53	0.31	1.72	0.085
	burn severity: low	0.33	0.23	1.46	0.144
	burn severity: high	0.19	0.31	0.61	0.541
Foliage – total	young × unburned (intercept)	2.48	0.16	15.86	<0.001
	pre-fire stand age: mid-seral	0.89	0.19	4.62	<0.001
	pre-fire stand age: late-seral	1.30	0.19	7.00	<0.001
	burn severity: low	-0.26	0.13	-2.07	0.039
	burn severity: high	-3.66	0.20	-18.35	<0.001
Foliage – live	young × unburned (intercept)	2.49	0.16	15.56	<0.001
	pre-fire stand age: mid-seral	0.89	0.20	4.52	<0.001
	pre-fire stand age: late-seral	1.27	0.19	6.72	<0.001
	burn severity: low	-0.28	0.13	-2.17	0.030
	burn severity: high	-3.85	0.20	-18.94	<0.001
Branches – total	young × unburned (intercept)	3.18	0.11	30.24	<0.001
	pre-fire stand age: mid-seral	1.03	0.12	8.77	<0.001
	pre-fire stand age: late-seral	1.36	0.11	12.22	<0.001
	burn severity: low	-0.05	0.10	-0.47	0.640

	burn severity: high	-0.68	0.09	-7.58	<0.001
Branches – live	young × unburned (intercept)	2.85	0.15	18.47	<0.001
	pre-fire stand age: mid-seral	1.08	0.19	5.67	<0.001
	pre-fire stand age: late-seral	1.58	0.18	8.54	<0.001
	burn severity: low	-0.13	0.13	-1.02	0.306
	burn severity: high	-3.50	0.20	-17.69	<0.001
Branches – dead	young × unburned (intercept)	1.64	0.13	12.42	<0.001
	pre-fire stand age: mid-seral	1.00	0.15	6.62	<0.001
	pre-fire stand age: late-seral	1.25	0.14	8.87	<0.001
	burn severity: low	0.08	0.13	0.63	0.530
	burn severity: high	0.92	0.11	8.14	<0.001
1-h branches – total	young × unburned (intercept)	2.26	0.11	20.76	<0.001
	pre-fire stand age: mid-seral	0.33	0.12	2.77	0.006
	pre-fire stand age: late-seral	0.34	0.11	2.98	0.003
	burn severity: low	-0.06	0.10	-0.58	0.563
	burn severity: high	-0.91	0.09	-10.18	<0.001
1-h branches – live	young × unburned (intercept)	1.87	0.13	14.01	<0.001
	pre-fire stand age: mid-seral	0.54	0.16	3.32	0.001
	pre-fire stand age: late-seral	0.72	0.16	4.60	<0.001
	burn severity: low	-0.32	0.11	-2.94	0.003
	burn severity: high	-3.70	0.17	-21.94	<0.001
1-h branches – dead	young × unburned (intercept)	0.34	0.13	2.59	0.010
	pre-fire stand age: mid-seral	0.30	0.15	2.08	0.038
	pre-fire stand age: late-seral	-0.01	0.14	-0.09	0.927
	burn severity: low	0.79	0.13	5.93	<0.001
	burn severity: high	1.16	0.11	10.33	<0.001
10-h branches – total	young × unburned (intercept)	2.43	0.10	25.51	<0.001
	pre-fire stand age: mid-seral	0.91	0.11	8.49	<0.001
	pre-fire stand age: late-seral	0.97	0.10	9.44	<0.001
	burn severity: low	-0.06	0.10	-0.58	0.559
	burn severity: high	-0.34	0.08	-4.19	<0.001
10-h branches – live	young × unburned (intercept)	2.10	0.14	15.15	<0.001
	pre-fire stand age: mid-seral	0.86	0.17	5.04	<0.001
	pre-fire stand age: late-seral	1.06	0.17	6.36	<0.001
	burn severity: low	-0.13	0.11	-1.17	0.240
	burn severity: high	-3.73	0.18	-21.05	<0.001
10-h branches – dead	young × unburned (intercept)	1.16	0.13	8.80	<0.001
	pre-fire stand age: mid-seral	0.91	0.15	6.00	<0.001
	pre-fire stand age: late-seral	0.88	0.14	6.23	<0.001
	burn severity: low	0.09	0.13	0.66	0.508
	burn severity: high	0.96	0.11	8.41	<0.001
100-h branches – total	young × unburned (intercept)	0.97	0.16	5.95	<0.001
	pre-fire stand age: mid-seral	2.32	0.19	11.94	<0.001

	pre-fire stand age: late-seral	3.09	0.18	16.73	<0.001
	burn severity: low	-0.16	0.17	-0.92	0.359
	burn severity: high	-1.14	0.15	-7.80	<0.001
100-h branches – live	young × unburned (intercept)	1.15	0.20	5.75	<0.001
	pre-fire stand age: mid-seral	1.84	0.24	7.55	<0.001
	pre-fire stand age: late-seral	2.63	0.24	11.08	<0.001
	burn severity: low	-0.03	0.15	-0.22	0.823
	burn severity: high	-3.24	0.26	-12.35	<0.001
100-h branches – dead	young × unburned (intercept)	-1.11	0.20	-5.65	<0.001
	pre-fire stand age: mid-seral	2.45	0.23	10.51	<0.001
	pre-fire stand age: late-seral	3.31	0.21	15.42	<0.001
	burn severity: low	-0.16	0.20	-0.79	0.429
	burn severity: high	0.77	0.17	4.49	<0.001
1000-h branches – live	young × unburned (intercept)	-3.46	0.55	-6.23	<0.001
	pre-fire stand age: mid-seral	2.43	0.60	4.08	<0.001
	pre-fire stand age: late-seral	2.97	0.60	4.97	<0.001
	burn severity: low	0.40	0.25	1.63	0.103
	burn severity: high	-1.48	0.41	-3.63	<0.001
Crown mass – total (foliage + branches)	young × unburned (intercept)	3.58	0.11	33.87	<0.001
	pre-fire stand age: mid-seral	1.00	0.12	8.52	<0.001
	pre-fire stand age: late-seral	1.34	0.11	11.89	<0.001
	burn severity: low	-0.11	0.11	-1.05	0.292
	burn severity: high	-1.05	0.09	-11.70	<0.001
Crown mass – live (foliage + branches)	young × unburned (intercept)	3.37	0.15	22.02	<0.001
	pre-fire stand age: mid-seral	1.01	0.19	5.32	<0.001
	pre-fire stand age: late-seral	1.47	0.18	8.03	<0.001
	burn severity: low	-0.18	0.13	-1.44	0.149
	burn severity: high	-3.61	0.20	-18.40	<0.001
Crown mass – dead (foliage + branches)	young × unburned (intercept)	1.64	0.13	12.36	<0.001
	pre-fire stand age: mid-seral	1.00	0.15	6.61	<0.001
	pre-fire stand age: late-seral	1.24	0.14	8.83	<0.001
	burn severity: low	0.12	0.13	0.91	0.363
	burn severity: high	0.92	0.11	8.11	<0.001

Notes: Both pre-fire stand age and burn severity were categorical predictors with three levels: young, mid-seral, and late-seral age; unburned, low-, and high-severity. Young unburned stands were incorporated into model intercepts. Outputs are not reported for dead foliage due to model convergence failure. Outputs are only presented for live 1000-h branches since no dead 1000-h branches were observed. β, coefficient estimate. SE, standard error. *z*, test statistic. *p*, p-value.

B.3 *Marginal comparisons among predictors*

Table 1.14. Comparison between mean effect size of pre-fire stand age and burn severity on post-fire aboveground biomass carbon and fuels components. Mean effect size is the average absolute difference in predicted means for pairwise comparisons across all levels of a predictor. Mean effect sizes are on the response scale (i.e., Mg ha^{-1}, unless otherwise indicated). Ratios compare mean effect sizes between predictors, with the effect size of the dominant predictor (i.e., predictor with the greater mean effect size) as the antecedent.

Response	Mean effect size (range)		Dominant predictor	Ratio
	Pre-fire stand age	Burn severity		
Aboveground biomass carbon (Mg C ha^{-1})				
Total	145.99 (58.09–218.98)	76.94 (22.26–115.40)	pre-fire stand age	1.9
Live	109.20 (79.98–163.79)	174.20 (15.70–261.31)	burn severity	1.6
Dead	64.65 (25.14–96.98)	96.65 (11.75–144.98)	burn severity	1.5
Woody	140.3 (54.51–210.45)	68.18 (26.14–102.27)	pre-fire stand age	2.1
Non-woody	2.62 (0.82–3.93)	10.83 (1.56–16.24)	burn severity	4.1
All trees	132.92 (45.57–199.39)	74.95 (26.16–112.42)	pre-fire stand age	1.8
Live trees	58.15 (30.41–87.22)	99.96 (4.30–149.94)	burn severity	1.7
Snags	51.89 (0.95–77.83)	110.25 (18.79–165.38)	burn severity	2.1
Stumps	0.62 (0.31–0.93)	0.16 (0.03–0.24)	pre-fire stand age	3.8
Stem wood – total	92.32 (29.27–138.48)	45.94 (25.84–68.91)	pre-fire stand age	2.0
Stem wood – live	38.44 (18.38–57.66)	68.61 (8.53–102.92)	burn severity	1.8
Stem wood – dead	34.24 (1.09–51.36)	78.05 (12.72–117.08)	burn severity	2.3
Stem bark – total	15.55 (1.54–23.32)	9.96 (6.73–14.95)	pre-fire stand age	1.6
Stem bark – live	6.47 (2.06–9.7)	13.48 (2.93–20.22)	burn severity	2.1
Stem bark – dead	7.81 (2.97–11.71)	15.25 (2.53–22.87)	burn severity	2.0
Down woody debris	13.69 (7.94–20.54)	4.66 (2.67–7.00)	pre-fire stand age	2.9
Live understory	0.30 (0.21–0.46)	0.53 (0.22–0.80)	burn severity	1.7
Charred wood	0.12 (0.03–0.17)	0.20 (0.07–0.29)	burn severity	1.7

Surface fuels (Mg ha^{-1})				
Down woody debris	27.19 (15.95–40.78)	9.57 (5.79–14.36)	pre-fire stand age	2.8
Coarse woody debris – total (1000-h)	23.31 (12.27–34.97)	7.68 (4.33–11.52)	pre-fire stand age	3.0
Sound 1000-h	15.52 (6.79–23.28)	4.70 (1.10–7.04)	pre-fire stand age	3.3
Rotten 1000-h	7.17 (4.70–10.75)	3.37 (1.32–5.06)	pre-fire stand age	2.1
Fine woody debris – total (1-, 10-, 100-h)	3.86 (2.14–5.79)	1.45 (1.03–2.17)	pre-fire stand age	2.7
1-h fuel	1.35 (0.94–2.02)	1.68 (0.11–2.51)	burn severity	1.2
10-h fuel	1.18 (0.65–1.77)	0.68 (0.32–1.02)	pre-fire stand age	1.7
100-h fuel	1.36 (0.67–2.04)	1.12 (0.47–1.68)	pre-fire stand age	1.2
Dead fuel depth (cm)	2.90 (2.13–4.35)	6.92 (3.48–10.38)	burn severity	2.4
Duff depth (cm)	1.30 (0.83–1.95)	3.71 (1.63–5.57)	burn severity	2.9
Litter depth (cm)	0.80 (0.59–1.19)	1.79 (1.15–2.68)	burn severity	2.2
Live fuel – total	0.67 (0.35–1.00)	1.16 (0.56–1.74)	burn severity	1.7
Live fuel – woody vegetation	0.46 (0.05–0.69)	1.23 (0.51–1.84)	burn severity	2.7
Live fuel – herbaceous vegetation	0.24 (0.06–0.36)	0.06 (0.02–0.08)	pre-fire stand age	4.2
Live fuel – woody shrubs	0.53 (0.20–0.79)	0.95 (0.49–1.43)	burn severity	1.8
Live seedlings & small saplings – total	0.32 (0.17–0.47)	0.32 (0.03–0.48)	burn severity	1.0
Live seedlings & small saplings – conifer	0.12 (0.00–0.18)	0.27 (0.02–0.40)	burn severity	2.2
Live seedlings & small saplings – broadleaf	0.04 (0.02–0.06)	0.03 (0.01–0.04)	pre-fire stand age	1.5
Canopy fuels (Mg ha^{-1})				
Available canopy fuel – total	7.68 (4.03–11.52)	21.7 (3.24–32.55)	burn severity	2.8
Available canopy fuel – live	7.65 (4.9–11.47)	16.24 (6.06–24.35)	burn severity	2.1
Available canopy fuel – dead	0.81 (0.03–1.22)	2.31 (0.93–3.47)	burn severity	2.8
Canopy bulk density (kg m^{-3})	0.02 (0.02–0.04)	0.12 (0.05–0.18)	burn severity	5.0
Canopy base height (m)	5.66 (0.98–8.49)	1.10 (0.77–1.65)	pre-fire stand age	5.2

Foliage – total	7.24 (5.03–10.86)	14.01 (5.02–21.02)	burn severity	1.9
Foliage – live	6.99 (4.65–10.49)	14.00 (5.30–21.00)	burn severity	2.0
Branches – total	36.21 (20.69–54.31)	23.63 (2.71–35.44)	pre-fire stand age	1.5
Branches – live	36.56 (21.15–54.84)	24.11 (3.50–36.16)	pre-fire stand age	1.5
Branches – dead	15.88 (11.74–23.82)	25.57 (4.82–38.36)	burn severity	1.6
1-h branches – total	14.12 (6.55–21.18)	14.63 (1.26–21.95)	burn severity	1.0
1-h branches – live	1.86 (0.09–2.79)	5.05 (0.74–7.58)	burn severity	2.7
1-h branches – dead	1.52 (0.74–2.29)	4.77 (2.00–7.16)	burn severity	3.1
10-h branches – total	0.77 (0.04–1.15)	2.29 (1.57–3.43)	burn severity	3.0
10-h branches – live	10.72 (1.37–16.08)	5.11 (1.44–7.66)	pre-fire stand age	2.1
10-h branches – dead	3.64 (1.48–5.46)	8.14 (1.57–12.21)	burn severity	2.2
100-h branches – total	5.40 (0.36–8.10)	7.60 (0.65–11.40)	burn severity	1.4
100-h branches – live	24.72 (16.2–37.08)	17.24 (5.50–25.86)	pre-fire stand age	1.4
100-h branches – dead	10.05 (6.25–15.07)	11.82 (0.62–17.72)	burn severity	1.2
1000-h branches – live	8.35 (5.02–12.52)	5.09 (0.85–7.64)	pre-fire stand age	1.6
Crown mass – total (foliage + branches)	47.05 (27.11–70.58)	46.45 (11.24–69.67)	pre-fire stand age	1.0
Crown mass – live (foliage + branches)	22.91 (16.52–34.37)	39.59 (10.14–59.39)	burn severity	1.7
Crown mass – dead (foliage + branches)	14.2 (6.54–21.30)	14.64 (1.87–21.97)	burn severity	1.1

Notes: Mean effect sizes are not presented for dead foliage due to model convergence failure. Mean effect sizes are only presented for live 1000-h branches since no dead 1000-h branches were observed.

Table 1.15. Marginal comparisons of the effects of pre-fire stand age and burn severity on post-fire aboveground biomass carbon and fuels components. Estimates represent the difference in model predicted means for all pairwise contrasts between levels of a predictor. Estimates are on the response scale (i.e., Mg ha^{-1}, unless otherwise indicated).

Response	Predictor	Contrast	Estimate	SE	*z*	*p*
Aboveground biomass carbon (Mg C ha^{-1})						
Total	burn severity	high − low	-115.40	19.59	-5.89	<0.001
		high − unburned	-93.14	16.62	-5.60	<0.001
		low − unburned	22.26	23.14	0.96	0.336
	pre-fire stand age	late-seral − mid-seral	58.09	17.37	3.34	0.001
		late-seral − young	218.98	13.81	15.86	<0.001
		mid-seral − young	160.89	13.72	11.73	<0.001
Live	burn severity	high − low	-245.60	59.29	-4.14	<0.001
		high − unburned	-261.31	60.75	-4.30	<0.001
		low − unburned	-15.70	84.85	-0.19	0.853
	pre-fire stand age	late-seral − mid-seral	79.98	44.71	1.79	0.074
		late-seral − young	163.79	41.41	3.96	<0.001
		mid-seral − young	83.81	29.11	2.88	0.004
Dead	burn severity	high − low	133.22	10.98	12.14	<0.001
		high − unburned	144.98	10.39	13.95	<0.001
		low − unburned	11.75	4.65	2.53	0.012
	pre-fire stand age	late-seral − mid-seral	25.14	9.11	2.76	0.006
		late-seral − young	96.98	7.72	12.57	<0.001
		mid-seral − young	71.84	7.45	9.65	<0.001
Woody	burn severity	high − low	-102.27	18.92	-5.40	<0.001
		high − unburned	-76.12	15.87	-4.80	<0.001
		low − unburned	26.14	21.99	1.19	0.235
	pre-fire stand age	late-seral − mid-seral	54.51	16.78	3.25	0.001
		late-seral − young	210.45	13.31	15.82	<0.001
		mid-seral − young	155.94	13.28	11.75	<0.001
Non-woody	burn severity	high − low	-14.68	2.52	-5.84	<0.001
		high − unburned	-16.24	2.42	-6.72	<0.001
		low − unburned	-1.56	3.45	-0.45	0.651
	pre-fire stand age	late-seral − mid-seral	3.93	1.66	2.37	0.018
		late-seral − young	3.12	2.07	1.51	0.131
		mid-seral − young	-0.82	1.98	-0.41	0.679
All trees	burn severity	high − low	-112.42	20.42	-5.51	<0.001
		high − unburned	-86.26	16.91	-5.10	<0.001
		low − unburned	26.16	24.09	1.09	0.277
	pre-fire stand age	late-seral − mid-seral	45.57	18.18	2.51	0.012
		late-seral − young	199.39	14.14	14.10	<0.001
		mid-seral − young	153.82	14.39	10.69	<0.001

Live trees	burn severity	high − low	-149.94	15.01	-9.99	<0.001
		high − unburned	-145.65	14.23	-10.24	<0.001
		low − unburned	4.30	20.92	0.21	0.837
	pre-fire stand age	late-seral − mid-seral	30.41	13.29	2.29	0.022
		late-seral − young	87.22	11.66	7.48	<0.001
		mid-seral − young	56.81	10.76	5.28	<0.001
Snags	burn severity	high − low	146.59	17.45	8.40	<0.001
		high − unburned	165.38	17.01	9.72	<0.001
		low − unburned	18.79	3.52	5.33	<0.001
	pre-fire stand age	late-seral − mid-seral	-0.95	13.08	-0.07	0.942
		late-seral − young	76.88	10.35	7.43	<0.001
		mid-seral − young	77.83	12.21	6.38	<0.001
Stumps	burn severity	high − low	-0.22	0.27	-0.82	0.411
		high − unburned	-0.24	0.16	-1.57	0.117
		low − unburned	-0.03	0.27	-0.09	0.926
	pre-fire stand age	late-seral − mid-seral	-0.31	0.17	-1.83	0.067
		late-seral − young	-0.93	0.42	-2.24	0.025
		mid-seral − young	-0.62	0.47	-1.32	0.186
Stem wood – total	burn severity	high − low	-68.91	14.51	-4.75	<0.001
		high − unburned	-43.07	11.69	-3.69	<0.001
		low − unburned	25.84	16.59	1.56	0.119
	pre-fire stand age	late-seral − mid-seral	29.27	12.88	2.27	0.023
		late-seral − young	138.48	9.96	13.91	<0.001
		mid-seral − young	109.21	10.25	10.65	<0.001
Stem wood – live	burn severity	high − low	-102.92	11.95	-8.62	<0.001
		high − unburned	-94.39	10.78	-8.76	<0.001
		low − unburned	8.53	16.26	0.52	0.600
	pre-fire stand age	late-seral − mid-seral	18.38	10.37	1.77	0.076
		late-seral − young	57.66	8.98	6.42	<0.001
		mid-seral − young	39.28	8.46	4.64	<0.001
Stem wood – dead	burn severity	high − low	104.36	10.23	10.20	<0.001
		high − unburned	117.08	9.92	11.81	<0.001
		low − unburned	12.72	2.34	5.44	<0.001
	pre-fire stand age	late-seral − mid-seral	1.09	7.93	0.14	0.890
		late-seral − young	51.36	6.21	8.28	<0.001
		mid-seral − young	50.26	7.17	7.01	<0.001
Stem bark – total	burn severity	high − low	-14.95	3.82	-3.92	<0.001
		high − unburned	-8.22	2.96	-2.78	0.005
		low − unburned	6.73	4.34	1.55	0.121
	pre-fire stand age	late-seral − mid-seral	1.54	3.35	0.46	0.646
		late-seral − young	23.32	2.52	9.25	<0.001
		mid-seral − young	21.78	2.84	7.67	<0.001
Stem bark – live	burn severity	high − low	-20.22	2.62	-7.70	<0.001

		high − unburned	-17.29	2.21	-7.84	<0.001
		low − unburned	2.93	3.46	0.85	0.398
	pre-fire stand age	late-seral − mid-seral	2.06	2.23	0.92	0.356
		late-seral − young	9.70	1.95	4.98	<0.001
		mid-seral − young	7.64	1.98	3.86	<0.001
Stem bark – dead	burn severity	high − low	20.34	2.83	7.18	<0.001
		high − unburned	22.87	2.76	8.30	<0.001
		low − unburned	2.53	0.62	4.09	<0.001
	pre-fire stand age	late-seral − mid-seral	-2.97	2.31	-1.29	0.198
		late-seral − young	8.74	1.57	5.58	<0.001
		mid-seral − young	11.71	2.25	5.21	<0.001
Down woody debris	burn severity	high − low	-2.67	2.15	-1.24	0.215
		high − unburned	-7.00	2.20	-3.17	0.001
		low − unburned	-4.33	2.61	-1.66	0.097
	pre-fire stand age	late-seral − mid-seral	12.60	2.06	6.12	<0.001
		late-seral − young	20.54	1.92	10.72	<0.001
		mid-seral − young	7.94	1.46	5.42	<0.001
Live understory	burn severity	high − low	0.22	0.11	1.95	0.051
		high − unburned	-0.58	0.23	-2.56	0.010
		low − unburned	-0.80	0.22	-3.58	<0.001
	pre-fire stand age	late-seral − mid-seral	-0.24	0.16	-1.48	0.139
		late-seral − young	-0.46	0.26	-1.77	0.077
		mid-seral − young	-0.21	0.29	-0.73	0.464
Charred wood	burn severity	high − low	0.07	0.06	1.08	0.281
		high − unburned	0.29	0.04	6.83	<0.001
		low − unburned	0.23	0.05	5.00	<0.001
	pre-fire stand age	late-seral − mid-seral	0.15	0.05	3.09	0.002
		late-seral − young	0.17	0.05	3.18	0.001
		mid-seral − young	0.03	0.04	0.69	0.492
Surface fuels (Mg ha^{-1})						
Down woody debris	burn severity	high − low	-5.79	4.23	-1.37	0.171
		high − unburned	-14.36	4.34	-3.30	0.001
		low − unburned	-8.57	5.15	-1.66	0.096
	pre-fire stand age	late-seral − mid-seral	24.83	4.02	6.17	<0.001
		late-seral − young	40.78	3.76	10.84	<0.001
		mid-seral − young	15.95	2.89	5.52	<0.001
Coarse woody debris – total (1000-h)	burn severity	high − low	-4.33	3.95	-1.09	0.274
		high − unburned	-11.52	4.20	-2.74	0.006
		low − unburned	-7.19	4.94	-1.46	0.145
	pre-fire stand age	late-seral – mid-seral	22.70	3.89	5.83	<0.001
		late-seral − young	34.97	3.56	9.83	<0.001
		mid-seral − young	12.27	2.12	5.79	<0.001
Sound 1000-h	burn severity	high − low	-5.94	3.37	-1.77	0.078

		high − unburned	-7.04	3.17	-2.22	0.026
		low − unburned	-1.10	4.04	-0.27	0.785
	pre-fire stand age	late-seral − mid-seral	16.49	3.08	5.35	<0.001
		late-seral − young	23.28	2.86	8.13	<0.001
		mid-seral − young	6.79	1.36	5.01	<0.001
Rotten 1000-h	burn severity	high − low	1.32	2.10	0.63	0.530
		high − unburned	-3.74	2.49	-1.50	0.133
		low − unburned	-5.06	2.64	-1.92	0.055
	pre-fire stand age	late-seral − mid-seral	6.05	2.20	2.75	0.006
		late-seral − young	10.75	2.05	5.24	<0.001
		mid-seral − young	4.70	1.60	2.94	0.003
Fine woody debris – total (1-, 10-, 100-h)	burn severity	high − low	-1.14	1.30	-0.88	0.381
		high − unburned	-2.17	1.23	-1.76	0.078
		low − unburned	-1.03	1.47	-0.70	0.485
	pre-fire stand age	late-seral − mid-seral	2.14	1.19	1.79	0.073
		late-seral − young	5.79	1.24	4.66	<0.001
		mid-seral − young	3.65	1.27	2.87	0.004
1-h fuel	burn severity	high − low	-2.51	0.50	-4.98	<0.001
		high − unburned	-2.41	0.44	-5.45	<0.001
		low − unburned	0.11	0.63	0.17	0.867
	pre-fire stand age	late-seral − mid-seral	0.94	0.42	2.25	0.025
		late-seral − young	2.02	0.43	4.71	<0.001
		mid-seral − young	1.08	0.42	2.55	0.011
10-h fuel	burn severity	high − low	-0.32	0.46	-0.69	0.491
		high − unburned	-1.02	0.46	-2.21	0.027
		low − unburned	-0.70	0.54	-1.29	0.196
	pre-fire stand age	late-seral − mid-seral	0.65	0.44	1.50	0.134
		late-seral − young	1.77	0.45	3.90	<0.001
		mid-seral − young	1.12	0.47	2.38	0.017
100-h fuel	burn severity	high − low	1.68	0.74	2.27	0.023
		high − unburned	1.21	0.71	1.69	0.090
		low − unburned	-0.47	0.72	-0.66	0.511
	pre-fire stand age	late-seral − mid-seral	0.67	0.69	0.98	0.326
		late-seral − young	2.04	0.73	2.79	0.005
		mid-seral − young	1.37	0.75	1.81	0.070
Dead fuel depth (cm)	burn severity	high − low	-10.38	3.06	-3.39	0.001
		high − unburned	-3.48	2.11	-1.65	0.099
		low − unburned	6.90	3.33	2.07	0.038
	pre-fire stand age	late-seral − mid-seral	2.13	2.27	0.94	0.347
		late-seral − young	4.35	2.58	1.69	0.092
		mid-seral − young	2.21	2.66	0.83	0.406
Duff depth (cm)	burn severity	high − low	-1.63	0.41	-4.00	<0.001
		high − unburned	-5.57	0.94	-5.95	<0.001

		low − unburned	-3.94	1.01	-3.90	<0.001
	pre-fire stand age	late-seral − mid-seral	1.12	0.62	1.82	0.069
		late-seral − young	1.95	0.58	3.33	0.001
		mid-seral − young	0.83	0.54	1.52	0.128
Litter depth (cm)	burn severity	high − low	-1.15	0.29	-3.92	<0.001
		high − unburned	-2.68	0.41	-6.60	<0.001
		low − unburned	-1.53	0.48	-3.19	0.001
	pre-fire stand age	late-seral − mid-seral	0.60	0.31	1.91	0.057
		late-seral − young	1.19	0.33	3.67	<0.001
		mid-seral − young	0.59	0.31	1.90	0.058
Live fuel – total	burn severity	high − low	0.56	0.24	2.37	0.018
		high − unburned	-1.18	0.48	-2.44	0.015
		low − unburned	-1.74	0.47	-3.68	<0.001
	pre-fire stand age	late-seral − mid-seral	-0.65	0.37	-1.77	0.077
		late-seral − young	-1.00	0.56	-1.80	0.072
		mid-seral − young	-0.35	0.65	-0.54	0.587
Live fuel – woody vegetation	burn severity	high − low	0.51	0.18	2.92	0.004
		high − unburned	-1.33	0.52	-2.57	0.010
		low − unburned	-1.84	0.51	-3.61	<0.001
	pre-fire stand age	late-seral − mid-seral	-0.69	0.39	-1.79	0.074
		late-seral − young	-0.64	0.46	-1.38	0.167
		mid-seral − young	0.05	0.59	0.08	0.933
Live fuel – herbaceous vegetation	burn severity	high – low	0.02	0.11	0.20	0.843
		high − unburned	0.08	0.09	0.93	0.352
		low − unburned	0.06	0.11	0.57	0.566
	pre-fire stand age	late-seral − mid-seral	-0.06	0.08	-0.77	0.442
		late-seral − young	-0.36	0.19	-1.92	0.055
		mid-seral − young	-0.29	0.20	-1.48	0.139
Live fuel – woody shrubs	burn severity	high − low	0.49	0.17	2.82	0.005
		high − unburned	-0.94	0.44	-2.11	0.035
		low − unburned	-1.43	0.43	-3.29	0.001
	pre-fire stand age	late-seral − mid-seral	-0.79	0.37	-2.13	0.033
		late-seral − young	-0.59	0.40	-1.47	0.140
		mid-seral − young	0.20	0.55	0.37	0.713
Live tree seedlings & small saplings – total	burn severity	high − low	0.03	0.02	1.29	0.197
		high − unburned	-0.45	0.20	-2.27	0.023
		low − unburned	-0.48	0.19	-2.46	0.014
	pre-fire stand age	late-seral − mid-seral	0.17	0.06	2.77	0.006
		late-seral − young	-0.30	0.28	-1.09	0.274
		mid-seral − young	-0.47	0.29	-1.65	0.100
Live tree seedlings & small saplings – conifer	burn severity	high − low	-0.02	0.00	-3.59	<0.001
		high − unburned	-0.40	0.10	-3.89	<0.001
		low − unburned	-0.38	0.10	-3.72	<0.001

	pre-fire stand age	late-seral − mid-seral	0.18	0.05	3.29	0.001
		late-seral − young	0.18	0.06	3.06	0.002
		mid-seral − young	0.00	0.02	0.20	0.840
Live tree seedlings & small saplings – broadleaf	burn severity	high − low	0.04	0.02	2.01	0.044
		high − unburned	0.01	0.04	0.39	0.695
		low − unburned	-0.03	0.03	-0.94	0.350
	pre-fire stand age	late-seral − mid-seral	0.02	0.02	0.96	0.336
		late-seral − young	-0.04	0.06	-0.73	0.465
		mid-seral − young	-0.06	0.06	-1.09	0.277
Canopy fuels (Mg ha^{-1})						
Available canopy fuel – total	burn severity	high − low	-29.28	3.09	-9.49	<0.001
		high − unburned	-32.85	2.94	-11.17	<0.001
		low − unburned	-3.56	4.25	-0.84	0.402
	pre-fire stand age	late-seral − mid-seral	4.17	2.40	1.74	0.082
		late-seral − young	11.68	2.35	4.96	<0.001
		mid-seral − young	7.51	2.38	3.16	0.002
Available canopy fuel – live	burn severity	high − low	-18.28	1.69	-10.81	<0.001
		high − unburned	-24.57	2.13	-11.52	<0.001
		low − unburned	-6.29	2.78	-2.27	0.023
	pre-fire stand age	late-seral − mid-seral	5.02	1.73	2.91	0.004
		late-seral − young	11.62	1.61	7.20	<0.001
		mid-seral − young	6.61	1.44	4.58	<0.001
Available canopy fuel − dead	burn severity	high − low	0.93	0.55	1.69	0.092
		high − unburned	3.46	0.40	8.70	<0.001
		low − unburned	2.53	0.43	5.90	<0.001
	pre-fire stand age	late-seral − mid-seral	-1.21	0.44	-2.74	0.006
		late-seral − young	-0.03	0.46	-0.06	0.954
		mid-seral − young	1.19	0.55	2.18	0.030
Canopy bulk density (kg m^{-3})	burn severity	high − low	-0.13	0.02	-6.15	<0.001
		high − unburned	-0.18	0.02	-7.77	<0.001
		low − unburned	-0.05	0.03	-1.59	0.112
	pre-fire stand age	late-seral − mid-seral	0.02	0.02	0.98	0.329
		late-seral − young	-0.02	0.03	-0.78	0.434
		mid-seral − young	-0.04	0.03	-1.38	0.169
Canopy base height (m)	burn severity	high − low	-0.77	1.76	-0.44	0.663
		high − unburned	0.88	1.51	0.58	0.561
		low − unburned	1.65	1.17	1.41	0.159
	pre-fire stand age	late-seral − mid-seral	-7.50	1.71	-4.38	<0.001
		late-seral − young	0.98	0.52	1.89	0.058
		mid-seral − young	8.49	1.70	5.00	<0.001
Foliage – total	burn severity	high − low	-16.00	1.51	-10.62	<0.001
		high − unburned	-21.02	1.88	-11.19	<0.001
		low − unburned	-5.02	2.45	-2.05	0.040

	pre-fire stand age	late-seral − mid-seral	5.03	1.52	3.30	0.001
		late-seral − young	10.86	1.41	7.68	<0.001
		mid-seral − young	5.83	1.20	4.85	<0.001
Foliage − live	burn severity	high − low	-15.70	1.50	-10.45	<0.001
		high − unburned	-21.00	1.90	-11.06	<0.001
		low − unburned	-5.30	2.47	-2.15	0.032
	pre-fire stand age	late-seral − mid-seral	4.65	1.53	3.03	0.002
		late-seral − young	10.49	1.42	7.41	<0.001
		mid-seral − young	5.84	1.23	4.73	<0.001
Branches – total	burn severity	high − low	-32.66	5.87	-5.56	<0.001
		high − unburned	-36.16	5.44	-6.65	<0.001
		low − unburned	-3.50	7.47	-0.47	0.639
	pre-fire stand age	late-seral − mid-seral	21.15	5.30	3.99	<0.001
		late-seral − young	54.84	4.41	12.44	<0.001
		mid-seral − young	33.69	3.96	8.50	<0.001
Branches − live	burn severity	high − low	-33.54	3.12	-10.77	<0.001
		high − unburned	-38.36	3.47	-11.04	<0.001
		low − unburned	-4.82	4.71	-1.02	0.307
	pre-fire stand age	late-seral − mid-seral	11.74	2.94	4.00	<0.001
		late-seral − young	23.82	2.65	8.99	<0.001
		mid-seral − young	12.08	2.07	5.83	<0.001
Branches − dead	burn severity	high − low	20.69	3.23	6.40	<0.001
		high − unburned	21.95	3.02	7.27	<0.001
		low − unburned	1.26	2.01	0.63	0.532
	pre-fire stand age	late-seral − mid-seral	6.55	2.84	2.31	0.021
		late-seral − young	21.18	2.38	8.91	<0.001
		mid-seral − young	14.62	2.29	6.39	<0.001
1-h branches – total	burn severity	high − low	-6.84	0.99	-6.92	<0.001
		high − unburned	-7.58	0.90	-8.40	<0.001
		low − unburned	-0.74	1.28	-0.58	0.562
	pre-fire stand age	late-seral − mid-seral	0.09	0.84	0.11	0.912
		late-seral − young	2.79	0.87	3.21	0.001
		mid-seral − young	2.70	0.93	2.89	0.004
1-h branches − live	burn severity	high − low	-5.15	0.42	-12.38	<0.001
		high − unburned	-7.16	0.52	-13.71	<0.001
		low − unburned	-2.00	0.69	-2.92	0.003
	pre-fire stand age	late-seral − mid-seral	0.74	0.43	1.72	0.085
		late-seral − young	2.29	0.44	5.22	<0.001
		mid-seral − young	1.55	0.44	3.54	<0.001
1-h branches − dead	burn severity	high − low	1.57	0.50	3.12	0.002
		high − unburned	3.43	0.40	8.68	<0.001
		low − unburned	1.86	0.37	5.07	<0.001
	pre-fire stand age	late-seral − mid-seral	-1.15	0.42	-2.75	0.006

		late-seral − young	-0.04	0.44	-0.09	0.927
		mid-seral − young	1.11	0.52	2.15	0.032
10-h branches – total	burn severity	high − low	-6.22	2.06	-3.02	0.003
		high − unburned	-7.66	1.92	-3.99	<0.001
		low − unburned	-1.44	2.46	-0.59	0.558
	pre-fire stand age	late-seral − mid-seral	1.37	1.98	0.69	0.490
		late-seral − young	16.08	1.57	10.21	<0.001
		mid-seral − young	14.71	1.75	8.42	<0.001
10-h branches − live	burn severity	high − low	-10.64	0.88	-12.03	<0.001
		high − unburned	-12.21	0.96	-12.79	<0.001
		low − unburned	-1.57	1.34	-1.17	0.240
	pre-fire stand age	late-seral − mid-seral	1.48	0.84	1.77	0.077
		late-seral − young	5.46	0.75	7.24	<0.001
		mid-seral − young	3.98	0.75	5.32	<0.001
10-h branches − dead	burn severity	high − low	10.75	1.62	6.62	<0.001
		high − unburned	11.40	1.52	7.50	<0.001
		low − unburned	0.65	0.99	0.66	0.511
	pre-fire stand age	late-seral − mid-seral	-0.36	1.48	-0.25	0.806
		late-seral − young	7.74	1.16	6.66	<0.001
		mid-seral − young	8.10	1.37	5.90	<0.001
100-h branches – total	burn severity	high − low	-20.36	4.13	-4.93	<0.001
		high − unburned	-25.86	4.59	-5.64	<0.001
		low − unburned	-5.50	6.03	-0.91	0.361
	pre-fire stand age	late-seral − mid-seral	20.88	3.89	5.37	<0.001
		late-seral − young	37.08	3.55	10.45	<0.001
		mid-seral − young	16.20	2.02	8.01	<0.001
100-h branches − live	burn severity	high − low	-17.10	1.97	-8.69	<0.001
		high − unburned	-17.72	2.04	-8.67	<0.001
		low − unburned	-0.62	2.79	-0.22	0.823
	pre-fire stand age	late-seral − mid-seral	8.82	1.77	4.98	<0.001
		late-seral − young	15.07	1.59	9.48	<0.001
		mid-seral − young	6.25	0.92	6.77	<0.001
100-h branches − dead	burn severity	high − low	7.64	1.66	4.61	<0.001
		high − unburned	6.78	1.64	4.14	<0.001
		low − unburned	-0.85	1.08	-0.79	0.429
	pre-fire stand age	late-seral − mid-seral	7.50	1.53	4.90	<0.001
		late-seral − young	12.52	1.40	8.93	<0.001
		mid-seral − young	5.02	0.73	6.90	<0.001
1000-h branches − live	burn severity	high − low	-0.28	0.06	-4.96	<0.001
		high − unburned	-0.17	0.05	-3.65	<0.001
		low − unburned	0.11	0.07	1.63	0.103
	pre-fire stand age	late-seral − mid-seral	0.11	0.05	2.25	0.025
		late-seral − young	0.24	0.04	6.14	<0.001

		mid-seral − young	0.14	0.03	4.84	<0.001
Crown mass – total (foliage + branches)	burn severity	high − low	-58.43	7.77	-7.52	<0.001
		high − unburned	-69.67	7.69	-9.06	<0.001
		low − unburned	-11.24	10.64	-1.06	0.291
	pre-fire stand age	late-seral − mid-seral	27.11	6.96	3.89	<0.001
		late-seral − young	70.58	5.85	12.07	<0.001
		mid-seral − young	43.47	5.27	8.25	<0.001
Crown mass – live (foliage + branches)	burn severity	high − low	-49.25	4.54	-10.86	<0.001
		high − unburned	-59.39	5.28	-11.25	<0.001
		low − unburned	-10.14	7.05	-1.44	0.150
	pre-fire stand age	late-seral − mid-seral	16.52	4.39	3.77	<0.001
		late-seral − young	34.37	3.99	8.61	<0.001
		mid-seral − young	17.86	3.23	5.52	<0.001
Crown mass – dead (foliage + branches)	burn severity	high − low	20.10	3.28	6.14	<0.001
		high − unburned	21.97	3.03	7.24	<0.001
		low − unburned	1.87	2.07	0.90	0.367
	pre-fire stand age	late-seral − mid-seral	6.54	2.87	2.28	0.023
		late-seral − young	21.30	2.40	8.88	<0.001
		mid-seral − young	14.76	2.32	6.38	<0.001

Notes: Marginal contrast outputs are not presented for dead foliage due to model convergence failure. Marginal contrast outputs are only presented for live 1000-h branches since no dead 1000-h branches were observed. SE, standard error. *z*, test statistic. *p*, p-value.

Table 1.16. Marginal predictions of the effects of pre-fire stand age and burn severity on post-fire aboveground biomass carbon and fuels components. Estimates represent the mean of model predicted means for each predictor level across all levels of the other predictor. Estimates are on the response scale (i.e., Mg ha^{-1}, unless otherwise indicated).

Response	Predictor	Level	Estimate	SE	*z*	*p*
Aboveground biomass carbon (Mg C ha^{-1})						
Total	burn severity	high	179.5	8.0	22.4	<0.001
		low	347.9	19.7	17.7	<0.001
		unburned	275.4	14.4	19.2	<0.001
	pre-fire stand age	late-seral	310.7	12.5	24.8	<0.001
		mid-seral	251.9	12.7	19.8	<0.001
		young	77.9	5.4	14.4	<0.001
Live	burn severity	high	3.2	0.6	5.4	<0.001
		low	290.4	69.2	4.2	<0.001
		unburned	250.6	56.8	4.4	<0.001
	pre-fire stand age	late-seral	213.8	42.9	5.0	<0.001
		mid-seral	132.2	29.5	4.5	<0.001
		young	29.9	9.1	3.3	0.001
Dead	burn severity	high	177.1	9.5	18.6	<0.001
		low	62.8	4.2	14.8	<0.001
		unburned	42.1	2.6	16.1	<0.001
	pre-fire stand age	late-seral	127.9	6.8	18.9	<0.001
		mid-seral	102.3	6.4	16.0	<0.001
		young	44.8	3.9	11.6	<0.001
Woody	burn severity	high	179.1	8.0	22.3	<0.001
		low	332.4	18.8	17.6	<0.001
		unburned	258.5	13.5	19.1	<0.001
	pre-fire stand age	late-seral	298.6	12.0	24.8	<0.001
		mid-seral	243.2	12.3	19.8	<0.001
		young	75.5	5.2	14.4	<0.001
Non-woody	burn severity	high	0.2	0.0	7.7	<0.001
		low	15.5	2.6	6.1	<0.001
		unburned	16.2	2.4	6.8	<0.001
	pre-fire stand age	late-seral	11.5	1.5	7.6	<0.001
		mid-seral	7.5	1.2	6.4	<0.001
		young	6.0	1.5	4.0	<0.001
All trees	burn severity	high	161.0	8.2	19.7	<0.001
		low	323.5	20.8	15.5	<0.001
		unburned	245.2	14.5	17.0	<0.001
	pre-fire stand age	late-seral	281.2	12.9	21.7	<0.001
		mid-seral	234.9	13.5	17.4	<0.001
		young	69.6	5.3	13.1	<0.001

Live trees	burn severity	high	10.5	1.9	5.4	<0.001
		low	184.3	16.9	10.9	<0.001
		unburned	149.7	13.1	11.4	<0.001
	pre-fire stand age	late-seral	126.9	10.2	12.4	<0.001
		mid-seral	96.1	9.7	9.9	<0.001
		young	25.0	4.0	6.3	<0.001
Snags	burn severity	high	164.6	15.8	10.4	<0.001
		low	33.2	3.9	8.6	<0.001
		unburned	9.4	1.0	9.5	<0.001
	pre-fire stand age	late-seral	93.9	9.5	9.9	<0.001
		mid-seral	92.6	11.1	8.4	<0.001
		young	27.2	4.0	6.8	<0.001
Stumps	burn severity	high	0.3	0.1	2.9	0.003
		low	0.3	0.1	2.5	0.012
		unburned	0.6	0.2	3.7	<0.001
	pre-fire stand age	late-seral	0.2	0.0	3.2	0.001
		mid-seral	0.5	0.2	3.2	0.002
		young	1.0	0.4	2.8	0.005
Stem wood – total	burn severity	high	120.9	6.2	19.6	<0.001
		low	225.0	14.6	15.4	<0.001
		unburned	163.4	9.7	16.8	<0.001
	pre-fire stand age	late-seral	196.3	9.1	21.7	<0.001
		mid-seral	166.3	9.6	17.3	<0.001
		young	49.6	3.8	13.0	<0.001
Stem wood – live	burn severity	high	7.7	1.6	4.7	<0.001
		low	127.0	13.4	9.4	<0.001
		unburned	98.0	9.9	9.9	<0.001
	pre-fire stand age	late-seral	84.8	7.8	10.8	<0.001
		mid-seral	66.1	7.7	8.6	<0.001
		young	16.7	3.1	5.4	<0.001
Stem wood – dead	burn severity	high	119.3	9.3	12.8	<0.001
		low	25.0	2.5	10.1	<0.001
		unburned	8.8	0.8	11.1	<0.001
	pre-fire stand age	late-seral	68.5	5.6	12.2	<0.001
		mid-seral	66.0	6.5	10.2	<0.001
		young	25.6	3.2	7.9	<0.001
Stem bark – total	burn severity	high	22.8	1.5	14.8	<0.001
		low	44.2	3.8	11.5	<0.001
		unburned	31.0	2.5	12.6	<0.001
	pre-fire stand age	late-seral	35.8	2.2	16.1	<0.001
		mid-seral	34.2	2.6	12.9	<0.001
		young	10.6	1.1	9.7	<0.001
Stem bark – live	burn severity	high	1.9	0.4	4.3	<0.001

		low	25.0	2.9	8.7	<0.001
		unburned	18.5	2.0	9.2	<0.001
	pre-fire stand age	late-seral	15.8	1.6	9.9	<0.001
		mid-seral	13.7	1.7	7.9	<0.001
		young	3.8	0.8	4.9	<0.001
Stem bark – dead	burn severity	high	23.1	2.6	9.0	<0.001
		low	4.7	0.7	7.2	<0.001
		unburned	1.6	0.2	8.0	<0.001
	pre-fire stand age	late-seral	12.0	1.4	8.6	<0.001
		mid-seral	14.5	2.1	7.1	<0.001
		young	4.8	0.9	5.7	<0.001
Down woody debris	burn severity	high	17.4	1.1	15.1	<0.001
		low	23.8	2.0	12.0	<0.001
		unburned	24.5	1.9	13.2	<0.001
	pre-fire stand age	late-seral	28.8	1.7	17.1	<0.001
		mid-seral	16.3	1.2	13.8	<0.001
		young	8.2	0.8	9.9	<0.001
Live understory	burn severity	high	0.6	0.1	6.0	<0.001
		low	0.3	0.1	4.7	<0.001
		unburned	1.1	0.2	5.3	<0.001
	pre-fire stand age	late-seral	0.5	0.1	6.4	<0.001
		mid-seral	0.7	0.2	4.9	<0.001
		young	1.1	0.3	4.0	<0.001
Charred wood	burn severity	high	0.3	0.0	7.9	<0.001
		low	0.3	0.0	6.2	<0.001
		unburned	0.0	0.0	3.0	0.002
	pre-fire stand age	late-seral	0.3	0.0	7.4	<0.001
		mid-seral	0.2	0.0	6.6	<0.001
		young	0.1	0.0	4.0	<0.001
Surface fuels (Mg ha^{-1})						
Down woody debris	burn severity	high	34.6	2.3	15.2	<0.001
		low	47.4	3.9	12.2	<0.001
		unburned	48.6	3.6	13.4	<0.001
	pre-fire stand age	late-seral	57.0	3.3	17.3	<0.001
		mid-seral	32.4	2.3	14.0	<0.001
		young	16.1	1.7	9.7	<0.001
Coarse woody debris – total (1000-h)	burn severity	high	22.1	2.1	10.3	<0.001
		low	32.2	3.8	8.5	<0.001
		unburned	33.1	3.6	9.3	<0.001
	pre-fire stand age	late-seral	41.2	3.4	12.2	<0.001
		mid-seral	18.7	1.9	9.8	<0.001
		young	6.3	0.9	6.8	<0.001
Sound 1000-h	burn severity	high	12.0	1.6	7.5	<0.001

		low	22.1	3.5	6.3	<0.001
		unburned	18.6	2.7	6.9	<0.001
	pre-fire stand age	late-seral	25.9	2.9	9.1	<0.001
		mid-seral	9.3	1.3	7.4	<0.001
		young	2.3	0.5	4.7	<0.001
Rotten 1000-h	burn severity	high	9.9	1.3	7.4	<0.001
		low	10.2	1.7	6.1	<0.001
		unburned	13.6	2.0	6.6	<0.001
	pre-fire stand age	late-seral	14.7	1.7	8.5	<0.001
		mid-seral	8.9	1.3	6.9	<0.001
		young	4.4	1.0	4.6	<0.001
Fine woody debris – total (1-, 10-, 100-h)	burn severity	high	12.8	0.7	17.7	<0.001
		low	15.1	1.1	13.7	<0.001
		unburned	14.9	1.0	15.4	<0.001
	pre-fire stand age	late-seral	15.7	0.8	19.3	<0.001
		mid-seral	13.6	0.9	15.6	<0.001
		young	9.9	0.9	11.2	<0.001
1-h fuel	burn severity	high	2.5	0.2	14.3	<0.001
		low	5.5	0.5	11.1	<0.001
		unburned	4.9	0.4	12.4	<0.001
	pre-fire stand age	late-seral	4.7	0.3	15.2	<0.001
		mid-seral	3.8	0.3	12.5	<0.001
		young	2.4	0.3	9.0	<0.001
10-h fuel	burn severity	high	3.9	0.3	15.2	<0.001
		low	4.6	0.4	11.8	<0.001
		unburned	4.9	0.4	13.3	<0.001
	pre-fire stand age	late-seral	4.9	0.3	16.6	<0.001
		mid-seral	4.3	0.3	13.4	<0.001
		young	3.2	0.3	9.6	<0.001
100-h fuel	burn severity	high	6.3	0.5	12.3	<0.001
		low	5.0	0.5	9.5	<0.001
		unburned	5.1	0.5	10.7	<0.001
	pre-fire stand age	late-seral	6.1	0.5	13.4	<0.001
		mid-seral	5.5	0.5	10.8	<0.001
		young	4.4	0.6	7.7	<0.001
Dead fuel depth (cm)	burn severity	high	13.1	1.2	11.1	<0.001
		low	24.5	2.8	8.6	<0.001
		unburned	16.4	1.7	9.7	<0.001
	pre-fire stand age	late-seral	18.9	1.6	11.8	<0.001
		mid-seral	16.6	1.7	9.7	<0.001
		young	12.2	1.7	7.0	<0.001
Duff depth (cm)	burn severity	high	0.7	0.1	7.2	<0.001
		low	2.6	0.4	6.1	<0.001

		unburned	6.1	0.9	6.9	<0.001
	pre-fire stand age	late-seral	3.5	0.5	7.3	<0.001
		mid-seral	2.6	0.4	6.2	<0.001
		young	1.8	0.4	4.8	<0.001
Litter depth (cm)	burn severity	high	1.3	0.1	11.9	<0.001
		low	2.6	0.3	9.2	<0.001
		unburned	3.9	0.4	10.3	<0.001
	pre-fire stand age	late-seral	2.8	0.2	12.1	<0.001
		mid-seral	2.3	0.2	10.4	<0.001
		young	1.7	0.2	7.3	<0.001
Live fuel – total	burn severity	high	1.2	0.2	5.8	<0.001
		low	0.5	0.1	4.7	<0.001
		unburned	2.4	0.5	5.2	<0.001
	pre-fire stand age	late-seral	1.0	0.2	6.4	<0.001
		mid-seral	1.6	0.3	4.7	<0.001
		young	2.4	0.6	3.8	<0.001
Live fuel – woody vegetation	burn severity	high	0.8	0.2	4.8	<0.001
		low	0.2	0.1	3.9	<0.001
		unburned	2.2	0.5	4.2	<0.001
	pre-fire stand age	late-seral	0.7	0.1	5.0	<0.001
		mid-seral	1.4	0.4	3.7	<0.001
		young	1.7	0.6	3.1	0.002
Live fuel – herbaceous vegetation	burn severity	high	0.4	0.1	5.3	<0.001
		low	0.3	0.1	4.2	<0.001
		unburned	0.3	0.1	4.8	<0.001
	pre-fire stand age	late-seral	0.3	0.0	6.0	<0.001
		mid-seral	0.3	0.1	4.8	<0.001
		young	0.6	0.2	3.5	<0.001
Live fuel – woody shrubs	burn severity	high	0.7	0.2	4.4	<0.001
		low	0.2	0.1	3.7	<0.001
		unburned	1.7	0.4	4.0	<0.001
	pre-fire stand age	late-seral	0.5	0.1	4.7	<0.001
		mid-seral	1.3	0.4	3.5	<0.001
		young	1.4	0.5	3.0	0.003
Live tree seedlings & small saplings – total	burn severity	high	0.1	0.0	3.4	0.001
		low	0.0	0.0	2.6	0.010
		unburned	0.6	0.2	2.4	0.017
	pre-fire stand age	late-seral	0.2	0.1	3.3	0.001
		mid-seral	0.0	0.0	2.7	0.007
		young	0.7	0.4	1.7	0.081
Live tree seedlings & small saplings – conifer	burn severity	high	0.0	0.0	4.5	<0.001
		low	0.0	0.0	3.7	<0.001
		unburned	0.4	0.1	4.0	<0.001

	pre-fire stand age	late-seral	0.2	0.1	3.8	<0.001
		mid-seral	0.0	0.0	3.1	0.002
		young	0.1	0.0	3.0	0.003
Live tree seedlings & small saplings – broadleaf	burn severity	high	0.1	0.0	2.2	0.027
		low	0.0	0.0	0.8	0.427
		unburned	0.0	0.0	1.0	0.338
	pre-fire stand age	late-seral	0.0	0.0	1.5	0.140
		mid-seral	0.0	0.0	1.4	0.147
		young	0.1	0.1	1.3	0.195
Canopy fuels (Mg ha^{-1})						
Available canopy fuel – total	burn severity	high	5.3	0.4	14.4	<0.001
		low	37.3	3.2	11.5	<0.001
		unburned	37.2	2.8	13.1	<0.001
	pre-fire stand age	late-seral	27.5	1.8	15.4	<0.001
		mid-seral	23.6	2.0	12.1	<0.001
		young	12.7	1.5	8.4	<0.001
Available canopy fuel – live	burn severity	high	0.5	0.1	5.6	<0.001
		low	21.3	1.9	11.2	<0.001
		unburned	23.9	2.0	12.1	<0.001
	pre-fire stand age	late-seral	17.1	1.3	12.8	<0.001
		mid-seral	12.3	1.2	10.1	<0.001
		young	4.4	0.7	6.5	<0.001
Available canopy fuel − dead	burn severity	high	5.0	0.4	13.4	<0.001
		low	4.2	0.4	10.4	<0.001
		unburned	1.6	0.1	11.9	<0.001
	pre-fire stand age	late-seral	3.3	0.2	14.6	<0.001
		mid-seral	4.4	0.4	11.4	<0.001
		young	3.1	0.4	8.3	<0.001
Canopy bulk density (kg m^{-3})	burn severity	high	0.04	0.00	10.80	<0.001
		low	0.16	0.02	8.37	<0.001
		unburned	0.22	0.02	9.44	<0.001
	pre-fire stand age	late-seral	0.13	0.01	11.13	<0.001
		mid-seral	0.12	0.01	9.01	<0.001
		young	0.14	0.02	6.23	<0.001
Canopy base height (m)	burn severity	high	5.5	1.5	3.7	<0.001
		low	6.1	1.1	5.6	<0.001
		unburned	3.9	0.7	5.8	<0.001
	pre-fire stand age	late-seral	2.4	0.4	6.9	<0.001
		mid-seral	10.0	1.7	6.0	<0.001
		young	1.3	0.3	3.9	<0.001
Foliage – total	burn severity	high	0.5	0.1	5.6	<0.001
		low	18.8	1.7	11.1	<0.001
		unburned	20.4	1.7	11.8	<0.001

	pre-fire stand age	late-seral	15.2	1.2	12.6	<0.001
		mid-seral	10.4	1.0	10.0	<0.001
		young	3.5	0.5	6.4	<0.001
Foliage − live	burn severity	high	0.4	0.1	5.4	<0.001
		low	18.4	1.7	10.8	<0.001
		unburned	20.3	1.8	11.6	<0.001
	pre-fire stand age	late-seral	14.8	1.2	12.3	<0.001
		mid-seral	10.4	1.1	9.7	<0.001
		young	3.5	0.6	6.3	<0.001
Branches – total	burn severity	high	35.8	2.2	16.2	<0.001
		low	80.2	6.1	13.2	<0.001
		unburned	69.7	4.8	14.5	<0.001
	pre-fire stand age	late-seral	74.6	4.1	18.4	<0.001
		mid-seral	53.5	3.7	14.6	<0.001
		young	17.5	1.6	10.6	<0.001
Branches − live	burn severity	high	1.1	0.2	5.6	<0.001
		low	40.1	3.6	11.2	<0.001
		unburned	37.2	3.2	11.7	<0.001
	pre-fire stand age	late-seral	30.9	2.4	12.8	<0.001
		mid-seral	19.2	1.9	10.2	<0.001
		young	5.0	0.8	6.5	<0.001
Branches − dead	burn severity	high	34.9	2.7	13.0	<0.001
		low	17.9	1.7	10.3	<0.001
		unburned	13.8	1.2	11.4	<0.001
	pre-fire stand age	late-seral	29.1	2.1	13.9	<0.001
		mid-seral	22.5	2.0	11.5	<0.001
		young	9.6	1.2	8.3	<0.001
1-h branches – total	burn severity	high	5.0	0.3	16.7	<0.001
		low	12.5	1.0	13.1	<0.001
		unburned	12.4	0.8	14.9	<0.001
	pre-fire stand age	late-seral	9.9	0.5	18.1	<0.001
		mid-seral	9.9	0.7	14.4	<0.001
		young	6.3	0.6	10.3	<0.001
1-h branches − live	burn severity	high	0.2	0.0	6.5	<0.001
		low	5.8	0.4	13.1	<0.001
		unburned	7.1	0.5	14.4	<0.001
	pre-fire stand age	late-seral	4.5	0.3	14.8	<0.001
		mid-seral	3.9	0.3	11.8	<0.001
		young	1.9	0.2	7.5	<0.001
1-h branches − dead	burn severity	high	4.9	0.4	13.4	<0.001
		low	3.5	0.3	10.4	<0.001
		unburned	1.6	0.1	11.9	<0.001
	pre-fire stand age	late-seral	3.1	0.2	14.5	<0.001

		mid-seral	4.2	0.4	11.4	<0.001
		young	3.1	0.4	8.3	<0.001
10-h branches – total	burn severity	high	18.0	1.0	18.1	<0.001
		low	27.8	1.9	14.3	<0.001
		unburned	25.3	1.6	15.8	<0.001
	pre-fire stand age	late-seral	26.0	1.3	20.2	<0.001
		mid-seral	24.8	1.5	16.1	<0.001
		young	9.5	0.8	11.7	<0.001
10-h branches − live	burn severity	high	0.3	0.0	6.3	<0.001
		low	12.3	1.0	12.5	<0.001
		unburned	12.0	0.9	13.4	<0.001
	pre-fire stand age	late-seral	8.6	0.6	14.3	<0.001
		mid-seral	7.2	0.6	11.2	<0.001
		young	2.4	0.3	7.2	<0.001
10-h branches − dead	burn severity	high	17.8	1.4	13.1	<0.001
		low	8.5	0.8	10.3	<0.001
		unburned	6.8	0.6	11.3	<0.001
	pre-fire stand age	late-seral	12.9	0.9	13.8	<0.001
		mid-seral	13.1	1.2	11.4	<0.001
		young	6.1	0.8	8.1	<0.001
100-h branches – total	burn severity	high	11.5	1.2	9.9	<0.001
		low	39.2	4.8	8.2	<0.001
		unburned	35.0	4.2	8.3	<0.001
	pre-fire stand age	late-seral	39.3	3.5	11.1	<0.001
		mid-seral	18.4	2.1	8.9	<0.001
		young	1.6	0.2	6.5	<0.001
100-h branches − live	burn severity	high	0.7	0.2	4.2	<0.001
		low	21.3	2.3	9.1	<0.001
		unburned	17.0	1.9	9.2	<0.001
	pre-fire stand age	late-seral	16.9	1.6	10.5	<0.001
		mid-seral	7.8	0.9	8.4	<0.001
		young	0.9	0.2	5.0	<0.001
100-h branches − dead	burn severity	high	11.8	1.4	8.2	<0.001
		low	6.0	0.9	6.7	<0.001
		unburned	5.3	0.7	7.3	<0.001
	pre-fire stand age	late-seral	12.7	1.4	9.4	<0.001
		mid-seral	5.3	0.7	7.7	<0.001
		young	0.5	0.1	5.3	<0.001
1000-h branches − live	burn severity	high	0.0	0.0	2.8	0.005
		low	0.4	0.1	6.2	<0.001
		unburned	0.2	0.0	5.3	<0.001
	pre-fire stand age	late-seral	0.3	0.0	6.7	<0.001
		mid-seral	0.2	0.0	5.5	<0.001

		young	0.0	0.0	1.8	0.075
Crown mass – total (foliage + branches)	burn severity	high	35.8	2.2	16.1	<0.001
		low	109.4	8.4	13.1	<0.001
		unburned	101.5	7.1	14.4	<0.001
	pre-fire stand age	late-seral	97.1	5.4	17.9	<0.001
		mid-seral	70.4	4.9	14.2	<0.001
		young	22.8	2.2	10.4	<0.001
Crown mass – live (foliage + branches)	burn severity	high	1.6	0.3	5.7	<0.001
		low	58.5	5.2	11.3	<0.001
		unburned	57.6	4.9	11.8	<0.001
	pre-fire stand age	late-seral	45.8	3.6	12.9	<0.001
		mid-seral	29.5	2.9	10.2	<0.001
		young	8.5	1.3	6.5	<0.001
Crown mass – dead (foliage + branches)	burn severity	high	34.9	2.7	12.9	<0.001
		low	18.6	1.8	10.3	<0.001
		unburned	13.8	1.2	11.4	<0.001
	pre-fire stand age	late-seral	29.4	2.1	13.9	<0.001
		mid-seral	22.7	2.0	11.5	<0.001
		young	9.6	1.2	8.2	<0.001

Notes: Marginal predictions are not presented for dead foliage due to model convergence failure. Marginal predictions are only presented for live 1000-h branches since no dead 1000-h branches were observed. SE, standard error. *z*, test statistic. *p*, p-value.

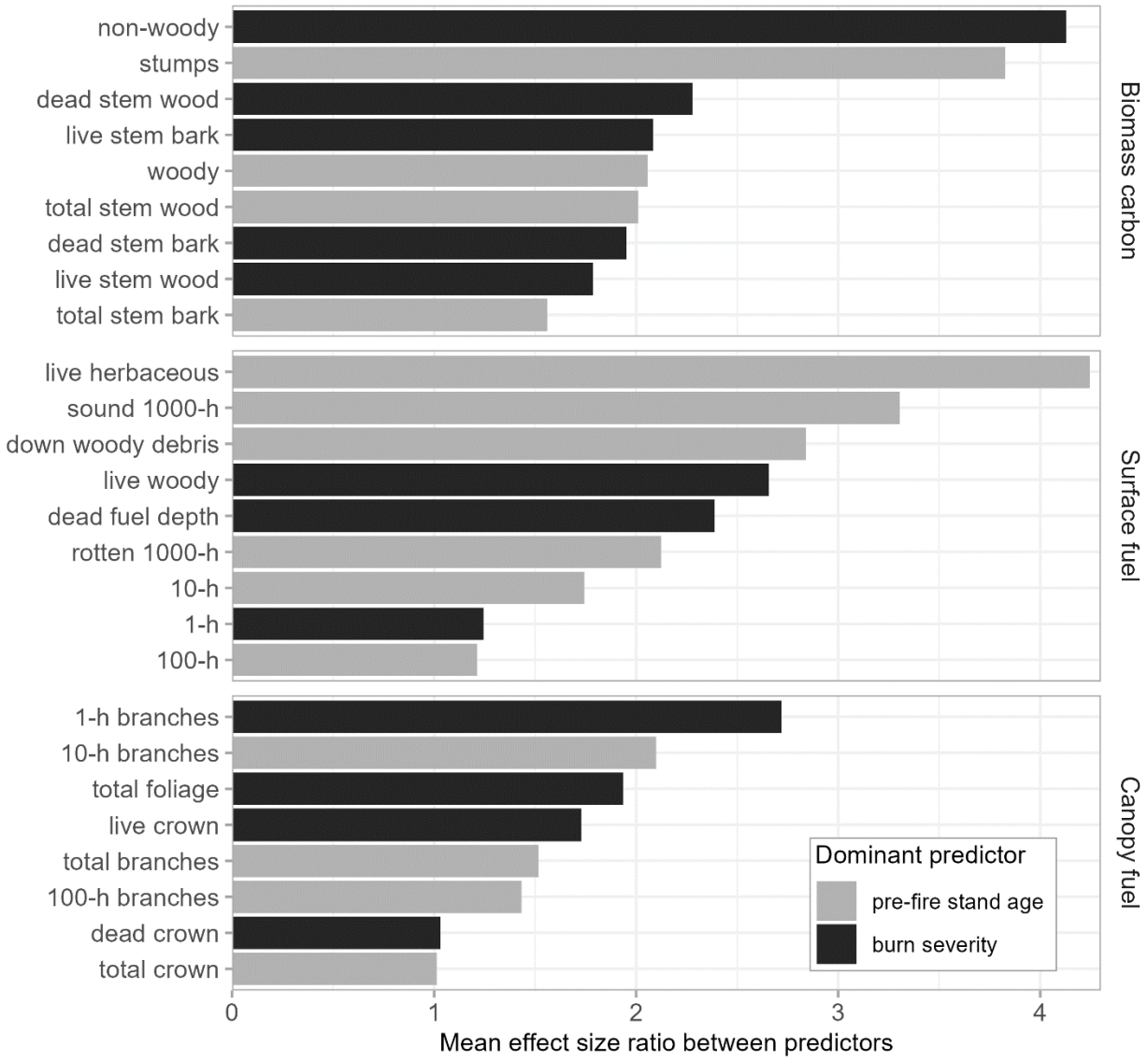

Figure 1.11. Mean effect size ratios for additional post-fire responses relative to the dominant predictor (i.e., predictor with the greater mean effect size): pre-fire stand age (gray) and burn severity (black). See Table 1.14 and Table 1.15 for detailed effect size and marginal comparisons among predictors.

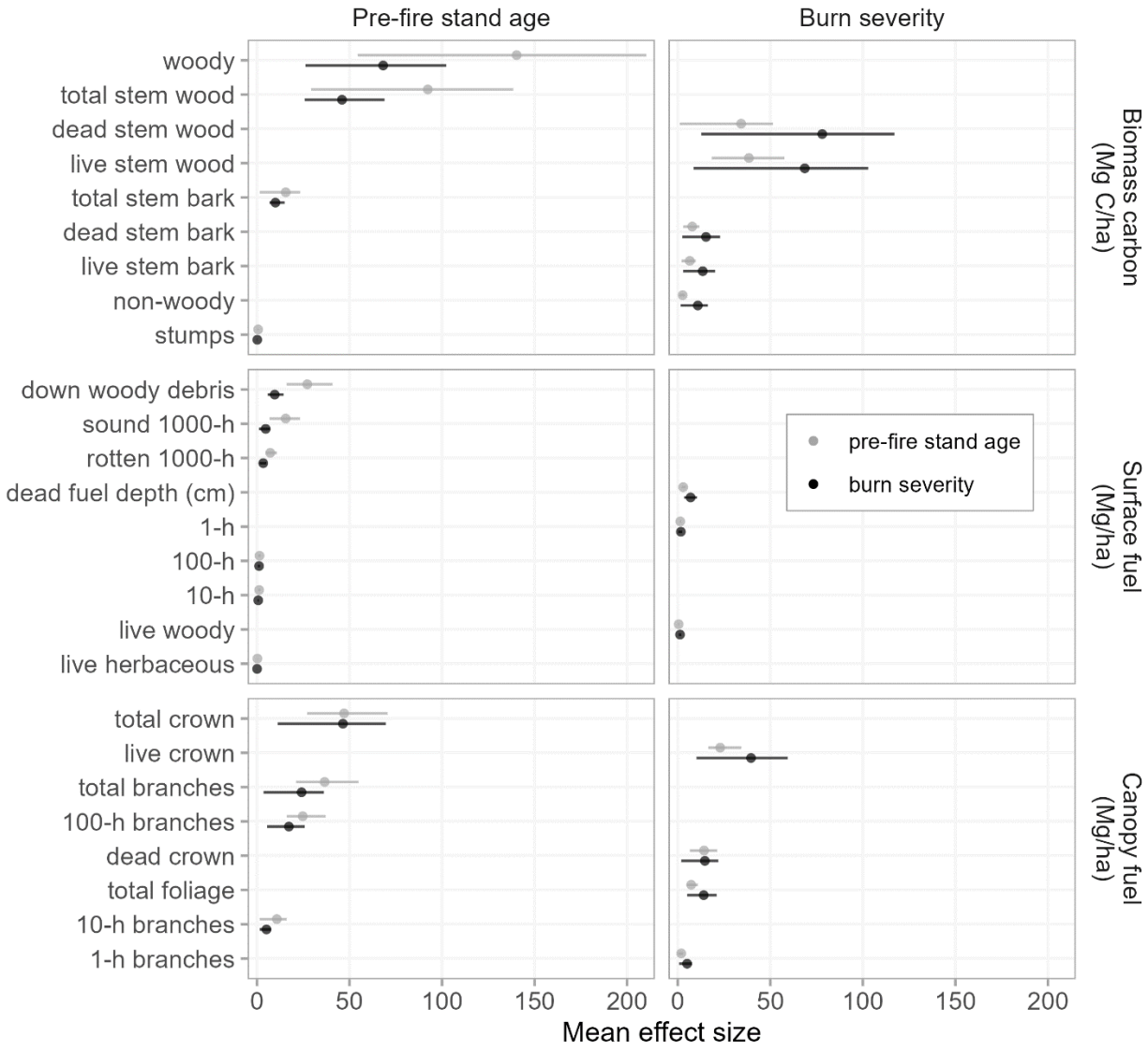

Figure 1.12. Marginal comparisons in mean effect sizes of pre-fire stand age (gray) and burn severity (black) on additional post-fire responses. Values are the mean (min–max) of pairwise contrasts for all levels of a predictor. Estimates are on the response scale and appear in the column of the dominant predictor (i.e., predictor with the greater mean effect size). See Table 1.14 and Table 1.15 for detailed effect size and marginal comparisons among predictors.

1.8 REFERENCES

Acker, S., and M. Easter. 1993. Unpublished data. Oregon State University, Forest Science Department, Corvallis, OR.

Agee, J. 1993. Fire ecology of Pacific Northwest forests. Island Press, Washington D.C.

Agee, J. 1998. The landscape ecology of western forest fire regimes. Northwest Science 72:24–34.

Agee, J. K., and M. H. Huff. 1987. Fuel succession in a western hemlock/Douglas-fir forest. Canadian Journal of Forest Research 17:697–704.

Alaback, P. B. 1986. Biomass regression equations for understory plants in Coastal Alaska: effects of species and sampling design on estimates. Northwest Science 60:90–103.

Alexander, M. E. 1978. Estimating fuel weights of two common shrubs in Colorado lodgepole pine stands. Research Note RM-RN-354, U.S. Department of Agriculture, Forest Service, Rocky Mountain Forest and Range Experiment Station, Fort Collins, CO.

Aphalo, P. J. 2024. *ggpmisc: Miscellaneous Extensions to "ggplot2."*

Arel-Bundock, V. 2024. *marginaleffects: Predictions, Comparisons, Slopes, Marginal Means, and Hypothesis Tests*.

Ares, A., T. A. Terry, K. B. Piatek, R. B. Harrison, R. E. Miller, B. L. Flaming, C. W. Licata, B. D. Strahm, C. A. Harrington, R. Meade, H. W. Anderson, L. C. Brodie, and J. M. Kraft. 2007. The Fall River Long-term Site Productivity Study in Coastal Washington: Site Characteristics, Methods, and Biomass and Carbon and Nitrogen Stores Before and After Harvest. Gen. Tech. Rep. PNW-GTR-691, U.S. Department of Agriculture, Forest Service, Pacific Northwest Research Station, Portland, OR.

Auguie, B. 2019. *egg: Extensions for "ggplot2": Custom Geom, Custom Themes, Plot Alignment, Labelled Panels, Symmetric Scales, and Fixed Panel Size*.

Bassett, M., S. W. J. Leonard, E. K. Chia, M. F. Clarke, and A. F. Bennett. 2017. Interacting effects of fire severity, time since fire and topography on vegetation structure after wildfire. Forest Ecology and Management 396:26–34.

Berner, L. T., and B. E. Law. 2016. Plant traits, productivity, biomass and soil properties from forest sites in the Pacific Northwest, 1999–2014. Scientific Data 3:160002.

Bird, M. I., J. G. Wynn, G. Saiz, C. M. Wurster, and A. McBeath. 2015. The pyrogenic carbon cycle. Annual Review of Earth and Planetary Sciences 43:273–298.

Boyd, R., editor. 1999. Indians, Fire and the Land in the Pacific Northwest. Oregon State University Press, Corvallis, Oregon.

Branca, C., and C. Di Blasi. 2003. Global Kinetics of Wood Char Devolatilization and Combustion. Energy & Fuels 17:1609–1615.

Braziunas, K. H., N. G. Kiel, and M. G. Turner. 2023. Less fuel for the next fire? Short-interval fire delays forest recovery and interacting drivers amplify effects. Ecology 104:e4042.

Brooks, M. E., K. Kristensen, K. J. van Benthem, A. Magnusson, C. W. Berg, A. Nielsen, H. J. Skaug, M. Maechler, and B. M. Bolker. 2017. glmmTMB balances speed and flexibility

among packages for zero-inflated generalized linear mixed modeling. The R Journal 9:378–400.

Brown, J. K. 1974. Handbook for inventorying downed woody material. Gen. Tech. Rep. INT-16, U.S. Department of Agriculture, Forest Service, Intermountain Forest and Range Experiment Station, Ogden, UT.

Brown, J. K. 1978. Weight and density of crowns of Rocky Mountain conifers. Research Paper INT-197, U.S. Department of Agriculture, Forest Service, Intermountain Forest and Range Experiment Station, Ogden, UT.

Brown, J. K., and C. M. Johnston. 1976. Debris Prediction System. Fuel Science RWU 2104, U.S. Department of Agriculture, Forest Service, Intermountain Forest and Range Experiment Station, Missoula, MT.

Buma, B., S. Weiss, K. Hayes, and M. Lucash. 2020. Wildland fire reburning trends across the US West suggest only short-term negative feedback and differing climatic effects. Environmental Research Letters 15:034026.

Burrascano, S., W. S. Keeton, F. M. Sabatini, and C. Blasi. 2013. Commonality and variability in the structural attributes of moist temperate old-growth forests: A global review. Forest Ecology and Management 291:458–479.

Campbell, J., D. Donato, D. Azuma, and B. Law. 2007. Pyrogenic carbon emission from a large wildfire in Oregon, United States. Journal of Geophysical Research: Biogeosciences 112.

Case, M. J., B. G. Johnson, K. J. Bartowitz, and T. W. Hudiburg. 2021. Forests of the future: Climate change impacts and implications for carbon storage in the Pacific Northwest, USA. Forest Ecology and Management 482:118886.

Cawson, J. G., T. J. Duff, K. G. Tolhurst, C. C. Baillie, and T. D. Penman. 2017. Fuel moisture in Mountain Ash forests with contrasting fire histories. Forest Ecology and Management 400:568–577.

Chen, J., J. F. Franklin, and T. A. Spies. 1993. Contrasting microclimates among clearcut, edge, and interior of old-growth Douglas-fir forest. Agricultural and Forest Meteorology 63:219–237.

Cruz, M. G., M. E. Alexander, and R. H. Wakimoto. 2004. Modeling the likelihood of crown fire occurrence in conifer forest stands. Forest Science 50:640–658.

Curtis, J. T., and R. P. McIntosh. 1951. An Upland Forest Continuum in the Prairie-Forest Border Region of Wisconsin. Ecology 32:476–496.

Dietenberger, M. 2002. Update for combustion properties of wood components. Fire and Materials 26:255–267.

Donato, D. C., J. L. Campbell, J. B. Fontaine, and B. E. Law. 2009a. Quantifying char in postfire woody detritus inventories. Fire Ecology 5:104–115.

Donato, D. C., J. B. Fontaine, and J. L. Campbell. 2016. Burning the legacy? Influence of wildfire reburn on dead wood dynamics in a temperate conifer forest. Ecosphere 7:e01341.

Donato, D. C., J. B. Fontaine, J. L. Campbell, W. D. Robinson, J. B. Kauffman, and B. E. Law. 2009b. Conifer regeneration in stand-replacement portions of a large mixed-severity

wildfire in the Klamath–Siskiyou Mountains. Canadian Journal of Forest Research 39:823–838.

Donato, D. C., J. B. Fontaine, J. B. Kauffman, W. D. Robinson, and B. E. Law. 2013a. Fuel mass and forest structure following stand-replacement fire and post-fire logging in a mixed-evergreen forest. International Journal of Wildland Fire 22:652.

Donato, D. C., J. S. Halofsky, and M. J. Reilly. 2020. Corralling a black swan: natural range of variation in a forest landscape driven by rare, extreme events. Ecological Applications 30:e02013.

Donato, D. C., B. J. Harvey, W. H. Romme, M. Simard, and M. G. Turner. 2013b. Bark beetle effects on fuel profiles across a range of stand structures in Douglas-fir forests of Greater Yellowstone. Ecological Applications 23:3–20.

Dye, A. W., M. J. Reilly, A. McEvoy, R. Lemons, K. L. Riley, J. B. Kim, and B. K. Kerns. 2024. Simulated Future Shifts in Wildfire Regimes in Moist Forests of Pacific Northwest, USA. Journal of Geophysical Research: Biogeosciences 129:e2023JG007722.

Fahnestock, G. R., and J. K. Agee. 1983. Biomass consumption and smoke production by prehistoric and modern forest fires in western Washington. Journal of Forestry 81:653–657.

Firke, S. 2023. *janitor: Simple Tools for Examining and Cleaning Dirty Data*.

Franklin, J. F., and C. T. Dyrness. 1973. Natural vegetation of Oregon and Washington. Gen. Tech. Rep. PNW-GTR-008, U.S. Department of Agriculture, Forest Service, Pacific Northwest Research Station, Portland, OR.

Franklin, J. F., D. Lindenmayer, J. A. MacMahon, A. McKee, J. Magnuson, D. A. Perry, R. Waide, and D. Foster. 2000. Threads of continuity. Conservation in Practice 1:8–17.

Franklin, J. F., T. A. Spies, R. V. Pelt, A. B. Carey, D. A. Thornburgh, D. R. Berg, D. B. Lindenmayer, M. E. Harmon, W. S. Keeton, D. C. Shaw, K. Bible, and J. Chen. 2002. Disturbances and structural development of natural forest ecosystems with silvicultural implications, using Douglas-fir forests as an example. Forest Ecology and Management 155:399–423.

Gholz, H. L., C. C. Grier, A. G. Campbell, and A. T. Brown. 1979. Equations and their use for estimating biomass and leaf area of plants in the Pacific Northwest. Research Paper 41, Forest Research Laboratoy, Oregon State University, Corvallis, OR.

Gray, A. N., and J. F. Franklin. 1997. Effects of multiple fires on the structure of southwestern Washington forests. Northwest Science 71:174–185.

Gray, A. N., T. R. Whittier, and M. E. Harmon. 2016. Carbon stocks and accumulation rates in Pacific Northwest forests: role of stand age, plant community, and productivity. Ecosphere 7:e01224.

Halpern, C. B., and E. Miller. 1993. Unpublished data. University of Washington, College of Forest Resources, Seattle, WA.

Halpern, C. B., E. A. Miller, and M. A. Geyer. 1996. Equations for predicting above-ground biomass of plant species in early successional forests of the western Cascade Range, Oregon. Northwest Science 70:306–320.

Harmon, M. E., B. Fasth, C. W. Woodall, and J. Sexton. 2013. Carbon concentration of standing and downed woody detritus: Effects of tree taxa, decay class, position, and tissue type. Forest Ecology and Management 291:259–267.

Harmon, M. E., W. K. Ferrell, and J. F. Franklin. 1990. Effects on Carbon Storage of Conversion of Old-Growth Forests to Young Forests. Science 247:699–702.

Harmon, M. E., J. F. Franklin, F. J. Swanson, P. Sollins, S. V. Gregory, J. D. Lattin, N. H. Anderson, S. P. Cline, N. G. Aumen, J. R. Sedell, G. W. Lienkaemper, K. Cromack, and K. W. Cummins. 1986. Ecology of coarse woody debris in temperate ecosystems. Advances in Ecological Research 15:133–302.

Harmon, M. E., C. W. Woodall, B. Fasth, and J. Sexton. 2008. Woody detritus density and density reduction factors for tree species in the United States: a synthesis. Gen. Tech. Rep. NRS-29, U.S. Department of Agriculture, Forest Service, Northern Research Station, Newtown Square, PA, Newtown Square, PA.

Harmon, M. E., C. W. Woodall, B. Fasth, J. Sexton, and M. Yatkov. 2011. Differences between standing and downed dead tree wood density reduction factors: A comparison across decay classes and tree species. Research Paper, U.S. Department of Agriculture, Forest Service, Northern Research Station, Newtown Square, PA.

Helgerson, O. T., K. Cromack, S. Stafford, R. E. Miller, and R. Slagle. 1988. Equations for estimating aboveground components of young Douglas-fir and red alder in a coastal Oregon plantation. Canadian Journal of Forest Research 18:1082–1085.

Hoecker, T. J., and M. G. Turner. 2022. A short-interval reburn catalyzes departures from historical structure and composition in a mesic mixed-conifer forest. Forest Ecology and Management 504:119814.

Hudiburg, T., J. Mathias, K. Bartowitz, D. M. Berardi, K. Bryant, E. Graham, C. A. Kolden, R. A. Betts, and L. Lynch. 2023. Terrestrial carbon dynamics in an era of increasing wildfire. Nature Climate Change 13:1306–1316.

Jain, T. B., R. T. Graham, and D. Adams. 2010. Carbon concentrations and carbon pool distributions in dry, moist, and cold mid-aged forests of the Rocky Mountains. Pages 39–59 Integrated management of carbon sequestration and biomass utilization opportunities in a changing climate: Proceedings of the 2009 National Silviculture Workshop. Proceedings RMRS-P-61. U.S. Department of Agriculture, Forest Service, Rocky Mountain Research Station, Fort Collins, CO.

Janisch, J. E., and M. E. Harmon. 2002. Successional changes in live and dead wood carbon stores: implications for net ecosystem productivity. Tree Physiology 22:77–89.

Johnston, J. D., M. R. Schmidt, A. G. Merschel, W. M. Downing, M. R. Coughlan, and D. G. Lewis. 2023. Exceptional variability in historical fire regimes across a western Cascades landscape, Oregon, USA. Ecosphere 14:e4735.

Johnstone, J. F., C. D. Allen, J. F. Franklin, L. E. Frelich, B. J. Harvey, P. E. Higuera, M. C. Mack, R. K. Meentemeyer, M. R. Metz, G. L. Perry, T. Schoennagel, and M. G. Turner. 2016. Changing disturbance regimes, ecological memory, and forest resilience. Frontiers in Ecology and the Environment 14:369–378.

Kashian, D. M., W. H. Romme, D. B. Tinker, M. G. Turner, and M. G. Ryan. 2006. Carbon

Storage on Landscapes with Stand-replacing Fires. BioScience 56:598–606.

Kassambara, A. 2023. *ggpubr: "ggplot2" Based Publication Ready Plots*.

Kattge, J., G. Bönisch, S. Díaz, S. Lavorel, I. C. Prentice, P. Leadley, S. Tautenhahn, G. D. A. Werner, T. Aakala, M. Abedi, A. T. R. Acosta, G. C. Adamidis, K. Adamson, M. Aiba, C. H. Albert, J. M. Alcántara, C. Alcázar C, I. Aleixo, H. Ali, B. Amiaud, C. Ammer, M. M. Amoroso, M. Anand, C. Anderson, N. Anten, J. Antos, D. M. G. Apgaua, T.-L. Ashman, D. H. Asmara, G. P. Asner, M. Aspinwall, O. Atkin, I. Aubin, L. Baastrup-Spohr, K. Bahalkeh, M. Bahn, T. Baker, W. J. Baker, J. P. Bakker, D. Baldocchi, J. Baltzer, A. Banerjee, A. Baranger, J. Barlow, D. R. Barneche, Z. Baruch, D. Bastianelli, J. Battles, W. Bauerle, M. Bauters, E. Bazzato, M. Beckmann, H. Beeckman, C. Beierkuhnlein, R. Bekker, G. Belfry, M. Belluau, M. Beloiu, R. Benavides, L. Benomar, M. L. Berdugo-Lattke, E. Berenguer, R. Bergamin, J. Bergmann, M. Bergmann Carlucci, L. Berner, M. Bernhardt-Römermann, C. Bigler, A. D. Bjorkman, C. Blackman, C. Blanco, B. Blonder, D. Blumenthal, K. T. Bocanegra-González, P. Boeckx, S. Bohlman, K. Böhning-Gaese, L. Boisvert-Marsh, W. Bond, B. Bond-Lamberty, A. Boom, C. C. F. Boonman, K. Bordin, E. H. Boughton, V. Boukili, D. M. J. S. Bowman, S. Bravo, M. R. Brendel, M. R. Broadley, K. A. Brown, H. Bruelheide, F. Brumnich, H. H. Bruun, D. Bruy, S. W. Buchanan, S. F. Bucher, N. Buchmann, R. Buitenwerf, D. E. Bunker, J. Bürger, S. Burrascano, D. F. R. P. Burslem, B. J. Butterfield, C. Byun, M. Marques, M. C. Scalon, M. Caccianiga, M. Cadotte, M. Cailleret, J. Camac, J. J. Camarero, C. Campany, G. Campetella, J. A. Campos, L. Cano-Arboleda, R. Canullo, M. Carbognani, F. Carvalho, F. Casanoves, B. Castagneyrol, J. A. Catford, J. Cavender-Bares, B. E. L. Cerabolini, M. Cervellini, E. Chacón-Madrigal, K. Chapin, F. S. Chapin, S. Chelli, S.-C. Chen, A. Chen, P. Cherubini, F. Chianucci, B. Choat, K.-S. Chung, M. Chytrý, D. Ciccarelli, L. Coll, C. G. Collins, L. Conti, D. Coomes, J. H. C. Cornelissen, W. K. Cornwell, P. Corona, M. Coyea, J. Craine, D. Craven, J. P. G. M. Cromsigt, A. Csecserits, K. Cufar, M. Cuntz, A. C. da Silva, K. M. Dahlin, M. Dainese, I. Dalke, M. Dalle Fratte, A. T. Dang-Le, J. Danihelka, M. Dannoura, S. Dawson, A. J. de Beer, A. De Frutos, J. R. De Long, B. Dechant, S. Delagrange, N. Delpierre, G. Derroire, A. S. Dias, M. H. Diaz-Toribio, P. G. Dimitrakopoulos, M. Dobrowolski, D. Doktor, P. Dřevojan, N. Dong, J. Dransfield, S. Dressler, L. Duarte, E. Ducouret, S. Dullinger, W. Durka, R. Duursma, O. Dymova, A. E-Vojtkó, R. L. Eckstein, H. Ejtehadi, J. Elser, T. Emilio, K. Engemann, M. B. Erfanian, A. Erfmeier, A. Esquivel-Muelbert, G. Esser, M. Estiarte, T. F. Domingues, W. F. Fagan, J. Fagúndez, D. S. Falster, Y. Fan, J. Fang, E. Farris, F. Fazlioglu, Y. Feng, F. Fernandez-Mendez, C. Ferrara, J. Ferreira, A. Fidelis, B. Finegan, J. Firn, T. J. Flowers, D. F. B. Flynn, V. Fontana, E. Forey, C. Forgiarini, L. François, M. Frangipani, D. Frank, C. Frenette-Dussault, G. T. Freschet, E. L. Fry, N. M. Fyllas, G. G. Mazzochini, S. Gachet, R. Gallagher, G. Ganade, F. Ganga, P. García-Palacios, V. Gargaglione, E. Garnier, J. L. Garrido, A. L. de Gasper, G. Gea-Izquierdo, D. Gibson, A. N. Gillison, A. Giroldo, M.-C. Glasenhardt, S. Gleason, M. Gliesch, E. Goldberg, B. Göldel, E. Gonzalez-Akre, J. L. Gonzalez-Andujar, A. González-Melo, A. González-Robles, B. J. Graae, E. Granda, S. Graves, W. A. Green, T. Gregor, N. Gross, G. R. Guerin, A. Günther, A. G. Gutiérrez, L. Haddock, A. Haines, J. Hall, A. Hambuckers, W. Han, S. P. Harrison, W. Hattingh, J. E. Hawes, T. He, P. He, J. M. Heberling, A. Helm, S. Hempel, J. Hentschel, B. Hérault, A.-M. Hereş, K. Herz, M. Heuertz, T. Hickler, P. Hietz, P. Higuchi, A. L. Hipp, A. Hirons, M. Hock, J. A. Hogan, K. Holl, O. Honnay, D. Hornstein, E. Hou, N. Hough-Snee, K. A.

Hovstad, T. Ichie, B. Igić, E. Illa, M. Isaac, M. Ishihara, L. Ivanov, L. Ivanova, C. M. Iversen, J. Izquierdo, R. B. Jackson, B. Jackson, H. Jactel, A. M. Jagodzinski, U. Jandt, S. Jansen, T. Jenkins, A. Jentsch, J. R. P. Jespersen, G.-F. Jiang, J. L. Johansen, D. Johnson, E. J. Jokela, C. A. Joly, G. J. Jordan, G. S. Joseph, D. Junaedi, R. R. Junker, E. Justes, R. Kabzems, J. Kane, Z. Kaplan, T. Kattenborn, L. Kavelenova, E. Kearsley, A. Kempel, T. Kenzo, A. Kerkhoff, M. I. Khalil, N. L. Kinlock, W. D. Kissling, K. Kitajima, T. Kitzberger, R. Kjøller, T. Klein, M. Kleyer, J. Klimešová, J. Klipel, B. Kloeppel, S. Klotz, J. M. H. Knops, T. Kohyama, F. Koike, J. Kollmann, B. Komac, K. Komatsu, C. König, N. J. B. Kraft, K. Kramer, H. Kreft, I. Kühn, D. Kumarathunge, J. Kuppler, H. Kurokawa, Y. Kurosawa, S. Kuyah, J.-P. Laclau, B. Lafleur, E. Lallai, E. Lamb, A. Lamprecht, D. J. Larkin, D. Laughlin, Y. Le Bagousse-Pinguet, G. le Maire, P. C. le Roux, E. le Roux, T. Lee, F. Lens, S. L. Lewis, B. Lhotsky, Y. Li, X. Li, J. W. Lichstein, M. Liebergesell, J. Y. Lim, Y.-S. Lin, J. C. Linares, C. Liu, D. Liu, U. Liu, S. Livingstone, J. Llusià, M. Lohbeck, Á. López-García, G. Lopez-Gonzalez, Z. Lososová, F. Louault, B. A. Lukács, P. Lukeš, Y. Luo, M. Lussu, S. Ma, C. Maciel Rabelo Pereira, M. Mack, V. Maire, A. Mäkelä, H. Mäkinen, A. C. M. Malhado, A. Mallik, P. Manning, S. Manzoni, Z. Marchetti, L. Marchino, V. Marcilio-Silva, E. Marcon, M. Marignani, L. Markesteijn, A. Martin, C. Martínez-Garza, J. Martínez-Vilalta, T. Mašková, K. Mason, N. Mason, T. J. Massad, J. Masse, I. Mayrose, J. McCarthy, M. L. McCormack, K. McCulloh, I. R. McFadden, B. J. McGill, M. Y. McPartland, J. S. Medeiros, B. Medlyn, P. Meerts, Z. Mehrabi, P. Meir, F. P. L. Melo, M. Mencuccini, C. Meredieu, J. Messier, I. Mészáros, J. Metsaranta, S. T. Michaletz, C. Michelaki, S. Migalina, R. Milla, J. E. D. Miller, V. Minden, R. Ming, K. Mokany, A. T. Moles, A. Molnár V, J. Molofsky, M. Molz, R. A. Montgomery, A. Monty, L. Moravcová, A. Moreno-Martínez, M. Moretti, A. S. Mori, S. Mori, D. Morris, J. Morrison, L. Mucina, S. Mueller, C. D. Muir, S. C. Müller, F. Munoz, I. H. Myers-Smith, R. W. Myster, M. Nagano, S. Naidu, A. Narayanan, B. Natesan, L. Negoita, A. S. Nelson, E. L. Neuschulz, J. Ni, G. Niedrist, J. Nieto, Ü. Niinemets, R. Nolan, H. Nottebrock, Y. Nouvellon, A. Novakovskiy, T. N. Network, K. O. Nystuen, A. O'Grady, K. O'Hara, A. O'Reilly-Nugent, S. Oakley, W. Oberhuber, T. Ohtsuka, R. Oliveira, K. Öllerer, M. E. Olson, V. Onipchenko, Y. Onoda, R. E. Onstein, J. C. Ordonez, N. Osada, I. Ostonen, G. Ottaviani, S. Otto, G. E. Overbeck, W. A. Ozinga, A. T. Pahl, C. E. T. Paine, R. J. Pakeman, A. C. Papageorgiou, E. Parfionova, M. Pärtel, M. Patacca, S. Paula, J. Paule, H. Pauli, J. G. Pausas, B. Peco, J. Penuelas, A. Perea, P. L. Peri, A. C. Petisco-Souza, A. Petraglia, A. M. Petritan, O. L. Phillips, S. Pierce, V. D. Pillar, J. Pisek, A. Pomogaybin, H. Poorter, A. Portsmuth, P. Poschlod, C. Potvin, D. Pounds, A. S. Powell, S. A. Power, A. Prinzing, G. Puglielli, P. Pyšek, V. Raevel, A. Rammig, J. Ransijn, C. A. Ray, P. B. Reich, M. Reichstein, D. E. B. Reid, M. Réjou-Méchain, V. R. de Dios, S. Ribeiro, S. Richardson, K. Riibak, M. C. Rillig, F. Riviera, E. M. R. Robert, S. Roberts, B. Robroek, A. Roddy, A. V. Rodrigues, A. Rogers, E. Rollinson, V. Rolo, C. Römermann, D. Ronzhina, C. Roscher, J. A. Rosell, M. F. Rosenfield, C. Rossi, D. B. Roy, S. Royer-Tardif, N. Rüger, R. Ruiz-Peinado, S. B. Rumpf, G. M. Rusch, M. Ryo, L. Sack, A. Saldaña, B. Salgado-Negret, R. Salguero-Gomez, I. Santa-Regina, A. C. Santacruz-García, J. Santos, J. Sardans, B. Schamp, M. Scherer-Lorenzen, M. Schleuning, B. Schmid, M. Schmidt, S. Schmitt, J. V. Schneider, S. D. Schowanek, J. Schrader, F. Schrodt, B. Schuldt, F. Schurr, G. Selaya Garvizu, M. Semchenko, C. Seymour, J. C. Sfair, J. M. Sharpe, C. S. Sheppard, S. Sheremetiev, S.

Shiodera, B. Shipley, T. A. Shovon, A. Siebenkäs, C. Sierra, V. Silva, M. Silva, T. Sitzia, H. Sjöman, M. Slot, N. G. Smith, D. Sodhi, P. Soltis, D. Soltis, B. Somers, G. Sonnier, M. V. Sørensen, E. E. Sosinski Jr, N. A. Soudzilovskaia, A. F. Souza, M. Spasojevic, M. G. Sperandii, A. B. Stan, J. Stegen, K. Steinbauer, J. G. Stephan, F. Sterck, D. B. Stojanovic, T. Strydom, M. L. Suarez, J.-C. Svenning, I. Svitková, M. Svitok, M. Svoboda, E. Swaine, N. Swenson, M. Tabarelli, K. Takagi, U. Tappeiner, R. Tarifa, S. Tauugourdeau, C. Tavsanoglu, M. te Beest, L. Tedersoo, N. Thiffault, D. Thom, E. Thomas, K. Thompson, P. E. Thornton, W. Thuiller, L. Tichý, D. Tissue, M. G. Tjoelker, D. Y. P. Tng, J. Tobias, P. Török, T. Tarin, J. M. Torres-Ruiz, B. Tóthmérész, M. Treurnicht, V. Trivellone, F. Trolliet, V. Trotsiuk, J. L. Tsakalos, I. Tsiripidis, N. Tysklind, T. Umehara, V. Usoltsev, M. Vadeboncoeur, J. Vaezi, F. Valladares, J. Vamosi, P. M. van Bodegom, M. van Breugel, E. Van Cleemput, M. van de Weg, S. van der Merwe, F. van der Plas, M. T. van der Sande, M. van Kleunen, K. Van Meerbeek, M. Vanderwel, K. A. Vanselow, A. Vårhammar, L. Varone, M. Y. Vasquez Valderrama, K. Vassilev, M. Vellend, E. J. Veneklaas, H. Verbeeck, K. Verheyen, A. Vibrans, I. Vieira, J. Villacís, C. Violle, P. Vivek, K. Wagner, M. Waldram, A. Waldron, A. P. Walker, M. Waller, G. Walther, H. Wang, F. Wang, W. Wang, H. Watkins, J. Watkins, U. Weber, J. T. Weedon, L. Wei, P. Weigelt, E. Weiher, A. W. Wells, C. Wellstein, E. Wenk, M. Westoby, A. Westwood, P. J. White, M. Whitten, M. Williams, D. E. Winkler, K. Winter, C. Womack, I. J. Wright, S. J. Wright, J. Wright, B. X. Pinho, F. Ximenes, T. Yamada, K. Yamaji, R. Yanai, N. Yankov, B. Yguel, K. J. Zanini, A. E. Zanne, D. Zelený, Y.-P. Zhao, J. Zheng, J. Zheng, K. Ziemińska, C. R. Zirbel, G. Zizka, I. C. Zo-Bi, G. Zotz, and C. Wirth. 2020. TRY plant trait database – enhanced coverage and open access. Global Change Biology 26:119–188.

Kauffman, J. B., L. M. Ellsworth, D. M. Bell, S. Acker, and J. Kertis. 2019. Forest structure and biomass reflects the variable effects of fire and land use 15 and 29 years following fire in the western Cascades, Oregon. Forest Ecology and Management 453:117570.

Keeley, J. E. 2009. Fire intensity, fire severity and burn severity: a brief review and suggested usage. International Journal of Wildland Fire 18:116.

Koerper, G. 1983. Progress Report: Biomass to cover relations for riparian species and wet meadow communities. Oregon State University, Forest Science Department, Corvallis, OR.

Lam, O., S. Tautenhahn, G. Walther, G. Boenisch, P. Baddam, and J. Kattge. 2023. *rtry: Preprocessing Plant Trait Data* .

Lamlom, S. H., and R. A. Savidge. 2003. A reassessment of carbon content in wood: variation within and between 41 North American species. Biomass and Bioenergy 25:381–388.

Landesmann, J. B., F. Tiribelli, J. Paritsis, T. T. Veblen, and T. Kitzberger. 2021. Increased fire severity triggers positive feedbacks of greater vegetation flammability and favors plant community-type conversions. Journal of Vegetation Science 32:e12936.

Laughlin, M. M., L. K. Rangel-Parra, J. E. Morris, D. C. Donato, J. S. Halofsky, and B. J. Harvey. 2023. Patterns and drivers of early conifer regeneration following stand-replacing wildfire in Pacific Northwest (USA) temperate maritime forests. Forest Ecology and Management 549:121491.

Law, B. E., D. Turner, J. Campbell, O. J. Sun, S. Van Tuyl, W. D. Ritts, and W. B. Cohen. 2004. Disturbance and climate effects on carbon stocks and fluxes across Western Oregon USA.

Global Change Biology 10:1429–1444.

Lemon, J. 2006. Plotrix: a package in the red light district of R. R-News 6:8–12.

Li, Y., and B. Shipley. 2017. An experimental test of CSR theory using a globally calibrated ordination method. PLOS ONE 12:e0175404.

Lindenmayer, D. B., G. E. Likens, and J. F. Franklin. 2010. Rapid responses to facilitate ecological discoveries from major disturbances. Frontiers in Ecology and the Environment 8:527–532.

Losapio, G., M. de la Cruz, A. Escudero, B. Schmid, and C. Schöb. 2018. The assembly of a plant network in alpine vegetation. Journal of Vegetation Science 29:999–1006.

Lutes, D. C., R. E. Keane, J. F. Caratti, C. H. Key, N. C. Benson, S. Sutherland, and L. J. Gangi. 2006. FIREMON: Fire effects monitoring and inventory system. Gen. Tech. Rep. RMRS-GTR-164, U.S. Department of Agriculture, Forest Service, Rocky Mountain Research Station, Fort Collins, CO.

Martin, A. R., M. Doraisami, and S. C. Thomas. 2018. Global patterns in wood carbon concentration across the world's trees and forests. Nature Geoscience 11:915–920.

Means, J. E., H. A. Hansen, G. J. Koerper, P. B. Alaback, and M. W. Klopsch. 1994. Software for computing plant biomass - BIOPAK users guide. Gen. Tech. Rep. PNW-GTR-340, U.S. Department of Agriculture, Forest Service, Pacific Northwest Research Station, Portland, OR.

Meigs, G. W., D. P. Turner, W. D. Ritts, Z. Yang, and B. E. Law. 2011. Landscape-scale simulation of heterogeneous fire effects on pyrogenic carbon emissions, tree mortality, and net ecosystem production. Ecosystems 14:758–775.

Minore, D. 1979. Comparative autecological characteristics of northwestern tree species - a literature review. Gen. Tech. Rep. PNW-GTR-087, U.S. Department of Agriculture, Forest Service, Pacific Northwest Research Station, Portland, OR.

Monzingo, D. S., L. A. Shipley, R. C. Cook, and J. G. Cook. 2022. Factors influencing predictions of understory vegetation biomass from visual cover estimates. Wildlife Society Bulletin 46:e1300.

Moore, P. T., H. Van Miegroet, and N. S. Nicholas. 2007. Relative role of understory and overstory in carbon and nitrogen cycling in a southern Appalachian spruce–fir forest. Canadian Journal of Forest Research 37:2689–2700.

Namm, B. H., and J.-P. Berrill. 2012. Accounting for variation in root wood density and percent carbon in belowground carbon estimates. Pages 293–302 Proceedings of the coast redwood forests in a changing California: A symposium for scientists and managers. U.S. Department of Agriculture, Forest Service, Pacific Southwest Research Station, Santa Cruz, CA.

Ohmann, L. F., D. F. Grigal, and L. L. Rogers. 1981. Estimating plant biomass for undergrowth species of northeastern Minnesota forest communiities. Gen. Tech. Rep. NC-61, U.S. Department of Agriculture, Forest Service, North Central Forest Experiment Station, St. Paul, MN.

Olson, C. M., and R. E. Martin. 1981. Estimating biomass of shrubs and forbs in Central Washington Douglas-fir stands. Research Note PNW-380, U.S. Department of

Agriculture, Forest Service, Pacific Northwest Forest and Range Experiment Station, Bend, OR.

Ottmar, R. D., R. E. Vihnanek, and J. C. Regelbrugge. 2000. Stereo photo series for quantifying natural fuels. Volume IV: pinyon-juniper, chaparral, and sagebrush types in the Southwestern United States. PMS 833, National Wildland Coordinating Group, National Interagency Fire Center, Boise, ID.

Pedersen, T. 2024. *patchwork: The Composer of Plots*.

Peters, D. P. C., A. E. Lugo, F. S. Chapin III, S. T. A. Pickett, M. Duniway, A. V. Rocha, F. J. Swanson, C. Laney, and J. Jones. 2011. Cross-system comparisons elucidate disturbance complexities and generalities. Ecosphere 2:art81.

Pickett, S. T. A., and P. S. White, editors. 1985. The Ecology of Natural Disturbance and Patch Dynamics. Academic Press, Inc, San Diego, California.

Pregitzer, K. S., and E. S. Euskirchen. 2004. Carbon cycling and storage in world forests: biome patterns related to forest age. Global Change Biology 10:2052–2077.

PRISM Climate Group. 2024, January. Norm91m: 30-Year Normals, 1991-2020. Oregon State University, https://prism.oregonstate.edu, accessed 1 May 2024.

Pugh, T. A. M., A. Arneth, M. Kautz, B. Poulter, and B. Smith. 2019. Important role of forest disturbances in the global biomass turnover and carbon sinks. Nature Geoscience 12:730–735.

R Core Team. 2024. *R: A Language and Environment for Statistical Computing*. R Foundation for Statistical Computing, Vienna, Austria.

Raymond, C. L., and D. McKenzie. 2012. Carbon dynamics of forests in Washington, USA: 21st century projections based on climate-driven changes in fire regimes. Ecological Applications 22:1589–1611.

Rebain, S. A. 2010. The Fire and Fuels Extension to the Forest Vegetation Simulator: Updated Model Documentation. Internal Rep., U.S. Department of Agriculture, Forest Service, Forest Management Service Center, Fort Collins, CO.

Reilly, M. J., J. E. Halofsky, M. A. Krawchuk, D. C. Donato, P. F. Hessburg, J. D. Johnston, A. G. Merschel, M. E. Swanson, J. S. Halofsky, and T. A. Spies. 2021. Fire Ecology and Management in Pacific Northwest Forests. Pages 393–435 *in* C. H. Greenberg and B. Collins, editors. Fire Ecology and Management: Past, Present, and Future of US Forested Ecosystems. Springer International Publishing, Cham.

Reilly, M. J., A. Zuspan, J. S. Halofsky, C. Raymond, A. McEvoy, A. W. Dye, D. C. Donato, J. B. Kim, B. E. Potter, N. Walker, R. Davis, C. J. Dunn, D. M. Bell, M. J. Gregory, J. D. Johnston, B. J. Harvey, J. E. Halofsky, and B. K. Kerns. 2022. Cascadia Burning: the historic, but not historically unprecedented, 2020 wildfires in the Pacific Northwest, USA. Ecosphere 13:e4070.

Reinhardt, E., D. Lutes, and J. Scott. 2006a. FuelCalc: A method for estimating fuel characteristics. Pages 273–282 Conference Proceedings RMRS-P-41. U.S. Department of Agriculture, Forest Service, Rocky Mountain Research Station, Portland, OR.

Reinhardt, E., J. Scott, K. Gray, and R. Keane. 2006b. Estimating canopy fuel characteristics in five conifer stands in the western United States using tree and stand measurements.

Canadian Journal of Forest Research 36:2803–2814.

Ross, D. W., and J. D. Walstad. 1986. Estimating aboveground biomass of shrubs and young ponderosa and lodgepole pines in southcentral Oregon. Research Bulletin 57, Forest Research Laboratory, Oregon State University, Corvallis, OR.

Sando, R. W., and C. H. Wick. 1972. A method of evaluating crown fuels in forest stands. Research Paper NC-84, U.S. Department of Agriculture, Forest Service, North Central Forest Experiment Station, St. Paul, MN.

Santín, C., S. H. Doerr, E. S. Kane, C. A. Masiello, M. Ohlson, J. M. de la Rosa, C. M. Preston, and T. Dittmar. 2016. Towards a global assessment of pyrogenic carbon from vegetation fires. Global Change Biology 22:76–91.

Scott, J. H., and E. D. Reinhardt. 2001. Assessing crown fire potential by linking models of surface and crown fire behavior. Research Paper RMRS-RP-29, U.S. Department of Agriculture, Forest Service, Rocky Mountain Research Station, Fort Collins, CO.

Seidl, R., W. Rammer, and T. A. Spies. 2014. Disturbance legacies increase the resilience of forest ecosystem structure, composition, and functioning. Ecological Applications 24:2063–2077.

Seidl, R., D. Thom, M. Kautz, D. Martin-Benito, M. Peltoniemi, G. Vacchiano, J. Wild, D. Ascoli, M. Petr, J. Honkaniemi, M. J. Lexer, V. Trotsiuk, P. Mairota, M. Svoboda, M. Fabrika, T. A. Nagel, and C. P. O. Reyer. 2017. Forest disturbances under climate change. Nature Climate Change 7:395–402.

Seidl, R., and M. G. Turner. 2022. Post-disturbance reorganization of forest ecosystems in a changing world. Proceedings of the National Academy of Sciences 119:e2202190119.

Shaw, D. L., Jr. 1979. Biomass equations for Douglas-fir, western hemlock and red cedar in Washington and Oregon. Pages 763–781 *in* W. E. Frayer, editor. Forest Resource Inventories Workshop Proceedings. International Union of Forest Research Organizations, Colorado State University, Fort Collins, CO.

Sillett, S. C., R. Van Pelt, J. A. Freund, J. Campbell-Spickler, A. L. Carroll, and R. D. Kramer. 2018. Development and dominance of Douglas-fir in North American rainforests. Forest Ecology and Management 429:93–114.

Simard, M., W. H. Romme, J. M. Griffin, and M. G. Turner. 2011. Do mountain pine beetle outbreaks change the probability of active crown fire in lodgepole pine forests? Ecological Monographs 81:3–24.

Smith, N. G., and J. S. Dukes. 2017. LCE: leaf carbon exchange data set for tropical, temperate, and boreal species of North and Central America. Ecology 98:2978–2978.

Snell, J. A. K., and S. N. Little. 1983. Predicting crown weight and bole volume of five Western hardwoods. Gen. Tech. Rep. PNW-GTR-151, U.S. Department of Agriculture, Forest Service, Pacific Northwest Forest and Range Experiment Station, Portland, OR.

Spies, T. A. 1991. Plant species diversity and occurrence in young, mature, and old-growth Douglas-fir stands in western Oregon and Washington. Pages 111–121 *in* L. F. Ruggiero, K. B. Aubry, A. B. Carey, and M. H. Huff, editors. Wildlife and vegetation of unmanaged Douglas-fir forests. U.S. Department of Agriculture, Forest Service, Pacific Northwest Research Station, Portland, OR.

Spies, T. A., J. F. Franklin, and T. B. Thomas. 1988. Coarse woody debris in Douglas-fir forests of western Oregon and Washington. Ecology 69:1689–1702.

Spies, T. A., P. A. Stine, R. Gravenmier, J. W. Long, and M. J. Reilly. 2018. Synthesis of science to inform land management within the Northwest Forest Plan area. Gen. Tech. Rep. PNW-GTR-966, U.S. Department of Agriculture, Forest Service, Pacific Northwest Research Station, Portland, OR.

Spies, T., and M. Easter. 1991. Unpublished data. Oregon State University, Forest Science Department, Corvallis, OR.

Standish, J. T., G. H. Manning, and J. P. Demaerschalk. 1985. Development of biomass equations for British Columbia tree species. Information Report BC-X-264, Canadian Forestry Service, Pacific Forest Research Centre, Victoria, B.C.

Stevens, J. T., M. M. Kling, D. W. Schwilk, J. M. Varner, and J. M. Kane. 2020. Biogeography of fire regimes in western U.S. conifer forests: A trait-based approach. Global Ecology and Biogeography 29:944–955.

Swanson, M. E., J. F. Franklin, R. L. Beschta, C. M. Crisafulli, D. A. DellaSala, R. L. Hutto, D. B. Lindenmayer, and F. J. Swanson. 2011. The forgotten stage of forest succession: early-successional ecosystems on forest sites. Frontiers in Ecology and the Environment 9:117–125.

Tepley, A. J., F. J. Swanson, and T. A. Spies. 2013. Fire-mediated pathways of stand development in Douglas-fir/western hemlock forests of the Pacific Northwest, USA. Ecology 94:1729–1743.

Thomas, S. C., and A. R. Martin. 2012. Carbon Content of Tree Tissues: A Synthesis. Forests 3:332–352.

Thompson, J. R., T. A. Spies, and L. M. Ganio. 2007. Reburn severity in managed and unmanaged vegetation in a large wildfire. Proceedings of the National Academy of Sciences 104:10743–10748.

Tichý, L. 2016. Field test of canopy cover estimation by hemispherical photographs taken with a smartphone. Journal of Vegetation Science 27:427–435.

Topik, C., N. M. Halverson, and D. G. Brockway. 1986. Plant association and management guide for the western hemlock zone. R6-ECOL-230A-1986, USDA Forest Service, Pacific Northwest Region.

Van Pelt, R. 2007. Identifying Mature and Old Forests in Western Washington. Washington State Department of Natural Resources.

Volkova, L., K. I. Paul, S. H. Roxburgh, and C. J. Weston. 2022. Tree mortality and carbon emission as a function of wildfire severity in south-eastern Australian temperate forests. Science of the Total Environment 853:158705.

Wickham, H., M. Averick, J. Bryan, W. Chang, L. McGowan, R. François, G. Grolemund, A. Hayes, L. Henry, J. Hester, M. Kuhn, T. Pedersen, E. Miller, S. Bache, K. Müller, J. Ooms, D. Robinson, D. Seidel, V. Spinu, K. Takahashi, D. Vaughan, C. Wilke, K. Woo, and H. Yutani. 2019. Welcome to the tidyverse. Journal of Open Source Software 4:1686.

Zeileis, A., and G. Grothendieck. 2005. zoo: S3 infrastructure for regular and irregular time series. Journal of Statistical Software 14:1–27.

Chapter 2. DRIVERS OF SHORT-INTERVAL REBURN POTENTIAL IN NORTHWESTERN CASCADIA FORESTS

2.1 ABSTRACT

Climate-driven increases in fire activity promote the likelihood of reburns with potential consequences for forest structure and function. Critical understanding of reburn dynamics is missing in high productivity wet forests characterized by infrequent fires. We simulated potential fire behavior and effects in wet temperate forests across northwestern Cascadia 2–5 years post-fire to characterize the relative importance of bottom-up and top-drown drivers of short-interval reburn potential in these systems. Using the Fire and Fuels Extension to the Forest Vegetation Simulator (FFE-FVS) initialized with field data from 95 long-term monitoring plots established in five recent fires across the region, we asked: how do (1) fuel variability, (2) fire weather, and (3) microclimate influence potential fire behavior and effects in reburns? We used generalized linear models to compare outputs of potential fire behavior (flame lengths, torching probability, torching and crowning indices) and effects (tree mortality) under moderate and extreme fire weather conditions with and without microclimate adjustments across pre-fire stand age and burn severity classes. While post-fire fuel loads in all stands were generally sufficient to support subsequent fire occurrence, we found that initial fuel variability influenced some aspects of short-interval reburn potential. Stands burned at high severity in the first fire had reduced potential crown fire behavior and increased potential tree mortality in reburns compared to unburned and low-severity stands. Stands that were mid-seral prior to the first fire had the lowest reburn potential, while both mid- and late-seral stands had less potential tree mortality in reburns compared to young stands, regardless of burn severity in the first fire. Extreme fire weather is likely to override these effects and result in stand-replacing fire effects in reburns regardless of

differences in initial fuel variability among stands. Similarly, stands with cooler and wetter microclimate settings may experience reduced reburn potential, though these effects were limited under extreme fire weather conditions. Collectively, our findings suggest the dominance of top-down drivers on short-interval reburn potential in wet temperate forests, with implications for the design of effective strategies for adapting to increasing fire activity in northwestern Cascadia. By exploring how short-interval post-fire reburn potential varies across dimensions of stand age, burn severity, fire weather, and microclimate, this study builds fundamental understanding of reburn dynamics in wet temperate forests.

2.2 INTRODUCTION

Anticipating the causes and consequences of disturbance interactions is critical for ecosystem management (Burton et al. 2020). In forest ecosystems, climate-driven increases in fire activity (Jolly et al. 2015, Westerling 2016, Abatzoglou and Williams 2016, Jones et al. 2022) promote the likelihood of fire × fire interactions (i.e., reburns). Reburns are fundamental drivers of change (Bowman et al. 2020) and can shape forest successional trajectories by altering vegetation structure and composition (Gray and Franklin 1997). However, when occurring at short intervals, reburns can also produce compound effects (Paine et al. 1998) on forest conditions that may cause abrupt shifts in forest dynamics (Landesmann et al. 2021, Hoecker and Turner 2022) and alter landscape heterogeneity (Harvey et al. 2023), with potential consequences for forest recovery (Busby et al. 2020, Braziunas et al. 2023). Thus, characterizing how one fire changes the probability and timing of reburning in subsequent fires remains a key priority for managing forest landscapes (McLauchlan et al. 2020).

Multiple fires can interact as linked disturbances (Simard et al. 2011) where an initial fire alters reburn likelihood or extent. By consuming available fuels and altering vegetation structure

and composition, past fires can act as temporary barriers to future fire spread and mitigate subsequent burn severity (Parks et al. 2014, 2015). These relationships have been well-studied in forest systems characterized by fuel-limited fire regimes (e.g., dry forests; Prichard et al. 2017) or relatively low productivity rates (e.g., subalpine forests; Harvey et al. 2016), and highlight the roles of initial burn severity and productivity as key determinants of reburn intervals (Buma et al. 2020) and effects (Tortorelli et al. 2024). In contrast, critical understanding of reburn dynamics is missing in high productivity wet forests characterized by climate-limited fire regimes that include infrequent, stand-replacing fire events (Halofsky et al. 2018a). In these forest systems, past fires may not reduce reburn likelihood or severity due to rapid accumulation of live biomass after fire (Halofsky et al. 2018a, 2020, Reilly et al. 2021). Further, growth of more flammable vegetation (e.g., sclerophyllous shrubs) and possible changes in microclimate conditions following stand-replacing fire may increase reburn likelihood relative to unburned areas (Landesmann et al. 2021, Wolf et al. 2021b). However, due to limited data on past fire events, mechanisms and impacts of reburns in wet forests are not well understood.

Improved understanding of drivers of reburn potential in high productivity systems is needed to support forest management decisions aimed at fostering resilience to increasing fire activity (McLauchlan et al. 2020). Reburn dynamics depend largely on biological legacies (i.e., individuals and organic structures that persist following disturbance; Franklin et al. 2000) produced by the previous fire event and subsequent fire weather conditions. Post-fire biological legacies are key bottom-up drivers of reburn potential, shaping the abundance, arrangement, and character of fuels available for reburning (Coppoletta et al. 2016). Two major controls on post-fire fuel variability include stand age prior to fire and burn severity, both of which influence the amount, size, density, and proportion of live and dead fuels (Agee and Huff 1987, Meigs et al.

2011). Fire weather conditions, including temperature, windspeed, and fuel moisture content, are key top-down drivers of reburn potential, influencing critical aspects of fire behavior such as fire intensity, flame length, and rate of spread (Agee 1993). Additionally, the interaction between post-fire biological legacies and fire weather can influence reburn potential through bottom-up effects on microclimate. Residual live and dead canopy cover can buffer subcanopy temperatures, windspeeds, and moisture conditions through effects on intercepted radiation, evapotranspiration, and surface roughness (Chen et al. 1993, Davis et al. 2019, De Frenne et al. 2019), with likely consequences for fuel flammability and fire spread (Wilson et al. 2022).

Wet temperate forests in the Cascade Range of western Washington and northwestern Oregon, USA (hereafter 'northwestern Cascadia'), are an exceptional example of high productivity systems characterized by climate-limited fire regimes. These conifer-dominated forests support very high amounts of biomass (Waring and Franklin 1979) and typically experience large fire events on an interval of one to several centuries (Reilly et al. 2021). In the near future, warming conditions are unlikely to affect fire frequency or severity in northwestern Cascadia (Halofsky et al. 2020). However, in the mid- to longer-term, these wet forest systems are projected to experience the largest proportional increase in area burned within the region (Littell et al. 2018) as drier conditions and human land use increase the potential for small to moderate sized fires (Cattau et al. 2020, Abatzoglou et al. 2021). Further, historical evidence indicates these forests can burn multiple times in the decades following an initial fire (Gray and Franklin 1997, Reilly et al. 2022), suggesting fuel limitation may be minimal. Given the importance of northwestern Cascadia forests to regional and global ecological, economic, and cultural services (Spies et al. 2018, Case et al. 2021), there is considerable interest from tribal, state, and federal agencies in managing post-fire landscapes to reduce fire risk to communities

and forest ecosystem services. In the last decade, more than 0.25 million ha have burned within the region (Reilly et al. 2022), creating a rare opportunity to characterize the relative importance of bottom-up and top-down drivers of short-interval reburn potential in wet temperate forests. Using a common stand simulation model initialized with field data from long-term monitoring plots established 2–5 years following five recent fires across northwestern Cascadia, we asked: how do (1) initial post-fire fuel variability, (2) fire weather conditions, and (3) microclimate influence potential fire behavior and effects in reburns?

2.3 METHODS

2.3.1 *Study area*

Northwestern Cascadia comprises 6.1 million ha of wet temperate forests west of the Cascade Range crest in Washington and northern Oregon, USA. The regional climate is Mediterranean, with mild seasonal temperatures, wet winters, and dry summer (Franklin and Dyrness 1973). Across our sampled area, annual mean temperature range is 4.0–10.7 °C, and total precipitation range is 1,435–3,273 mm, 76% of which occurs November to April (30-year normals, 1991–2020; PRISM Climate Group 2024). Dominant forest types include the *Tsuga heterophylla* and *Abies amabilis* zones (Franklin and Dyrness 1973). The *Tsuga heterophylla* Zone is found at lower elevations (<1,000 m) and dominated by Douglas-fir (*Pseudotsuga menziesii*), western hemlock (*Tsuga heterophylla*), and western redcedar (*Thuja plicata*), with minor components of broadleaf species such as red alder (*Alnus rubra*) and bigleaf maple (*Acer macrophyllum*). The *Abies amabilis* Zone is prevalent at relatively cooler and wetter middle elevations (1,000–1,600 m) and dominated by noble fir (*Abies procera*) and Pacific silver fir (*Abies amabilis*), with common associates including mountain hemlock (*Tsuga mertensiana*). Forest understories are

characterized by abundant cover of shrub, fern, and forb species (Spies 1991). These forests are unique in their evergreen species dominance and high biomass accumulations (Waring and Franklin 1979) which have contributed to their global ecological and economic importance (Spies et al. 2018).

While intermittent non-stand-replacing fires were often more common, an archetypal fire regime within these forests includes large (10^4–10^6 ha), infrequent (200–600 year fire return intervals), stand-replacing fire events limited primarily by climate and weather controls on fuel flammability (Agee 1993). Most fires occur in late summer or early fall following prolonged periods of high heat and low moisture conditions necessary for sufficient drying of fine fuels to ignite and carry fire (Littell et al. 2009, Reilly et al. 2021). Fires typically burn on the surface and as passive or active crown fires, producing coarse-scale spatial mosaics of burn severity dominated by large, high severity patches of near-total overstory tree mortality (Agee 1993, Reilly et al. 2021). The largest fires are driven by synoptic east wind events that bring warm and dry continental air towards the ocean, further decreasing fuel moisture and contributing to rapid fire spread (Reilly et al. 2022). We selected recent (2017–2020) fires across northwestern Cascadia for our study, all of which burned large areas of federal lands under both moderate and east wind-driven conditions, reflecting a range a stand ages and management histories along a latitudinal climate gradient (Spies et al. 2018, Reilly et al. 2022): Norse Peak (2017), Eagle Creek (2017), Big Hollow (2020), Riverside (2020), and Lionshead (2020).

2.3.2 *Field measurements*

We measured initial (2–5 years) post-fire stand structure and fuel loads in 95 1-ha long-term monitoring plots distributed within five recent fires across northwestern Cascadia. Field methods are described in detail in Chapter 1 and summarized here. Plots were systematically stratified by

stand age prior to the first fire (young, mid-seral, late-seral; Van Pelt 2007) and burn severity in the first fire (i.e., percent basal area mortality; unburned, 0%; low, <30%; high, ≥90%). We were unable to locate any large patches of accessible young stands that burned at low severity, thus this condition is not represented here.

Within each plot, we measured general site characteristics and post-fire stand structure and surface fuel profiles. General site characteristics (slope, aspect, elevation, topography) were recorded at plot center using standard methods. Stand structure (basal area, stem density) was characterized in variable-radius subplots for all trees (diameter at breast height [dbh] ≥ 10 cm), saplings (dbh < 10 cm and height ≥ 30 cm), and live seedlings (height < 30 cm). For trees, measures included species, status (live or dead), decay class, dbh, total height, percent bark at dbh, and percent total stem remaining. Burn severity measures (wood char, bark char, char height, needle scorch) were also recorded for trees in burned stands. For saplings, measures included species, status, dbh, total height, and presence of broken top. For seedlings, measures included species, total height, and presence of top damage. Canopy cover was estimated from hemispherical digital photographs taken at five positions throughout each plot (Tichý 2016). Surface fuel profiles of down woody debris, litter, and duff were measured in planar intercept transects using standard methods (Brown 1974, Lutes et al. 2006).

2.3.3 *Potential fire behavior modeling*

We modeled stand-level reburn potential using the Westside Cascades variant (FVS Staff 2008) of the Fire and Fuels Extension to the Forest Vegetation Simulator (FFE-FVS; Rebain 2010). FFE-FVS combines models of fire behavior (Rothermel 1972, Van Wagner 1977, Scott and Reinhardt 2001), fire effects (Reinhardt et al. 1997), and fuel and snag dynamics (Rebain 2010) with a deterministic individual tree growth and yield model (Dixon 2002) to support forest

management decisions. We chose this modeling approach because FFE-FVS is a well-documented tool with a broad geographic scope and long history of use by both scientific and management communities (Rebain 2010), allowing for easier interpretation and comparison of our outputs with other studies.

Vegetation inputs — We initialized FFE-FVS with stand and tree inputs derived from each of our post-fire field plots ($N = 95$). Stand inputs included inventory year (2019–2023), Forest Service region, state, National Forest location code, aspect, slope, elevation, topography code, and dead surface fuel loads. Dead surface fuels included fine and coarse woody debris, litter, and duff. Methods for deriving fuel loads are described in detail in Chapter 1. Briefly, we used species-, size-, and region-specific allometric equations (Means et al. 1994) to convert our field measures into stand-level fuel profiles. Surface fuel profiles were adjusted for volume and density loss from decay (Harmon et al. 2008, 2011, Donato et al. 2013) and deep wood charring (Donato et al. 2009). Fine woody debris was summarized by standard time-lag size class (1-, 10-, 100-h particles), and coarse woody debris (1000-h particles) was summarized by decay (sound vs. rotten) and size classes based on diameter (Brown 1974). We converted stand-level mean depths of litter and duff into biomass using standard methods (Brown et al. 1982, Woodall and Monleon 2008) and bulk density values averaged across relevant sources for Douglas-fir forests (Williams and Dyrness 1967, Lutes et al. 2006, Woodall and Monleon 2008, Prichard et al. 2013). Surface fuel inputs are summarized in Appendix C: Table 2.3. Tree inputs included the species, per-hectare count, history code (live, dead, or pre-fire snag), diameter, total height, live crown base height, crown ratio, and broken top damage code for all live and dead individuals. Diameter inputs represented dbh for trees with height ≥ 1.37 m and diameter at root collar for height < 1.37 m. Small saplings (height 0.3–1.37 m) and seedlings (height < 0.3 m) were

assigned a small non-zero diameter (0.25 cm) according to suggested practice (Dixon 2002, Crookston et al. 2003). Tree inputs are summarized in Chapter 1.

Fuel model selection — Within each stand, we used FFE-FVS to generate projections of potential fire behavior (surface and total flame lengths, torching probability, torching and crowning indices) and effects (basal area mortality) under moderate and extreme fire weather conditions. We used the new model selection logic to dynamically determine a weighted set of two standard fire behavior fuel models for each stand, drawing from the compiled set of all 53 fuel models. Sensitivity analyses revealed similar qualitative trends in potential fire behavior outputs among strata when using this approach to assign primary and secondary fuel models versus selecting from just the original 13 (Albini 1976, Anderson 1982) or new 40 (Scott and Burgan 2005) standard fire behavior fuel models (Appendix C: Figs. 2.6–2.10). We also adjusted default settings to include both conifer and hardwood tree species in canopy fuel calculations.

Fire weather scenarios — We defined two scenarios of baseline temperature, wind speed, and surface fuel moisture inputs to compare potential fire behavior in reburns under both moderate and extreme fire weather conditions (Table 2.1). Temperature and wind speed values were derived from statistical climate-fire relationships for the region based on meteorological data extracted from 27 fires that burned >400 ha within northwestern Cascadia between 2003 and 2021 (Raymond et al., in prep). Moderate fire weather values represented average conditions sufficient to support ecologically small to moderate-sized fires (<10,000 ha). Extreme fire weather values represented conditions enabling very large east wind-driven fires (40,000 ha), based on observations from the day of the most area burned in the 2020 Beachie Creek fire – the largest contemporary fire within the study area (78,336 ha; Reilly et al. 2022). Moisture contents of surface fuel components for moderate and extreme fire weather conditions were represented

by variant-specific FFE-FVS defaults from the "moist" and "very dry" moisture groups, respectively (Table 2.1; Rebain 2010).

Table 2.1. Baseline temperature, wind speed, and fuel moisture content inputs for modeling two scenarios of potential fire weather in reburns. Inputs were based on meteorological data from recent (2003–2021) fires observed within northwestern Cascadia. Moderate scenario values represent conditions typical for moderate-sized (<10,000 ha) wildfires. Extreme scenario values represent conditions typical for very large (>40,000 ha) east wind-driven wildfires.

Variable	**Potential fire weather scenario**	
	moderate	**extreme**
Air temperature (°C)	18.0	25.6
20-ft wind speed (m/s)	4.0	13.6
Surface fuel moisture content (%)		
1-h fuels (0–0.6 cm)	12	4
10-h fuels (0.6–2.5 cm)	12	4
100-h fuels (2.5–7.6 cm)	14	5
1000-h fuels (>7.6 cm)	25	10
Duff	125	15
Live woody and herbaceous fuels	150	70

Microclimate adjustments — We incorporated differences in microclimate conditions into our FFE-FVS simulations by adjusting fire weather inputs based on stand structure. We synthesized data from relevant literature in wet temperate forests to derive linear relationships between microclimate variables and canopy cover (Appendix C). Using these relationships, we adjusted baseline values of temperature and fine (1-h, 10-h, 100-h) fuel moisture content for each stand based on total canopy cover. We assumed baseline values represented open conditions (i.e., 0% canopy cover) to account for the buffering effects of canopy cover. Adjusted temperature and fine fuel moisture inputs for both moderate and extreme fire weather scenarios are summarized across stand age × burn severity strata in Appendix C: Table 2.6. We kept inputs for all other fire weather variables at their baseline values since canopy cover effects on wind speed are already

built into the fire submodel of FFE-FVS (Rebain 2010), and we found limited evidence to support robust relationships between canopy cover and moisture content of coarse (1000-h) fuels, duff, and live surface fuels.

2.3.4 *Analysis*

We assessed the effects of post-fire fuel variability, fire weather, and microclimate on short-interval reburn potential by constructing generalized linear models for each potential fire behavior (surface flame length, total flame length, torching probability, torching index, crowning index) and effects (tree mortality) output from FFE-FVS (Rebain 2010). To address Question 1, we modeled these outputs as a function of stand age prior to and burn severity in the first fire. Models of non-negative continuous responses (flame lengths, fire behavior indices) used a gamma distribution with log link function and zero-inflation term. Models of proportional responses (torching probability, tree mortality) used a beta distribution with ordered logit link function (Kubinec 2023). To address Question 2, we created separate models for outputs generated under both moderate and extreme fire weather scenarios, using the same model form as Question 1 (i.e., response ~ stand age × burn severity). To address Question 3, we created separate models for outputs generated using baseline versus microclimate-adjusted fire weather inputs, using the same model form as Questions 1 and 2. For all questions, differences among strata were considered significant when confidence intervals for a response did not overlap. Analyses were conducted in R, version 4.4.0 (R Core Team 2024) using the following packages: *glmmTMB*, version 1.1.9 (Brooks et al. 2017); *openxlsx*, version 4.2.7.1 (Schauberger and Walker 2024); *patchwork*, version 1.2.0 (Pedersen 2024); and *tidyverse*, version 2.0.0 (Wickham et al. 2019).

2.4 RESULTS

2.4.1 *Fuel variability*

Fuel variability was a significant predictor of short-interval (2–5 years) post-fire reburn potential, though direction and magnitude of differences varied by stand age prior to and burn severity in the first fire. Stand age prior to the first fire generally had a negative relationship with most potential fire behavior and effects responses (Appendix C: Table 2.7). Stand age effects were driven primarily by differences of young stands from mid- and late-seral stands. Compared to young stands, total flame lengths in reburns across all burn severity classes were 37% shorter under moderate fire weather conditions in mid-seral stands, with stronger differences between unburned stands (Fig. 1c), though the actual height difference in flame lengths was only ~0.5 m (Table 2.2). Compared to young stands, torching probabilities in reburns across both fire weather scenarios were 27–47% lower in unburned late- and mid-seral stands, respectively, with stronger differences under moderate fire weather conditions (Fig. 1e–f). Compared to young stands, potential tree mortality in reburns across all burn severity classes was 52–62% less under moderate fire weather conditions in mid- and late-seral stands, respectively, with stronger differences between unburned stands (Fig. 2a). Compared to young stands, crowning indices in reburns were 57% greater in unburned late-seral stands (Fig. 3b). We found no significant differences in potential fire behavior and effects in reburns between stands that were mid- and late-seral prior to the first fire.

Burn severity in the first fire did not have a consistent relationship with potential fire behavior and effects responses in reburns (Appendix C: Table 2.7). Effects of burn severity in the first fire on response variables were frequently driven by differences of stands burned at high severity from unburned and stands burned at low severity in the first fire, especially under

extreme fire weather conditions. Compared to unburned stands, surface flame lengths in reburns across all stand age classes were 34–52% taller under moderate fire weather conditions in stands first burned at low and high severity, respectively (Fig. 1a), though the actual height difference in flame lengths was only ~0.2–0.4 m (Table 2.2). Under extreme fire weather conditions, all stands burned at high severity in the first fire, regardless of age prior to the first fire, also had 137% taller surface flame lengths in reburns than unburned stands (Fig. 1b) and 80–82% shorter total flame lengths in reburns than stands burned at low severity and unburned stands (Fig. 1d). Compared to unburned stands, torching probabilities in reburns were 56–66% lower in low-severity late- and mid-seral stands, respectively, with stronger differences under moderate fire weather conditions (Fig. 1e–f). Torching probabilities were near zero in all stands first burned at high severity regardless of stand age prior to the first fire or reburn fire weather conditions (Fig. 1e–f). Compared to unburned and low-severity stands, potential tree mortality in reburns across all stand age classes was generally 24–133% greater under moderate fire weather conditions in stands burned at high severity in the first fire, though this relationship was only significant for late-seral stands (Fig. 2a). Torching indices in reburns were similar between burned and unburned stands, but nearly 400% greater in stands burned at low versus high severity in the first fire (Fig. 3a). Crowning indices in reburns were similar between unburned and low-severity stands, but 256–282% greater in mid- and late-seral stands burned at high severity in the first fire, respectively (Fig. 3b).

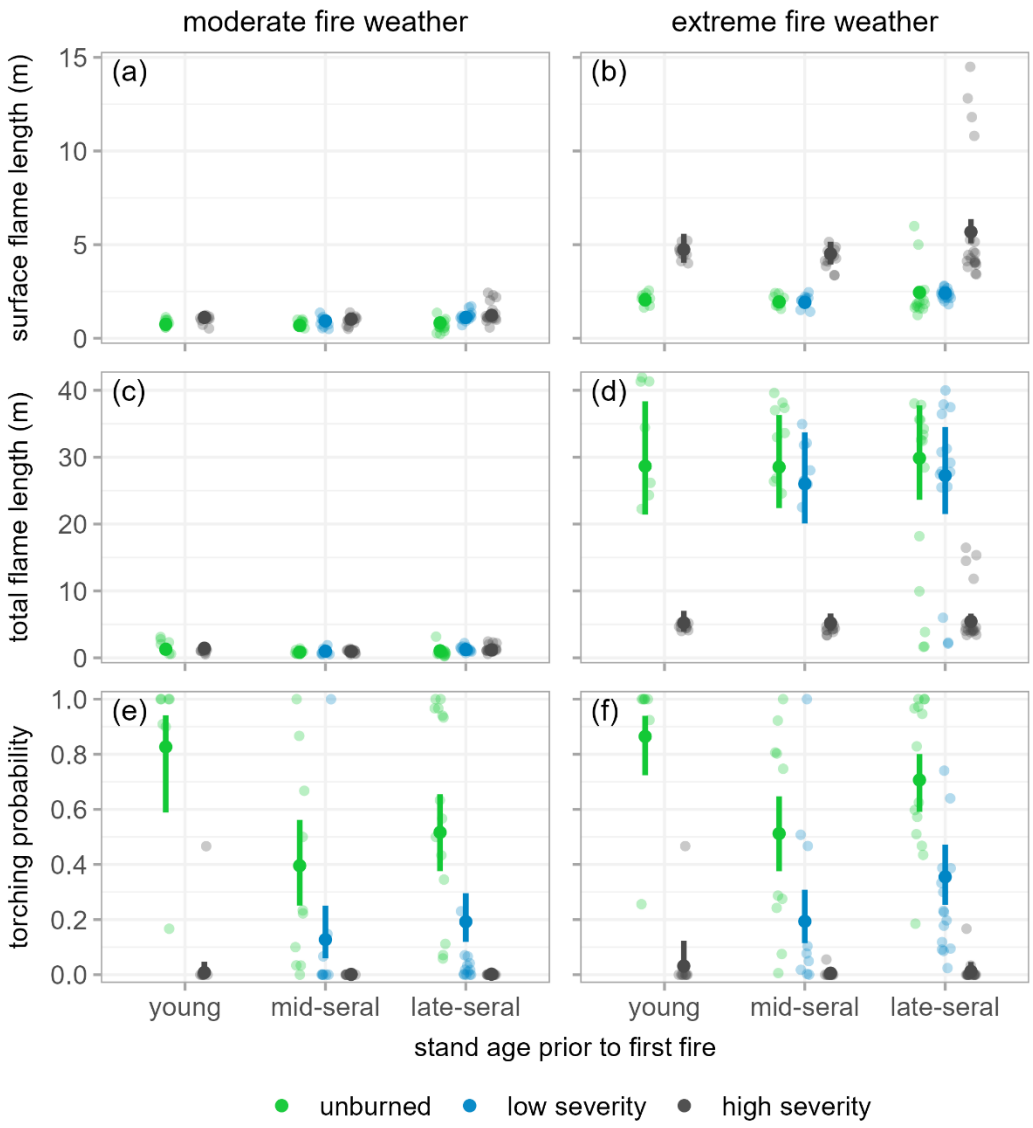

Figure 2.1. Potential fire behavior in reburns 2–5 years post-fire under moderate (*left*) and extreme (*right*) fire weather conditions. Fire weather conditions include plot-level adjustments to temperature and fine fuel moisture content account for structural effects on microclimate. Bold points and lines are generalized linear model-predicted means and 95% confidence intervals for each stand age class, colored by burn severity in the first fire: unburned, low severity (≤30% mortality), high severity (≥90% mortality). Light points are plot-level values. See Appendix C: Table 2.7 for model summaries.

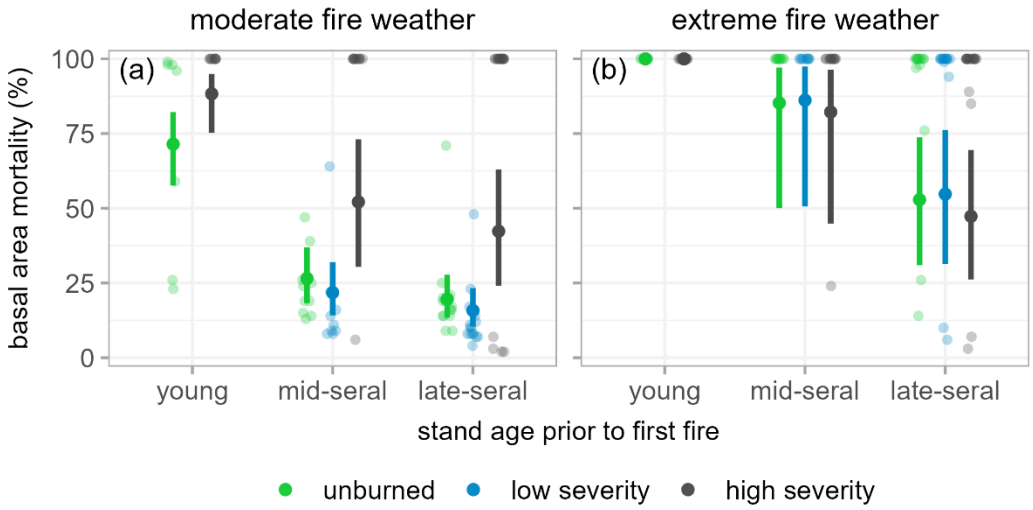

Figure 2.2. Potential fire effects in reburns 2–5 years post-fire under moderate (*left*) and extreme (*right*) fire weather conditions. Fire weather conditions include plot-level adjustments to temperature and fine fuel moisture content account for structural effects on microclimate. Bold points and lines are generalized linear model-predicted means and 95% confidence intervals for each stand age class, colored by burn severity in the first fire: unburned, low severity (≤30% mortality), high severity (≥90% mortality). Light points are plot-level values. See Appendix C: Table 2.7 for model summaries.

2.4.2 *Fire weather*

Fire weather moderated the effects of fuel variability on short-interval (2–5 years) post-fire reburn potential. In general, potential flame lengths and tree mortality in reburns were greater under extreme versus moderate fire weather conditions (Appendix C: Table 2.7). Compared to moderate conditions, surface flame lengths in reburns were 2–5 times taller (Fig. 1a–b), total flame lengths in reburns were 4–45 times taller (Fig. 1c–d), and tree mortality in reburns was 14–291% greater (Fig. 2) under extreme fire weather conditions across all stands. Significant effects of fuel variability on flame lengths in reburns were only maintained under extreme fire weather for the late-seral and high-severity stands (Fig. 1a–d), and effects of fuel variability on tree mortality in reburns were diminished under extreme fire weather (Fig. 2). Torching probabilities

in reburns were similar under both fire weather scenarios (Fig. 1e–f).

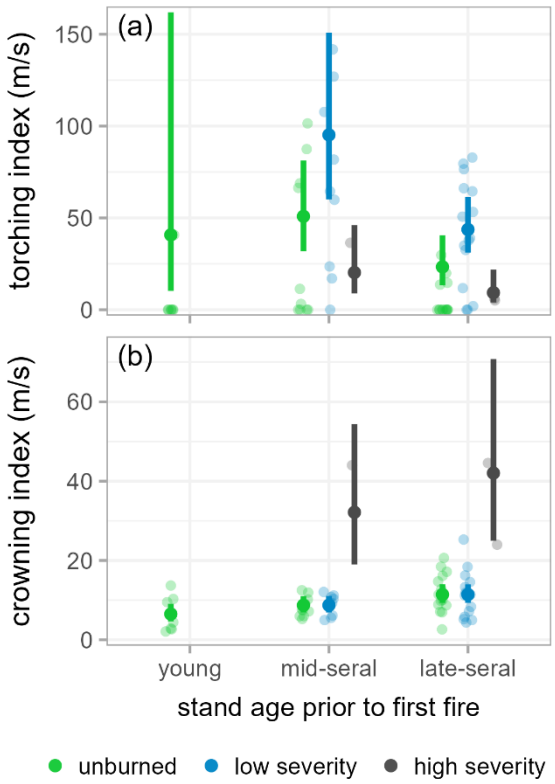

Figure 2.3. Indices of torching (a) and crowning (b) potential fire behavior in reburns 2–5 years post-fire. Bold points and lines are generalized linear model-predicted means and 95% confidence intervals for each stand age class, colored by burn severity in the first fire: unburned, low severity (≤30% mortality), high severity (≥90% mortality). Light points are plot-level values. Predicted outputs for young × high-severity stands are not shown since canopy base heights were undefined due to sparse canopy fuels. See Appendix C: Table 2.7 for model summaries.

2.4.3 *Microclimate*

Incorporating structural effects on microclimate into fire weather inputs had a buffering effect on short-interval (2–5 years) post-fire reburn potential, but did not change overall patterns with fuel variability and fire weather drivers for most response variables (Appendix C: Tables 2.7–2.8). Microclimate buffering was greatest in unburned stands and under the moderate fire weather scenario (Appendix C: Table 2.6). In general, including microclimate adjustments lowered

potential surface and total flame lengths in unburned stands by 36–43% and 62–67%, respectively, with greater reductions for older stands (Table 2.2). Including microclimate adjustments also lowered potential basal area mortality in high severity mid- and late-seral stands by 45–54%, respectively (Table 2.2). Compared to unadjusted simulations, microclimate adjustments maintained consistent relationships of stand age prior to and burn severity in the first fire with potential fire behavior and effects in reburns under extreme fire weather conditions (Appendix C: Tables 2.7–2.8). These relationships were also consistent under moderate fire weather conditions for all outputs except potential flame lengths and torching index. Incorporating microclimate adjustments eliminated the significant positive effect of stand age and negative effect of burn severity on potential surface and total flame lengths, respectively, and indicated a significant positive effect of burn severity on potential surface flame lengths not indicated in unadjusted simulations (Appendix C: Tables 2.7–2.8). Incorporating microclimate adjustments also indicated a significant negative effect of high burn severity on torching index not indicated in unadjusted simulations (Appendix C: Tables 2.7–2.8).

Table 2.2. Model-predicted means and 95% confidence intervals for initial (2–5 years) post-fire potential fire behavior and effects in reburns across pre-fire stand age × burn severity strata (N = 95). Separate generalized linear models were fit for outputs simulated under moderate and extreme scenarios of reburn fire weather conditions, both with (adjusted) and without (unadjusted) stand-level microclimate adjustments.

Variable	young		mid-seral			late-seral		
	unburned	high	unburned	low	high	unburned	low	high
moderate fire weather								
surface flame length (m)								
adjusted	0.7 (0.6-0.9)	1.1 (0.9-1.3)	0.7 (0.6-0.8)	0.9 (0.8-1.1)	1.0 (0.9-1.2)	0.8 (0.7-0.9)	1.1 (1.0-1.3)	1.2 (1.1-1.4)
unadjusted	1.1 (0.9-1.3)	1.1 (0.9-1.4)	1.1 (0.9-1.3)	1.1 (1.0-1.4)	1.1 (1.0-1.3)	1.4 (1.2-1.6)	1.5 (1.3-1.7)	1.4 (1.3-1.6)
total flame length (m)								
adjusted	1.3 (1.0-1.6)	1.4 (1.1-1.8)	0.8 (0.7-1.0)	1.0 (0.8-1.2)	0.9 (0.8-1.1)	1.0 (0.9-1.3)	1.2 (1.0-1.5)	1.2 (1.0-1.4)
unadjusted	3.4 (2.5-4.8)	1.6 (1.1-2.3)	2.3 (1.7-3.1)	1.5 (1.1-2.1)	1.0 (0.8-1.4)	3.0 (2.2-3.9)	2.0 (1.5-2.6)	1.4 (1.1-1.7)
torching probability								
adjusted	0.83 (0.59-0.94)	0.01 (0.00-0.05)	0.40 (0.25-0.56)	0.13 (0.06-0.25)	0.00 (0.00-0.01)	0.52 (0.38-0.65)	0.19 (0.12-0.30)	0.00 (0.00-0.01)
unadjusted	0.77 (0.57-0.90)	0.02 (0.00-0.07)	0.38 (0.26-0.52)	0.10 (0.05-0.17)	0.00 (0.00-0.01)	0.58 (0.45-0.69)	0.19 (0.12-0.29)	0.01 (0.00-0.03)
basal area mortality (%)								
adjusted	71 (58-82)	88 (75-95)	27 (18-37)	22 (14-32)	52 (30-73)	20 (13-28)	16 (10-23)	42 (24-63)
unadjusted	73 (56-85)	98 (92-100)	44 (30-59)	35 (22-50)	94 (79-99)	37 (26-51)	29 (19-41)	92 (75-98)
extreme fire weather								
surface flame length (m)								
adjusted	2.0 (1.7-2.4)	4.7 (4.0-5.6)	1.9 (1.7-2.2)	1.9 (1.7-2.2)	4.5 (3.9-5.2)	2.4 (2.2-2.8)	2.4 (2.1-2.8)	5.7 (5.1-6.4)
unadjusted	2.4 (2.0-2.8)	4.8 (4.1-5.6)	2.3 (2.0-2.7)	2.3 (2.0-2.6)	4.7 (4.1-5.4)	2.9 (2.6-3.3)	2.8 (2.5-3.2)	5.9 (5.2-6.5)
total flame length (m)								
adjusted	28.7 (21.4-38.4)	5.2 (3.9-7.0)	28.5 (22.4-36.3)	26.0 (20.1-33.7)	5.2 (4.1-6.6)	29.9 (23.6-37.8)	27.2 (21.5-34.5)	5.5 (4.5-6.6)
unadjusted	32.3 (24.8-42.0)	5.2 (4.0-6.7)	33.3 (26.8-41.5)	28.4 (22.6-35.9)	5.4 (4.3-6.7)	36.1 (29.2-44.5)	30.8 (24.9-38.1)	5.8 (4.9-6.9)
torching probability								
adjusted	0.86 (0.72-0.94)	0.03 (0.01-0.12)	0.51 (0.38-0.65)	0.19 (0.11-0.31)	0.01 (0.00-0.02)	0.71 (0.59-0.80)	0.36 (0.25-0.47)	0.01 (0.00-0.05)
unadjusted	0.84 (0.65-0.94)	0.03 (0.01-0.13)	0.56 (0.43-0.68)	0.25 (0.17-0.37)	0.01 (0.00-0.03)	0.70 (0.59-0.80)	0.39 (0.29-0.50)	0.01 (0.00-0.05)
basal area mortality (%)								
adjusted	100 (100-100)	100 (100-100)	85 (50-97)	86 (51-97)	82 (45-96)	53 (31-74)	55 (31-76)	47 (26-69)
unadjusted	100 (100-100)	100 (100-100)	90 (60-98)	86 (50-98)	82 (47-96)	63 (39-83)	54 (29-78)	47 (26-69)

fire behavior indices								
torching index (m/s)								
adjusted	41 (10-162)	16 (3-85)	51 (32-81)	95 (60-151)	20 (9-46)	23 (13-41)	44 (31-61)	9 (4-22)
unadjusted	30 (8-113)	16 (3-75)	35 (23-55)	78 (50-122)	18 (8-40)	17 (10-30)	38 (27-53)	9 (4-20)
crowning index (m/s)								
adjusted	7 (5-9)	24 (13-45)	9 (7-11)	9 (7-11)	32 (19-54)	11 (9-14)	11 (9-14)	42 (25-71)
unadjusted	6 (4-8)	23 (11-45)	8 (6-10)	8 (6-10)	31 (17-54)	10 (8-13)	10 (8-13)	41 (23-72)

Notes: Torching and crowning indices are based on extreme fire weather conditions.

2.5 DISCUSSION

2.5.1 *Fuel variability can influence short-interval reburn potential under moderate fire weather*

Our findings suggest that initial post-fire fuel variability can influence some measures of short-interval reburn potential in northwestern Cascadia. Burn severity in the first fire has important consequences for subsequent fire behavior and effects (Busby et al. 2020). Potential surface fire behavior in reburns 2–5 years post-fire may be similar regardless of burn severity in the first fire, despite small increases in potential surface flame lengths in burned stands due to greater proportions of dead surface fuels. However, both low and high burn severity in the first fire may reduce the likelihood of torching in reburns due to reductions in surface and ladder fuels via combustion. In contrast, only high burn severity in the first fire may reduce potential crown fire behavior in reburns due to near-complete overstory mortality and reduction in crown fuels compared to unburned stands. Low burn severity in the first fire is unlikely to result in different crown fire behavior in reburns than unburned stands due to similarities in live stand structure and canopy fuel loads following the first fire (Agee 1993). However, reburn severity can still be high in the absence of crown fire behavior (Raymond and Peterson 2005). High burn severity in the

first fire may increase potential tree mortality in reburns relative to unburned and low-severity stands until regenerating trees are able to develop more fire-resistant traits (e.g., thicker bark, taller crown base heights). This aligns with findings in similar forest types (Thompson et al. 2007, Collins et al. 2021) and fire regimes (Harvey et al. 2016), but contrasts with dry frequent-fire systems where past fires have been found to decrease severity of subsequent burns for a decade or more (Prichard and Kennedy 2014, Cansler et al. 2021).

Stand age prior to the first fire may also influence potential fire behavior and effects in reburns but is likely a weaker driver than burn severity and may be more easily overridden under extreme fire weather conditions. Mid-seral stands may have lower reburn potential 2–5 years post-fire due to taller canopy base heights decreasing the likelihood of torching. This aligns with findings from chronosequence fuel studies in the region which highlight the strongest buffering effects of stand age on surface fire behavior in mid-seral stands (Agee and Huff 1987). In contrast, late-seral stands may have increased potential surface fire intensity in reburns due to greater surface fuel loads of fine and coarse woody debris, litter, and duff (Appendix C: Table 2.3). Compared to young stands, mid- and late-seral stands may experience lower burn severity in reburns under moderate weather. Greater abundance of larger trees in older stands may offer greater resistance to subsequent fire-induced tree mortality, similar to findings from field-based (Busby et al. 2023) and remotely-sensed (Evers et al. 2022) observations within the study area. Young stands are likely to experience severe fire effects in reburns regardless of fire weather and prior burn severity due to smaller tree stature and abundant fine surface fuels that result in low fire resistance and high fuel availability (Thompson et al. 2007). This aligns with similar field observations of higher mortality in recently-burned young stands across northwestern Cascadia (Busby et al. 2023), and provides support for our inability to locate any large patches of

accessible young stands burned at low severity across the study region.

While we demonstrated some effects of initial post-fire fuel variability on short-interval reburn potential, our findings are limited by model handling of live and dead surface fuels. FFE-FVS represents live woody shrubs and herbaceous surface fuels based on relationships with overstory canopy cover, rather than as an explicit model input (Rebain 2010). This may result in an inability to capture accurate dynamics of live surface fuel abundance and flammability traits on reburn potential in northwestern Cascadia, as demonstrated in other wet temperate forests (Tiribelli et al. 2018, Landesmann et al. 2021, Brown et al. 2024). Rapid growth of shrubs and resprouting vegetation following high severity fire has also been shown to promote severe reburns in other systems with stand-replacing fire regimes (Agne et al. 2023) and in dry fire-prone forests (Coppoletta et al. 2016). Additionally, the use of stylized fire behavior fuel models to represent fuelbed conditions, rather than explicit fuel load inputs, may obscure finer-scale effects of initial fuel variability on reburn potential (Noonan-Wright et al. 2014).

2.5.2 *Fire weather may override effects of fuel variability on short-interval reburn potential*

Our findings suggest the dominance of top-down drivers on short-interval reburn potential in wet temperate forests. Extreme fire weather conditions (i.e., higher temperature, faster windspeed, and lower fuel moisture) may override effects of initial fuel variability on potential fire behavior and effects in reburns by promoting fire occurrence, spread, and size. Effects of stand age prior to the first fire may be more easily overridden than effects of burn severity in the first fire, due to less influence of fuel amount compared to fuel character (i.e., live vs. dead) on potential fire behavior in reburns. Although potential tree mortality in reburns may be lower in stands that were older prior to the first fire, extreme fire weather in reburns is likely to result in stand-replacing fire effects regardless of differences in initial fuel variability among stands due to

limited adaptations of dominant tree species to resist high intensity fire. This aligns with findings of reduced strength of fuel limitations on reburn potential under warmer, drier, and windier conditions in northwestern Cascadia (Reilly et al. 2022, Evers et al. 2022, Busby et al. 2023), other wet temperate forests (Leonard et al. 2014) and stand-replacing fire regimes (Turner and Romme 1994), and more fire-prone dry forests (Parks et al. 2018; though see Prichard and Kennedy 2014 and Tortorelli et al. 2024).

While we used statistical fire-climate relationships to define thresholds for moderate and extreme fire weather conditions, the relatively small sample size of recent fires in the region limits the quantitative strength of these relationships (Raymond et al., in prep). Continued refinement of fire-climate relationships in northwestern Cascadia and use of site-specific weather inputs (e.g., FireFamily Plus; Bradshaw and McCormick 2009) could strengthen our ability to disentangle the effects of fuels and fire weather on reburn potential under changing climate (Littell et al. 2018) and increase the accuracy of our simulations (Hummel et al. 2013).

2.5.3 *Microclimate conditions buffer the effects of fire weather in reburns*

Our findings suggest that microclimate conditions can moderate the effects of fire weather on reburn potential in wet temperate forests. Incorporating buffering effects of post-fire canopy cover on fire weather thresholds reduced potential fire behavior and effects in reburns through reductions in temperature, windspeed, and fuel aridity. Accordingly, buffering effects were greatest for older and unburned stands. These findings align with microclimate studies in northwestern Cascadia (Chen et al. 1993, Frey et al. 2016, Wolf et al. 2021a) and other wet temperate forest systems (Millikin et al. 2024) which have demonstrated greater temperature, wind, and moisture buffering capacity of old and dense forests due to effects of canopy cover on intercepted radiation, evapotranspiration, and surface roughness. However, microclimate

conditions may only be effective at reducing reburn potential under moderate fire weather and do not meaningfully reduce torching probability. Buffering effects were reduced under extreme fire weather conditions, supporting findings of limited benefits of canopy cover on reducing temperatures under extreme hot and dry conditions (Brackett et al. 2024).

Due to limited available studies on fire-microclimate relationships in northwestern Cascadia, our representation of microclimate effects by modifying fire weather thresholds based on canopy cover was relatively simple, and likely unable to capture more detailed and dynamic drivers of microclimate in wet forests. For example, understory vegetation abundance and type can moderate surface fuel moisture (Pickering et al. 2021), and the strength of canopy buffering may change under future climate (Davis et al. 2019). Thus, explicit measures of microclimate in recently burned stands over time will be important for accurately characterizing the relationships between structure and reburn potential in these systems.

2.5.4 *Management implications and future research*

These findings build fundamental understanding of the drivers of short-interval reburn potential in wet temperate forests. By exploring how potential fire behavior and effects in reburns 2–5 years post-fire vary across dimensions of stand age, burn severity, fire weather, and microclimate, application of this research can help forest managers design strategies for adapting to increasing fire activity in northwestern Cascadia. There is particular interest among regional forest managers in effects of fuel treatments on fire risk in unburned stands (Powers 2021, Powers and Kertis 2022). Our results suggest that fire has a limited role as an effective stand-scale fuel reduction treatment in high productivity systems shaped by infrequent fire events (Halofsky et al. 2018b). While traditional fuel treatments such as mechanical thinning and prescribed fire can be useful for decreasing fire intensity and severity in dry forests (Agee and

Skinner 2005), these actions are typically assumed to be less effective at moderating fire behavior in wet forests (Halofsky et al. 2018b). However, few opportunities exist to robustly test these assumptions in northwestern Cascadia. Our results demonstrate similar subsequent fire behavior and effects between unburned and low-severity stands despite reductions in surface and ladder fuels following low severity fire. Our findings also highlight that any potential fuel-reduction effects from recent wildfire on reburn potential are likely to be overridden under extreme fire weather. Additionally, while our results demonstrated that an initial high severity fire may reduce crown fire behavior in short-interval reburns, this kind of fuel reduction by fire may predispose stands to heightened reburn severity. Further, given the high productivity and rapid recovery of live fuels following fire, maintaining these effects would require frequent re-treatment, and reductions in fuels to this intensity may present undesirable tradeoffs with fundamental structural and functional attributes of these ecosystems (Halofsky et al. 2018b, Millikin et al. 2024).

Our study highlights several directions for future research to further address uncertainties about drivers of reburn potential in northwestern Cascadia. While our study provided useful insights into potential fire behavior and effects in reburns 2–5 years post-fire, this timeframe may be too short to adequately capture realistic reburn dynamics. For instance, historical evidence from the 1902 Yacolt Burn and 1933 Tillamook Burn observed reburn intervals of 6–30 years (Neiland 1958, Gray and Franklin 1997), while typical fire return intervals range from one to several centuries (Reilly et al. 2021). Thus, continued monitoring and repeated measurement of these long-term plots over time, and additional sampling of reburned areas, will be critical for characterization of patterns in structure and fuel profiles throughout stand development. Combining field data with simulation modeling approaches could be a useful way to extend field

insights and get at reburn dynamics over longer time scales (Loehman et al. 2020). Simulation modeling could also enable exploration of reburn dynamics under future climate and management scenarios (e.g., Hansen et al. 2020) and incorporate spatial dimensions relevant to post-fire stand development trajectories (e.g., distance to seed source; Harvey et al. 2023, Buonanduci et al. 2024).

Future work could also consider modeling approaches that better represent the influences of live surface fuels and microclimate on potential fire behavior and effects. These factors are highly relevant to reburn potential in northwestern Cascadia (Agee and Huff 1987, Gray et al. 2002) and other wet temperate forest systems (Cawson et al. 2017, Pickering et al. 2021, Lindenmayer et al. 2022), but not captured well by FFE-FVS. Use of more complex fire behavior models (e.g., Hoffman et al. 2018) combined with empirical observations of microclimate conditions within our recently burned stands across the region (e.g., Wolf et al. 2021b) could help improve our understanding of reburn potential in these forest types.

2.6 APPENDIX C: SUPPLEMENTAL METHODS, RESULTS, AND STATISTICAL MODEL OUTPUTS

C.1 *Model inputs*

Table 2.3. Summary of surface fuel input variables across stand age × burn severity strata. Values are the mean (minimum-maximum) fuel loads (Mg/ha) across all replicates within each strata combination (N = 95). Fuel loads for 1000-h particles are separated by decay status (sound, rotten) and binned by diameter size classes.

Variable	**young** (*n* = 16)		**mid-seral** (*n* = 31)			**late-seral** (*n* = 48)		
	unburned (*n* = 7)	**high** (*n* = 9)	**unburned** (*n* = 10)	**low** (*n* = 9)	**high** (*n* = 12)	**unburned** (*n* = 14)	**low** (*n* = 15)	**high** (*n* = 19)
litter	10.2 (8.6-12.7)	3.1 (0.3-6.6)	16.9 (9.7-27.8)	7.9 (4.7-14.8)	3.4 (0.5-8.7)	13.0 (7.5-28.6)	10.4 (6.5-20.7)	6.3 (1.5-11.7)
duff	54.1 (32.0-93.6)	5.1 (0.3-23.5)	81.7 (25.3-166.4)	31.7 (10.0-79.7)	2.7 (0.0-12.9)	85.5 (33.0-144.1)	34.2 (9.5-85.4)	14.0 (0.0-40.6)
1-h	3.7 (1.8-5.7)	1.5 (0.8-3.3)	4.9 (3.4-7.2)	4.7 (2.6-6.3)	2.3 (0.7-5.2)	5.2 (3.1-8.6)	5.9 (3.9-8.4)	3.2 (0.4-9.2)
10-h	3.8 (1.9-6.2)	2.7 (0.9-4.4)	5.3 (3.1-6.8)	4.5 (1.6-9.8)	3.4 (1.5-6.8)	5.1 (3.0-9.8)	4.6 (2.9-8.7)	4.9 (1.1-11.6)
100-h	4.5 (1.2-9.0)	4.2 (1.1-8.7)	5.0 (0.8-7.9)	4.5 (1.2-9.3)	6.7 (1.4-16.5)	5.4 (1.7-9.0)	5.4 (2.9-11.2)	7.3 (2.5-15.0)
1000-h, sound (cm)								
7.6–15.2	1.2 (0.0-3.8)	1.0 (0.0-3.9)	3.1 (0.1-5.8)	1.5 (0.8-1.9)	0.9 (0.3-1.8)	1.2 (0.4-2.8)	1.3 (0.0-2.2)	1.3 (0.0-4.0)
15.2–30.5	1.1 (0.0-3.0)	0.7 (0.0-2.0)	5.5 (0.0-9.0)	4.2 (0.8-12.7)	1.9 (0.0-7.2)	5.4 (0.0-12.9)	6.1 (0.0-16.7)	4.6 (0.0-10.2)
30.5–50.8	0.0 (0.0-0.0)	0.0 (0.0-0.0)	2.3 (0.0-10.0)	3.7 (0.0-11.9)	2.2 (0.0-12.2)	10.2 (0.0-23.8)	11.3 (4.3-27.2)	7.2 (0.7-18.1)
50.8–88.9	0.0 (0.0-0.0)	0.0 (0.0-0.0)	1.1 (0.0-11.5)	2.2 (0.0-12.8)	1.3 (0.0-5.3)	12.2 (0.0-42.0)	9.3 (0.0-31.9)	7.5 (0.0-45.2)
88.9–127.0	0.0 (0.0-0.0)	0.0 (0.0-0.0)	0.0 (0.0-0.0)	0.0 (0.0-0.0)	0.0 (0.0-0.0)	3.4 (0.0-25.1)	0.0 (0.0-0.0)	0.0 (0.0-0.0)
>127.0	0.0 (0.0-0.0)	0.0 (0.0-0.0)	0.0 (0.0-0.0)	0.0 (0.0-0.0)	0.0 (0.0-0.0)	0.0 (0.0-0.0)	0.0 (0.0-0.0)	0.0 (0.0-0.0)
1000-h, rotten (cm)								
7.6–15.2	0.7 (0.0-1.4)	0.7 (0.0-1.5)	1.2 (0.1-3.5)	0.5 (0.0-1.0)	1.0 (0.1-2.6)	0.6 (0.0-1.1)	0.5 (0.0-1.4)	0.6 (0.1-1.3)
15.2–30.5	0.8 (0.0-1.9)	1.0 (0.0-2.3)	2.7 (1.2-4.8)	1.3 (0.5-3.0)	2.7 (0.8-6.6)	3.2 (0.5-8.6)	2.8 (0.7-6.0)	2.9 (0.4-7.1)
30.5–50.8	1.4 (0.0-3.7)	1.3 (0.0-6.2)	3.5 (0.0-6.3)	1.9 (0.0-6.7)	3.3 (0.0-11.1)	8.2 (1.9-15.7)	4.4 (0.0-12.2)	4.7 (0.0-20.0)

50.8–88.9	1.3 (0.0-7.9)	1.1 (0.0-6.3)	5.9 (0.0-16.0)	1.6 (0.0-14.4)	1.3 (0.0-5.1)	5.3 (0.0-35.3)	3.9 (0.0-14.6)	3.6 (0.0-20.5)
88.9–127.0	0.0 (0.0-0.0)	0.0 (0.0-0.0)	0.0 (0.0-0.0)	0.6 (0.0-5.3)	0.0 (0.0-0.0)	1.1 (0.0-7.8)	1.9 (0.0-21.0)	1.2 (0.0-9.3)
>127.0	0.0 (0.0-0.0)	0.0 (0.0-0.0)	0.0 (0.0-0.0)	0.0 (0.0-0.0)	0.0 (0.0-0.0)	0.0 (0.0-0.0)	0.0 (0.0-0.0)	0.0 (0.0-0.0)

C.2 *Microclimate adjustments*

We examined the effects of microclimate on initial reburn potential by modifying baseline FFE-FVS fire weather inputs based on stand structure. We modeled relationships between structure and microclimate variables based on a synthesis of field studies conducted in wet temperate forests. This synthesis revealed strong relationships of canopy cover with both air temperature (Chen et al. 1993, Barg and Edmonds 1999, Heithecker and Halpern 2007, Frey et al. 2016, Lindenmayer et al. 2022, Brackett et al. 2024, Millikin et al. 2024) and fine (1-, 10-, 100-h) fuel moisture content (Cawson et al. 2017, Brown et al. 2024, Millikin et al. 2024). We compiled the data reported by these studies and derived the proportional changes in temperature and fine fuel moisture content as a function of relative change in canopy cover (Table 2.4; Table 2.5; Fig. 2.4). We fit linear models to proportional changes in temperature (ΔpT) and fine fuel moisture content ($\Delta pFMC$) as a function of total percent canopy cover ($cover$):

$$\Delta pT = \beta_1 \cdot cover$$

$$\Delta pFMC = \beta_1 \cdot cover$$

Models were fit to all compiled literature values, regardless of time scale (e.g., annual, growing season) or type (e.g., mean, maximum, minimum). We set the model intercepts at 0 to reflect the assumption of baseline fire weather inputs representing open conditions (i.e., 0% canopy cover). Regression coefficients (β_1) were –0.00188 for ΔpT and 0.00809 for $\Delta pFMC$ (Fig. 2.5).

We used these relationships to determine the microclimate-adjusted values of temperature (T_{adj}) and fine fuel moisture content (FMC_{adj}) for each stand:

$$T_{adj} = T_{base} + (T_{base} \cdot \Delta pT)$$

$$FMC_{adj} = FMC_{base} + (FMC_{base} \cdot \Delta pFMC),$$

where T_{base} and FMC_{base} are the baseline values of temperature and fine fuel moisture content,

respectively, for each fire weather scenario (Table 2.6).

We kept the fire weather inputs for wind speed at their baseline values since structural effects on wind are built into the default simulation processes of FFE-FVS, with the model adjusting wind speeds based on stand canopy cover (Rebain 2010). We also kept the inputs for fuel moisture content of other surface fuel components (1000-h coarse fuels, duff, live fuels) at their baseline values due to limited available studies on relationships between canopy cover and these variables in wet temperate forests.

Table 2.4. Literature synthesis of air temperature (T) as a function of canopy cover in wet temperate forests. Differences (Δ) in absolute (°C) and proportional temperatures were derived from observed values and reported per percent change in canopy cover, relative to open conditions (i.e., 0% cover).

Relative cover change (%)	Observed T (°C)	Type and scale	ΔT (°C)	ΔT (proportion)	Source
0	36.6	mean annual	–	–	Barg & Edmonds 1999
23.5	34.2	mean annual	-0.5	-0.07	Barg & Edmonds 1999[1]
89	28.6	mean annual	-1.9	-0.22	Barg & Edmonds 1999[1]
0	42	max daily	–	–	Brackett et al. 2024
60	34	max daily	-8	-0.19	Brackett et al. 2024
0	16.33	mean daily	–	–	Chen et al. 1993
75	15.72	mean daily	-0.61	-0.04	Chen et al. 1993
0	13.2	max spring	–	–	Frey et al. 2016
100	12.7	max spring	-0.5	-0.04	Frey et al. 2016
0	23	mean summer	–	–	Heithecker & Halpern 2007
9	13	mean summer	-10	-0.43	Heithecker & Halpern 2007[1]
0	7	median daily	–	–	Lindenmayer et al. 2022
100	5	median daily	-2	-0.29	Lindenmayer et al. 2022
0	6.8	median daily	–	–	Lindenmayer et al. 2022
30	5.4	median daily	-1.5	-0.21	Lindenmayer et al. 2022
0	26.7	mean summer	–	–	Millikin et al. 2024
29.5	25.2	mean summer	-1.5	-0.06	Millikin et al. 2024[1]

[1] Cover value represents midpoint of reported range.

Table 2.5. Dead fine surface fuel moisture content (FMC) as a function of canopy cover in wet temperate forests. Differences (Δ) in absolute (%) and proportional fuel moisture contents were derived from observed values and reported relative to percent change in canopy cover.

Relative cover change (%)	Observed FMC (%)	Type and scale	ΔFMC (%)	ΔFMC (proportion)	Source
0	20	mean annual	–	–	Brown et al. 2024
75	45	mean annual	18.5	1.25	Brown et al. 2024[1]
0	11.4	min daily	–	–	Cawson et al. 2017
75	20.9	min daily	15	0.83	Cawson et al. 2017[1]
0	23.7	mean summer	–	–	Millikin et al. 2024
29.5	33.3	mean summer	9.6	0.41	Millikin et al. 2024[2]

[1] Unburned and/or forested conditions were assigned 75% cover.

[2] Cover value represents midpoint of reported range.

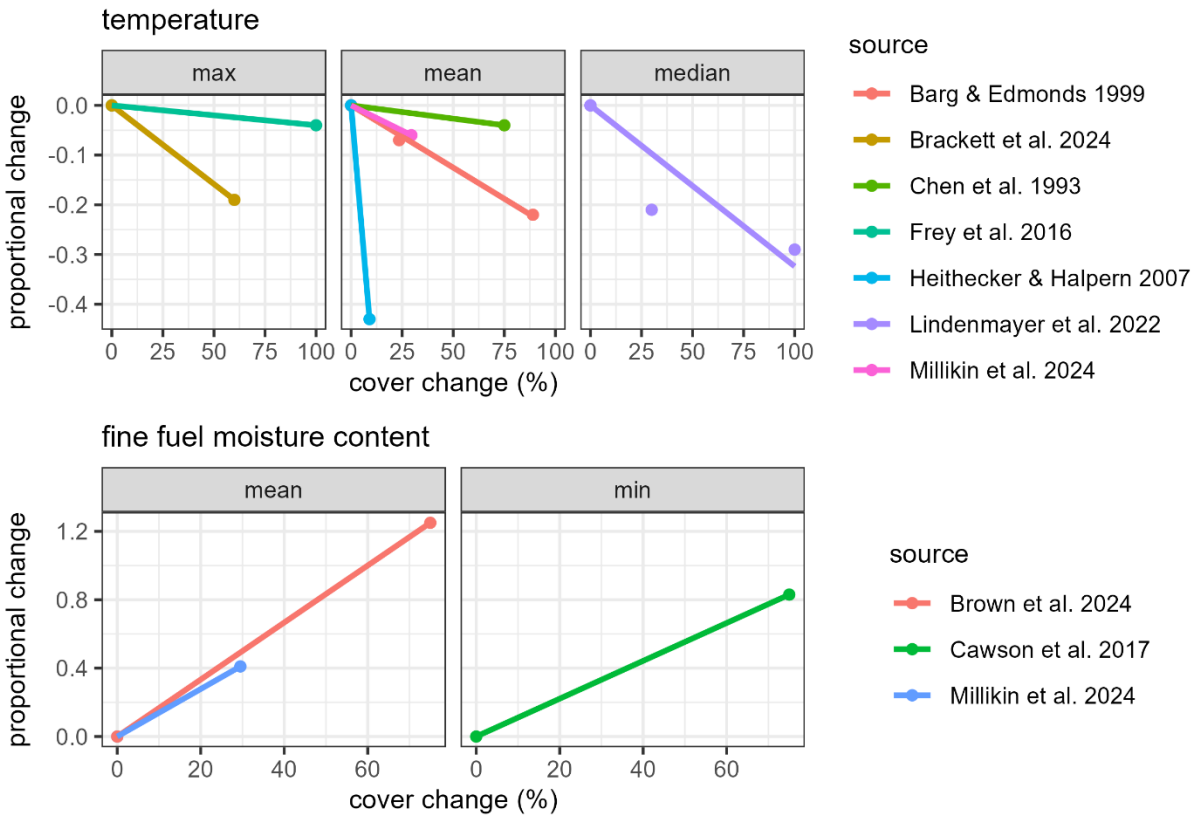

Figure 2.4. Literature sources used to derive the relationship between relative change in canopy cover and the proportional change in both temperature (*top*) and fine fuel moisture content (*bottom*). Sources were specific to wet temperate forests and presented trends in maximum, mean, and median temperature, and mean and minimum fine fuel moisture content across a range of stand ages and structural conditions.

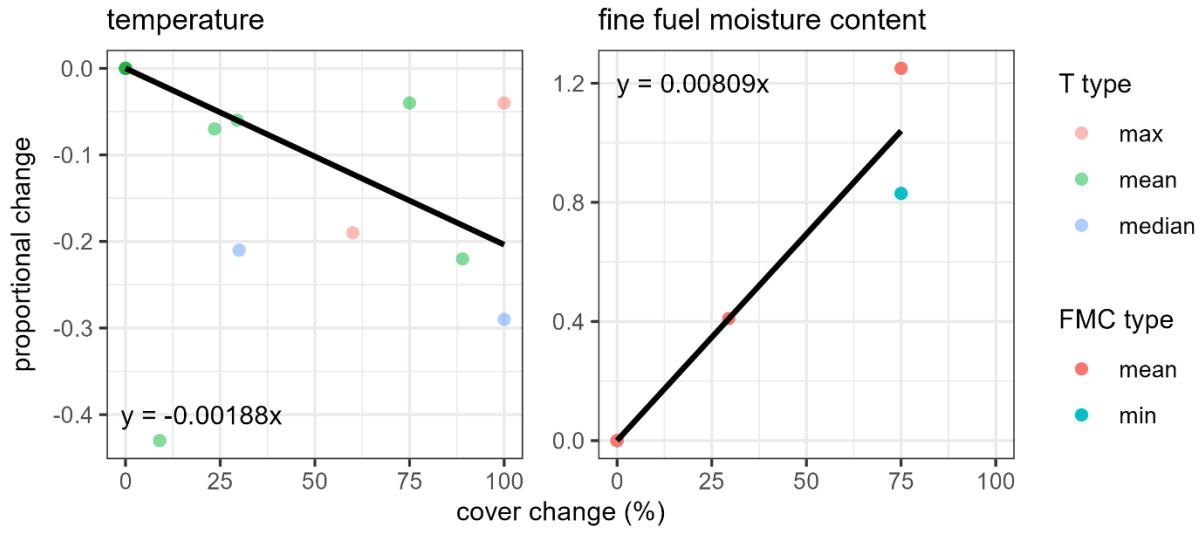

Figure 2.5. Linear regression models of proportional change in temperature (T; *left*) and fine fuel moisture content (FMC; *right*) as a function of relative change in canopy cover. Models were fit across all literature sources and reported value types (i.e., mean, maximum, median, minimum). Model intercepts were set at 0 to represent microclimate changes relative to open conditions (i.e., 0% canopy cover).

Table 2.6. Potential fire weather inputs adjusted for structural effects on microclimate conditions. Values are the mean and range in stand-level conditions across stand age × burn severity strata for moderate and extreme fire weather scenarios. Baseline inputs (bracketed values) for each scenario were adjusted to account for buffering effects of tree canopies on temperature and moisture variables, based on differences in total post-fire canopy cover among strata.

Variable	young		mid-seral			late-seral		
	unburned	**high**	**unburned**	**low**	**high**	**unburned**	**low**	**high**
air temperature (°C)								
moderate [18.0]	15.3 (14.9–15.7)	17.7 (17.5–17.9)	15.0 (14.7–15.4)	15.4 (15.0–16.2)	17.0 (16.4–17.5)	15.2 (14.9–15.4)	15.8 (15.2–16.7)	17.1 (16.6–17.5)
extreme [25.6]	21.7 (21.2–22.3)	25.1 (24.9–25.4)	21.3 (21.0–21.9)	21.9 (21.4–23.0)	24.3 (23.3–24.9)	21.6 (21.1–21.9)	22.4 (21.6–23.7)	24.4 (23.6–24.9)
surface fuel moisture content (%), 1- & 10-h fuels								
moderate [12]	20 (19–21)	13 (12–13)	21 (19–21)	19 (17–21)	15 (13–17)	20 (19–21)	18 (16–20)	15 (14–16)
extreme [4]	7 (6–7)	4 (4–4)	7 (6–7)	7 (6–7)	5 (4–6)	7 (6–7)	6 (5–7)	5 (5–5)
surface fuel moisture content (%), 100-h fuels								
moderate [14]	23 (22–24)	15 (14–16)	24 (23–25)	23 (20–24)	17 (16–19)	24 (23–25)	21 (18–23)	17 (16–19)
extreme [5]	8 (8–9)	5 (5–6)	9 (8–9)	8 (7–9)	6 (6–7)	8 (8–9)	8 (7–8)	6 (6–7)
canopy cover (%)								
total	80.5 (68.0–91.4)	10.1 (4.1–15.1)	89.2 (76.7–96.3)	77.0 (54.1–88.0)	28.0 (14.9–48.5)	83.6 (75.9–92.8)	66.1 (39.4–83.0)	26.1 (15.6–42.5)

C.3 *Fire behavior fuel model selection*

We tested the sensitivity of FFE-FVS fuel model selection logic on potential fire behavior and effects outputs by running the same simulations using the original 13 (Albini 1976, Anderson 1982), new 40 (Scott and Burgan 2005), and combined pool of all 53 fire behavior fuel models. Fire weather conditions were represented by baseline values (i.e., no microclimate adjustments). Primary and secondary fuel model assignments for each stand age × burn severity strata varied across the different fuel model pools (Fig. 2.6; Fig. 2.7). Overall patterns in potential fire behavior (Fig. 2.8; Fig. 2.9) and effects (Fig. 2.10) outputs among strata and fire weather conditions were consistent across all three fuel model pools, though the magnitude of output values varied.

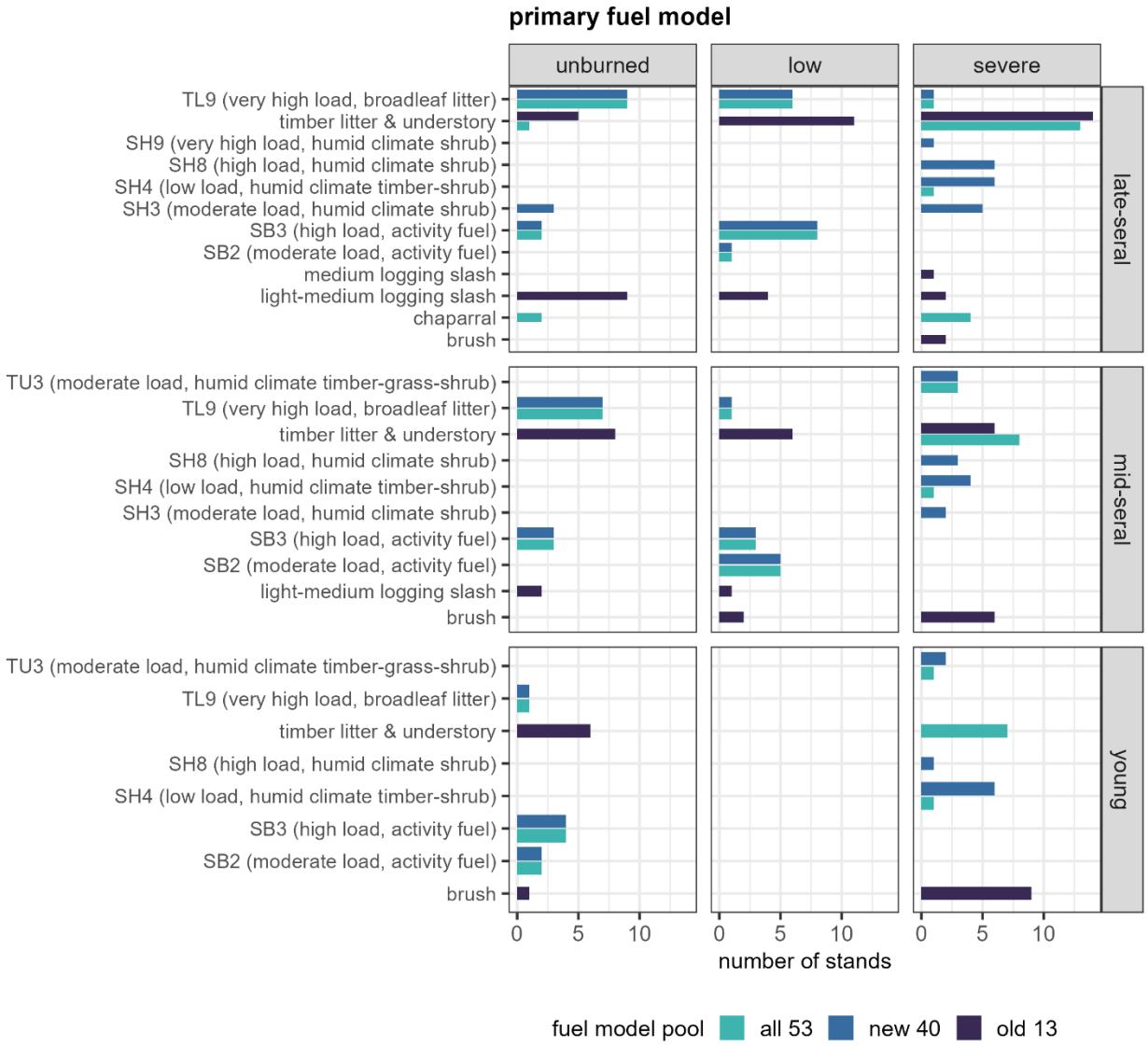

Figure 2.6. Comparison of primary fuel model selection for stand age × burn severity strata between FFE-FVS simulations run using the original 13, new 40, or all 53 fire behavior fuel model pools. Bars indicate the number of stands within each stratum assigned to each primary fuel model, colored by fuel model pool.

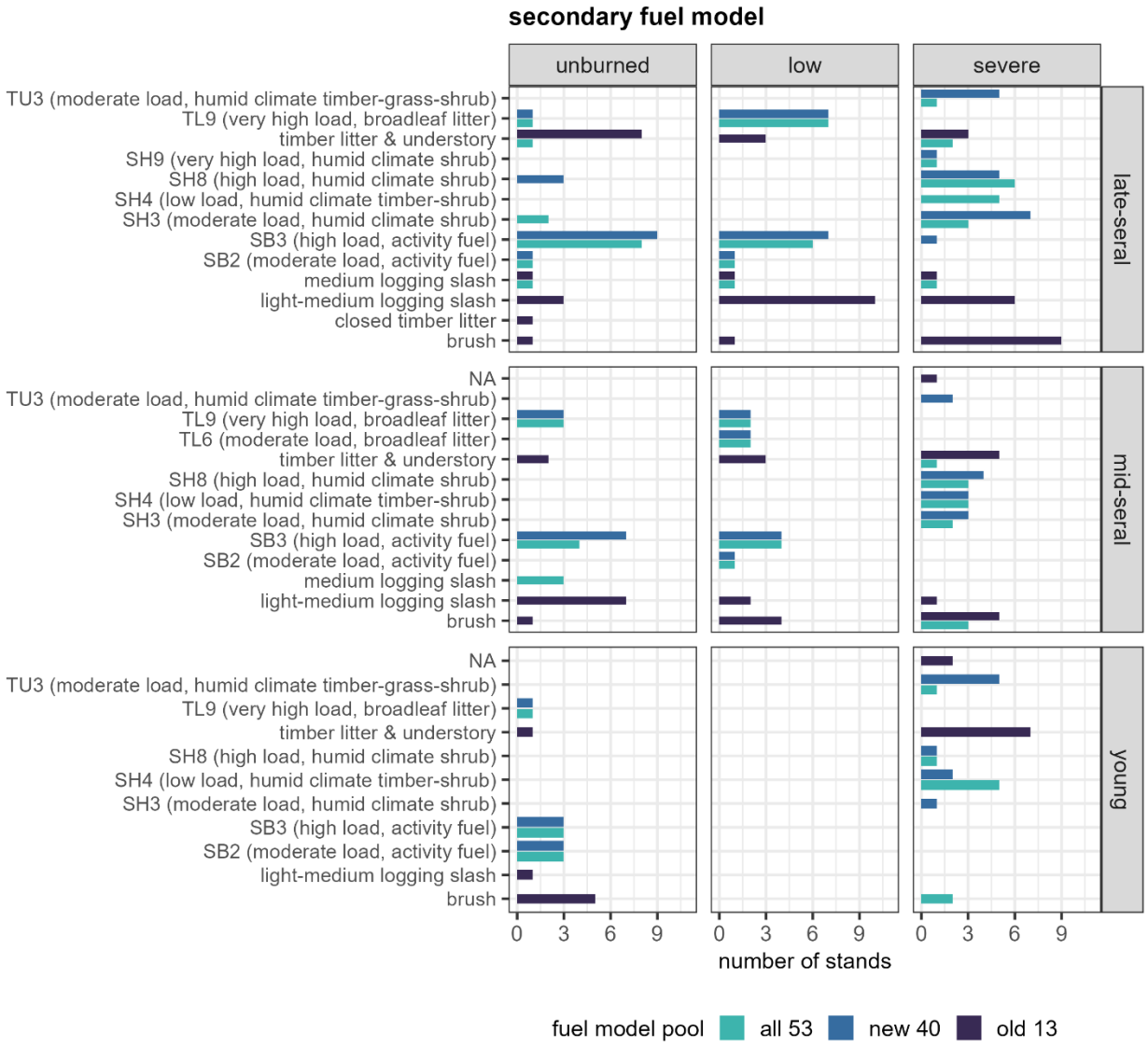

Figure 2.7. Comparison of secondary fuel model selection for stand age × burn severity strata between FFE-FVS simulations run using the original 13, new 40, or all 53 fire behavior fuel model pools. Bars indicate the number of stands within each stratum assigned to each secondary fuel model, colored by fuel model pool.

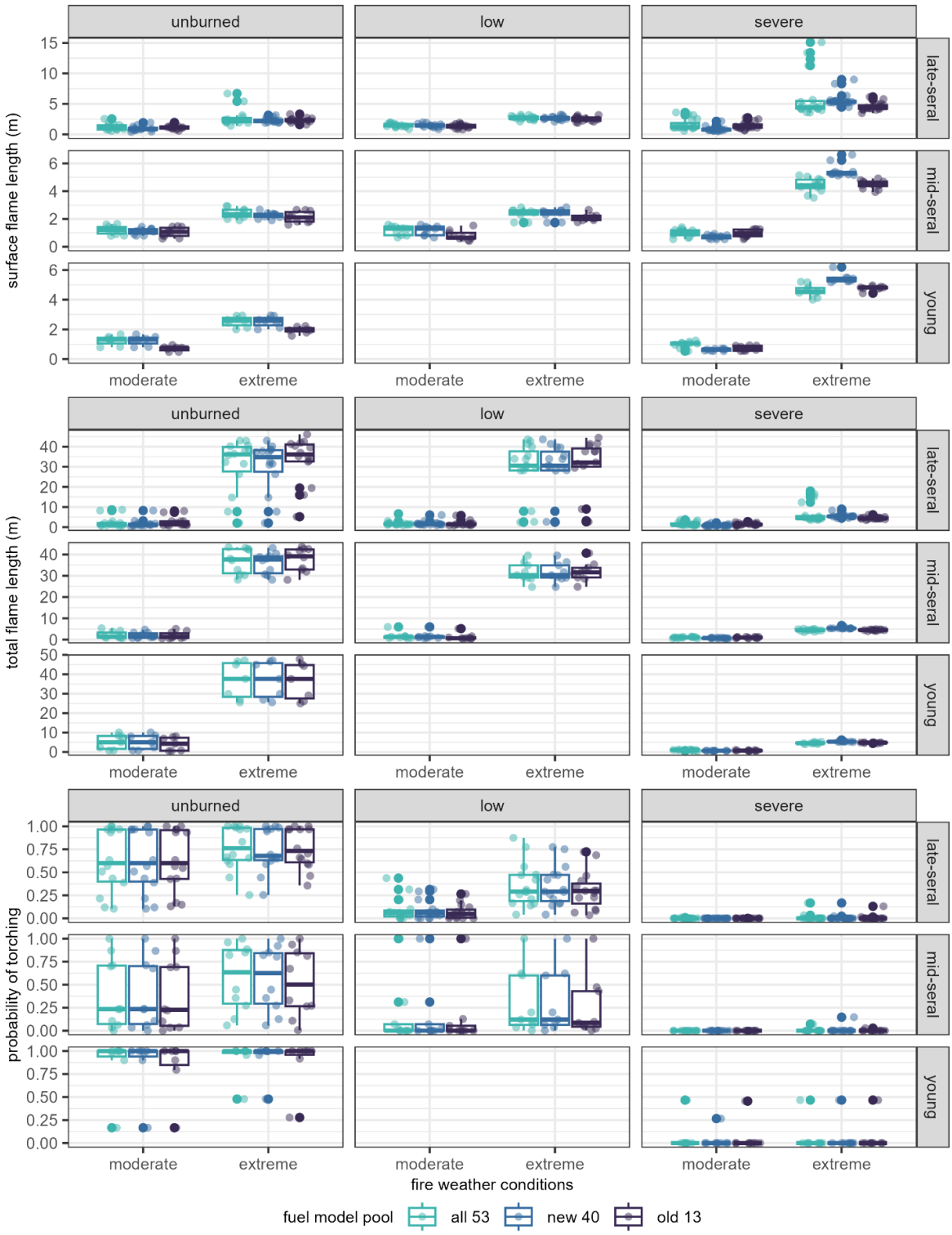

Figure 2.8. Comparison of potential reburn fire behavior outputs between FFE-FVS simulations run using the original 13, new 40, or all 53 fire behavior fuel model pools. Standard boxplots summarize outputs across all individual stand replicates (points) within each stratum (stand age × burn severity in the first fire), colored by fuel model pool.

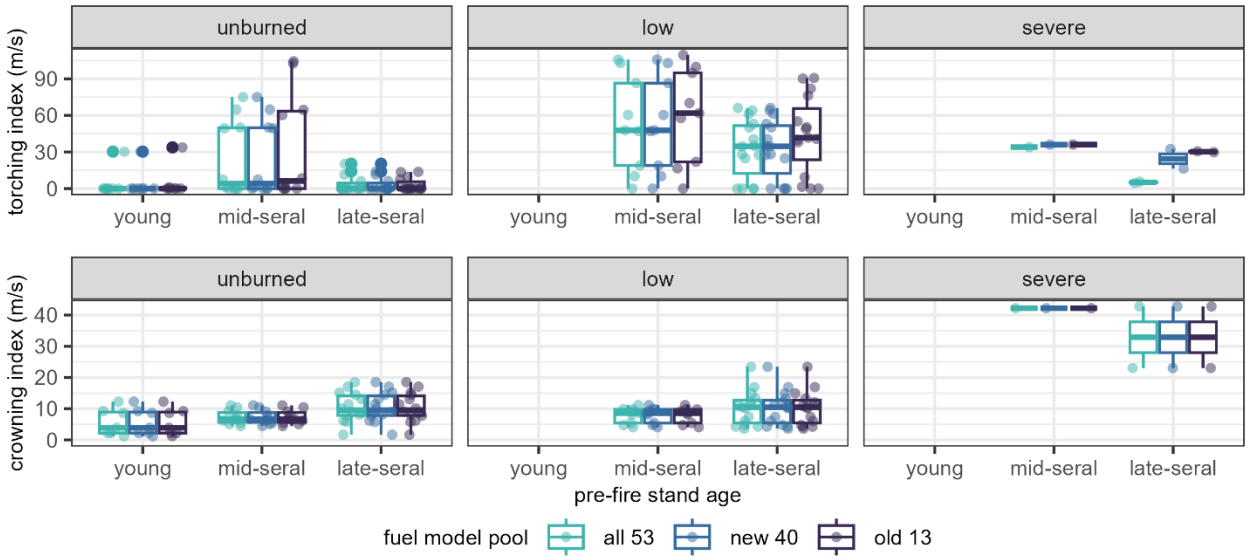

Figure 2.9. Comparison of potential reburn torching and crowning indices between FFE-FVS simulations run using the original 13, new 40, or all 53 fire behavior fuel model pools. Standard boxplots summarize outputs across all individual stand replicates (points) within each stratum (stand age × burn severity in the first fire), colored by fuel model pool.

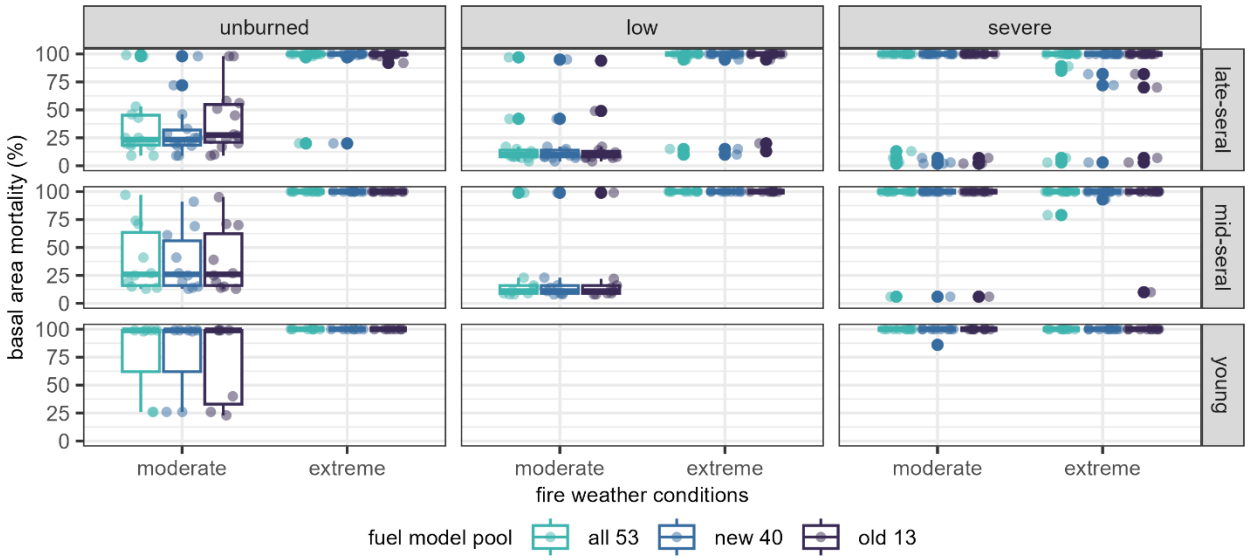

Figure 2.10. Comparison of potential reburn fire effects outputs between FFE-FVS simulations run using the original 13, new 40, or all 53 fire behavior fuel model pools. Standard boxplots summarize outputs across all individual stand replicates (points) within each stratum (stand age × burn severity in the first fire), colored by fuel model pool.

C.4 *Statistical model outputs*

Table 2.7. Output from generalized linear models testing for effects of stand age and burn severity on initial (2–5 years) post-fire potential fire behavior and effects. Fire weather conditions included stand-level microclimate adjustments (Table 2.6). All models had the same form: response ~ stand age prior to first fire + burn severity in first fire. Separate models were fit for flame length, torching probability, and mortality responses simulated under moderate and extreme scenarios of reburn fire weather conditions.

***Response* & predictors**	**moderate fire weather**				**extreme fire weather**			
	β	**SE**	***z***	***p***	**β**	**SE**	***z***	***p***
Surface flame length								
young × unburned (intercept)	-0.30	0.09	-3.24	0.001	0.72	0.09	8.32	0.000
mid-seral	-0.09	0.10	-0.84	0.402	-0.05	0.10	-0.52	0.605
late-seral	0.10	0.10	0.97	0.331	0.18	0.09	1.99	0.047
low severity	0.31	0.09	3.27	0.001	-0.02	0.09	-0.19	0.850
high severity	0.40	0.08	5.05	0.000	0.84	0.07	11.52	0.000
Total flame length								
young × unburned (intercept)	0.24	0.12	2.07	0.038	3.36	0.15	22.57	0.000
mid-seral	-0.42	0.14	-2.95	0.003	-0.01	0.17	-0.03	0.977
late-seral	-0.20	0.14	-1.45	0.147	0.04	0.16	0.25	0.799
low severity	0.16	0.13	1.23	0.218	-0.09	0.15	-0.61	0.544
high severity	0.11	0.11	1.05	0.295	-1.70	0.13	-13.08	0.000
Torching probability								
young × unburned (intercept)	1.56	0.62	2.54	0.011	1.85	0.45	4.08	0.000
mid-seral	-1.99	0.66	-3.01	0.003	-1.81	0.50	-3.58	0.000
late-seral	-1.50	0.63	-2.37	0.018	-0.98	0.47	-2.10	0.036
low severity	-1.50	0.37	-4.07	0.000	-1.48	0.32	-4.59	0.000
high severity	-6.38	0.94	-6.82	0.000	-5.28	0.71	-7.45	0.000
Percent basal area mortality								
young × unburned (intercept)	0.92	0.31	2.94	0.003	21.93	22830.93	0.00	0.999
mid-seral	-1.94	0.40	-4.86	0.000	-20.18	22830.93	0.00	0.999
late-seral	-2.33	0.39	-5.95	0.000	-21.82	22830.93	0.00	0.999
low severity	-0.26	0.28	-0.93	0.352	0.08	0.58	0.13	0.897
high severity	1.10	0.42	2.64	0.008	-0.22	0.56	-0.40	0.690

***Response* and predictors**	**β**	**SE**	***z***	***p***
Torching index				
young × unburned (intercept)	3.71	0.70	5.27	0.000
mid-seral	0.22	0.74	0.30	0.765
late-seral	-0.56	0.76	-0.74	0.462
low severity	0.63	0.29	2.20	0.028
high severity	-0.92	0.46	-1.99	0.047
Crowning index				
young × unburned (intercept)	1.87	0.17	11.03	0.000
mid-seral	0.30	0.21	1.42	0.156
late-seral	0.56	0.20	2.82	0.005
low severity	0.00	0.13	-0.01	0.995
high severity	1.30	0.28	4.74	0.000

Notes: Both stand age prior to and burn severity in the first fire were categorical predictors with three levels: young, mid-, and late-seral age; unburned, low, and high severity. Young × unburned stands were incorporated into model intercepts. Torching and crowning indices are based on extreme fire weather conditions. β, coefficient estimate. SE, standard error. *z*, test statistic. *p*, p-value.

Table 2.8. Output from generalized linear models testing for effects of stand age and burn severity on initial (2–5 years) post-fire potential fire behavior and effects. Fire weather conditions were represented by baseline values (i.e., no microclimate adjustments; Table 2.6). All models had the same form: response ~ stand age prior to first fire + burn severity in first fire. Separate models were fit for flame length, torching probability, and mortality responses simulated under moderate and extreme scenarios of reburn fire weather conditions.

***Response* and predictors**	**moderate fire weather**				**extreme fire weather**			
	β	**SE**	***z***	***p***	**β**	**SE**	***z***	***p***
Surface flame length								
young × unburned (intercept)	0.09	0.10	0.87	0.382	0.87	0.08	10.33	0.000
mid-seral	0.00	0.11	0.01	0.988	-0.02	0.09	-0.18	0.858
late-seral	0.26	0.11	2.42	0.015	0.20	0.09	2.21	0.027
low severity	0.05	0.10	0.51	0.613	-0.04	0.08	-0.46	0.643
high severity	0.03	0.09	0.30	0.768	0.70	0.07	9.79	0.000
Total flame length								
young × unburned (intercept)	1.24	0.17	7.39	0.000	3.47	0.13	25.92	0.000
mid-seral	-0.42	0.20	-2.04	0.041	0.03	0.15	0.20	0.838
late-seral	-0.15	0.19	-0.77	0.443	0.11	0.14	0.77	0.444
low severity	-0.40	0.18	-2.17	0.030	-0.16	0.14	-1.16	0.244
high severity	-0.79	0.16	-5.04	0.000	-1.83	0.12	-15.66	0.000
Torching probability								
young × unburned (intercept)	1.22	0.48	2.54	0.011	1.68	0.53	3.16	0.002
mid-seral	-1.72	0.53	-3.24	0.001	-1.44	0.55	-2.60	0.009
late-seral	-0.90	0.50	-1.82	0.068	-0.81	0.53	-1.52	0.128
low severity	-1.75	0.33	-5.24	0.000	-1.32	0.29	-4.46	0.000
high severity	-5.18	0.66	-7.80	0.000	-5.07	0.69	-7.31	0.000
Percent basal area mortality								
young × unburned (intercept)	0.97	0.38	2.56	0.011	21.88	19991.55	0.00	0.999
mid-seral	-1.21	0.46	-2.60	0.009	-19.66	19991.55	0.00	0.999
late-seral	-1.49	0.45	-3.32	0.001	-21.33	19991.55	0.00	0.999
low severity	-0.40	0.34	-1.17	0.240	-0.37	0.66	-0.56	0.575
high severity	3.00	0.68	4.41	0.000	-0.68	0.61	-1.12	0.265

***Response* and predictors**	**β**	**SE**	***z***	***p***
Torching index				
young × unburned (intercept)	3.41	0.67	5.09	0.000
mid-seral	0.16	0.71	0.22	0.823
late-seral	-0.56	0.72	-0.78	0.436
low severity	0.79	0.28	2.82	0.005
high severity	-0.66	0.44	-1.49	0.135
Crowning index				
young × unburned (intercept)	1.73	0.19	9.36	0.000
mid-seral	0.30	0.23	1.34	0.179
late-seral	0.58	0.22	2.68	0.007
low severity	0.02	0.14	0.12	0.906
high severity	1.38	0.30	4.61	0.000

Notes: Both stand age prior to and burn severity in the first fire were categorical predictors with three levels: young, mid-, and late-seral age; unburned, low, and high severity. Young × unburned stands were incorporated into model intercepts. Torching and crowning indices are based on extreme fire weather conditions. β, coefficient estimate. SE, standard error. *z*, test statistic. *p*, p-value.

2.7 REFERENCES

Abatzoglou, J. T., D. E. Rupp, L. W. O'Neill, and M. Sadegh. 2021. Compound extremes drive the western Oregon wildfires of September 2020. Geophysical Research Letters 48:e2021GL092520.

Abatzoglou, J. T., and A. P. Williams. 2016. Impact of anthropogenic climate change on wildfire across western US forests. Proceedings of the National Academy of Sciences 113:11770–11775.

Agee, J. 1993. Fire ecology of Pacific Northwest forests. Island Press, Washington D.C.

Agee, J. K., and M. H. Huff. 1987. Fuel succession in a western hemlock/Douglas-fir forest. Canadian Journal of Forest Research 17:697–704.

Agne, M., J. Fontaine, N. Enright, S. Bisbing, and B. Harvey. 2023. Rapid fuel recovery after stand-replacing fire in closed-cone pine forests and implications for short-interval severe reburns. Forest Ecology and Management 545:121263.

Albini, F. A. 1976. Estimating wildfire behavior and effects. Pages 1–68. Gen. Tech. Rep. INT-30, U.S. Department of Agriculture, Forest Service, Intermountain Forest and Range Experiment Station, Ogden, UT.

Anderson, H. E. 1982. Aids to determining fuel models for estimating fire behavior. Pages 1–22. Gen. Tech. Rep. INT-GTR-122, U.S. Department of Agriculture, Forest Service, Intermountain Forest and Range Experiment Station, Ogden, UT.

Barg, A. K., and R. L. Edmonds. 1999. Influence of partial cutting on site microclimate, soil nitrogen dynamics, and microbial biomass in Douglas-fir stands in western Washington. Canadian Journal of Forest Research 29:705–713.

Bowman, D. M. J. S., C. A. Kolden, J. T. Abatzoglou, F. H. Johnston, G. R. van der Werf, and M. Flannigan. 2020. Vegetation fires in the Anthropocene. Nature Reviews Earth & Environment 1:500–515.

Brackett, A. E., C. J. Still, and K. J. Puettmann. 2024. Residual canopy cover provides buffering of near-surface temperatures, but benefits are limited under extreme conditions. Canadian Journal of Forest Research.

Bradshaw, L. S., and E. McCormick. 2009. FireFamily Plus user's guide, version 4.0. Page 282. USDA Forest Service, Fire and Aviation Management, Boise, ID.

Braziunas, K. H., N. G. Kiel, and M. G. Turner. 2023. Less fuel for the next fire? Short-interval fire delays forest recovery and interacting drivers amplify effects. Ecology 104:e4042.

Brooks, M. E., K. Kristensen, K. J. van Benthem, A. Magnusson, C. W. Berg, A. Nielsen, H. J. Skaug, M. Maechler, and B. M. Bolker. 2017. glmmTMB balances speed and flexibility among packages for zero-inflated generalized linear mixed modeling. The R Journal 9:378–400.

Brown, J. K. 1974. Handbook for inventorying downed woody material. Gen. Tech. Rep. INT-16, U.S. Department of Agriculture, Forest Service, Intermountain Forest and Range Experiment Station, Ogden, UT.

Brown, J. K., R. D. Oberheu, and C. M. Johnston. 1982. Handbook for inventorying surface fuels and biomass in the Interior West. Page INT-GTR-129. U.S. Department of Agriculture, Forest Service, Intermountain Forest and Range Experiment Station, Ogden, UT.

Brown, T. P., T. J. Duff, A. Inbar, P. N. J. Lane, and G. J. Sheridan. 2024. Forest reorganisation effects on fuel moisture content can exceed changes due to climate warming in wet temperate forests. Global Change Biology 30:e17023.

Buma, B., S. Weiss, K. Hayes, and M. Lucash. 2020. Wildland fire reburning trends across the US West suggest only short-term negative feedback and differing climatic effects. Environmental Research Letters 15:034026.

Buonanduci, M. S., D. C. Donato, J. S. Halofsky, M. C. Kennedy, and B. J. Harvey. 2024. Few large or many small fires: Using spatial scaling of severe fire to quantify effects of fire-size distribution shifts. Ecosphere 15:e4875.

Burton, P. J., A. Jentsch, and L. R. Walker. 2020. The Ecology of Disturbance Interactions. BioScience 70:854–870.

Busby, S. U., A. M. Klock, and J. S. Fried. 2023. Inventory analysis of fire effects wrought by wind-driven megafires in relation to weather and pre-fire forest structure in the western Cascades. Fire Ecology 19:58.

Busby, S. U., K. B. Moffett, and A. Holz. 2020. High-severity and short-interval wildfires limit forest recovery in the Central Cascade Range. Ecosphere 11:e03247.

Cansler, C. A., V. R. Kane, P. F. Hessburg, J. T. Kane, S. M. A. Jeronimo, J. A. Lutz, N. A. Povak, D. J. Churchill, and A. J. Larson. 2021. Previous wildfires and management treatments moderate subsequent fire severity. Forest Ecology and Management 504.

Case, M. J., B. G. Johnson, K. J. Bartowitz, and T. W. Hudiburg. 2021. Forests of the future: Climate change impacts and implications for carbon storage in the Pacific Northwest, USA. Forest Ecology and Management 482:118886.

Cattau, M., C. Wessman, A. Mahood, and J. Balch. 2020. Anthropogenic and lightning-started fires are becoming larger and more frequent over a longer season length in the U.S.A. Global Ecology and Biogeography 29.

Cawson, J. G., T. J. Duff, K. G. Tolhurst, C. C. Baillie, and T. D. Penman. 2017. Fuel moisture in Mountain Ash forests with contrasting fire histories. Forest Ecology and Management 400:568–577.

Chen, J., J. F. Franklin, and T. A. Spies. 1993. Contrasting microclimates among clearcut, edge, and interior of old-growth Douglas-fir forest. Agricultural and Forest Meteorology 63:219–237.

Collins, L., A. Hunter, S. McColl-Gausden, T. D. Penman, and P. Zylstra. 2021. The Effect of Antecedent Fire Severity on Reburn Severity and Fuel Structure in a Resprouting Eucalypt Forest in Victoria, Australia. Forests 12:450.

Coppoletta, M., K. E. Merriam, and B. M. Collins. 2016. Post-fire vegetation and fuel development influences fire severity patterns in reburns. Ecological Applications 26:686–699.

Crookston, N., D. L. Gammel, S. Rebain, D. Robinson, C. E. Keyser, C. A. Dahl, L. R. David, and M. A. Shettles. 2003. Users Guide to the Database Extension of the Forest Vegetation

Simulator Version 2.0. Page 64. Internal Rep, U.S. Department of Agriculture, Forest Service, Forest Management Service Center, Fort Collins, CO.

Davis, K. T., S. Z. Dobrowski, Z. A. Holden, P. E. Higuera, and J. T. Abatzoglou. 2019. Microclimatic buffering in forests of the future: the role of local water balance. Ecography 42:1–11.

De Frenne, P., F. Zellweger, F. Rodríguez-Sánchez, B. R. Scheffers, K. Hylander, M. Luoto, M. Vellend, K. Verheyen, and J. Lenoir. 2019. Global buffering of temperatures under forest canopies. Nature Ecology & Evolution 3:744–749.

Dixon, G. E. 2002. Essential FVS: A user's guide to the Forest Vegetation Simulator. Page 226. Internal Rep, U.S. Department of Agriculture, Forest Service, Forest Management Service Center, Fort Collins, CO.

Donato, D. C., J. L. Campbell, J. B. Fontaine, and B. E. Law. 2009. Quantifying char in postfire woody detritus inventories. Fire Ecology 5:104–115.

Donato, D. C., B. J. Harvey, W. H. Romme, M. Simard, and M. G. Turner. 2013. Bark beetle effects on fuel profiles across a range of stand structures in Douglas-fir forests of Greater Yellowstone. Ecological Applications 23:3–20.

Evers, C., A. Holz, S. Busby, and M. Nielsen-Pincus. 2022. Extreme winds alter influence of fuels and topography on megafire burn severity in seasonal temperate rainforests under record fuel aridity. Fire 5:41.

Franklin, J. F., and C. T. Dyrness. 1973. Natural vegetation of Oregon and Washington. Gen. Tech. Rep. PNW-GTR-008, U.S. Department of Agriculture, Forest Service, Pacific Northwest Research Station, Portland, OR.

Franklin, J. F., D. Lindenmayer, J. A. MacMahon, A. McKee, J. Magnuson, D. A. Perry, R. Waide, and D. Foster. 2000. Threads of continuity. Conservation in Practice 1:8–17.

Frey, S. J. K., A. S. Hadley, S. L. Johnson, M. Schulze, J. A. Jones, and M. G. Betts. 2016. Spatial models reveal the microclimatic buffering capacity of old-growth forests. Science Advances 2:e1501392.

FVS Staff. 2008. Westside Cascades (WC) Variant Overview of the Forest Vegetation Simulator. Page 85. Internal Rep, U.S. Department of Agriculture, Forest Service, Forest Management Service Center, Fort Collins, CO.

Gray, A. N., and J. F. Franklin. 1997. Effects of multiple fires on the structure of southwestern Washington forests. Northwest Science 71:174–185.

Gray, A. N., T. A. Spies, and M. J. Easter. 2002. Microclimatic and soil moisture responses to gap formation in coastal Douglas-fir forests. Canadian Journal of Forest Research 32:332–343.

Halofsky, J. E., D. L. Peterson, and B. J. Harvey. 2020. Changing wildfire, changing forests: the effects of climate change on fire regimes and vegetation in the Pacific Northwest, USA. Fire Ecology 16:4.

Halofsky, J. S., D. R. Conklin, D. C. Donato, J. E. Halofsky, and J. B. Kim. 2018a. Climate change, wildfire, and vegetation shifts in a high-inertia forest landscape: Western Washington, U.S.A. PLOS ONE 13:e0209490.

Halofsky, J. S., D. C. Donato, J. F. Franklin, J. E. Halofsky, D. L. Peterson, and B. J. Harvey. 2018b. The nature of the beast: examining climate adaptation options in forests with stand-replacing fire regimes. Ecosphere 9:e02140.

Hansen, W. D., D. Abendroth, W. Rammer, R. Seidl, and M. G. Turner. 2020. Can wildland fire management alter 21st-century subalpine fire and forests in Grand Teton National Park, Wyoming, USA. Ecological Applications 30.

Harmon, M. E., C. W. Woodall, B. Fasth, and J. Sexton. 2008. Woody detritus density and density reduction factors for tree species in the United States: a synthesis. Gen. Tech. Rep. NRS-29, U.S. Department of Agriculture, Forest Service, Northern Research Station, Newtown Square, PA, Newtown Square, PA.

Harmon, M. E., C. W. Woodall, B. Fasth, J. Sexton, and M. Yatkov. 2011. Differences between standing and downed dead tree wood density reduction factors: A comparison across decay classes and tree species. Research Paper, U.S. Department of Agriculture, Forest Service, Northern Research Station, Newtown Square, PA.

Harvey, B. J., M. S. Buonanduci, and M. G. Turner. 2023. Spatial interactions among short-interval fires reshape forest landscapes. Global Ecology and Biogeography:geb.13634.

Harvey, B. J., D. C. Donato, and M. G. Turner. 2016. Burn me twice, shame on who? Interactions between successive forest fires across a temperate mountain region. Ecology 97:2272–2282.

Heithecker, T. D., and C. B. Halpern. 2007. Edge-related gradients in microclimate in forest aggregates following structural retention harvests in western Washington. Forest Ecology and Management 248:163–173.

Hoecker, T. J., and M. G. Turner. 2022. A short-interval reburn catalyzes departures from historical structure and composition in a mesic mixed-conifer forest. Forest Ecology and Management 504:119814.

Hoffman, C., C. Sieg, R. Linn, W. Mell, R. Parsons, J. Ziegler, and J. Hiers. 2018. Advancing the science of wildland fire dynamics using process-based models. Fire 1:32.

Hummel, S., M. Kennedy, and E. Ashley Steel. 2013. Assessing forest vegetation and fire simulation model performance after the Cold Springs wildfire, Washington USA. Forest Ecology and Management 287:40–52.

Jolly, W. M., M. A. Cochrane, P. H. Freeborn, Z. A. Holden, T. J. Brown, G. J. Williamson, and D. M. J. S. Bowman. 2015. Climate-induced variations in global wildfire danger from 1979 to 2013. Nature Communications 6:1–11.

Jones, M. W., J. T. Abatzoglou, S. Veraverbeke, N. Andela, G. Lasslop, M. Forkel, A. J. P. Smith, C. Burton, R. A. Betts, G. R. van der Werf, S. Sitch, J. G. Canadell, C. Santín, C. Kolden, S. H. Doerr, and C. Le Quéré. 2022. Global and Regional Trends and Drivers of Fire Under Climate Change. Reviews of Geophysics 60:e2020RG000726.

Kubinec, R. 2023. Ordered beta regression: A parsimonious, well-fitting model for continuous data with lower and upper bounds. Political Analysis 31:519–536.

Landesmann, J. B., F. Tiribelli, J. Paritsis, T. T. Veblen, and T. Kitzberger. 2021. Increased fire severity triggers positive feedbacks of greater vegetation flammability and favors plant community-type conversions. Journal of Vegetation Science 32:e12936.

Leonard, S. W. J., A. F. Bennett, and M. F. Clarke. 2014. Determinants of the occurrence of unburnt forest patches: Potential biotic refuges within a large, intense wildfire in south-eastern Australia. Forest Ecology and Management 314:85–93.

Lindenmayer, D., W. Blanchard, L. McBurney, E. Bowd, K. Youngentob, K. Marsh, and C. Taylor. 2022. Stand age related differences in forest microclimate. Forest Ecology and Management 510:120101.

Littell, J. S., D. McKenzie, D. L. Peterson, and A. L. Westerling. 2009. Climate and wildfire area burned in western U.S. ecoprovinces, 1916–2003. Ecological Applications 19:1003–1021.

Littell, J. S., D. McKenzie, H. Y. Wan, and S. A. Cushman. 2018. Climate Change and Future Wildfire in the Western United States: An Ecological Approach to Nonstationarity. Earth's Future 6:1097–1111.

Loehman, R. A., R. E. Keane, and L. M. Holsinger. 2020. Simulation modeling of complex climate, wildfire, and vegetation dynamics to address wicked problems in land management. Frontiers in Forests and Global Change 3:3.

Lutes, D. C., R. E. Keane, J. F. Caratti, C. H. Key, N. C. Benson, S. Sutherland, and L. J. Gangi. 2006. FIREMON: Fire effects monitoring and inventory system. Gen. Tech. Rep. RMRS-GTR-164, U.S. Department of Agriculture, Forest Service, Rocky Mountain Research Station, Fort Collins, CO.

McLauchlan, K. K., P. E. Higuera, J. Miesel, B. M. Rogers, J. Schweitzer, J. K. Shuman, A. J. Tepley, J. M. Varner, T. T. Veblen, S. A. Adalsteinsson, J. K. Balch, P. Baker, E. Batllori, E. Bigio, P. Brando, M. Cattau, M. L. Chipman, J. Coen, R. Crandall, L. Daniels, N. Enright, W. S. Gross, B. J. Harvey, J. A. Hatten, S. Hermann, R. E. Hewitt, L. N. Kobziar, J. B. Landesmann, M. M. Loranty, S. Y. Maezumi, L. Mearns, M. Moritz, J. A. Myers, J. G. Pausas, A. F. A. Pellegrini, W. J. Platt, J. Roozeboom, H. Safford, F. Santos, R. M. Scheller, R. L. Sherriff, K. G. Smith, M. D. Smith, and A. C. Watts. 2020. Fire as a fundamental ecological process: Research advances and frontiers. Journal of Ecology 108:2047–2069.

Means, J. E., H. A. Hansen, G. J. Koerper, P. B. Alaback, and M. W. Klopsch. 1994. Software for computing plant biomass - BIOPAK users guide. Gen. Tech. Rep. PNW-GTR-340, U.S. Department of Agriculture, Forest Service, Pacific Northwest Research Station, Portland, OR.

Meigs, G. W., D. P. Turner, W. D. Ritts, Z. Yang, and B. E. Law. 2011. Landscape-scale simulation of heterogeneous fire effects on pyrogenic carbon emissions, tree mortality, and net ecosystem production. Ecosystems 14:758–775.

Millikin, R. L., W. J. Braun, M. E. Alexander, and S. Fani. 2024. The Impact of Fuel Thinning on the Microclimate in Coastal Rainforest Stands of Southwestern British Columbia, Canada. Fire 7:285.

Neiland, B. J. 1958. Forest and adjacent burn in the Tillamook Burn area of northwestern Oregon. Ecology 39:660–671.

Noonan-Wright, E. K., N. M. Vaillant, and A. L. Reiner. 2014. The Effectiveness and Limitations of Fuel Modeling Using the Fire and Fuels Extension to the Forest Vegetation Simulator. Forest Science 60:231–240.

Paine, R. T., M. J. Tegner, and E. A. Johnson. 1998. Compounded perturbations yield ecological surprises. Ecosystems 1:535–545.

Parks, S. A., L. M. Holsinger, C. Miller, and C. R. Nelson. 2015. Wildland fire as a self-regulating mechanism: the role of previous burns and weather in limiting fire progression. Ecological Applications 25:1478–1492.

Parks, S. A., C. Miller, C. R. Nelson, and Z. A. Holden. 2014. Previous fires moderate burn severity of subsequent wildland fires in two large western US wilderness areas. Ecosystems 17:29–42.

Parks, S. A., M. Parisien, C. Miller, L. M. Holsinger, and L. S. Baggett. 2018. Fine-scale spatial climate variation and drought mediate the likelihood of reburning. Ecological Applications 28:573–586.

Pedersen, T. 2024. *patchwork: The Composer of Plots*.

Pickering, B. J., T. J. Duff, C. Baillie, and J. G. Cawson. 2021. Darker, cooler, wetter: forest understories influence surface fuel moisture. Agricultural and Forest Meteorology 300:108311.

Powers, M. D. 2021. Silviculture treatment impacts on fuels and wildfire behavior in moist, westside Pacific Northwest forests: A summary of relevant literature. Pages 1–28. Central Cascades Adaptive Management Partnership, Willamette National Forest.

Powers, M. D., and J. Kertis. 2022. Fuel treatment impacts on landscape-scale wildfire behavior in moist, westside Pacific Northwest forests: A summary of relevant literature. Pages 1–50. Central Cascades Adaptive Management Partnership, Willamette National Forest.

Prichard, S. J., and M. C. Kennedy. 2014. Fuel treatments and landform modify landscape patterns of burn severity in an extreme fire event. Ecological Applications 24:571–590.

Prichard, S. J., D. V. Sandberg, R. D. Ottmar, E. Eberhardt, A. Andreu, P. Eagle, and Kjell. Swedin. 2013. Fuel Characteristic Classification System version 3.0: technical documentation. Page PNW-GTR-887. U.S. Department of Agriculture, Forest Service, Pacific Northwest Research Station, Portland, OR.

Prichard, S. J., C. S. Stevens-Rumann, and P. F. Hessburg. 2017. Tamm Review: Shifting global fire regimes: Lessons from reburns and research needs. Forest Ecology and Management 396:217–233.

PRISM Climate Group. 2024, January. Norm91m: 30-Year Normals, 1991-2020. Oregon State University, https://prism.oregonstate.edu, accessed 1 May 2024.

R Core Team. 2024. *R: A Language and Environment for Statistical Computing*. R Foundation for Statistical Computing, Vienna, Austria.

Raymond, C. L., and D. L. Peterson. 2005. Fuel treatments alter the effects of wildfire in a mixed-evergreen forest, Oregon, USA. Canadian Journal of Forest Research 35:15.

Rebain, S. A. 2010. The Fire and Fuels Extension to the Forest Vegetation Simulator: Updated Model Documentation. Internal Rep., U.S. Department of Agriculture, Forest Service, Forest Management Service Center, Fort Collins, CO.

Reilly, M. J., J. E. Halofsky, M. A. Krawchuk, D. C. Donato, P. F. Hessburg, J. D. Johnston, A. G. Merschel, M. E. Swanson, J. S. Halofsky, and T. A. Spies. 2021. Fire Ecology and

Management in Pacific Northwest Forests. Pages 393–435 *in* C. H. Greenberg and B. Collins, editors. Fire Ecology and Management: Past, Present, and Future of US Forested Ecosystems. Springer International Publishing, Cham.

Reilly, M. J., A. Zuspan, J. S. Halofsky, C. Raymond, A. McEvoy, A. W. Dye, D. C. Donato, J. B. Kim, B. E. Potter, N. Walker, R. Davis, C. J. Dunn, D. M. Bell, M. J. Gregory, J. D. Johnston, B. J. Harvey, J. E. Halofsky, and B. K. Kerns. 2022. Cascadia Burning: the historic, but not historically unprecedented, 2020 wildfires in the Pacific Northwest, USA. Ecosphere 13:e4070.

Reinhardt, E. D., R. E. Keane, and J. K. Brown. 1997. First Order Fire Effects Model: FOFEM 4.0, user's guide. Page INT-GTR-344. U.S. Department of Agriculture, Forest Service, Intermountain Research Station, Ogden, UT.

Rothermel, R. C. 1972. A mathematical model for predicting fire spread in wildland fuels. U.S. Department of Agriculture, Forest Service, Intermountain Forest and Range Experiment Station, Ogden, UT.

Schauberger, P., and A. Walker. 2024. *openxlsx: Read, Write and Edit xlsx Files*.

Scott, J. H., and R. E. Burgan. 2005. Standard fire behavior fuel models: a comprehensive set for use with Rothermel's surface fire spread model. Page RMRS-GTR-153. U.S. Department of Agriculture, Forest Service, Rocky Mountain Research Station, Ft. Collins, CO.

Scott, J. H., and E. D. Reinhardt. 2001. Assessing crown fire potential by linking models of surface and crown fire behavior. Research Paper RMRS-RP-29, U.S. Department of Agriculture, Forest Service, Rocky Mountain Research Station, Fort Collins, CO.

Simard, M., W. H. Romme, J. M. Griffin, and M. G. Turner. 2011. Do mountain pine beetle outbreaks change the probability of active crown fire in lodgepole pine forests? Ecological Monographs 81:3–24.

Spies, T. A. 1991. Plant species diversity and occurrence in young, mature, and old-growth Douglas-fir stands in western Oregon and Washington. Pages 111–121 *in* L. F. Ruggiero, K. B. Aubry, A. B. Carey, and M. H. Huff, editors. Wildlife and vegetation of unmanaged Douglas-fir forests. U.S. Department of Agriculture, Forest Service, Pacific Northwest Research Station, Portland, OR.

Spies, T. A., P. A. Stine, R. Gravenmier, J. W. Long, and M. J. Reilly. 2018. Synthesis of science to inform land management within the Northwest Forest Plan area. Gen. Tech. Rep. PNW-GTR-966, U.S. Department of Agriculture, Forest Service, Pacific Northwest Research Station, Portland, OR.

Thompson, J. R., T. A. Spies, and L. M. Ganio. 2007. Reburn severity in managed and unmanaged vegetation in a large wildfire. Proceedings of the National Academy of Sciences 104:10743–10748.

Tichý, L. 2016. Field test of canopy cover estimation by hemispherical photographs taken with a smartphone. Journal of Vegetation Science 27:427–435.

Tiribelli, F., T. Kitzberger, and J. M. Morales. 2018. Changes in vegetation structure and fuel characteristics along post-fire succession promote alternative stable states and positive fire–vegetation feedbacks. Journal of Vegetation Science 29:147–156.

Tortorelli, C. M., A. M. Latimer, and D. J. N. Young. 2024. Moderating effects of past wildfire on reburn severity depend on climate and initial severity in Western US forests. Ecological Applications 34:e3023.

Turner, M. G., and W. H. Romme. 1994. Landscape dynamics in crown fire ecosystems. Landscape Ecology 9:59–77.

Van Pelt, R. 2007. Identifying Mature and Old Forests in Western Washington. Washington State Department of Natural Resources.

Van Wagner, C. E. 1977. Conditions for the start and spread of crown fire. Canadian Journal of Forest Research 7:23–34.

Waring, R. H., and J. F. Franklin. 1979. Evergreen coniferous forests of the Pacific Northwest. Science 204:1380–1386.

Westerling, A. L. 2016. Increasing western US forest wildfire activity: sensitivity to changes in the timing of spring. Philosophical Transactions of the Royal Society B: Biological Sciences 371:1–10.

Wickham, H., M. Averick, J. Bryan, W. Chang, L. McGowan, R. François, G. Grolemund, A. Hayes, L. Henry, J. Hester, M. Kuhn, T. Pedersen, E. Miller, S. Bache, K. Müller, J. Ooms, D. Robinson, D. Seidel, V. Spinu, K. Takahashi, D. Vaughan, C. Wilke, K. Woo, and H. Yutani. 2019. Welcome to the tidyverse. Journal of Open Source Software 4:1686.

Williams, C. B., and C. T. Dyrness. 1967. Some characteristics of forest floors and soils under true fir-hemlock stands in the Cascade range. Page 19. Research Paper, U.S. Department of Agriculture, Forest Service, Pacific Northwest Forest and Range Experiment Station, Corvallis, OR.

Wilson, N., R. Bradstock, and M. Bedward. 2022. Disturbance causes variation in sub-canopy fire weather conditions. Agricultural and Forest Meteorology 323:109077.

Wolf, C., D. M. Bell, H. Kim, M. P. Nelson, M. Schulze, and M. G. Betts. 2021a. Temporal consistency of undercanopy thermal refugia in old-growth forest. Agricultural and Forest Meteorology 307:108520.

Wolf, K. D., P. E. Higuera, K. T. Davis, and S. Z. Dobrowski. 2021b. Wildfire impacts on forest microclimate vary with biophysical context. Ecosphere 12:e03467.

Woodall, C. W., and V. J. Monleon. 2008. Sampling protocol, estimation, and analysis procedures for the down woody materials indicator of the FIA program. Gen. Tech. Rep. NRS-GTR-22, U.S. Department of Agriculture, Forest Service, Northern Research Station, Newtown Square, PA.

Chapter 3. TRADEOFFS FOR MANAGING POST-FIRE FOREST TRAJECTORIES IN NORTHWESTERN CASCADIA UNDER CHANGING CLIMATE

3.1 ABSTRACT

Forecasting ecosystem dynamics under warming climate and increasing fire activity is a critical priority for forest management. Forest conditions following stand-replacing fire present a key opportunity for implementing climate adaptation strategies and steering forest recovery towards desirable trajectories. We combined empirical and simulation approaches to examine potential tradeoffs for managing post-fire forest conditions in wet temperate forests across western Washington and northwestern Oregon, USA. Using the individual-based landscape model, iLand, we simulated 80 years of stand development following high severity fire in stands across the region to examine the effects of pre-fire stand age on post-fire trajectories of (a) early-seral conditions, (b) tree regeneration, and (c) fuel profiles under two future climate scenarios. We found that early-seral conditions persisted for 40–60 years after stand-replacing fire, with longer durations in severely burned mid- and late-seral stands. Similarly, older stands had greater live tree regeneration and dead surface fuel loads following fire, suggesting post-fire recovery and biological legacies may be more robust in stands that are older at the time of fire. Post-fire trajectories were similar under both future climate scenarios, suggesting the positive effects of warming and greater atmospheric CO_2 concentrations on productivity may outweigh potential negative effects of drying through the end of the century. These findings highlight potential tradeoffs among common post-fire management strategies of cultural burning, reforestation, and fuel reduction treatments on stand structural complexity, carbon storage, and fire risk in

northwestern Cascadia. Collectively, our findings help strengthen the simulation-modeling infrastructure for the region and build critical understanding of post-fire responses in wet temperate forests under changing climate.

3.2 INTRODUCTION

Predicting future forest dynamics is a critical but challenging task for facilitating adaptation to changing climate. Across western North America, climate warming and drying has driven increases in fire activity (Abatzoglou and Williams 2016), including fire season length (Jolly et al. 2015), number of large fires (Dennison et al. 2014), and area burned at high severity (Parks and Abatzoglou 2020). While high severity patches are a natural component of many fire regimes, increasing stand-replacing fire activity raises concerns about post-fire forest structure and function (Coop et al. 2020). Further, critical understanding of large and severe fire effects is missing in forests where fire can be infrequent, such as wet temperate forests west of the Cascade Range crest in Washington and northern Oregon, USA (hereafter 'northwestern Cascadia'). These forests are likely to experience increases in area burned under warmer and drier climate conditions (Littell et al. 2018), highlighting interest from Tribal, state, and federal agencies in anticipating future forest dynamics and possible management responses to support the resilience of communities and forest resources to future change (Washington Department of Natural Resources 2020, USFS 2022, Whitely-Binder and Schneider 2022, Tulalip Planning Commission 2023).

Forest conditions following stand-replacing fire present a key opportunity for implementing climate adaptation strategies and steering forest recovery towards desirable trajectories (Halofsky et al. 2018b). Stand age at the time of fire is a key driver of post-fire forest conditions (Johnstone et al. 2016) with implications for future forest structure and composition

(Seidl and Turner 2022). In northwestern Cascadia, key priorities for post-fire management include restoring important successional stages and cultural resources by enhancing early-seral conditions, maintaining forest resilience to fire by ensuring adequate post-fire tree regeneration, and reducing subsequent fire risk by managing fuels, especially in the wildland-urban interface (Spies et al. 2018, Whitely-Binder and Schneider 2022). The early-seral "pre-forest" stage occurs prior to canopy closure after stand-replacing fire (Franklin et al. 2002) and is currently the most underrepresented successional stage across the region (Donato et al. 2020). Early-seral conditions are characterized by dominance of non-tree vegetation (e.g., shrubs, forbs), complex structure, and high biodiversity (Swanson et al. 2011, Donato et al. 2012), providing important ecosystem services including the provisioning of wildlife habitat and culturally important foods and medicines (Boyd 1999, Swanson et al. 2014). Post-fire tree regeneration is a key mechanism of forest resilience (i.e., ability to retain similar structure and function following disturbance; Walker et al. 2004) to stand-replacing fire (Johnstone et al. 2016). Regeneration timelines and densities are typically quicker and more robust in high severity patches positioned closer to unburned live seed sources, and during favorable post-fire climate conditions (Stevens-Rumann and Morgan 2019, Laughlin et al. 2023). Subsequent fire risk is typically reduced for several years after stand-replacing fire due to combustion of available fuel (Parks et al. 2015). However, this fuel limitation may be short-lived in highly productive systems (Buma et al. 2020), and could be enhanced by changes in microclimate conditions (Wilson et al. 2022). Until the last decade, there have been few empirical opportunities to examine fire effects in northwestern Cascadia. Recent fires have burned more than 200,000 ha in the region (Reilly et al. 2022), providing an opportunity to characterize post-fire forest structure and function in these ecosystems.

While initiating field studies soon after stand-replacing fire is critical for understanding short-term post-fire forest dynamics (Lindenmayer et al. 2010), successional development in wet temperate forests plays out over decades to centuries (Winter et al. 2002, Franklin et al. 2002, Freund et al. 2014), and future dynamics are unknown in an era of rapid global change (Halofsky et al. 2020). Simulation models can be useful tools for overcoming the spatial and temporal limitations of empirical studies and guiding management actions by extending field observations into the future (Seidl 2017, Loehman et al. 2020). Individual-based models are considered especially useful for representing realistic forest structural and functional dynamics through pattern-oriented representation of demographic and environmental processes across multiple scales (Grimm et al. 2017). We combined empirical and simulation modeling approaches to examine potential tradeoffs for managing post-fire forest conditions in a changing climate. Using field data from recently burned wet temperate forests across northwestern Cascadia paired with the individual-based landscape model, iLand, we simulated stand development trajectories following stand-replacing fire under two future climate scenarios. Specifically, we asked: (1) How does pre-fire stand age influence post-fire trajectories of (a) early-seral conditions, (b) tree regeneration, and (c) fuel profiles? (2) What are expected post-fire stand development trajectories under future climate conditions? (3) How might the type and timing of management interventions influence post-fire recovery outcomes?

3.3 METHODS

3.3.1 *Study area*

Northwestern Cascadia is defined by wet temperate forests adapted to infrequent, climate-limited fire regimes (Reilly et al. 2021), in addition to intermittent non-stand-replacing fires. Regional

forests are dominated by conifer tree species, high levels of biomass, and abundant cover of shrub, fern, and forb species in the understory (Waring and Franklin 1979, Spies 1991). Tree species composition varies by forest zone. The *Tsuga heterophylla* Zone is dominated by Douglas-fir (*Pseudotsuga menziesii*), western hemlock (*Tsuga heterophylla*), and western redcedar (*Thuja plicata*), with common associates including western white pine (*Pinus monticola*), grand fir (*Abies grandis*), and broadleaf tree species such as bigleaf maple (*Acer macrophyllum*), golden chinquapin (*Chrysolepis chrysophylla*), and bitter cherry (*Prunus emarginata*). The *Abies amabilis* Zone is generally cooler and higher in elevation than the *Tsuga heterophylla* Zone, and dominated by noble fir (*Abies procera*) and Pacific silver fir (*Abies amabilis*), with common associates including mountain hemlock (*Tsuga mertensiana*) along with Douglas-fir and western hemlock (Franklin and Dyrness 1973). Current structural conditions reflect a range of stand ages as a function of varied management histories (Spies et al. 2018). Regional forest cover is currently dominated by mid-seral stands and young plantations due to past and current management; complex early-seral and late-seral conditions are underrepresented compared to expected abundance from the estimated natural range of variation (Donato et al. 2020).

The climate in northwestern Cascadia is Mediterranean, with wet winters, dry summers, and mild seasonal temperatures. Recent climate normals (1991–2020) for annual mean temperature and total precipitation across our sampled area range from 4.0–10.7 °C and 1,435–3,273 mm, respectively, with 76% of precipitation falling from November through April (PRISM Climate Group 2024). Common soils include loamy, well-drained groups of volcanic and glacial origin that are typically rich in organic matter (Williams and Dyrness 1967, Franklin and Dyrness 1973). Fires in northwestern Cascadia are limited primarily by climatic controls on fuel

flammability, with strong climate-fire relationships with year-of-fire temperature and moisture (Agee 1993, Littell et al. 2009, Reilly et al. 2021). Large, stand-replacing fires typically occur at multi-century intervals (>200 years; Reilly et al. 2021). Smaller, more frequent fires are also represented in the historical fire regime, commonly associated with Indigenous fire use for management of cultural resources and travel corridors (Boyd 1999, Johnston et al. 2023).

3.3.2 *Sampling design*

We used field data collected 2–5 years following five recent fires across northwestern Cascadia. Detailed sampling design and field methods are described in Chapter 1. Briefly, we measured initial post-fire stand structure, tree regeneration, and fuel profiles 2–5 years in 40 1-ha stands burned at high severity (i.e., ≥90% overstory basal area mortality). Stands were stratified by pre-fire stand age based on structural development attributes (Van Pelt 2007) and classified as young (n = 9), mid-seral (n = 12), or late-seral (n = 19). Generally, young stands were ~50-year-old plantations established following clearcut harvesting in the 1970s and 1980s, mid-seral stands were ~120-year-old second-growth or fire-origin stands established after Euro-American settlement, and late-seral stands were fire-origin old-growth stands established ~>200 years ago prior to Euro-American settlement.

3.3.3 *Model overview*

We modeled post-fire stand development trajectories within each of our field-measured high-severity stands using the spatially explicit individual-based forest landscape and disturbance model, iLand (Seidl et al. 2012a, Rammer et al. 2024). iLand simulates growth, mortality, and regeneration of individual trees on stand to landscape scales by explicitly modeling competition for resources and environmental influences on forest processes. Tree characteristics and

behaviors are controlled by 66 species-specific parameters that define functional traits for each species (Thom et al. 2024). The model has been used to investigate the effects of climate change, disturbances, and management on forest dynamics over time and space in ecosystems across North America (e.g., Seidl et al. 2014, Hansen et al. 2021, Turner et al. 2022), Europe (e.g., Thom et al. 2018, Albrich et al. 2020), and Japan (e.g., Kobayashi et al. 2023). Detailed model documentation is available from the online wiki (https://iland-model.org).

We used parameters for 13 major tree species found within our field-measured stands. These included eight species from the original use of iLand in western Oregon (Seidl et al. 2012a, 2014), two species from the Northern Rocky Mountains (Braziunas et al. 2018), and three new tree species parameterized for this study (Thom et al. 2024). We re-calibrated these 13 species against regional forest inventory data for use in the western Cascades across Washington and Oregon, USA. For several tree species measured in our stands that have yet to be fully re-calibrated for iLand (n = 7), we used alternate species to serve as proxies, based on similar functional traits (Appendix D: Table 3.1).

3.3.4 *Model inputs*

Model inputs for initial vegetation, environment, and climate conditions were derived from field measures and geospatial datasets. We used our post-fire field data to initialize live trees and dead carbon pools within each simulated 1-ha stand (Appendix D: Table 3.2). Live vegetation inputs included individual trees (height > 4 m), saplings (height 1.3–4 m), and seedlings (height ≤ 1.3 m). Trees were initialized as unique individuals with species, dbh, and height information tracked at 2 m resolution. Sapling and seedlings were initialized with species and height information and treated as cohorts at 2-m resolution, eventually being recruited as individuals when surpassing the 4-m tree height threshold. Within each 1-ha stand, spatial positions of

individual trees and cohorts of saplings and seedlings are determined by a pseudo-random function based on light availability and existing basal area present in each 10-m cell (Seidl et al. 2012a). Live surface fuels and non-tree vegetation types (i.e., woody shrubs, herbaceous understory plants) are not currently represented in iLand.

Dead vegetation inputs included snags and surface fuels. Snags were initialized as stand-level densities and aboveground biomass carbon for standing dead trees (height ≥ 4 m). Surface fuels were initialized as stand-level aboveground biomass carbon in the labile soil pool (litter, duff, 1-h, 10-h fuels) and refractory soil pool (100-h, 1000-h fuels). Small snags (height < 4 m) and stumps were also included in surface biomass carbon pools according to diameter size class (labile ≤ 2.54 cm; refractory > 2.54 cm). Detailed methods for conversion of field measures into biomass carbon are described in Chapters 1 (aboveground biomass carbon for snags, down woody debris) and 2 (litter and duff biomass). In brief, we used species-, compartment-, and region-specific allometric equations and carbon fractions to derive biomass carbon stored in aboveground vegetation components (Brown 1974, Brown et al. 1982, Means et al. 1994, Woodall and Monleon 2008). We corrected biomass for loss of density and volume as a function of decay class and deep wood charring (Harmon et al. 2008, 2011, Donato et al. 2009, 2013). For litter and duff biomass, we assumed a dry-weight carbon proportion of 0.378 and 0.428, respectively, based on the average of forest floor biomass values reported for the Pacific Northwest (Smith and Heath 2002) and used in common fuel models (Prichard et al. 2013).

Stand-level environment inputs were extracted from 1-km gridded soil datasets using the geographic coordinates for each plot center (Appendix D: Table 3.3). Soil depth and texture (i.e., percent sand, silt, clay) were obtained from CONUS-SOIL (Miller and White 1998), and plant available nitrogen was derived from regional soil fertility maps (Coops et al. 2012). Stand-level

climate inputs were based on 1-km gridded meteorological data from Daymet version 4.1 (Thornton et al. 2022). We used these grids to extract daily values of minimum and maximum temperature, total precipitation, total radiation, and average vapor pressure deficit from 1981–2020 for each of our plot locations (Appendix E: Table 3.7).

3.3.5 *External seed availability*

We simulated external seed input to approximate realistic regeneration dynamics following stand-replacing fire. We used a buffer approach to establish a 200-m wide belt of available seeds surrounding each stand. Seed belts were positioned outside a non-forested buffer with a width equal to the distance of a stand from the nearest live seed source. Distance to live seed source was hand measured from the center of each stand using Google Earth satellite imagery collected in the same year as our field sampling. We defined live seed source as a patch of live trees at least 1-ha in area with less than 25% overstory mortality. Across our sampled stands, distance to live seed sources ranged from 38 to 1,610 m with a mean of 268 m (Appendix D: Fig. 3.6). We assigned each simulated high severity stand an external seed input species mix that matched the species composition of live mature trees (dbh ≥ 10 cm) in sampled unburned stands of the same stand age and forest zone class (Appendix D: Tables 3.5–3.6). We assumed an equal representation of each available species within the seed belt and allowed seeds to disperse into stands from all directions according to species-specific dispersal kernel functions (Seidl et al. 2012b).

3.3.6 *Future climate scenarios*

We examined the effects of climate change on post-fire stand development trajectories by constructing two future climate scenarios: a ‘control’ scenario representing no change from

present day conditions, and a 'warm' scenario representing projected increases in temperature with substantial greenhouse gas emissions. Both scenarios were constructed using the stand-level daily climate inputs from Daymet for 1981–2020. To simulate stand development trajectories through the end of the century (c. 2100), we derived an 80-year timeseries by linearly detrending and duplicating the 40-yr (1981–2020) daily climate inputs from Daymet and scaling these detrended values according to the trends for each scenario. For the 'control' scenario, we used the 40-yr averages in daily observations from 1981–2020 to scale the detrended values for each stand and assumed a static atmospheric CO_2 concentration of 400 ppm throughout the simulation. For the 'warm' scenario, we examined the effects of future warming and drying on post-fire stand development trajectories. We employed a simple climate perturbation approach (*sensu* Hsiao et al. 2024) to shift the observed meteorology data from Daymet based on global changes in mean temperature and relative humidity in accordance with SSP3-7.0 (Riahi et al. 2017). This scenario reflects substantial greenhouse gas emissions and projected increase in global mean temperature of +3.1 °C by 2100 under atmospheric CO_2 concentration of 850 ppm (Meinshausen et al. 2020, Lee et al. 2021). We used maps of monthly anomalies in temperature and relative humidity to scale these global trends to expected local patterns for each of our plots (Appendix E: Table 3.8, Figs. 3.7–3.8). Monthly anomaly maps were derived from multi-model mean projections from CMIP6 outputs (O'Neill et al. 2016) and reflect fairly consistent spatial patterns of temperature and relative humidity changes across climate models (Vargas Zeppetello et al. 2019). We applied these changes directly to our detrended meteorology data (Appendix E: Table 3.9, Figs. 3.9–3.10). This approach limits known biases in variability from singular climate models and preserves fine-scale temporal and spatial correlations between climate variables (Taylor et al. 2023). We generated minimum and maximum temperature inputs based on

differences in 40-year averages of monthly temperatures from the mean temperatures in each stand (Appendix E: Fig. 3.11), assuming constant diurnal temperature range due to uncertainties in projections from CMIP6 models (Wang and Clow 2020). We assumed no change in precipitation due to high uncertainty in the spatiotemporal pattern and magnitude of precipitation projections among climate models (Lee et al. 2021, Rogers and Mauger 2021). We also included an annual timeseries of atmospheric CO_2 concentration change based on SSP3-7.0 projections of ~415 ppm in 2021 to ~850 ppm by 2100 (Meinshausen et al. 2020). Inputs for each future climate scenario are summarized in Appendix D: Table 3.4.

3.3.7 *Simulations and outputs*

We simulated post-fire stand development trajectories in each high severity stand ($N = 40$) for 80 years (c. 2100) with no additional disturbance under the control and warm future climate scenarios. Stands were treated independently, with all resources and processes constrained to each stand within a continuous environment. We generated annual outputs of live and dead structural attributes and aboveground biomass carbon pools for each stand. We ran 20 simulation replicates of each stand for both climate scenarios and averaged results by stand to capture variability from stochastic processes in iLand (Rammer et al. 2024).

3.3.8 *Analyses*

To address Question 1, we compared mean and variability in simulated trajectories of early-seral conditions, regeneration, and fuel profile outputs among pre-fire stand age classes. We interpreted periods of non-overlap in confidence intervals to indicate meaningful differences in trends among strata (White et al. 2014).

Early-seral conditions — We examined the longevity of early-seral conditions using a

structure-based ruleset approach (e.g., Hoecker and Turner 2022). Since iLand does not currently simulate non-tree vegetation, we defined early-seral conditions based on stand-level forest attributes of live tree canopy cover and quadratic mean diameter. Canopy cover was extracted from annual raster outputs of the proportion of 2-m pixels within a stand covered by tree crown. We included all live conifer trees and saplings (i.e., individuals with dbh; height > 1.3 m) in the quadratic mean diameter calculations; hardwood species were omitted since they are commonly considered a distinguishing feature of early-seral communities (Swanson et al. 2014). We considered stands to be in an early-seral condition if, at the end of each simulation year, they had live tree canopy cover < 60% and live quadratic mean diameter < 12.7 cm. For stands containing any legacy trees (i.e., large trees which survived the fire; n = 5 stands), we applied an additional early-seral criterion limiting legacy tree canopy cover to 10%. These values generally correspond to the timing of canopy closure and recovery of tree dominance typically observed in wet temperate forests within the region (Franklin et al. 2002, Van Pelt 2007), and align with characterizations of early-seral conditions by regional studies (Burcsu et al. 2014, Reilly and Spies 2015, Donato et al. 2020).

Tree regeneration — We examined post-fire regeneration trajectories by tracking patterns in live basal area and density by size class over the 80-year simulation period. For each output, we assessed both total trends in magnitude and proportional trends by species categorized into three functional groups: broadleaf, shade-tolerant conifer, and shade-intolerant conifer species (Appendix D: Table 3.1).

Fuel profiles — We examined post-fire fuel profile trajectories by tracking patterns in biomass carbon stored in canopy and surface fuel components over the 80-year simulation period. Canopy fuel components included total crown fuel of foliage and branch biomass from

all live and dead standing trees (height > 4 m). Surface fuel components included down woody debris biomass of litter, duff, and dead woody fuels on or near the forest floor (height < 2 m).

To address Question 2, we compared post-fire aboveground biomass carbon trajectories among the control and warm future climate scenarios. We interpreted differences in 80-year trends among outputs from each scenario based on the same principles described for simulated data in Question 1. To address Question 3, we interpreted our simulated findings within a management context to discuss potential tradeoffs among common post-fire management strategies for achieving desired outcomes following high severity fire. All analyses and visualizations were done in R (v4.4.0; R Core Team 2024) using the following packages: *daymetr* (v1.7.1; Hufkens et al. 2018), *filesstrings* (v3.4.0; Nolan and Padilla-Parra 2017), *ncdf4* (v1.23; Pierce 2024), *patchwork* (v1.2.0; Pedersen 2024), *plotrix* (v3.8-4; Lemon 2006), *raster* (v3.6-30; Hijmans 2024a), *reshape2* (v1.4.4; Wickham 2007), *RSQLite* (v2.3.7; Müller et al. 2024), *sp* (v2.1-4; Pebesma and Bivand 2005), *terra* (v1.7-78; Hijmans 2024b), *tidyterra* (v0.6.1; Hernangómez 2023), and *tidyverse* (v2.0.0; Wickham et al. 2019).

3.4 RESULTS

3.4.1 *Early-seral conditions*

Early-seral conditions persisted for several decades following high severity fire, though duration varied by pre-fire stand age (Fig. 3.1). The proportion of stands in an early-seral condition declined over time (Fig. 3.1a) as live tree cover and size increased (Fig. 3.1b–c). Most stands (i.e., proportion > 0.5) remained within an early-seral condition for 30–40 years after sampling, though transition of all stands to tree dominated successional stages (i.e., proportion = 0) did not occur for another 10–20 years since sampling (Fig. 3.1a). This transition out of early-seral

condition occurred more rapidly for pre-fire young stands, occurring around year 40 after sampling compared to years 50–60 for mid- and late-seral stands (Fig. 3.1a).

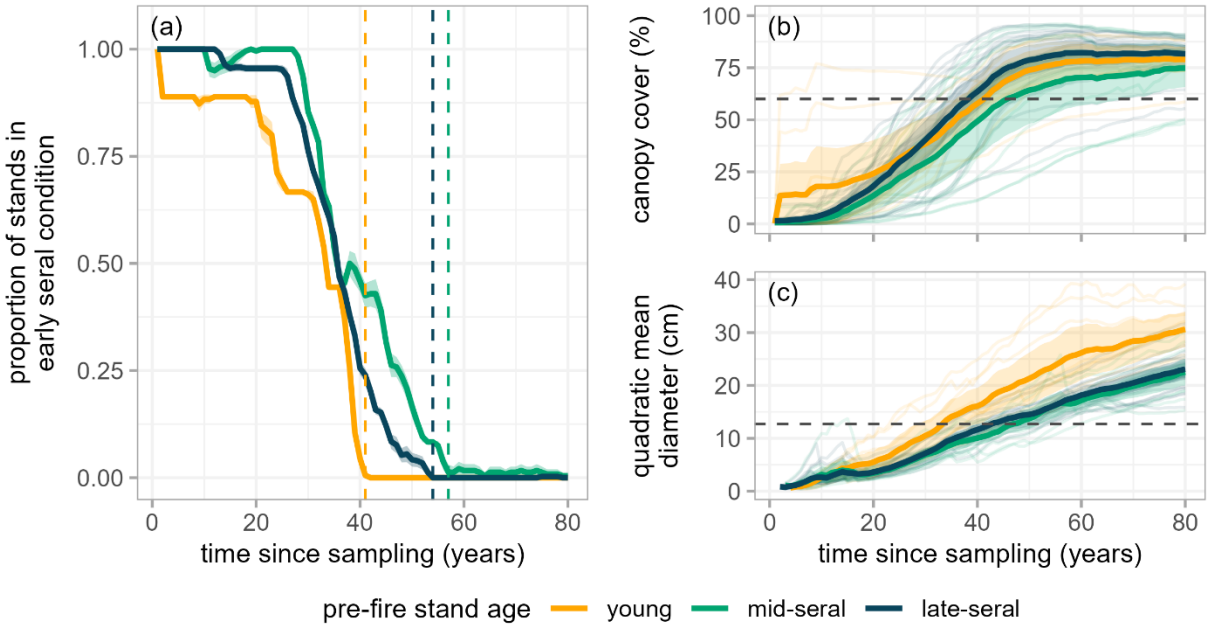

Figure 3.1. Simulated trajectories of early-seral conditions following high severity fire. Proportion of stands considered early seral was summarized annually for each pre-fire stand age class (a). Early-seral conditions were defined as live canopy cover < 60% (b) and live quadratic mean diameter < 12.7 cm (c). Quadratic mean diameter included all live conifer trees with dbh (i.e., height > 1.3 m). Bold lines are the mean and shaded 95% confidence interval for each pre-fire stand age class, based on stand-level values averaged across 20 simulation replicates (transparent lines). Vertical dashed lines (a) represent the timing of total transition out of the early-seral stage for each age class (i.e., proportion of early-seral stands = 0). Horizontal dashed lines represent the threshold values of live cover (b) and size (c) used to define early-seral conditions.

3.4.2 *Tree regeneration*

Post-fire tree regeneration was generally robust over time, though the shape, magnitude, and species composition of live tree recovery trajectories varied by pre-fire stand age and tree size class. Live basal area increased over time, with the greatest and most rapid increases occurring in

pre-fire late-seral stands (Fig. 3.2). Broadleaf species were a dominant proportion of live basal for the first five years before declining over time, though broadleaf dominance remained relatively high in pre-fire young stands through the full simulation (Fig. 3.2). Basal area proportion of shade-intolerant conifer species increased rapidly for 5–10 years after sampling before stabilizing or slowly declining over time. In contrast, basal area proportion of shade-tolerant conifer species steadily increased throughout the simulation. By year 80 after sampling, basal area proportion of live conifer species was similar between pre-fire mid- and late-seral stands, while proportions of shade-intolerant species were greater, and shade-tolerant species less, in young stands (Fig. 3.2).

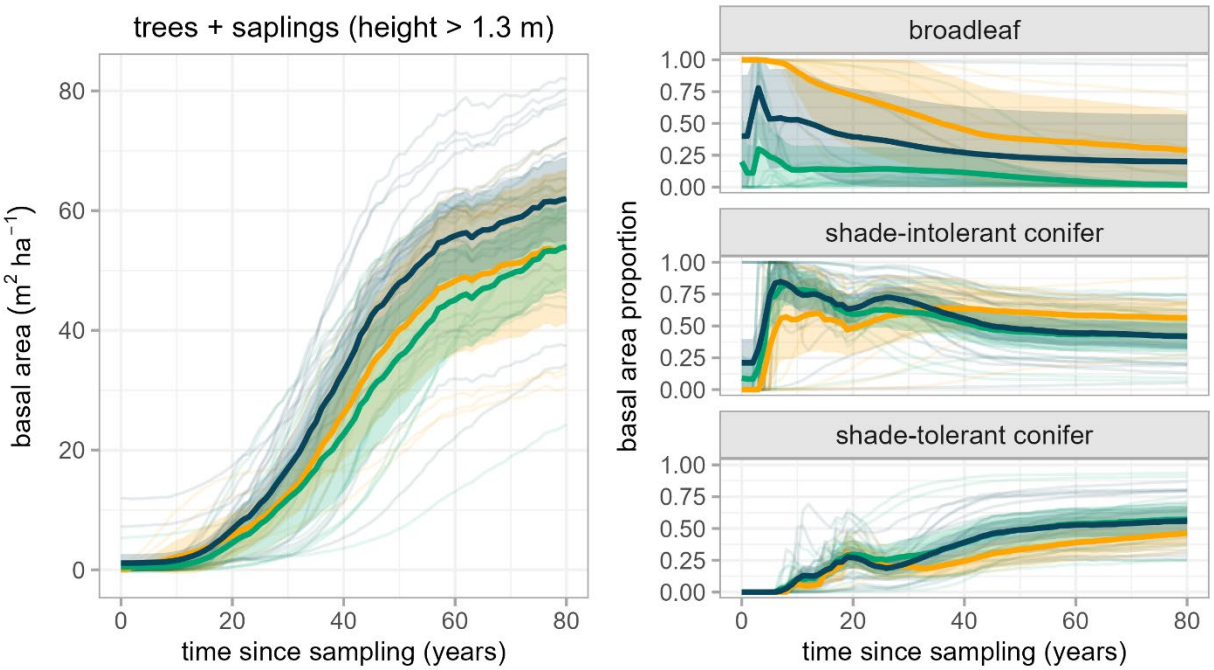

Figure 3.2. Simulated trajectories of total live basal area following high severity fire. Basal area includes live trees and saplings with height > 1.3 m, summarized for all individuals combined (*left*) and proportional share by species functional group (*right*; Appendix D: Table 3.1). Bold lines are the mean and shaded 95% confidence interval for each pre-fire stand age class, based on stand-level values averaged across 20 simulation replicates (transparent lines). Proportions among functional groups within a stand age class may exceed 1 due to aggregation of stand-level proportions across all replicates.

Live stem density displayed similar trends among pre-fire stand age classes for all size classes (Fig. 3.3). Tree increased for 50–60 years after sampling before declining for the remainder of the simulation (Fig. 3.3a). These trends were similar for saplings and seedlings, though the timing of declines in density were earlier, sapling density peaking around year 20 after sampling (Fig. 3.3b) and seedling density peaking first around year 10 then again around year 30 (Fig. 3.3c), reflecting the transition of individuals into taller size classes. Live stem densities were generally higher in pre-fire mid- and late-seral stands compared to young stands, though tree densities converged by year 80 after sampling. Density proportion of broadleaf species was highly variable across pre-fire stand age and size classes (Fig. 3.3). Density proportion of shade-intolerant conifer seedlings declined rapidly, remaining near 0 at 10 years after sampling for pre-fire mid- and late-seral stands (Fig. 3.3c). Density proportion of shade-tolerant conifer seedlings reflected a opposite trend, rapidly increasing for 10 years after sampling and remaining near 1 through year 80 (Fig. 3.3c). Pre-fire young stands maintained a higher density proportion of shade-intolerant conifer seedlings than mid- and late-seral stands throughout the simulation (Fig. 3.3c).

3.4.3 *Fuel profiles*

Post-fire fuel profiles were dominated by dead fuel biomass and varied by pre-fire stand age (Fig. 3.4). Biomass carbon in total crown fuels decreased sharply for 5 years after sampling before increasing over the remainder of the simulation period (Fig. 3.4a). This trend was similar among pre-fire stand age classes throughout the simulation. Biomass carbon in down woody debris displayed an opposite trend, increasing sharply in the first 5 years after sampling before declining until stabilizing around year 50 (Fig. 3.4b). Down woody debris was greater in pre-fire mid- and late-seral stands than young stands for at least 60 years after sampling (Fig. 3.4b).

Biomass carbon in down woody debris remained greater than crown fuel for 50 years after sampling in pre-fire young stands and for the full simulation in mid- and late-seral stands (Fig. 3.4).

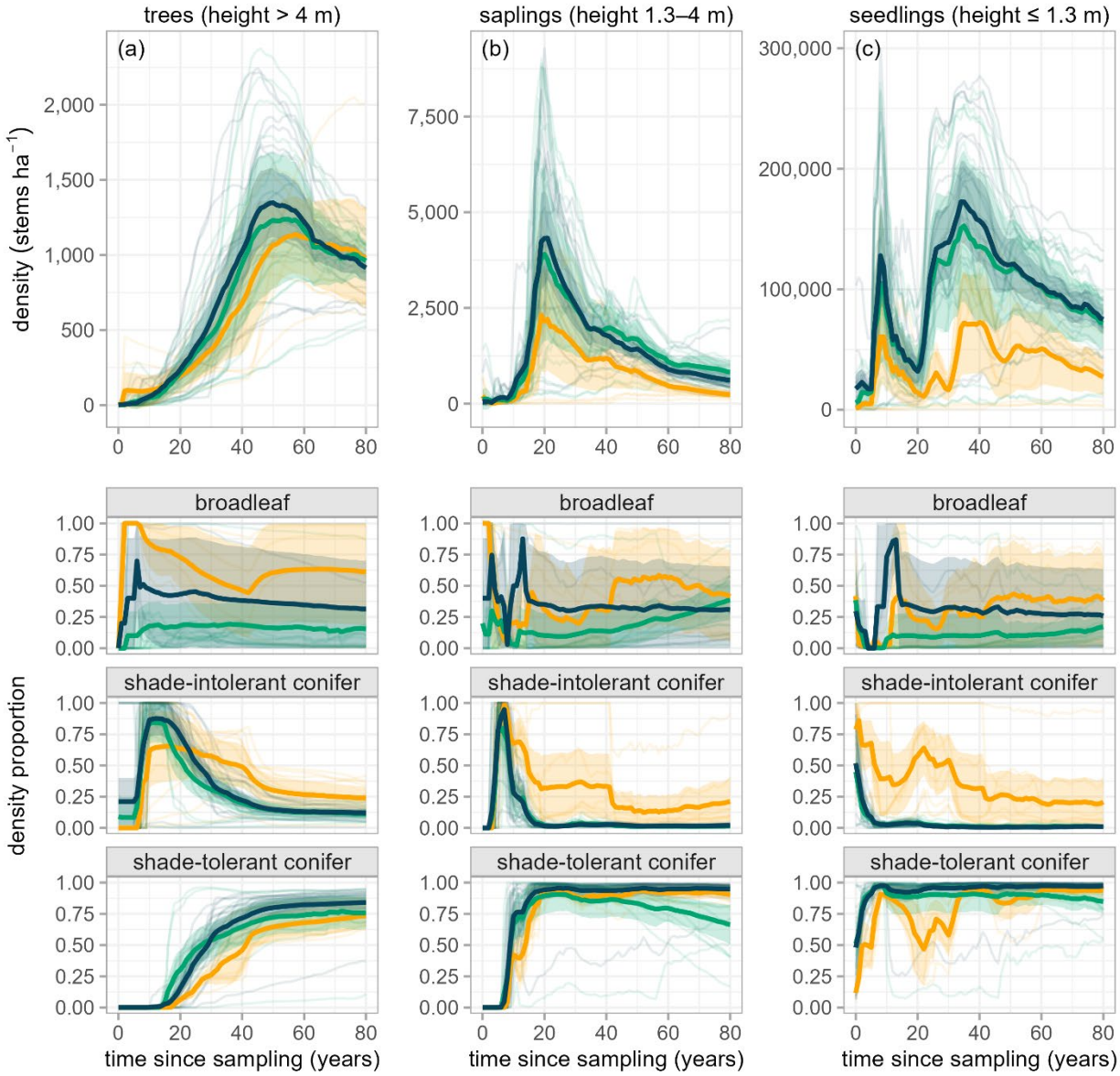

Figure 3.3. Simulated trajectories of live stem density by size class following high severity fire. Density of trees (a), saplings (b), and seedlings (c) is summarized for all individuals combined (*top*) and proportional share by species functional group (*bottom*; Appendix D: Table 3.1). Bold lines are the mean and shaded 95% confidence interval for each pre-fire stand age class, based on stand-level values averaged across 20 simulation replicates (transparent lines). Proportions among functional groups within a stand age class may exceed 1 due to aggregation of stand-level proportions across all replicates.

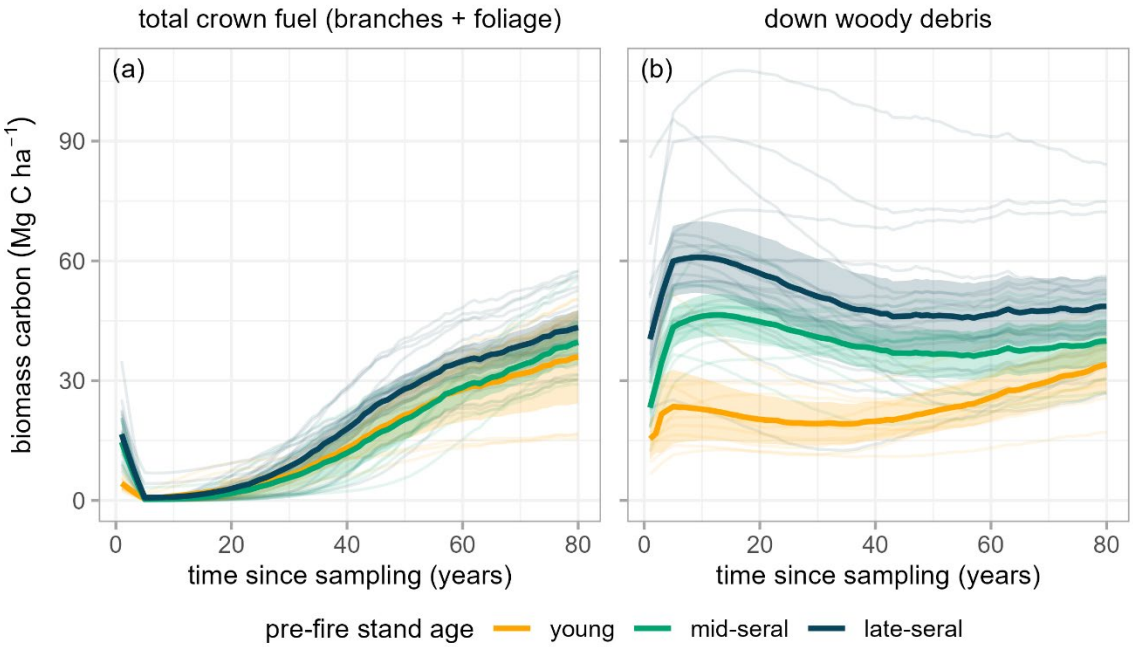

Figure 3.4. Simulated trajectories of aboveground biomass carbon in canopy (a) and surface (b) fuel components following high severity fire. Crown fuel includes foliage and branch biomass from all live and dead standing trees (height > 4 m). Down woody debris includes biomass from litter, duff, and dead woody fuels on or near the forest floor (height < 2 m). Bold lines are the mean and shaded 95% confidence interval for each pre-fire stand age class, based on stand-level values averaged across 20 simulation replicates (transparent lines).

3.4.4 *Future climate scenarios*

Post-fire stand trajectories were similar regardless of future climate scenario. Both the control and warm scenario projected similar overall patterns in total, live, and dead aboveground biomass carbon (Fig. 3.5). Live biomass carbon increased, and dead biomass carbon decreased over time. Total biomass carbon decreased for 30–40 years after sampling before increasing for the remainder of the simulation, reflecting the transition from dominance by dead to live biomass which occurred most rapidly in pre-fire young stands. By year 80 after sampling, total carbon was highest in pre-fire late-seral stands (Fig. 3.5). Overlap in trajectories between future climate scenarios decreased over time, with the warm scenario projecting greater live and less dead biomass carbon at the end of the simulation on average than the control scenario (Fig. 3.5).

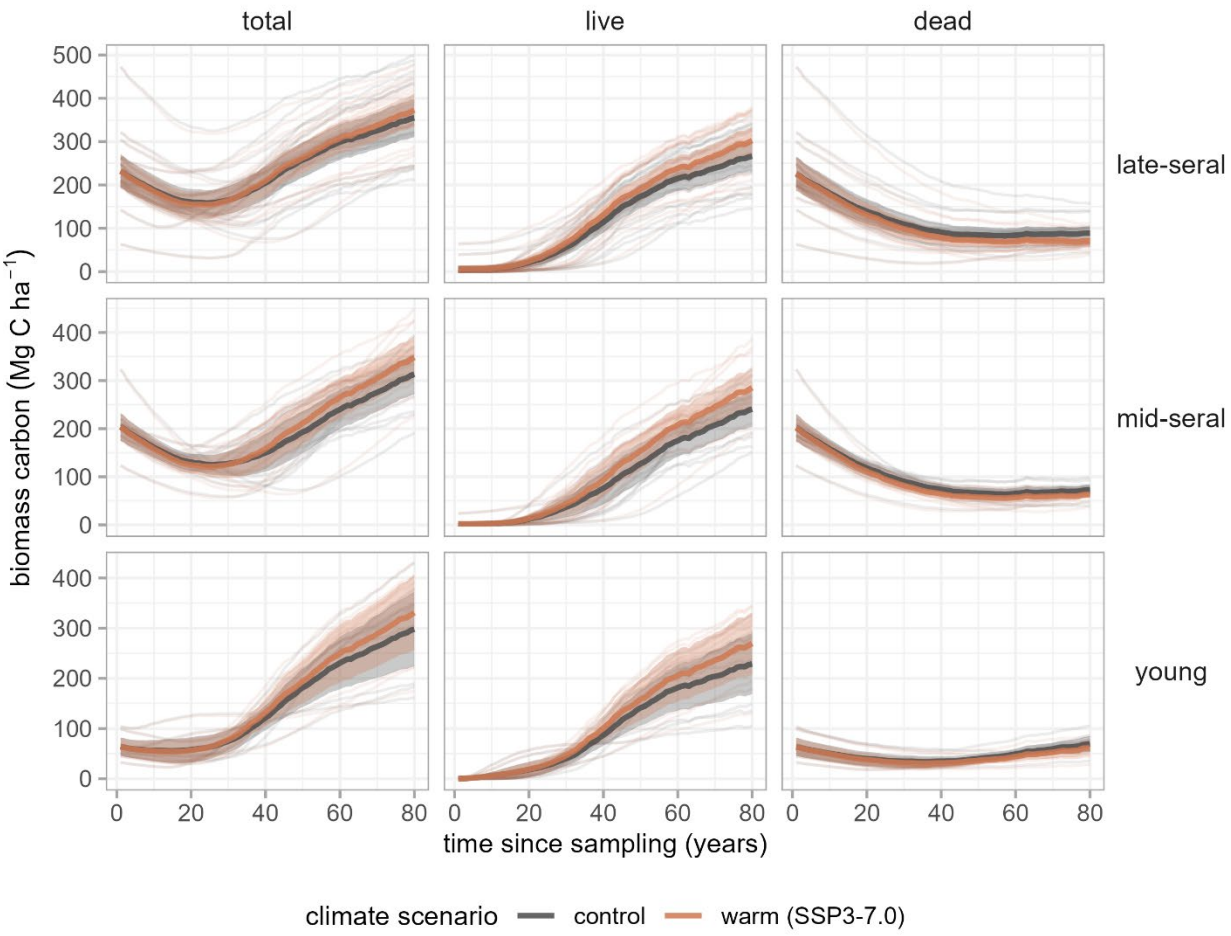

Figure 3.5. Comparison of simulated trajectories in total (*left*), live (*center*), and dead (*right*) aboveground biomass carbon following high severity fire across future climate scenarios. The control scenario (black) represents no change from baseline (1981–2020) conditions. The warm scenario (red) represents warming and drying conditions based on projected trends in temperature and relative humidity under substantial greenhouse gas emissions (SSP3-7.0). Bold lines are the mean and shaded 95% confidence interval for each pre-fire stand age class (young, mid-seral, late-seral) based on stand-level values averaged across 20 simulation replicates (transparent lines).

3.5 DISCUSSION

By simulating 80 years of stand development following high severity fire in wet temperate forest, our study demonstrates the lasting effects of pre-fire stand age on post-fire structure and composition. This work contributes to critical understanding of potential forest recovery trajectories after stand-replacing fire under future climate and supports post-fire management

strategies aimed at addressing climate adaptation in northwestern Cascadia.

3.5.1 *Pre-fire stand age directs forest recovery following stand-replacing fire*

Pre-fire stand age drove differences in trajectories of early-seral conditions, tree regeneration, and fuel profiles following stand-replacing fire.

Early-seral conditions — Early-seral conditions persisted for four to six decades following fire, generally aligning with reconstructions of establishment dynamics and stand initiation timelines for mature and old forests within the region (Winter et al. 2002, Tepley et al. 2014, Freund et al. 2014). The duration of the early-seral stage was shortest in pre-fire young stands with transition to tree dominance occurring 10–20 years sooner than in mid- and late-seral stands. This is likely due to faster growth of regenerating trees in pre-fire young stands as a result of less initial tree regeneration (Laughlin et al. 2023) and thus weaker resource competition among individuals. However, this effect may also be confounded with distance to seed source. Pre-fire young stands were on average 94–136 m closer to live mature trees than mid- and late-seral stands (Appendix D: Fig. 3.6), suggesting greater external seed pressure and faster tree establishment (Appendix F: Fig. 3.12; Laughlin et al. 2023).

These findings suggest greater ability of complex pre-fire stands to support complex post-fire dynamics. When burned, older stands may have greater potential than young stands to support early-seral ecosystem services and fulfill regional forest restoration priorities (Spies et al. 2018). Regardless of pre-fire stand age, stand-replacing fire may support the development of complex early-seral habitats for half a century or more, facilitating high biodiversity of plant and animal species that thrive in open environments (Swanson et al. 2014). These benefits are likely to last the longest in areas with slower rates of canopy closure, such as the interiors of large high severity patches far from live seed sources (Swanson et al. 2011) or areas at higher elevation

with lower productivity rates (Tepley et al. 2014).

Tree regeneration — Simulated trajectories of live tree regeneration followed expected patterns of stand development in northwestern Cascadia. Our findings highlighted that post-fire tree regeneration can occur over multiple decades, supporting observations of protracted establishment times from reconstructive studies throughout the region (Freund et al. 2014). For instance, simulated peaks in live tree density around year 50 correspond with the estimated timeframe for initial cohort establishment (Tepley et al. 2014) and transition into the competitive exclusion stage of stand development (Franklin et al. 2002). Tree regeneration trajectories also followed expected species successional dynamics, with early dominance by broadleaf and shade-intolerant conifer species, and continuous regeneration of shade-tolerant conifer species over the full simulation (Winter et al. 2002, Tepley et al. 2013). Similar to trends reported in existing regional studies (Tepley et al. 2014), variability in regeneration trajectories was high within stand age classes likely due to differences in distance to seed source, with stands closer to live mature seed sources having greater regeneration success than stands far from seed source (Stevens-Rumann and Morgan 2019, Laughlin et al. 2023).

Our findings suggest post-fire recovery may be more robust in stands that were older at the time of fire. Greater abundance of initial seedling and sapling densities in pre-fire mid- and late-seral stands (Laughlin et al. 2023) facilitates greater amounts and more rapid recovery of live basal area and density following fire. This supports findings in other wet temperate forest systems (Bowd et al. 2021). Regardless of pre-fire stand age, regeneration trajectories in all stands appear sufficient to achieve recovery of pre-fire forest structure and composition, implying that northwestern Cascadia stands are poised to be resilient to stand-replacing fire in the near future.

Post-fire stand development pathways may be distinct in pre-fire young stands compared to mid- and late-seral stands. Simulated trajectories of stand structural attributes, including coexistence of shade-tolerant and shade-intolerant conifer species and abundance of dead woody biomass, suggest all stands may support complex ecosystem functions comparable to old-growth stands regardless of pre-fire stand age (Donato et al. 2012). However, pre-fire young stands had greater quadratic mean diameter and lower densities than mid- and late-seral stands, as well as large proportions of broadleaf tree species and prolonged establishment of shade-intolerant conifer seedlings. These structural attributes suggest pre-fire young stands may follow a more open successional pathway, likely facilitated by lower abundance and diversity of initial seedling regeneration (Laughlin et al. 2023). This has potential implications for the continuity of complexity and subsequent ecosystem functions throughout stand development, though longer simulation timeframes will be necessary to test this.

Fuel profiles — Simulated trajectories of post-fire canopy and surface fuel profiles followed expected patterns of stand development in wet temperate forests. Biomass carbon in canopy fuels decreased initially as dead foliage and branches on fire-killed trees fell to the surface, then increased over time with establishment and growth of live trees. Biomass carbon in dead surface fuels displayed an opposite trend, first increasing with input of foliage and branches from decaying snags, then decreasing as decomposition became more dominant. This aligns with general patterns of fuel succession across stand development stages in northwestern Cascadia (Agee and Huff 1987). Canopy fuel loads were similar among pre-fire stand ages, reflecting similar trajectories of live tree regeneration. In contrast, dead surface fuels were greater in pre-fire mid- and late-seral stands, reflecting greater overall pre-fire biomass within older stands (Gray et al. 2016) and the persistence of dead fuels for decades after fire (Spies et al. 1988).

These findings suggest greater surface fire hazard after stand-replacing fire in late-seral stands, though differences may lessen over time and overall fire hazard may remain similar across all stands given the dominance of climate and fire weather conditions, rather than fuel loads, on reburn dynamics in wet temperate forests (Tepley et al. 2018, Evers et al. 2022, Busby et al. 2023).

3.5.2 *Climate warming may enhance live carbon trajectories*

Our simulations revealed similar post-fire trajectories of aboveground biomass carbon under both future climate scenarios. Thus, near-term effects of climate change may not fundamentally change the structure and function of post-fire forest recovery in northwestern Cascadia. However, divergence in trends over time implies potential increases in live biomass carbon under the warm scenario with a longer simulation timeline. This suggests that the positive effects of warming and greater atmospheric CO_2 concentrations on productivity (e.g., more growing degree days, CO_2 fertilization, enhanced water use efficiency) may outweigh potential negative effects of drying (e.g., carbon starvation, hydraulic failure), at least through the end of the century. This generally aligns with expectations of increased growth and productivity with higher temperatures and atmospheric CO_2 concentrations in wet forests where sufficient water is available during the growing seasons (Halofsky et al. 2018a, Case et al. 2021), though responses are likely to be spatially variable and species-specific (Case and Lawler 2016). For instance, several tree species in northwestern Cascadia, including bigleaf maple (Betzen et al. 2021) and western redcedar (Andrus et al. 2024), are displaying high rates of tree mortality and decline in portions of their range, which may be further enhanced with continued climate warming (Allen et al. 2010).

Our future climate scenarios did not incorporate changes in precipitation or represent extreme weather events. The timing, magnitude, and spatial patterns of precipitation projections

for the region are variable and uncertain, but generally suggest slight increases in annual precipitation and more extreme seasonality (i.e., wetter winters, drier summers) in the western Cascades (Rogers and Mauger 2021, Chegwidden et al. 2022). These changes in precipitation may reduce moisture available for growth and productivity during some times of the year. Extreme weather events are projected to become more frequent and intense with climate change (Seneviratne et al. 2021). These events, such as the 2021 Heat Dome which brought record-breaking heat and aridity to northwestern Cascadia (Thompson et al. 2022), may have profound impacts on productivity (Still et al. 2023), mortality (Jain et al. 2024), and regeneration (Brackett et al. 2024) dynamics following fire. Further, our simulations were run without additional disturbances. Disturbance activity is likely to continue to increase under further climate warming (Seidl et al. 2017), with implications for live and dead forest carbon trajectories (Raymond and McKenzie 2012). Future simulations could explore additional climate scenarios that incorporate potential changes in precipitation, capture extreme events, and incorporate disturbance dynamics not currently represented in our simulations.

3.5.3 *Management implications*

Our findings have important implications for potential tradeoffs among management strategies to achieve desired post-fire recovery outcomes. Aligning management strategies with natural disturbance dynamics is important for maintaining forest integrity (Franklin et al. 2018). In forests shaped in part by infrequent stand-replacing fires, appropriate post-fire management for protecting and restoring key ecosystem services can range from no direct action to interventions such as cultural burning, reforestation, and fuel reduction treatments (Lindenmayer et al. 2022). Tradeoffs will likely change through time and vary based on management strategy and future climate conditions (Halofsky et al. 2017). Management options are further complicated by

existing policy barriers, organizational capacity, and public acceptance (Schoennagel et al. 2017, Halofsky et al. 2018b). Adopting an adaptive co-production approach through inclusive engagement between researchers, practitioners, and decision-makers can help balance these priorities, enhancing the capacity to facilitate forest resilience following fire and manage for a range of post-fire conditions across the region (Lebel et al. 2006, Armitage et al. 2009).

Cultural burning — Cultural fire use by Indigenous communities can promote early-seral conditions by encouraging the dominance of non-tree species. These conditions can enhance plant species richness and diversity (Hoffman et al. 2017, Greenwood et al. 2024), and provide critical habitat for supporting cultural resources (Boyd 1999, Lake et al. 2017, Long et al. 2021). However, by lengthening regeneration timelines and delaying return to tree dominance, this management strategy may also present tradeoffs with carbon storage (Harmon et al. 1990) and economic objectives related to timber production (Spies et al. 2018), though the magnitude of these effects will depend on the amount of cultural burning applied.

Our simulations suggest cultural burning may be most effective at promoting early-seral conditions in pre-fire young stands, given the high proportion of broadleaf species regeneration and potentially more open conditions. Accordingly, these stands present an opportunity for embracing both western science and Indigenous Knowledge to enhance cultural resources and work towards restoring the proportion of early-seral area in alignment with the natural range of variation in the region (Donato et al. 2020, Eisenberg et al. 2024). However, meaningful implementation of this post-fire management strategy will require enabling Indigenous leadership and removing barriers for practicing cultural fire (Maclean et al. 2023), including federal policies related to fire suppression, Tribal sovereignty, and use of fire as a management tool (Clark et al. 2024).

Reforestation — Planting tree seedlings following high severity fire can be useful for accelerating forest recovery timelines and return to tree dominance by ensuring adequate tree regeneration (Rodman et al. 2024). Rapid live tree recovery is particularly important for promoting economic objectives related to timber production and live carbon storage (Law et al. 2004, Kline et al. 2016). Post-fire planting can also present an opportunity for enhancing forest resilience to climate change through adaptation strategies such as assisted population migration (Halofsky et al. 2018a, Agne et al. 2025). Given our findings of robust live tree regeneration trajectories within our simulated stands, post-fire planting may be unnecessary to ensure forest recovery and resilience to future fire and climate conditions in northwestern Cascadia, depending on management objective. Additionally, planting presents tradeoffs for stand complexity, early-seral conditions, and potential fire risk that are important to consider.

A key management objective for northwestern Cascadia forests is accelerating the development of older forest structure and composition across the landscape (Spies et al. 2018). Depending on the chosen species and site preparation activities used, post-fire planting may hinder these efforts by simplifying the natural "precocious" complexity of early post-fire stand structure and composition as suggested by our simulations (Donato et al. 2012). By accelerating tree dominance, post-fire planting diminishes the temporal and spatial extent of early-seral conditions with corresponding effects including reduced understory plant diversity, including culturally important foods and medicines, and reduced habitat for animal species that utilize open-forest conditions (Boyd 1999, Swanson et al. 2014). By adding live vegetation to the system, post-fire planting alters fuel profiles. This is less likely to impact fire potential in climate-limited fire regimes due to limited effects of manipulation of fuel and stand structure on fire behavior (Halofsky et al. 2018b). However, the tendency of wet temperate forests to reburn

multiple times in the decades following an initial fire (Gray and Franklin 1997) suggests that post-fire planting may impact fire behavior or severity of reburns in moist forests by elevating surface fuel loads and spatial connectivity. Yet, these effects may be marginal given the natural propensity for high severity fire in these systems, particularly under extreme fire weather conditions, and likely depend on site preparation activities (e.g., snag thinning, pile burning). Finally, given the high monetary and human costs of implementation, planting is likely to be most worth it in stands where natural post-fire forest recovery is unlikely (Davis et al. 2023, Dobrowski et al. 2024).

Fuel reduction treatments — There is particular interest among forest managers across the region in understanding the effects of fuel reduction treatments on fire risk in northwestern Cascadia. In the absence of east winds, the potential for small to moderate sized fire in wet temperate forests is expected to increase due to drier conditions (Halofsky et al. 2018a, 2020) and increased probability of ignition due to human population growth, recreation pressure, and greater development in the wildland urban interface (Syphard et al. 2017, Cattau et al. 2020). Reburn risk may also increase due to increased frequency and magnitude of warmer and drier conditions that promote fuel drying (Reilly et al. 2022). Further, increasing co-occurrence of compounding extremes (e.g., fuel aridity and east winds) under climate change may increase the risk of small to moderate fires becoming large extreme events (Abatzoglou et al. 2021). Fuel reduction treatments including mechanical thinning and prescribed fire can be useful for reducing fire risk in dry forests (Bernal et al. 2025), but may be less effective at moderating fire behavior and effects in wet forests (Halofsky et al. 2018b). Rapid recovery of live fuels following fire, as illustrated by our simulations, coupled with possible increases in flammability through alteration of post-fire microclimate conditions (Millikin et al. 2024) likely limits the role

of fire as an effective fuel reduction treatment in these systems (Halofsky et al. 2018b).

3.5.4 *Evaluation of simulation model performance*

In general, iLand captured realistic broad patterns of stand development following high severity fire, though our findings highlight areas for model improvement. While trajectories of live stand structure followed expected overall stand development trends for basal area, density, and species composition, the shape of these trajectories was influenced by iLand's size classifications. For example, the timing of pulses in density trajectories reflects transitions in recruitment of seedlings into saplings and saplings into tree height classes. Additionally, trajectories of broadleaf species exhibit an abrupt increase in density proportion around year 40 of the simulations for pre-fire young. This is likely attributed to the current parameterization of golden chinquapin regeneration. The age of maturity (i.e., minimum age for seed production) for this species is currently set at 45 years (Thom et al. 2024), contributing to a large pulse in broadleaf individuals in pre-fire young stands which had large components of golden chinquapin in initial post-fire field surveys. These dynamics suggest further refinement of species parameters, environment inputs, and landscape setup is necessary to improve the plausibility of our simulations.

Our findings point to several additional ways to improve the plausibility of our simulations. First, we treated stands as isolated entities, though they exist within a broader landscape context. The consequences of this simulation feature are particularly notable for regeneration dynamics. While our external seed buffer approach incorporated differences in distance to seed source and species composition among stands, seed was allowed to enter stands from all directions and all available species were considered equally abundant, ignoring spatial patterns of seed availability and relative species importance (Stevens-Rumann and Morgan

2019). Thus, simulated external seed pressure was likely greater in our simulations than would be expected for each stand, given actual spatial constraints on available seed sources. Representation of more realistic conditions of external seed availability among stands could be helpful for refining simulated post-fire regeneration dynamics and stand development trajectories.

Next, our simulations were also limited by the spatial scale of climate inputs. iLand models daily climate at the stand scale (100 m resolution) and reflects structural effects on light availability (Seidl et al. 2012a), but does not capture finer scale, within-stand variability in other microclimate conditions (e.g., temperature, moisture). These factors are important controls on growth, regeneration, mortality, and nutrient cycling processes, with important implications for post-fire forest structural and compositional trajectories (De Frenne et al. 2021). Current efforts are underway to build a microclimate module for iLand to reflect more realistic stand dynamics (Braziunas et al. 2025).

Finally, our simulations would be improved by representation of non-tree vegetation dynamics. Because vegetation in iLand is limited to trees (Seidl et al. 2012a), our simulations are missing important effects of non-tree vegetation on stand successional development. In wet temperate forests, rapid growth of live woody shrubs and herbaceous vegetation following stand-replacing fire has important effects on early-seral conditions, tree establishment and growth, and live surface fuel profiles (Tiribelli et al. 2018, Stevens-Rumann and Morgan 2019, Buma et al. 2020). Implementation of understory vegetation into iLand is an active area of model development (Rammer et al. 2024), and existing studies suggest ways of examining non-tree vegetation abundance and richness in iLand using species distribution models relating overstory structure with understory dynamics (Braziunas et al. 2024). Adopting this approach could be a

near-term way to improve our characterization of post-fire trajectories in northwestern Cascadia.

Despite these limitations, iLand remains a powerful tool for exploring complex landscape dynamics. Building capacity for simulation modeling is increasingly important to the field of ecology (Seidl 2017). By parameterizing additional tree species (Thom et al. 2024) and re-calibrating model performance across regional environmental and productivity gradients, we are helping strengthen the simulation-modeling infrastructure for the Pacific Northwest with which to complement empirical methods. Further calibration and evaluation efforts are ongoing to incorporate remaining tree species, improve productivity dynamics, operationalize the fire module, and enhance the ease and comparability of implementing common silvicultural and fuel treatments in iLand. Continued monitoring of our field-measured stands over time will be important for improving model performance by allowing for comparison of observed trends against simulated trends.

3.6 APPENDIX D: MODEL INPUTS

Table 3.1. Tree species measured within sampled stands. Species were categorized into three functional groups based on taxonomic division (i.e., conifer vs. broadleaf) and shade tolerance (Minore 1979).

Species	Common name	Code*	Alternate species†	Functional group
Abies amabilis[1]	Pacific silver fir	abam	–	shade tolerant conifer
Abies grandis[1]	grand fir	abgr	–	shade tolerant conifer
Abies lasiocarpa	subalpine fir	abla	*Picea engelmannii*	shade tolerant conifer
Abies procera[1]	noble fir	abpr	–	shade intolerant conifer
Acer macrophyllum[1]	bigleaf maple	acma	–	broadleaf
Alnus rubra	red alder	alru	*Prunus emarginata*	broadleaf
Callitropsis nootkatensis	yellow cedar	cano	*Thuja plicata*	shade tolerant conifer
Chrysolepis chrysophylla[3]	golden chinquapin	chch	–	broadleaf
Cornus nuttallii	Pacific dogwood	conu	*Prunus emarginata*	broadleaf
Larix occidentalis	western larch	laoc	*Pseudotsuga menziesii*	shade intolerant conifer
Pinus contorta	lodgepole pine	pico	*Pinus monticola*	shade intolerant conifer
Picea engelmannii[2]	Engelmann spruce	pien	–	shade tolerant conifer
Pinus monticola[2]	western white pine	pimo	–	shade intolerant conifer
Populus trichocarpa	black cottonwood	poba	*Acer macrophyllum*	broadleaf
Prunus emarginata[3]	bitter cherry	prem	–	broadleaf
Pseudotsuga menziesii[1]	Douglas-fir	psmem	–	shade intolerant conifer
Taxus brevifolia[3]	Pacific yew	tabr	–	shade tolerant conifer
Thuja plicata[1]	western redcedar	thpl	–	shade tolerant conifer
Tsuga heterophylla[1]	western hemlock	tshe	–	shade tolerant conifer
Tsuga mertensiana[1]	mountain hemlock	tsme	–	shade tolerant conifer

* Tree species codes used in iLand.

† For several species that have yet to be fully re-calibrated for iLand simulations in northwestern Cascadia, we assigned temporary alternate species based on similar functional traits (e.g., physical characteristics, physiological tolerances, reproductive strategies).

[1] Originally parameterized for western Oregon (Seidl et al. 2012a).

[2] Originally parameterized for the Northern Rockies (Braziunas et al. 2018).

[3] Newly parameterized for the Pacific Northwest (Thom et al. 2024).

Table 3.2. Summary of initial (2–5 years) post-fire live and dead vegetation inputs used to initialize iLand simulations in stands burned at high severity. Values are mean (standard error) minimum–maximum of live stand structure and dead carbon pools across all replicates (N = 40) within each pre-fire stand age class.

Vegetation input	pre-fire stand age		
	young (n = 9)	**mid-seral** (n = 12)	**late-seral** (n = 19)
Live basal area (m^2/ha)			
trees (height ≥ 4 m)	0 (–) 0-0	5.5 (–) 5.5-5.5	5.1 (2.5) 0.9-11.3
saplings (height 1.37–4 m)	0 (–) 0-0	0 (–) 0-0	0 (–) 0-0
Density (stems/ha)			
trees (height ≥ 4 m)	0 (–) 0-0	24 (–) 24-24	7 (4) 1-16
saplings (height 1.37–4 m)	421 (103) 198-596	1,193 (–) 1,193-1,193	464 (331) 132-795
seedlings (height < 1.37 m)	534 (148) 21-1,368	3,137 (1,535) 129-19,277	8,619 (3,569) 87-66,715
snags (height ≥ 4 m)	1,381 (290) 548-3,223	770 (91) 374-1,500	533 (51) 164-920
Aboveground biomass (Mg C/ha)			
snags (height ≥ 4 m)	53.5 (8.0) 21.9-97.8	191.1 (14.2) 107.4-323.4	198.1 (18.9) 43.2-447.2
labile soil pool	5.4 (1) 2.4-12.8	5.1 (0.7) 1.4-10.6	11.8 (1.4) 1.8-23.1
refractory soil pool	6.4 (0.9) 2.6-10	11.5 (1.4) 5.1-19.6	22.1 (3.3) 8.2-71.1

Notes: The labile soil pool includes litter, duff, 1-h and 10-h down woody debris, and small snags (height < 4 m) and stumps with diameter ≤ 2.54 cm. The refractory soil pool includes 100-h and 1000-h down woody debris, and small snags (height < 4 m) and stumps with diameter > 2.54 cm. Empty standard error values (–) indicate mean values correspond to a single stand.

Table 3.3. Summary of environment inputs used to initialize iLand simulations in stands burned at high severity. Values are mean (standard error) minimum–maximum of pre-fire soil conditions across all replicates ($N = 40$) within each pre-fire stand age class.

Environment input	**pre-fire stand age**		
	young ($n = 9$)	**mid-seral** ($n = 12$)	**late-seral** ($n = 19$)
Plant available nitrogen (kg ha^{-1} yr^{-1})	64 (1) 60-69	65 (1) 58-71	65 (1) 58-74
Soil depth (cm)	71.9 (4.1) 59.3-86.9	88.5 (3.7) 59.3-99.6	88.8 (3) 59.3-106.1
Sand (%)	48 (4) 38-68	54 (3) 34-68	49 (2) 34-60
Silt (%)	38 (3) 23-45	34 (2) 23-49	38 (2) 29-49
Clay (%)	14 (1) 9-17	12 (1) 9-17	13 (1) 11-17

Notes: Plant available nitrogen was derived from regional soil fertility rasters (Coops et al. 2012). Soil depth and texture values were obtained from the CONUS-SOIL geodatabase (Miller and White 1998).

Table 3.4. Climate inputs for each future climate scenario, summarized for 20-year periods within the 80-year simulations. Values are the mean (minimum–maximum) of each variable across all sampled high-severity plots.

***Climate variable* & simulation year**	**Future climate scenario**	
	Control	**Warming**
Minimum temperature (°C)		
1–20	2.0 (0.0–4.6)	3.0 (1.1–5.6)
21–40	1.8 (0.0–4.5)	3.8 (2.0–6.3)
41–60	2.0 (0.0–4.6)	5.0 (3.2–7.5)
61–80	1.8 (0.0–4.5)	6.1 (4.4–8.5)
Maximum temperature (°C)		
1–20	10.9 (7.8–14.4)	11.9 (8.8–15.4)
21–40	10.9 (7.6–14.4)	12.8 (9.7–16.2)
41–60	10.9 (7.8–14.4)	13.9 (10.9–17.3)
61–80	10.9 (7.6–14.4)	15.1 (12.1–18.4)
Annual precipitation (mm)		
1–20	2,311 (1,742–3,275)	2,311 (1,742–3,275)
21–40	2,218 (1,594–3,258)	2,218 (1,594–3,258)
41–60	2,311 (1,742–3,275)	2,311 (1,742–3,275)
61–80	2,218 (1,594–3,258)	2,218 (1,594–3,258)
Solar radiation (MJ m^{-2} day^{-1})		
1–20	12.8 (11.8–14.1)	12.8 (11.8–14.1)
21–40	12.9 (11.8–14.1)	12.9 (11.8–14.1)
41–60	12.8 (11.8–14.1)	12.8 (11.8–14.1)
61–80	12.9 (11.8–14.1)	12.9 (11.8–14.1)
Minimum vapor pressure deficit (kPa)		
1–20	0.03 (0.00–0.06)	0.02 (0.00–0.04)
21–40	0.02 (0.00–0.04)	0.03 (0.01–0.05)
41–60	0.03 (0.00–0.06)	0.03 (0.00–0.05)
61–80	0.02 (0.00–0.04)	0.03 (0.01–0.05)
Maximum vapor pressure deficit (kPa)		
1–20	1.80 (1.40–2.32)	2.11 (1.67–2.75)
21–40	1.83 (1.37–2.38)	2.37 (1.76–3.11)
41–60	1.80 (1.40–2.32)	2.65 (2.18–3.33)
61–80	1.83 (1.37–2.38)	3.07 (2.37–3.89)

Notes: Temperature and radiation variables are an average of daily values for each 20-year period. Precipitation is an average of annual totals for each 20-year period. Vapor pressure deficit variables are an average of annual minimum or maximum values for each 20-year period.

Table 3.5. Species composition of external seed input across pre-fire stand age and forest zone strata. *n* indicates the number of sampled high severity stands across strata ($N = 40$). Species are listed using iLand codes (Table 3.1).

***Forest zone* & pre-fire stand age**	***n***	**External seed species**
Tsuga heterophylla Zone		
young	3	pimo, psmem
mid-seral	10	abam, abgr, abpr, acma, psmem, thpl, tshe
late-seral	11	abam, abgr, abpr, psmem, tabr, thpl, tshe
Abies amabilis Zone		
young	6	abam, abpr, pimo, psmem, tshe
mid-seral	2	abam
late-seral	8	abam, abpr, psmem, tabr, thpl, tshe, tsme

Table 3.6. Importance values of live mature (dbh ≥ 10 cm) tree species in sampled unburned stands (N = 31) across pre-fire stand age and forest zone strata. Values represent an index of species dominance within a stand based on relative basal area, density, and frequency (Curtis and McIntosh 1951), and were used to inform the species composition of external seed input for high-severity stands (Table 3.5).

Species	***Tsuga heterophylla* Zone**			***Abies amabilis* Zone**		
	young (n = 1)	**mid-seral** (n = 9)	**late-seral** (n = 6)	**young** (n = 6)	**mid-seral** (n = 1)	**late-seral** (n = 8)
Abies amabilis	–	0.06	0.10	0.82	3.00	1.42
Abies grandis	–	0.04	0.07	0.86	–	–
Abies procera	–	0.04	0.13	–	–	0.05
Acer macrophyllum	–	0.11	–	–	–	–
Pinus monticola	1.10	–	–	0.06	–	–
Pseudotsuga menziesii	1.90	1.49	0.81	1.01	–	0.44
Taxus brevifolia	–	–	0.11	–	–	0.04
Thuja plicata	–	0.28	0.35	–	–	0.09
Tsuga heterophylla	–	0.97	1.44	0.25	–	0.82
Tsuga mertensiana	–	–	–	–	–	0.14

Notes: The importance value index ranges from 0 to 3, with higher values signifying greater importance of an individual species. Blank values (–) indicate no live mature individuals of that species were measured in sampled unburned stands of that stratum.

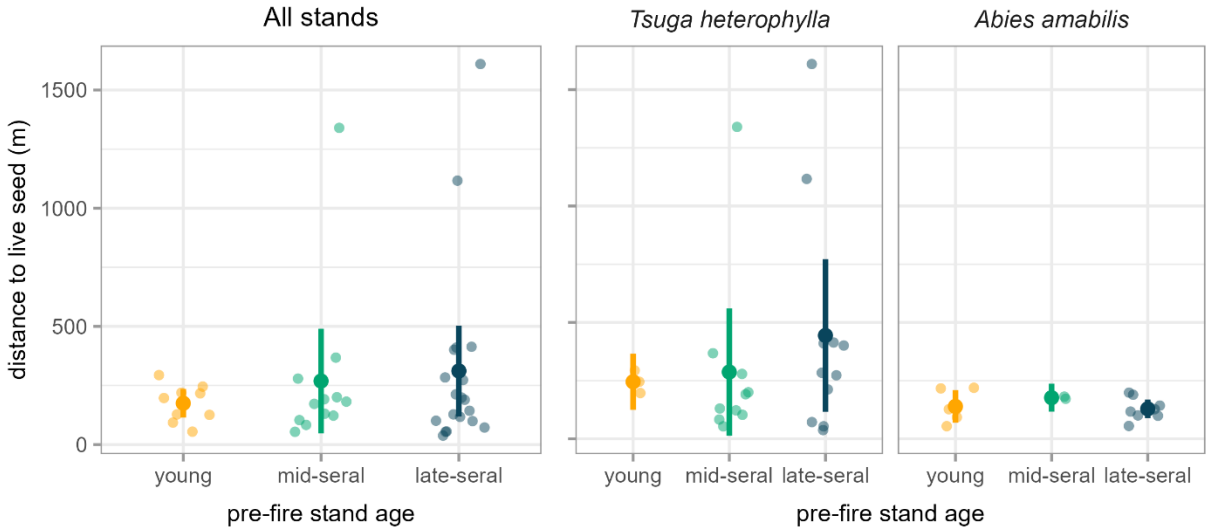

Figure 3.6. Distance to live seed source of sampled high-severity stands ($N = 40$), colored by pre-fire stand age and presented for all stands combined (*left*) and separated by forest zone (*right*). Bold points and lines are means and 95% confidence intervals for each stand age class. Translucent points show stand-level values.

3.7 APPENDIX E: FUTURE CLIMATE SCENARIOS

Table 3.7. Average climate conditions in sampled high-severity stands ($N = 40$) from 1981–2020.

Climate variable	Average conditions, 1981–2020		
	mean	minimum	maximum
minimum temperature (°C)	1.9	0.0	4.6
maximum temperature (°C)	10.9	7.7	14.4
annual precipitation (mm)	2,249	1,639	3,261
solar radiation (MJ m^{-2} day^{-1})	12.9	11.8	14.1
minimum vapor pressure deficit (kPa)	0.02	0.01	0.04
maximum vapor pressure deficit (kPa)	1.82	1.39	2.35

Notes: Temperature and radiation variables are an average of daily values for the 40-year period. Precipitation is an average of annual totals for the 40-year period. Vapor pressure deficit variables are an average of annual minimum or maximum values for the 40-year period. All climate variables were obtained from Daymet gridded meteorological data (Thornton et al. 2022).

Table 3.8. Scaling patterns of local anomalies in monthly mean temperature and relative humidity across sampled fires, arranged by latitude (north to south). Scalars represent local relationships in mean temperature (Fig. 3.7) and relative humidity (Fig. 3.8) anomalies relative to global mean temperature projections.

Fire	Jan	Feb	Mar	Apr	May	Jun	Jul	Aug	Sep	Oct	Nov	Dec
Temperature anomaly scalar												
Norse Peak	1.33	1.31	1.19	1.03	1.11	1.47	1.95	2.04	1.82	1.35	1.21	1.27
Big Hollow	1.11	1.06	0.99	0.93	1.05	1.35	1.72	1.83	1.71	1.32	1.13	1.10
Eagle Creek	1.11	1.06	0.99	0.93	1.05	1.35	1.72	1.83	1.71	1.32	1.13	1.10
Riverside	1.11	1.05	1.00	0.96	1.10	1.40	1.76	1.86	1.74	1.38	1.14	1.10
Lionshead	1.11	1.05	1.00	0.96	1.10	1.40	1.76	1.86	1.74	1.38	1.14	1.10
Relative humidity anomaly scalar												
Norse Peak	-0.28	-0.58	-0.58	-0.08	-0.21	-1.17	-2.21	-1.92	-1.24	-0.01	0.31	-0.01
Big Hollow	0.10	-0.03	0.06	0.17	-0.13	-0.86	-1.58	-1.42	-0.90	-0.09	0.34	0.23
Eagle Creek	0.10	-0.03	0.06	0.17	-0.13	-0.86	-1.58	-1.42	-0.90	-0.09	0.34	0.23
Riverside	-0.07	-0.11	-0.03	0.02	-0.28	-0.90	-1.52	-1.25	-0.75	-0.32	0.15	0.04
Lionshead	-0.07	-0.11	-0.03	0.02	-0.28	-0.90	-1.52	-1.25	-0.75	-0.32	0.15	0.04

Notes: Local anomaly scalars were extracted from global maps (0.25-degree resolution) of scaling patterns for monthly temperature and relative humidity anomalies, derived from multi-model mean climate projections from CMIP6 (Vargas Zeppetello et al. 2019).

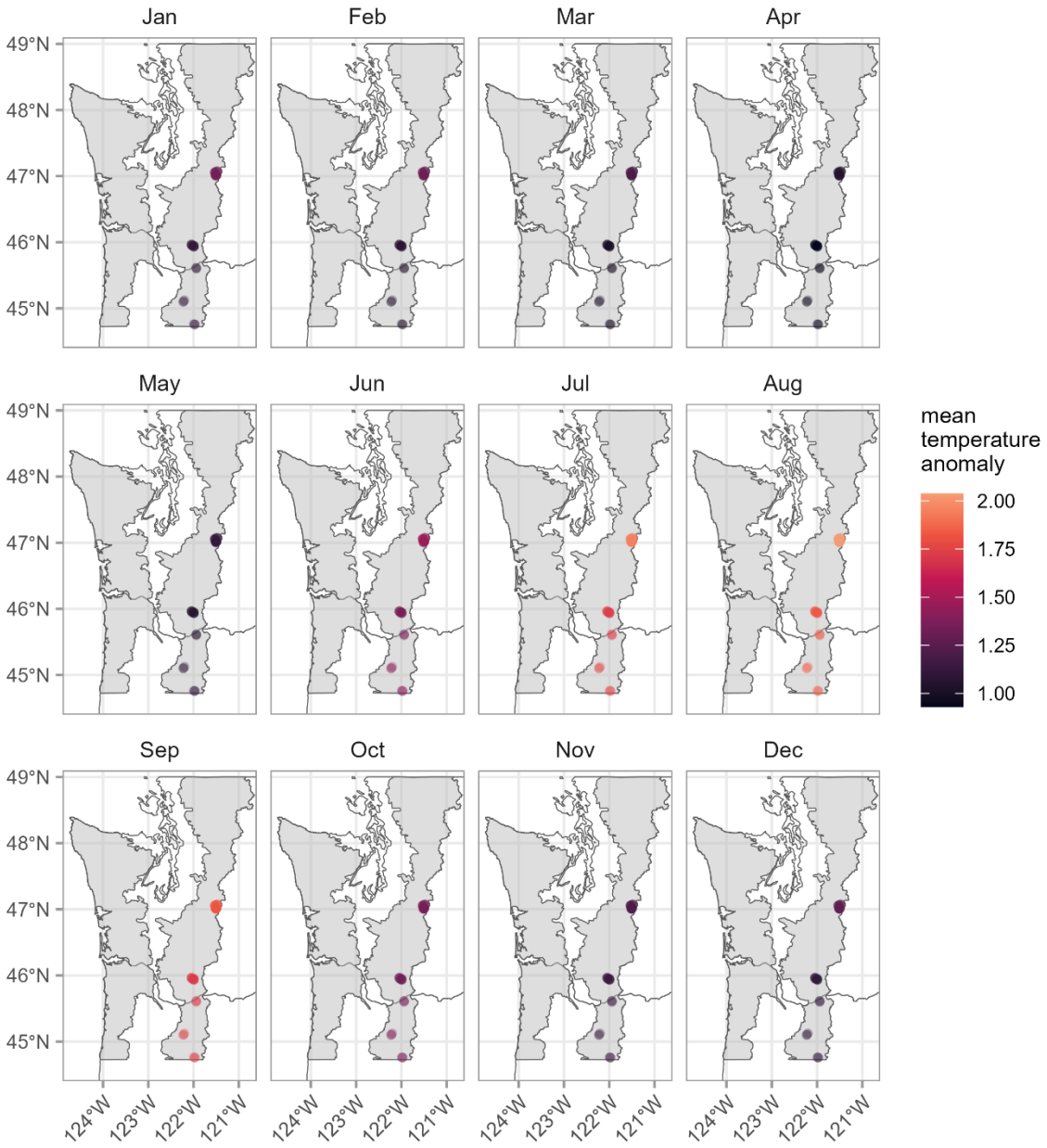

Figure 3.7. Monthly scalars for local mean temperature anomalies in sampled high-severity stands (colored points; $N = 40$) across northwestern Cascadia, USA (gray shaded area). Scalars represent local anomalies in mean temperature relative to global-scale temperature changes, and were extracted from maps of temperature scaling patterns based on multi-model mean climate projections from CMIP6 (Vargas Zeppetello et al. 2019).

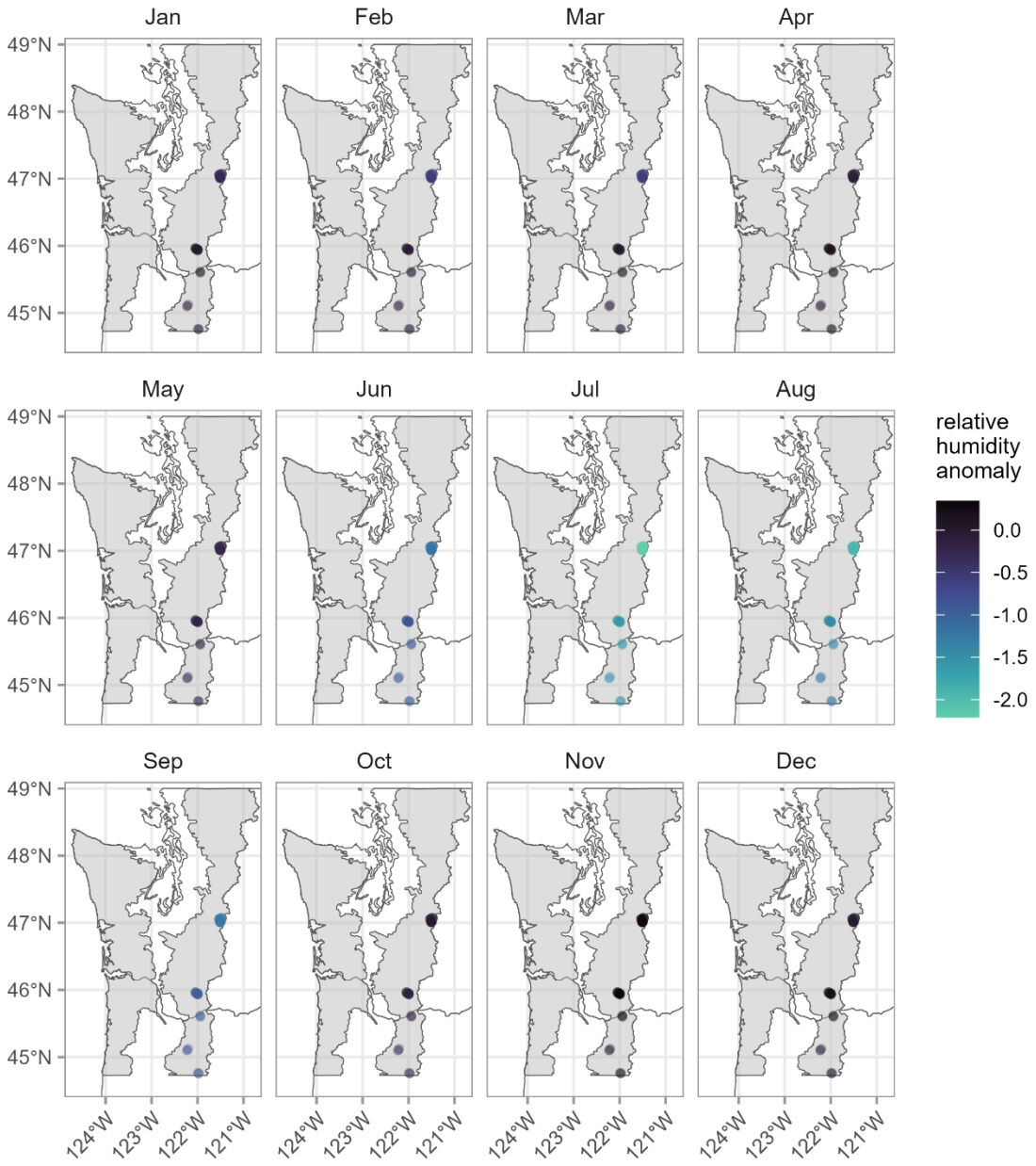

Figure 3.8. Monthly scalars for local relative humidity anomalies in sampled high-severity stands (colored points; $N = 40$) across northwestern Cascadia, USA (gray shaded area). Scalars represent local anomalies in relative humidity relative to global-scale temperature changes, and were extracted from maps of relative humidity scaling patterns based on multi-model mean climate projections from CMIP6 (Vargas Zeppetello et al. 2019).

Table 3.9. Summary of future trends in local anomalies of annual mean temperature (Fig. 3.9) and relative humidity (Fig. 3.10) in sampled stands across northwestern Cascadia, scaled to global climate projections under SSP3-7.0 (Lee et al. 2021).

Future time period	Global anomaly	Local anomaly	
		minimum	maximum
Mean surface air temperature (°C)			
2021–2040	+0.7	+0.9	+1.0
2041–2060	+1.4	+1.8	+2.0
2061–2080	+2.2	+2.8	+3.2
2081–2100	+3.1	+4.0	+4.5
Relative humidity over land (%)			
2021–2040	−1.5	−0.4	−0.8
2041–2060	−1.8	−1.0	−1.7
2061–2080	−2.6	−1.4	−2.6
2081–2100	−3.3	−1.9	−3.7

Notes: Global anomalies are relative to 1995–2014.

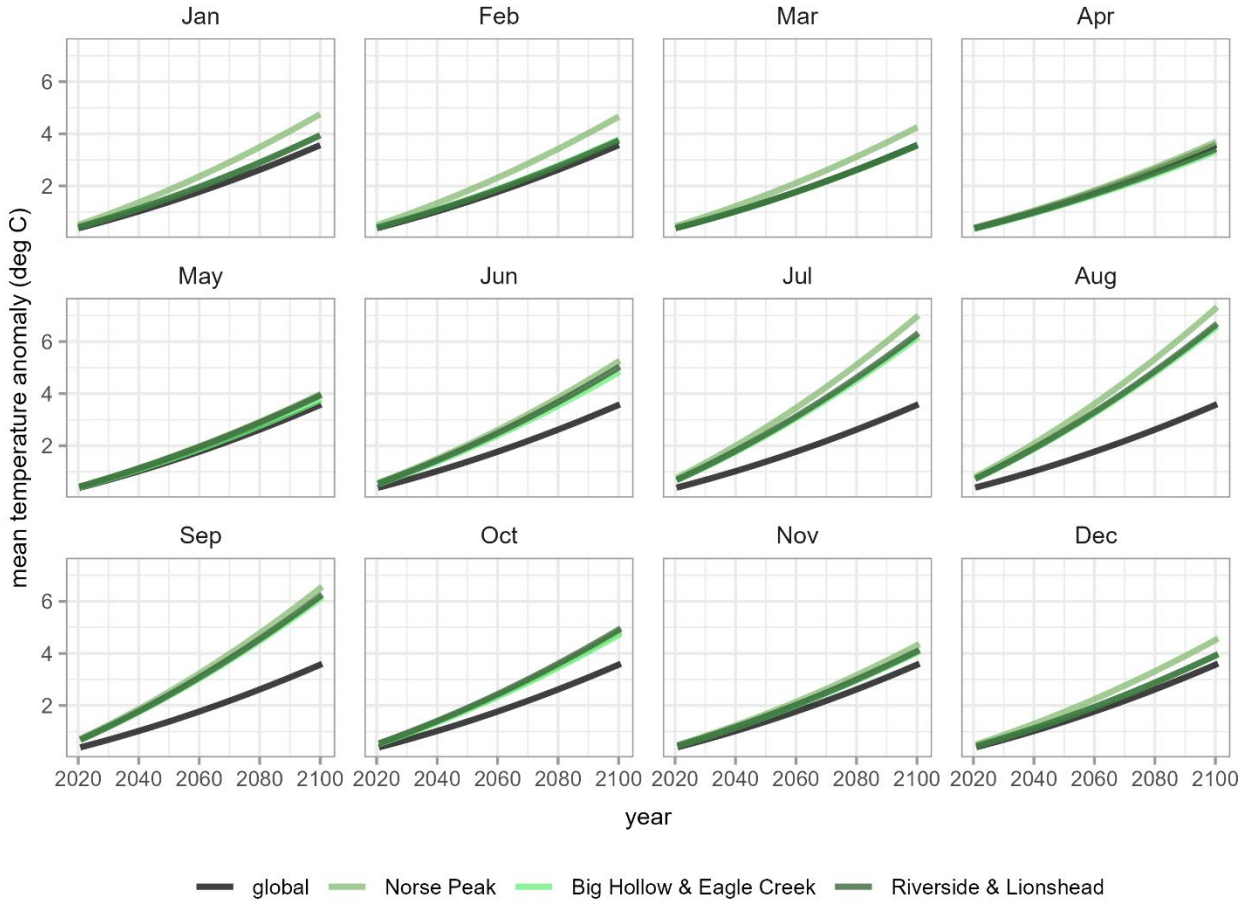

Figure 3.9. Projected future trends in monthly local anomalies of mean temperature (°C) for high-severity stands sampled in five recent fires across northwestern Cascadia (green lines). Trends are scaled to projections of annual global mean temperature under SSP3-7.0 (black lines; Lee et al. 2021). Sampled stands within each fire were positioned across three unique 0.25-degree pixels from global maps of mean temperature scaling patterns (Vargas Zeppetello et al. 2019).

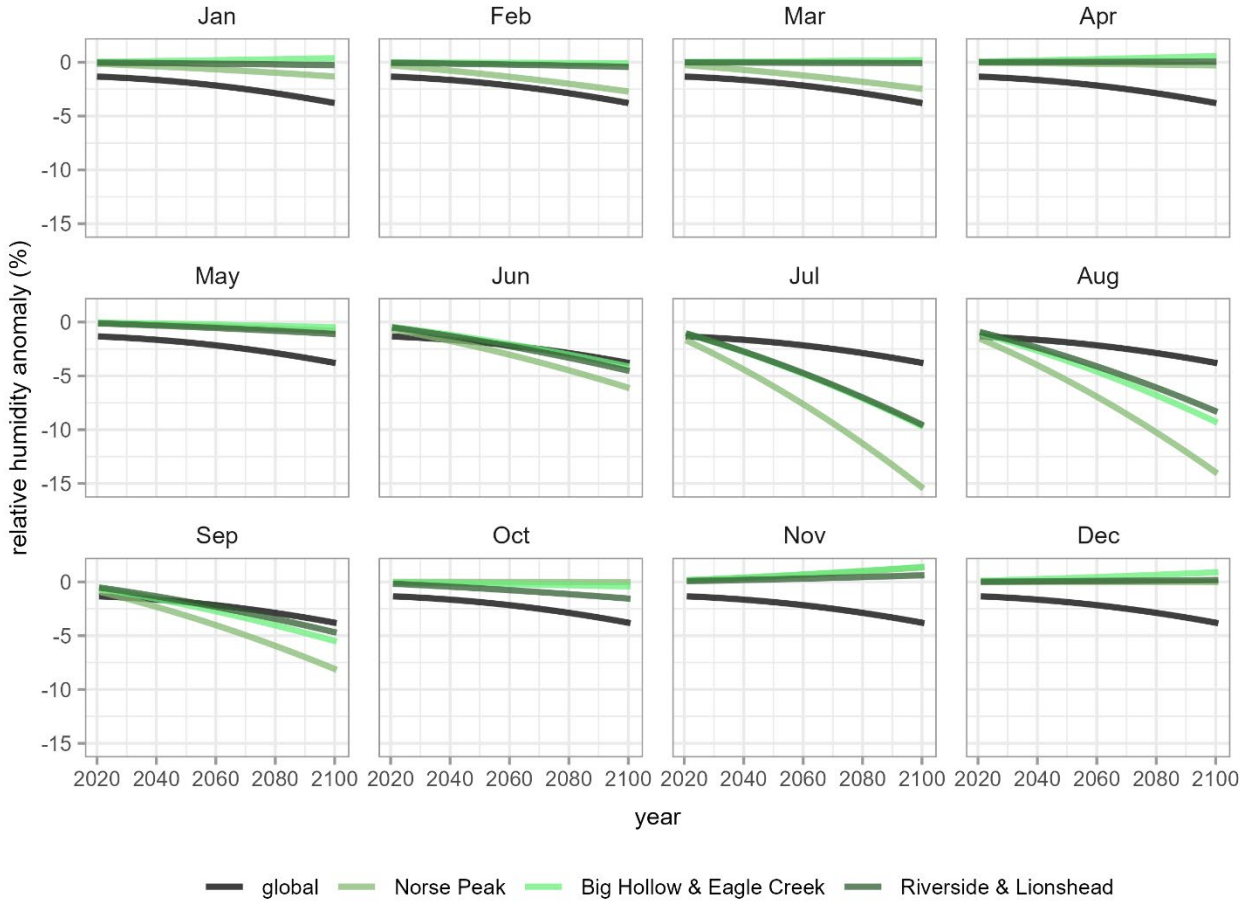

Figure 3.10. Projected future trends in monthly local anomalies of relative humidity (%) for high-severity stands sampled in five recent fires across northwestern Cascadia (green lines). Trends are scaled to projections of annual global mean relative humidity over land as a function of mean temperature under SSP3-7.0 (black lines; Lee et al. 2021). Sampled stands within each fire were positioned across three unique 0.25-degree pixels from global maps of mean temperature scaling patterns (Vargas Zeppetello et al. 2019).

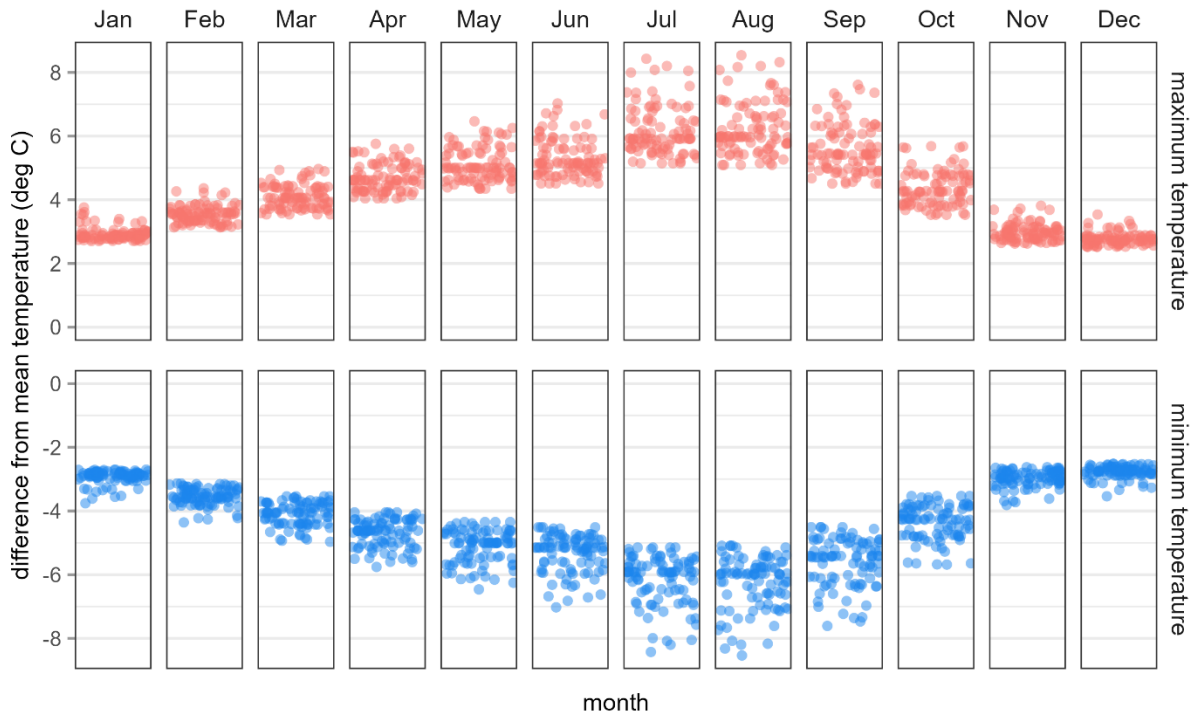

Figure 3.11. Stand-level differences (°C) of monthly minimum and maximum temperatures from the mean based on daily Daymet observations from 1981–2020 (Thornton et al. 2022).

3.8 APPENDIX F: SUPPLEMENTAL RESULTS

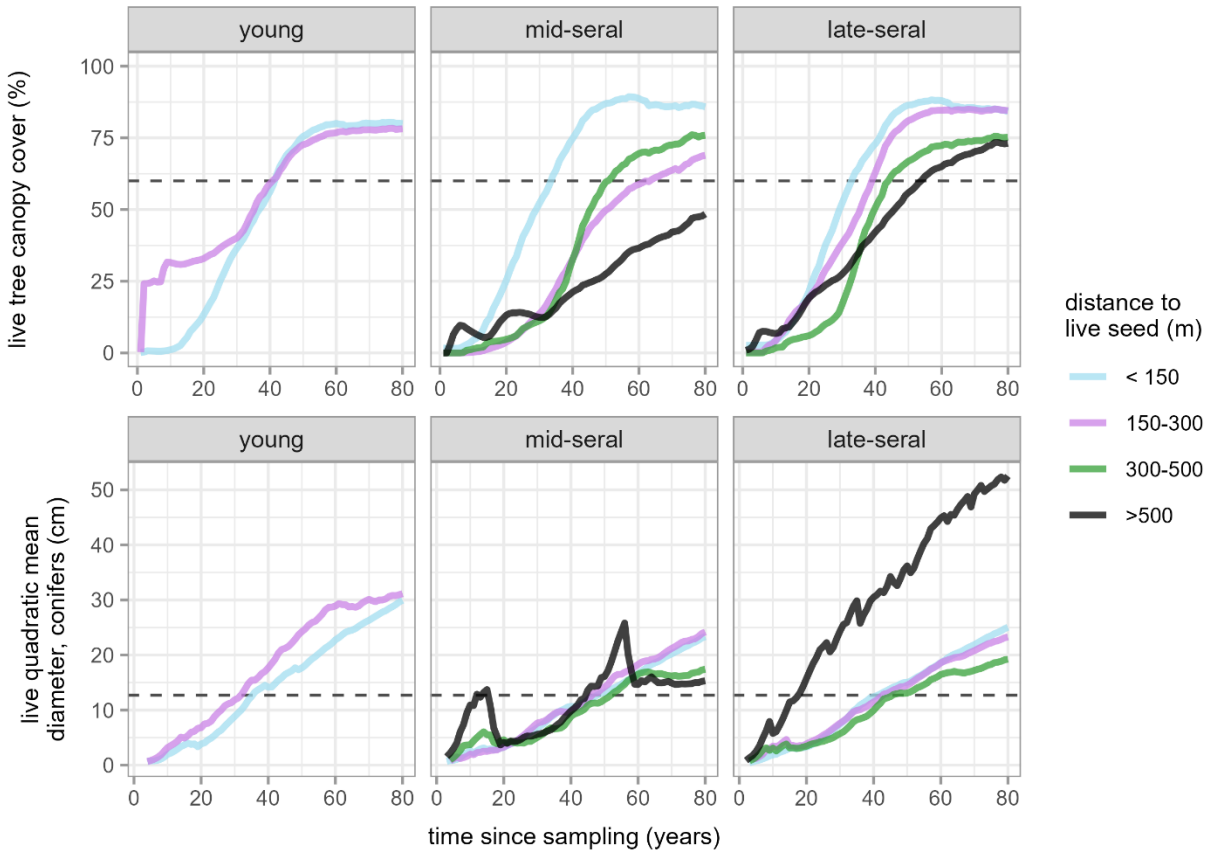

Figure 3.12. Relationship of distance to live seed source with simulated post-fire live canopy cover (*top*) and quadratic mean diameter (*bottom*) across pre-fire stand age class. Lines are strata-level means for all stands burned at high severity, colored by distance to live seed source. Live quadratic mean diameter includes all conifers with height > 1.3 m.

3.9 REFERENCES

Abatzoglou, J. T., D. E. Rupp, L. W. O'Neill, and M. Sadegh. 2021. Compound extremes drive the western Oregon wildfires of September 2020. Geophysical Research Letters 48:e2021GL092520.

Abatzoglou, J. T., and A. P. Williams. 2016. Impact of anthropogenic climate change on wildfire across western US forests. Proceedings of the National Academy of Sciences 113:11770–11775.

Agee, J. 1993. Fire ecology of Pacific Northwest forests. Island Press, Washington D.C.

Agee, J. K., and M. H. Huff. 1987. Fuel succession in a western hemlock/Douglas-fir forest. Canadian Journal of Forest Research 17:697–704.

Agne, M. C., R. A. Slesak, L. G. Mantecon, J. W. Wright, S. E. Kolpak, E. E. Baumgart, A. D. Bower, R. Darbyshire, C. Ellwanger, V. J. Erickson, A. R. Ferreria, C. E. Looney, B. A. Roskilly, and J. W. Sherlock. 2025. Informing reforestation with the Experimental Network for Assisted Migration and Establishment Silviculture (ENAMES). Gen Tech. Rep. PNW-GTR-1031. Portland, OR: U.S. Department of Agriculture, Forest Service, Pacific Northwest Research Station. 103 p. (Online Only) 1031.

Albrich, K., W. Rammer, and R. Seidl. 2020. Climate change causes critical transitions and irreversible alterations of mountain forests. Global Change Biology 26:4013–4027.

Allen, C. D., A. K. Macalady, H. Chenchouni, D. Bachelet, N. McDowell, M. Vennetier, T. Kitzberger, A. Rigling, D. D. Breshears, E. H. (Ted) Hogg, P. Gonzalez, R. Fensham, Z. Zhang, J. Castro, N. Demidova, J.-H. Lim, G. Allard, S. W. Running, A. Semerci, and N. Cobb. 2010. A global overview of drought and heat-induced tree mortality reveals emerging climate change risks for forests. Forest Ecology and Management 259:660–684.

Andrus, R. A., L. R. Peach, A. R. Cinquini, B. Mills, J. T. Yusi, C. Buhl, M. Fischer, B. A. Goodrich, J. M. Hulbert, A. Holz, A. J. H. Meddens, K. B. Moffett, A. Ramirez, and H. D. Adams. 2024. Canary in the forest?—Tree mortality and canopy dieback of western redcedar linked to drier and warmer summers. Journal of Biogeography 51:103–119.

Armitage, D. R., R. Plummer, F. Berkes, R. I. Arthur, A. T. Charles, I. J. Davidson-Hunt, A. P. Diduck, N. C. Doubleday, D. S. Johnson, M. Marschke, P. McConney, E. W. Pinkerton, and E. K. Wollenberg. 2009. Adaptive co-management for social–ecological complexity. Frontiers in Ecology and the Environment 7:95–102.

Bernal, A. A., S. L. Stephens, M. A. Callaham, B. M. Collins, J. S. Crotteau, M. B. Dickinson, D. L. Hagan, R. Hedges, S. M. Hood, T. F. Hutchinson, M. K. Taylor, and T. A. Coates. 2025. The national Fire and Fire Surrogate study: Effects of fuel treatments in the Western and Eastern United States after 20 years. Ecological Applications 35:e70003.

Betzen, J. J., A. Ramsey, D. Omdal, G. J. Ettl, and P. C. Tobin. 2021. Bigleaf maple, *Acer macrophyllum* Pursh, decline in western Washington, USA. Forest Ecology and Management 501:119681.

Bowd, E. J., D. P. Blair, and D. B. Lindenmayer. 2021. Prior disturbance legacy effects on plant recovery post-high-severity wildfire. Ecosphere 12:e03480.

Boyd, R., editor. 1999. Indians, Fire and the Land in the Pacific Northwest. Oregon State University Press, Corvallis, Oregon.

Brackett, A. E., C. J. Still, and K. J. Puettmann. 2024. Residual canopy cover provides buffering of near-surface temperatures, but benefits are limited under extreme conditions. Canadian Journal of Forest Research.

Braziunas, K. H., L. Geres, T. Richter, F. Glasmann, C. Senf, D. Thom, S. Seibold, and R. Seidl. 2024. Projected climate and canopy change lead to thermophilization and homogenization of forest floor vegetation in a hotspot of plant species richness. Global Change Biology 30:e17121.

Braziunas, K. H., W. D. Hansen, R. Seidl, W. Rammer, and M. G. Turner. 2018. Looking beyond the mean: Drivers of variability in postfire stand development of conifers in Greater Yellowstone. Forest Ecology and Management 430:460–471.

Braziunas, K. H., W. Rammer, P. De Frenne, J. Díaz-Calafat, P.-O. Hedwall, C. Senf, D. Thom, F. Zellweger, and R. Seidl. 2025. Microclimate temperature effects propagate across scales in forest ecosystems. Landscape Ecology 40:37.

Brown, J. K. 1974. Handbook for inventorying downed woody material. Gen. Tech. Rep. INT-16, U.S. Department of Agriculture, Forest Service, Intermountain Forest and Range Experiment Station, Ogden, UT.

Brown, J. K., R. D. Oberheu, and C. M. Johnston. 1982. Handbook for inventorying surface fuels and biomass in the Interior West. Page INT-GTR-129. U.S. Department of Agriculture, Forest Service, Intermountain Forest and Range Experiment Station, Ogden, UT.

Buma, B., S. Weiss, K. Hayes, and M. Lucash. 2020. Wildland fire reburning trends across the US West suggest only short-term negative feedback and differing climatic effects. Environmental Research Letters 15:034026.

Burcsu, T. K., J. S. Halofsky, S. A. Bisrat, T. A. Christopher, M. K. Creutzburg, E. B. Henderson, M. A. Hemstrom, F. J. Triepke, and M. Whitman. 2014. Chapter 2: Dynamic Vegetation Modeling of Forest, Woodland, Shrubland, and Grassland Vegetation Communities in the Pacific Northwest and Southwest Regions of the United States. Pages 15–70 Integrating Social, Economic, and Ecological Values Across Large Landscapes. U.S. Department of Agriculture, Forest Service, Pacific Northwest Research Station, Portland, OR.

Busby, S. U., A. M. Klock, and J. S. Fried. 2023. Inventory analysis of fire effects wrought by wind-driven megafires in relation to weather and pre-fire forest structure in the western Cascades. Fire Ecology 19:58.

Case, M. J., B. G. Johnson, K. J. Bartowitz, and T. W. Hudiburg. 2021. Forests of the future: Climate change impacts and implications for carbon storage in the Pacific Northwest, USA. Forest Ecology and Management 482:118886.

Case, M. J., and J. J. Lawler. 2016. Relative vulnerability to climate change of trees in western North America. Climatic Change 136:367–379.

Cattau, M., C. Wessman, A. Mahood, and J. Balch. 2020. Anthropogenic and lightning-started fires are becoming larger and more frequent over a longer season length in the U.S.A. Global Ecology and Biogeography 29.

Chegwidden, O. S., R. Hagen, K. Martin, M. Jones, A. Banihirwe, C. Chiao, S. Frank, J.

Freeman, and J. Hamman. 2022. Open data and tools for multiple methods of global climate downscaling. https://github.com/carbonplan/research.

Clark, S. A., J. N. Archer, S. L. Stephens, B. M. Collins, and D. L. Hankins. 2024. Realignment of federal environmental policies to recognize fire's role. Fire Ecology 20:74.

Coop, J. D., S. A. Parks, C. S. Stevens-Rumann, S. D. Crausbay, P. E. Higuera, M. D. Hurteau, A. Tepley, E. Whitman, T. Assal, B. M. Collins, K. T. Davis, S. Dobrowski, D. A. Falk, P. J. Fornwalt, P. Z. Fulé, B. J. Harvey, V. R. Kane, C. E. Littlefield, E. Q. Margolis, M. North, M.-A. Parisien, S. Prichard, and K. C. Rodman. 2020. Wildfire-driven forest conversion in western North American landscapes. BioScience 70:659–673.

Coops, N. C., R. H. Waring, and T. Hilker. 2012. Prediction of soil properties using a process-based forest growth model to match satellite-derived estimates of leaf area index. Remote Sensing of Environment 126:160–173.

Curtis, J. T., and R. P. McIntosh. 1951. An Upland Forest Continuum in the Prairie-Forest Border Region of Wisconsin. Ecology 32:476–496.

Davis, E. J., C. Wilmsen, M. A. Machado, and G. M. Alessi. 2023. Multiple Stories, Multiple Marginalities: The Labor-Intensive Forest and Fire Stewardship Workforce in Oregon. Fire 6:268.

De Frenne, P., J. Lenoir, M. Luoto, B. R. Scheffers, F. Zellweger, J. Aalto, M. B. Ashcroft, D. M. Christiansen, G. Decocq, K. De Pauw, S. Govaert, C. Greiser, E. Gril, A. Hampe, T. Jucker, D. H. Klinges, I. A. Koelemeijer, J. J. Lembrechts, R. Marrec, C. Meeussen, J. Ogée, V. Tyystjärvi, P. Vangansbeke, and K. Hylander. 2021. Forest microclimates and climate change: Importance, drivers and future research agenda. Global Change Biology 27:2279–2297.

Dennison, P. E., S. C. Brewer, J. D. Arnold, and M. A. Moritz. 2014. Large wildfire trends in the western United States, 1984–2011. Geophysical Research Letters 41:2928–2933.

Dobrowski, S. Z., M. M. Aghai, A. Chichilnisky Du Lac, R. Downer, J. Fargione, D. L. Haase, T. Hoecker, O. A. Kildisheva, A. Murdoch, S. Newman, M. North, P. Saksa, M. Sjoholm, T. Baribault, M. S. Buonanduci, M. E. Chambers, L. Gonzales-Kramer, B. J. Harvey, M. D. Hurteau, J. Loevner, H. D. Safford, and J. Sloan. 2024. 'Mind the Gap'—reforestation needs vs. reforestation capacity in the western United States. Frontiers in Forests and Global Change 7:1402124.

Donato, D. C., J. L. Campbell, J. B. Fontaine, and B. E. Law. 2009. Quantifying char in postfire woody detritus inventories. Fire Ecology 5:104–115.

Donato, D. C., J. L. Campbell, and J. F. Franklin. 2012. Multiple successional pathways and precocity in forest development: can some forests be born complex? Journal of Vegetation Science 23:576–584.

Donato, D. C., J. S. Halofsky, and M. J. Reilly. 2020. Corralling a black swan: natural range of variation in a forest landscape driven by rare, extreme events. Ecological Applications 30:e02013.

Donato, D. C., B. J. Harvey, W. H. Romme, M. Simard, and M. G. Turner. 2013. Bark beetle effects on fuel profiles across a range of stand structures in Douglas-fir forests of Greater Yellowstone. Ecological Applications 23:3–20.

Eisenberg, C., S. Prichard, M. P. Nelson, and P. Hessburg. 2024. Braiding Indigenous and Western Knowledge for Climate-Adapated Forests: An Ecocultural State of Science Report. Page 102.

Evers, C., A. Holz, S. Busby, and M. Nielsen-Pincus. 2022. Extreme winds alter influence of fuels and topography on megafire burn severity in seasonal temperate rainforests under record fuel aridity. Fire 5:41.

Franklin, J. F., and C. T. Dyrness. 1973. Natural vegetation of Oregon and Washington. Gen. Tech. Rep. PNW-GTR-008, U.S. Department of Agriculture, Forest Service, Pacific Northwest Research Station, Portland, OR.

Franklin, J. F., K. N. Johnson, and D. L. Johnson. 2018. Ecological Forest Management. Waveland Press.

Franklin, J. F., T. A. Spies, R. V. Pelt, A. B. Carey, D. A. Thornburgh, D. R. Berg, D. B. Lindenmayer, M. E. Harmon, W. S. Keeton, D. C. Shaw, K. Bible, and J. Chen. 2002. Disturbances and structural development of natural forest ecosystems with silvicultural implications, using Douglas-fir forests as an example. Forest Ecology and Management 155:399–423.

Freund, J. A., J. F. Franklin, A. J. Larson, and J. A. Lutz. 2014. Multi-decadal establishment for single-cohort Douglas-fir forests. Canadian Journal of Forest Research 44:1068–1078.

Gray, A. N., T. R. Whittier, and M. E. Harmon. 2016. Carbon stocks and accumulation rates in Pacific Northwest forests: role of stand age, plant community, and productivity. Ecosphere 7:e01224.

Greenwood, L., R. Bliege Bird, C. McGuire, N. Jadai, J. Price, A. Skroblin, S. van Leeuwen, and D. Nimmo. 2024. Indigenous pyrodiversity promotes plant diversity. Biological Conservation 291:110479.

Grimm, V., D. Ayllón, and S. F. Railsback. 2017. Next-Generation Individual-Based Models Integrate Biodiversity and Ecosystems: Yes We Can, and Yes We Must. Ecosystems 20:229–236.

Halofsky, J. E., D. L. Peterson, and B. J. Harvey. 2020. Changing wildfire, changing forests: the effects of climate change on fire regimes and vegetation in the Pacific Northwest, USA. Fire Ecology 16:4.

Halofsky, J. S., D. R. Conklin, D. C. Donato, J. E. Halofsky, and J. B. Kim. 2018a. Climate change, wildfire, and vegetation shifts in a high-inertia forest landscape: Western Washington, U.S.A. PLOS ONE 13:e0209490.

Halofsky, J. S., D. C. Donato, J. F. Franklin, J. E. Halofsky, D. L. Peterson, and B. J. Harvey. 2018b. The nature of the beast: examining climate adaptation options in forests with stand-replacing fire regimes. Ecosphere 9:e02140.

Halofsky, J. S., J. E. Halofsky, M. A. Hemstrom, A. T. Morzillo, X. Zhou, and D. C. Donato. 2017. Divergent trends in ecosystem services under different climate-management futures in a fire-prone forest landscape. Climatic Change 142:83–95.

Hansen, W. D., R. Fitzsimmons, J. Olnes, and A. P. Williams. 2021. An alternate vegetation type proves resilient and persists for decades following forest conversion in the North American boreal biome. Journal of Ecology 109:85–98.

Harmon, M. E., W. K. Ferrell, and J. F. Franklin. 1990. Effects on Carbon Storage of Conversion of Old-Growth Forests to Young Forests. Science 247:699–702.

Harmon, M. E., C. W. Woodall, B. Fasth, and J. Sexton. 2008. Woody detritus density and density reduction factors for tree species in the United States: a synthesis. Gen. Tech. Rep. NRS-29, U.S. Department of Agriculture, Forest Service, Northern Research Station, Newtown Square, PA, Newtown Square, PA.

Harmon, M. E., C. W. Woodall, B. Fasth, J. Sexton, and M. Yatkov. 2011. Differences between standing and downed dead tree wood density reduction factors: A comparison across decay classes and tree species. Research Paper, U.S. Department of Agriculture, Forest Service, Northern Research Station, Newtown Square, PA.

Hernangómez, D. 2023. Using the tidyverse with terra objects: the tidyterra package. Journal of Open Source Software 8:5751.

Hijmans, R. J. 2024a. *raster: Geographic Data Analysis and Modeling*.

Hijmans, R. J. 2024b. *terra: Spatial Data Analysis*.

Hoecker, T. J., and M. G. Turner. 2022. Combined effects of climate and fire-driven vegetation change constrain the distributions of forest vertebrates during the 21st century. Diversity and Distributions 28:727–744.

Hoffman, K. M., K. P. Lertzman, and B. M. Starzomski. 2017. Ecological legacies of anthropogenic burning in a British Columbia coastal temperate rain forest. Journal of Biogeography 44:2903–2915.

Hsiao, J., S.-H. Kim, D. J. Timlin, N. D. Mueller, and A. L. S. Swann. 2024. Model-aided climate adaptation for future maize in the US. Environmental Research: Food Systems 1:015004.

Hufkens, K., D. Basler, T. Milliman, E. K. Melaas, and A. D. Richardson. 2018. An integrated phenology modelling framework in R: modeling vegetation phenology with phenor. Methods in Ecology and Evolution 9:1–10.

Jain, P., A. R. Sharma, D. C. Acuna, J. T. Abatzoglou, and M. Flannigan. 2024. Record-breaking fire weather in North America in 2021 was initiated by the Pacific northwest heat dome. Communications Earth & Environment 5:1–10.

Johnston, J. D., M. R. Schmidt, A. G. Merschel, W. M. Downing, M. R. Coughlan, and D. G. Lewis. 2023. Exceptional variability in historical fire regimes across a western Cascades landscape, Oregon, USA. Ecosphere 14:e4735.

Johnstone, J. F., C. D. Allen, J. F. Franklin, L. E. Frelich, B. J. Harvey, P. E. Higuera, M. C. Mack, R. K. Meentemeyer, M. R. Metz, G. L. Perry, T. Schoennagel, and M. G. Turner. 2016. Changing disturbance regimes, ecological memory, and forest resilience. Frontiers in Ecology and the Environment 14:369–378.

Jolly, W. M., M. A. Cochrane, P. H. Freeborn, Z. A. Holden, T. J. Brown, G. J. Williamson, and D. M. J. S. Bowman. 2015. Climate-induced variations in global wildfire danger from 1979 to 2013. Nature Communications 6:1–11.

Kline, J. D., M. E. Harmon, T. A. Spies, A. T. Morzillo, R. J. Pabst, B. C. McComb, F. Schnekenburger, K. A. Olsen, B. Csuti, and J. C. Vogeler. 2016. Evaluating carbon storage, timber harvest, and habitat possibilities for a Western Cascades (USA) forest

landscape. Ecological Applications 26:2044–2059.

Kobayashi, Y., R. Seidl, W. Rammer, K. F. Suzuki, and A. S. Mori. 2023. Identifying effective tree planting schemes to restore forest carbon and biodiversity in Shiretoko National Park, Japan. Restoration Ecology 31:e13681.

Lake, F. K., V. Wright, P. Morgan, M. McFadzen, D. McWethy, and C. Stevens-Rumann. 2017. Returning Fire to the Land: Celebrating Traditional Knowledge and Fire. Journal of Forestry 115:343–353.

Laughlin, M. M., L. K. Rangel-Parra, J. E. Morris, D. C. Donato, J. S. Halofsky, and B. J. Harvey. 2023. Patterns and drivers of early conifer regeneration following stand-replacing wildfire in Pacific Northwest (USA) temperate maritime forests. Forest Ecology and Management 549:121491.

Law, B. E., D. Turner, J. Campbell, O. J. Sun, S. Van Tuyl, W. D. Ritts, and W. B. Cohen. 2004. Disturbance and climate effects on carbon stocks and fluxes across Western Oregon USA. Global Change Biology 10:1429–1444.

Lebel, L., J. M. Anderies, B. Campbell, C. Folke, S. Hatfield-Dodds, T. P. Hughes, and J. Wilson. 2006. Governance and the Capacity to Manage Resilience in Regional Social-Ecological Systems. Ecology and Society 11:art19.

Lee, J.-Y., J. Marotzke, G. Bala, L. Cao, S. Corti, J. P. Dunne, F. Engelbrecht, E. Fischer, J. C. Fyfe, C. Jones, A. Maycock, J. Mutemi, O. Ndiaye, S. Panickal, and T. Zhou. 2021. Future Global Climate: Scenario-Based Projections and Near-Term Information. Cambridge University Press, Cambridge, United Kingdom and New York, NY, USA.

Lemon, J. 2006. Plotrix: a package in the red light district of R. R-News 6:8–12.

Lindenmayer, D. B., E. J. Bowd, and P. Gibbons. 2022. Forest restoration in a time of fire: perspectives from tall, wet eucalypt forests subject to stand-replacing wildfires. Philosophical Transactions of the Royal Society B: Biological Sciences 378:20210082.

Lindenmayer, D. B., G. E. Likens, and J. F. Franklin. 2010. Rapid responses to facilitate ecological discoveries from major disturbances. Frontiers in Ecology and the Environment 8:527–532.

Littell, J. S., D. McKenzie, D. L. Peterson, and A. L. Westerling. 2009. Climate and wildfire area burned in western U.S. ecoprovinces, 1916–2003. Ecological Applications 19:1003–1021.

Littell, J. S., D. McKenzie, H. Y. Wan, and S. A. Cushman. 2018. Climate Change and Future Wildfire in the Western United States: An Ecological Approach to Nonstationarity. Earth's Future 6:1097–1111.

Loehman, R. A., R. E. Keane, and L. M. Holsinger. 2020. Simulation modeling of complex climate, wildfire, and vegetation dynamics to address wicked problems in land management. Frontiers in Forests and Global Change 3:3.

Long, J. W., F. K. Lake, and R. W. Goode. 2021. The importance of Indigenous cultural burning in forested regions of the Pacific West, USA. Forest Ecology and Management 500:119597.

Maclean, K., D. L. Hankins, A. C. Christianson, I. Oliveras, B. A. Bilbao, O. Costello, E. R. Langer, and C. J. Robinson. 2023. Revitalising Indigenous cultural fire practice: benefits

and partnerships. Trends in Ecology & Evolution 38:899–902.

Means, J. E., H. A. Hansen, G. J. Koerper, P. B. Alaback, and M. W. Klopsch. 1994. Software for computing plant biomass - BIOPAK users guide. Gen. Tech. Rep. PNW-GTR-340, U.S. Department of Agriculture, Forest Service, Pacific Northwest Research Station, Portland, OR.

Meinshausen, M., Z. R. J. Nicholls, J. Lewis, M. J. Gidden, E. Vogel, M. Freund, U. Beyerle, C. Gessner, A. Nauels, N. Bauer, J. G. Canadell, J. S. Daniel, A. John, P. B. Krummel, G. Luderer, N. Meinshausen, S. A. Montzka, P. J. Rayner, S. Reimann, S. J. Smith, M. Van Den Berg, G. J. M. Velders, M. K. Vollmer, and R. H. J. Wang. 2020. The shared socio-economic pathway (SSP) greenhouse gas concentrations and their extensions to 2500. Geoscientific Model Development 13:3571–3605.

Miller, D. A., and R. A. White. 1998. A Conterminous United States Multilayer Soil Characteristics Dataset for Regional Climate and Hydrology Modeling. Earth Interactions 2:1–26.

Millikin, R. L., W. J. Braun, M. E. Alexander, and S. Fani. 2024. The Impact of Fuel Thinning on the Microclimate in Coastal Rainforest Stands of Southwestern British Columbia, Canada. Fire 7:285.

Minore, D. 1979. Comparative autecological characteristics of northwestern tree species - a literature review. Gen. Tech. Rep. PNW-GTR-087, U.S. Department of Agriculture, Forest Service, Pacific Northwest Research Station, Portland, OR.

Müller, K., H. Wickham, D. A. James, and S. Falcon. 2024. *RSQLite: SQLite Interface for R*.

Nolan, R., and S. Padilla-Parra. 2017. *filesstrings*: An R package for file and string manipulation. Journal of Open Source Software 2.

O'Neill, B. C., C. Tebaldi, D. P. van Vuuren, V. Eyring, P. Friedlingstein, G. Hurtt, R. Knutti, E. Kriegler, J.-F. Lamarque, J. Lowe, G. A. Meehl, R. Moss, K. Riahi, and B. M. Sanderson. 2016. The Scenario Model Intercomparison Project (ScenarioMIP) for CMIP6. Geoscientific Model Development 9:3461–3482.

Parks, S. A., and J. T. Abatzoglou. 2020. Warmer and drier fire seasons contribute to increases in area burned at high severity in western US forests from 1985-2017. Geophysical Research Letters 47:e2020GL089858.

Parks, S. A., L. M. Holsinger, C. Miller, and C. R. Nelson. 2015. Wildland fire as a self-regulating mechanism: the role of previous burns and weather in limiting fire progression. Ecological Applications 25:1478–1492.

Pebesma, E., and R. Bivand. 2005. Classes and methods for spatial data in R. R-News 5:9–13.

Pedersen, T. 2024. *patchwork: The Composer of Plots*.

Pierce, D. 2024. *ncdf4: Interface to Unidata netCDF (Version 4 or Earlier) Format Data Files*.

Prichard, S. J., D. V. Sandberg, R. D. Ottmar, E. Eberhardt, A. Andreu, P. Eagle, and Kjell. Swedin. 2013. Fuel Characteristic Classification System version 3.0: technical documentation. Page PNW-GTR-887. U.S. Department of Agriculture, Forest Service, Pacific Northwest Research Station, Portland, OR.

PRISM Climate Group. 2024, January. Norm91m: 30-Year Normals, 1991-2020. Oregon State

University, https://prism.oregonstate.edu, accessed 1 May 2024.

R Core Team. 2024. *R: A Language and Environment for Statistical Computing*. R Foundation for Statistical Computing, Vienna, Austria.

Rammer, W., D. Thom, M. Baumann, K. Braziunas, C. Dollinger, J. Kerber, J. Mohr, and R. Seidl. 2024. The individual-based forest landscape and disturbance model iLand: Overview, progress, and outlook. Ecological Modelling:110785.

Raymond, C. L., and D. McKenzie. 2012. Carbon dynamics of forests in Washington, USA: 21st century projections based on climate-driven changes in fire regimes. Ecological Applications 22:1589–1611.

Reilly, M. J., J. E. Halofsky, M. A. Krawchuk, D. C. Donato, P. F. Hessburg, J. D. Johnston, A. G. Merschel, M. E. Swanson, J. S. Halofsky, and T. A. Spies. 2021. Fire Ecology and Management in Pacific Northwest Forests. Pages 393–435 *in* C. H. Greenberg and B. Collins, editors. Fire Ecology and Management: Past, Present, and Future of US Forested Ecosystems. Springer International Publishing, Cham.

Reilly, M. J., and T. A. Spies. 2015. Regional variation in stand structure and development in forests of Oregon, Washington, and inland Northern California. Ecosphere 6:art192.

Reilly, M. J., A. Zuspan, J. S. Halofsky, C. Raymond, A. McEvoy, A. W. Dye, D. C. Donato, J. B. Kim, B. E. Potter, N. Walker, R. Davis, C. J. Dunn, D. M. Bell, M. J. Gregory, J. D. Johnston, B. J. Harvey, J. E. Halofsky, and B. K. Kerns. 2022. Cascadia Burning: the historic, but not historically unprecedented, 2020 wildfires in the Pacific Northwest, USA. Ecosphere 13:e4070.

Riahi, K., D. P. Van Vuuren, E. Kriegler, J. Edmonds, B. C. O'Neill, S. Fujimori, N. Bauer, K. Calvin, R. Dellink, O. Fricko, W. Lutz, A. Popp, J. C. Cuaresma, S. Kc, M. Leimbach, L. Jiang, T. Kram, S. Rao, J. Emmerling, K. Ebi, T. Hasegawa, P. Havlik, F. Humpenöder, L. A. Da Silva, S. Smith, E. Stehfest, V. Bosetti, J. Eom, D. Gernaat, T. Masui, J. Rogelj, J. Strefler, L. Drouet, V. Krey, G. Luderer, M. Harmsen, K. Takahashi, L. Baumstark, J. C. Doelman, M. Kainuma, Z. Klimont, G. Marangoni, H. Lotze-Campen, M. Obersteiner, A. Tabeau, and M. Tavoni. 2017. The Shared Socioeconomic Pathways and their energy, land use, and greenhouse gas emissions implications: An overview. Global Environmental Change 42:153–168.

Rodman, K. C., P. J. Fornwalt, Z. A. Holden, J. E. Crouse, K. T. Davis, L. A. E. Marshall, M. T. Stoddard, R. A. Andrus, M. E. Chambers, T. B. Chapman, S. J. Hart, C. A. Schloegel, and C. S. Stevens-Rumann. 2024. Green is the New Black: Outcomes of post-fire tree planting across the US Interior West. Forest Ecology and Management 574:122358.

Rogers, M., and G. S. Mauger. 2021. Pacific Northwest Climate Projection Tool. University of Washington Climate Impacts Group.

Schoennagel, T., J. K. Balch, H. Brenkert-Smith, P. E. Dennison, B. J. Harvey, M. A. Krawchuk, N. Mietkiewicz, P. Morgan, M. A. Moritz, R. Rasker, M. G. Turner, and C. Whitlock. 2017. Adapt to more wildfire in western North American forests as climate changes. Proceedings of the National Academy of Sciences 114:4582–4590.

Seidl, R. 2017. To Model or not to Model, That is no Longer the Question for Ecologists. Ecosystems 20:222–228.

Seidl, R., W. Rammer, R. M. Scheller, and T. A. Spies. 2012a. An individual-based process model to simulate landscape-scale forest ecosystem dynamics. Ecological Modelling 231:87–100.

Seidl, R., W. Rammer, and T. A. Spies. 2014. Disturbance legacies increase the resilience of forest ecosystem structure, composition, and functioning. Ecological Applications 24:2063–2077.

Seidl, R., T. A. Spies, W. Rammer, E. A. Steel, R. J. Pabst, and K. Olsen. 2012b. Multi-scale drivers of spatial variation in old-growth forest carbon density disentangled with lidar and an individual-based landscape model. Ecosystems 15:1321–1335.

Seidl, R., D. Thom, M. Kautz, D. Martin-Benito, M. Peltoniemi, G. Vacchiano, J. Wild, D. Ascoli, M. Petr, J. Honkaniemi, M. J. Lexer, V. Trotsiuk, P. Mairota, M. Svoboda, M. Fabrika, T. A. Nagel, and C. P. O. Reyer. 2017. Forest disturbances under climate change. Nature Climate Change 7:395–402.

Seidl, R., and M. G. Turner. 2022. Post-disturbance reorganization of forest ecosystems in a changing world. Proceedings of the National Academy of Sciences 119:e2202190119.

Seneviratne, S. I., X. Zhang, M. Adnan, W. Badi, C. Dereczynski, A. Di Luca, S. Ghosh, I. Iskandar, J. Kossin, S. Lewis, F. Otto, I. Pinto, M. Satoh, S. M. Vicente-Serrano, M. Wehner, and B. Zhou. 2021. Weather and Climate Extreme Events in a Changing Climate. Cambridge University Press, Cambridge, United Kingdom and New York, NY, USA.

Smith, J. E., and L. S. Heath. 2002. A model of forest floor carbon mass for United States forest types. Research Paper, U.S. Department of Agriculture, Forest Service, Northeastern Research Station, Newtown Square, PA.

Spies, T. A. 1991. Plant species diversity and occurrence in young, mature, and old-growth Douglas-fir stands in western Oregon and Washington. Pages 111–121 *in* L. F. Ruggiero, K. B. Aubry, A. B. Carey, and M. H. Huff, editors. Wildlife and vegetation of unmanaged Douglas-fir forests. U.S. Department of Agriculture, Forest Service, Pacific Northwest Research Station, Portland, OR.

Spies, T. A., J. F. Franklin, and T. B. Thomas. 1988. Coarse woody debris in Douglas-fir forests of western Oregon and Washington. Ecology 69:1689–1702.

Spies, T. A., P. A. Stine, R. Gravenmier, J. W. Long, and M. J. Reilly. 2018. Synthesis of science to inform land management within the Northwest Forest Plan area. Gen. Tech. Rep. PNW-GTR-966, U.S. Department of Agriculture, Forest Service, Pacific Northwest Research Station, Portland, OR.

Stevens-Rumann, C. S., and P. Morgan. 2019. Tree regeneration following wildfires in the western US: a review. Fire Ecology 15:15.

Still, C. J., A. Sibley, D. DePinte, P. E. Busby, C. A. Harrington, M. Schulze, D. R. Shaw, D. Woodruff, D. E. Rupp, C. Daly, W. M. Hammond, and G. F. M. Page. 2023. Causes of widespread foliar damage from the June 2021 Pacific Northwest Heat Dome: more heat than drought. Tree Physiology 43:203–209.

Swanson, M. E., J. F. Franklin, R. L. Beschta, C. M. Crisafulli, D. A. DellaSala, R. L. Hutto, D. B. Lindenmayer, and F. J. Swanson. 2011. The forgotten stage of forest succession: early-

successional ecosystems on forest sites. Frontiers in Ecology and the Environment 9:117–125.

Swanson, M. E., N. M. Studevant, J. L. Campbell, and D. C. Donato. 2014. Biological associates of early-seral pre-forest in the Pacific Northwest. Forest Ecology and Management 324:160–171.

Syphard, A. D., J. E. Keeley, A. H. Pfaff, and K. Ferschweiler. 2017. Human presence diminishes the importance of climate in driving fire activity across the United States. Proceedings of the National Academy of Sciences 114:13750–13755.

Taylor, G. P., P. C. Loikith, C. M. Aragon, H. Lee, and D. E. Waliser. 2023. CMIP6 model fidelity at simulating large-scale atmospheric circulation patterns and associated temperature and precipitation over the Pacific Northwest. Climate Dynamics 60:2199–2218.

Tepley, A. J., F. J. Swanson, and T. A. Spies. 2013. Fire-mediated pathways of stand development in Douglas-fir/western hemlock forests of the Pacific Northwest, USA. Ecology 94:1729–1743.

Tepley, A. J., F. J. Swanson, and T. A. Spies. 2014. Post-fire tree establishment and early cohort development in conifer forests of the western Cascades of Oregon, USA. Ecosphere 5:art80.

Tepley, A. J., E. Thomann, T. T. Veblen, G. L. W. Perry, A. Holz, J. Paritsis, T. Kitzberger, and K. J. Anderson-Teixeira. 2018. Influences of fire–vegetation feedbacks and post-fire recovery rates on forest landscape vulnerability to altered fire regimes. Journal of Ecology 106:1925–1940.

Thom, D., W. Rammer, K. Albrich, K. H. Braziunas, L. Dobor, C. Dollinger, W. D. Hansen, B. J. Harvey, T. Hlásny, T. J. Hoecker, J. Honkaniemi, W. S. Keeton, Y. Kobayashi, S. S. Kruszka, A. Mori, J. E. Morris, S. Peters-Collaer, Z. Ratajczak, T. Simensen, I. Storms, K. F. Suzuki, A. R. Taylor, M. G. Turner, S. Willis, and R. Seidl. 2024. Parameters of 150 temperate and boreal tree species and provenances for an individual-based forest landscape and disturbance model. Data in Brief 55:110662.

Thom, D., W. Rammer, R. Garstenauer, and R. Seidl. 2018. Legacies of past land use have a stronger effect on forest carbon exchange than future climate change in a temperate forest landscape. Biogeosciences 15:5699–5713.

Thompson, V., A. T. Kennedy-Asser, E. Vosper, Y. T. E. Lo, C. Huntingford, O. Andrews, M. Collins, G. C. Hegerl, and D. Mitchell. 2022. The 2021 western North America heat wave among the most extreme events ever recorded globally. Science Advances 8:eabm6860.

Thornton, M., R. Shrestha, Y. Wei, P. Thornton, and S.-C. Kao. 2022. Daymet: Daily Surface Weather Data on a 1-km Grid for North America. ORNL DAAC, Oak Ridge, Tennessee, USA.

Tiribelli, F., T. Kitzberger, and J. M. Morales. 2018. Changes in vegetation structure and fuel characteristics along post-fire succession promote alternative stable states and positive fire–vegetation feedbacks. Journal of Vegetation Science 29:147–156.

Tulalip Planning Commission. 2023. Chapter 2: Land Use. Page Tulalip Tribes Comprehensive Land Use Plan.

Turner, M. G., K. H. Braziunas, W. D. Hansen, T. J. Hoecker, W. Rammer, Z. Ratajczak, A. L. Westerling, and R. Seidl. 2022. The magnitude, direction, and tempo of forest change in Greater Yellowstone in a warmer world with more fire. Ecological Monographs 92:e01485.

USFS. 2022. Confronting the Wildfire Crisis: a 10-year Implementation Plan. U.S. Department of Agriculture, Forest Service.

Van Pelt, R. 2007. Identifying Mature and Old Forests in Western Washington. Washington State Department of Natural Resources.

Vargas Zeppetello, L. R., D. S. Battisti, and M. B. Baker. 2019. The Origin of Soil Moisture Evaporation "Regimes." Journal of Climate 32:6939–6960.

Walker, B., C. S. Holling, S. R. Carpenter, and A. P. Kinzig. 2004. Resilience, adaptability and transformability in social-ecological systems. Ecology and Society 9:5.

Wang, K., and G. D. Clow. 2020. The Diurnal Temperature Range in CMIP6 Models: Climatology, Variability, and Evolution.

Waring, R. H., and J. F. Franklin. 1979. Evergreen coniferous forests of the Pacific Northwest. Science 204:1380–1386.

Washington Department of Natural Resources. 2020. Safeguarding Our Lands, Waters, and Communities: DNR's Plan for Climate Resilience. Pages 1–96. Washington State Department of Natural Resources, Olympia, WA.

White, J. W., A. Rassweiler, J. F. Samhouri, A. C. Stier, and C. White. 2014. Ecologists should not use statistical significance tests to interpret simulation model results. Oikos 123:385–388.

Whitely-Binder, L., and J. Schneider. 2022. King County Wildfire Risk Reduction Strategy. King County Climate Action Team, King County, Washington, USA.

Wickham, H. 2007. Reshaping Data with the reshape Package. Journal of Statistical Software 21:1–20.

Wickham, H., M. Averick, J. Bryan, W. Chang, L. McGowan, R. François, G. Grolemund, A. Hayes, L. Henry, J. Hester, M. Kuhn, T. Pedersen, E. Miller, S. Bache, K. Müller, J. Ooms, D. Robinson, D. Seidel, V. Spinu, K. Takahashi, D. Vaughan, C. Wilke, K. Woo, and H. Yutani. 2019. Welcome to the tidyverse. Journal of Open Source Software 4:1686.

Williams, C. B., and C. T. Dyrness. 1967. Some characteristics of forest floors and soils under true fir-hemlock stands in the Cascade range. Page 19. Research Paper, U.S. Department of Agriculture, Forest Service, Pacific Northwest Forest and Range Experiment Station, Corvallis, OR.

Wilson, N., R. Bradstock, and M. Bedward. 2022. Disturbance causes variation in sub-canopy fire weather conditions. Agricultural and Forest Meteorology 323:109077.

Winter, L. E., L. B. Brubaker, J. F. Franklin, E. A. Miller, and D. Q. DeWitt. 2002. Initiation of an old-growth Douglas-fir stand in the Pacific Northwest: a reconstruction from tree-ring records. Canadian Journal of Forest Research 32:1039–1056.

Woodall, C. W., and V. J. Monleon. 2008. Sampling protocol, estimation, and analysis procedures for the down woody materials indicator of the FIA program. Gen. Tech. Rep.

NRS-GTR-22, U.S. Department of Agriculture, Forest Service, Northern Research Station, Newtown Square, PA.

CONCLUSION

Understanding the drivers and effects of natural disturbances is critical for anticipating ecosystem dynamics in a time of rapid global change. Large infrequent disturbances play a profound role in shaping immediate and future landscape patterns and processes, though the inherent rarity of these events limits our understanding of their ecological effects. In this dissertation, I leveraged empirical and simulation modeling approaches to address priorities for anticipating the effects of large infrequent fires on future forest dynamics in northwestern Cascadia. Key findings from each chapter provide insights on drivers of aboveground disturbance legacies, short-interval disturbance interactions, and stand recovery trajectories following fire in wet temperate forests. Overall, this work advances our understanding of mechanisms behind disturbance-mediated change in ecosystems shaped by long intervals between large severe disturbances.

A key takeaway from this dissertation is that alterations to pre-disturbance legacies will have lasting effects on post-disturbance outcomes and recovery potential in these systems. Legacies are major determinants of ecosystem structure and function following large infrequent disturbances (Turner and Dale 1998, Franklin et al. 2000). The pre-disturbance ecosystem state drives total legacy amounts, while disturbance magnitude moderates legacy conditions. For example, in wet temperate forests, initial patterns in total aboveground biomass carbon and fuels following fire are driven by stand age at the time of fire, while burn severity controls the amount and arrangement of these legacies within live and dead pools (Chapter 1). These relationships suggest older forest stands may have more potential to support post-disturbance ecosystem functioning due to greater legacy abundance and complexity.

The abundance of available fuel following fire in high productivity systems shaped by large infrequent disturbances suggests that bottom-up constraints (i.e., fuel limitation) are unlikely to strongly limit subsequent fire behavior and severity. For example, in wet temperate forests, extreme fire weather conditions may override effects of initial post-fire fuel variability on potential fire behavior and effects in reburns (Chapter 2). This supports the predominance of positive linked interactions between multiple fire events in highly productive ecosystems where fire is limited primarily by fuel flammability. Additionally, feedbacks between fire effects and microclimate conditions will be important to characterize given increased likelihood of disturbance interactions with climate warming and potential for compound effects on ecosystem structure and function when disturbances interact at short intervals (Paine et al. 1998, Burton et al. 2020).

Tradeoffs exist among post-disturbance management interventions for guiding post-disturbance trajectories and are likely to change through time based on management strategies and future climate conditions. In the absence of additional disturbance, post-disturbance recovery may be more robust in older stands. For example, in wet temperate forests, pre-fire stand age has lasting effects on forest recovery for more than 80 years following high-severity fire, with longer persistence of early-seral conditions, more abundant tree regeneration, and greater fuel loads in stands older at the time of fire (Chapter 3). Accordingly, ecosystem conditions following large severe disturbances present a major opportunity for implementation of climate adaptation strategies (Halofsky et al. 2018)

Ultimately, this dissertation advances our understanding of severe fire effects in forests shaped by large infrequent disturbances and highlights key remaining knowledge gaps and directions for future research. Given that post-disturbance recovery processes play out over decades to

centuries (Franklin et al. 2002), continued monitoring and repeat measurements of these stands (beyond the 2–5-year post-fire window examined here) are necessary to capture patterns in structure and function throughout stand development and update models for improved future projections of forest dynamics. Additionally, more robust characterization of microclimate conditions is needed to improve understanding of reburn potential in systems with fire regimes primarily limited by flammability (Halofsky et al. 2020). Further, I focused solely on aboveground forest dynamics, but belowground responses to fire may differ with important consequences for vegetation patterns and ecosystem processes. Characterizing the effects of large infrequent fire events on soil properties and belowground biota will be important for developing a more robust understanding of fire effects on ecosystem structure and function (McLauchlan et al. 2020). Finally, all analyses and simulations were conducted at the scale of individual stands (i.e., 1 ha). Yet, large infrequent disturbances are contagious processes with extents that can exceed hundreds of thousands of hectares (Turner and Dale 1998). Conducting analyses at broader spatial scales could yield important insights into heterogeneity of disturbance effects and associated implications for ecosystem processes (Turner and Romme 1994, Agee 1998, Seidl and Turner 2022). Thus, continuing to strengthen landscape simulation modeling infrastructure through regional calibration efforts will be a powerful approach for addressing new objectives and challenges in ecology across a range of spatial and temporal scales (Seidl 2017).

REFERENCES

Agee, J. 1998. The landscape ecology of western forest fire regimes. Northwest Science 72:24–34.

Burton, P. J., A. Jentsch, and L. R. Walker. 2020. The Ecology of Disturbance Interactions. BioScience 70:854–870.

Franklin, J. F., D. Lindenmayer, J. A. MacMahon, A. McKee, J. Magnuson, D. A. Perry, R. Waide, and D. Foster. 2000. Threads of continuity. Conservation in Practice 1:8–17.

Franklin, J. F., T. A. Spies, R. V. Pelt, A. B. Carey, D. A. Thornburgh, D. R. Berg, D. B. Lindenmayer, M. E. Harmon, W. S. Keeton, D. C. Shaw, K. Bible, and J. Chen. 2002. Disturbances and structural development of natural forest ecosystems with silvicultural implications, using Douglas-fir forests as an example. Forest Ecology and Management 155:399–423.

Halofsky, J. E., D. L. Peterson, and B. J. Harvey. 2020. Changing wildfire, changing forests: the effects of climate change on fire regimes and vegetation in the Pacific Northwest, USA. Fire Ecology 16:4.

Halofsky, J. S., D. C. Donato, J. F. Franklin, J. E. Halofsky, D. L. Peterson, and B. J. Harvey. 2018. The nature of the beast: examining climate adaptation options in forests with stand-replacing fire regimes. Ecosphere 9:e02140.

McLauchlan, K. K., P. E. Higuera, J. Miesel, B. M. Rogers, J. Schweitzer, J. K. Shuman, A. J. Tepley, J. M. Varner, T. T. Veblen, S. A. Adalsteinsson, J. K. Balch, P. Baker, E. Batllori, E. Bigio, P. Brando, M. Cattau, M. L. Chipman, J. Coen, R. Crandall, L. Daniels, N. Enright, W. S. Gross, B. J. Harvey, J. A. Hatten, S. Hermann, R. E. Hewitt, L. N. Kobziar, J. B. Landesmann, M. M. Loranty, S. Y. Maezumi, L. Mearns, M. Moritz, J. A. Myers, J. G. Pausas, A. F. A. Pellegrini, W. J. Platt, J. Roozeboom, H. Safford, F. Santos, R. M. Scheller, R. L. Sherriff, K. G. Smith, M. D. Smith, and A. C. Watts. 2020. Fire as a fundamental ecological process: Research advances and frontiers. Journal of Ecology 108:2047–2069.

Paine, R. T., M. J. Tegner, and E. A. Johnson. 1998. Compounded perturbations yield ecological surprises. Ecosystems 1:535–545.

Seidl, R. 2017. To Model or not to Model, That is no Longer the Question for Ecologists. Ecosystems 20:222–228.

Seidl, R., and M. G. Turner. 2022. Post-disturbance reorganization of forest ecosystems in a changing world. Proceedings of the National Academy of Sciences 119:e2202190119.

Turner, M. G., and V. H. Dale. 1998. Comparing Large, Infrequent Disturbances: What Have We Learned? Ecosystems 1:493–496.

Turner, M. G., and W. H. Romme. 1994. Landscape dynamics in crown fire ecosystems. Landscape Ecology 9:59–77.